Alma Mater Studiorum – Università di Bologna

DOTTORATO DI RICERCA IN

MECCANICA E SCIENZE AVANZATE DELL'INGEGNERIA

Ciclo 33

Settore Concorsuale: 09/C1 – MACCHINE E ESISTEMI PER L'ENERGIA E L'AMBIENTE

Settore Scientifico Disciplinare: ING-IND/08 – MACCHINE A FLUIDO

DEFINITION OF MANAGEMENT CRITERIA AND DESIGN OF COMPLEX ELECTRICAL, THERMAL AND COOLING ENERGY AND FUEL DISTRIBUTION NETWORKS

Presentata da: Jessica Rosati

Coordinatore Dottorato	**Supervisore**
Prof. Marco Carricato	Prof. Francesco Melino
	Co-supervisore
	Prof. Michele Bianchi

Esame finale anno 2021

Contents

Introduction

The European and national legislations, as well as the international policies, have imposed strict constraints related to environmental issues in order to reduce the greenhouse gases emissions associated to the employment of fossil fuels and to increase the energy conversion efficiency. This have been resulted in an increasing diffusion of distributed generation systems, namely small-scale power generators or storage technologies, within the energy grid, and in particular to the ones based on the renewable energy sources exploitation, which led to a significant change in the traditional energy networks which have been moved from a centralized energy production paradigm into a more distributed one.

The need of integrating the distributed generation systems (renewable energy production systems and storage devices) with the traditional fossil fuel-based generators (operating with fossil fuels, and in particular natural gas), have led to an increase in the complexity of the existing grids both from the energy distribution and the network management points of view. It results in the development of the complex electrical, thermal and cooling energies and fuel distribution networks. In addition, the energy network, shifted towards a smart paradigm, in fact, the on-site installation of the distributed energy generators – such as photovoltaic panels, solar thermal panels, small-size combined heat and power units, etc. – involves the possibility of the one-site production and to self-consume the energy produced and, in case of energy surplus, to feed the energy network. This involves the possibility to allow a bidirectional heat exchange between the energy network and the end users which becomes a smart user (or prosumer) since it can act both as consumer and as a producer.

At the same time, the increasing diffusion of the distributed generation systems, have also involved some issue, related to the existing grid, in term of frequency and stability, as well as the possibility of black-out events in case of wrong demand forecast as well as issue related to the network management.

In this scenario, the main challenges related to the complex energy networks – characterized by the electrical, thermal, cooling energies and fuel fluxes – concern the definition of the optimal management criteria (such as the optimization of the energy systems scheduling) and the optimal design, namely the ideal setup of the energy systems. As it regards the network management, an important aspect concerns the optimization of the energy production mix and the operation of each energy system with the main purpose of maximizing the exploitation of the renewable energy source and of minimizing both the economic costs (especially the ones related to the fuel consumption) and the environmental impact.

These problems are generally addressed through the development and implementation of appropriate algorithms based on different techniques such as approximate or exact mathematical methods. Among the approximate (or heuristics) models, the most used within the complex energy networks field are the genetic algorithms, firefly algorithms and particle swarm optimization. As it concerns the exact method, instead, the linear programming, Mixed Integer Linear Programming and the Mixed Integer Non Linear Programming are used as optimization techniques.

This thesis addressed both the optimal design and the management of the complex energy grids both in the case of a singular energy flux – as for example the district heating networks, characterized by the only thermal energy production and distribution – and in the case of integrated networks characterized by electrical, thermal and cooling energies and fuel fluxes. Furthermore, another key aspect considered in this thesis is the transition into a smart paradigm, namely the possibility of converting a traditional energy network into a smart one.

To this purpose, the aim of this PhD thesis is to investigate the algorithm suitable for the aforementioned optimization problems by considering different software based on different resolution methods and implementing them to analyze different energy networks.

According to this objective, the originality of this thesis is the development of a novel software based on a non-heuristic algorithm which is able to address the non-linearity of the energy system scheduling.

Structure of the manuscript

This thesis is divided in four main parts:

Part I. The first part, corresponding to Chapter 1, presents an overview of the complex energy networks and the integration with the distributed generation systems. In particular, the main distributed generation systems are described along with innovative technologies, and the transition of the traditional electrical, thermal cooling and fuel grids into smart energy networks is addressed. Therefore, the main algorithms adopted within the complex energy networks field are presented.

Part II. The second part of the thesis focuses on the only thermal energy grids by addressing the conversion of the traditional district heating networks into smart networks. In detail, in Chapter 2 the importance of the smart user role is introduced and the optimal allocation of a smart user within a district heating network is investigated to point out a general guideline for the choice of the smart user. To this respect, in this section is presented the mathematical model of the existing software IHENA (Intelligent Heat Network Analysis), developed for the design and analysis of district heating networks. Furthermore, is also presented a novel additional tool (namely an integrating code) of software IHENA designed with the main aim of investigating the research of the more suitable thermal user to be upgraded into a smart user. The additional tool has been then used to investigate two small-size simplified district heating networks and, therefore, for the analysis of an existing medium-size thermal grid.

Part III. This section focuses on the adoption of the genetic algorithms to address both the design and management optimization problems with respect to the complex energy networks characterized by electrical, thermal and cooling energies and fuel fluxes. In Chapter 3 the mathematical model of software EGO (Energy Grid Optimizer), already developed for the optimization of the energy systems scheduling (and so used for the design optimization) is firstly presented. Therefore, as it concerns the definition of the optimal design, a residential neighborhood has been considered and implemented within the software EGO. In detail, the annual operation of the considered energy network has been analyzing by carrying out a parametric analysis by varying the total number of the considered households to outline the optimal range of each energy generation system. In Chapter 4, instead, the software genetic algorithm has been used to address the optimization problem related to the energy grids scheduling. To this respect, an isolated grid, consisting in a cruise ship, has been considered. In detail, different energy systems settings have been proposed, optimized under the operation point of view by using the software EGO and compared from the energy, economic and environmental viewpoints.

Part IV. The fourth part of this thesis focuses on the non-heuristic algorithms for the definition of optimal management criteria of complex energy networks. In particular, in Chapter 5 the mathematical model of a novel in-house developed software, called COMBO, which is able to address the nonlinearity of the scheduling problems by creating all the possible combinations of the energy systems loads and by evaluating each one of them, is presented along with its validation. To this respect, a residential energy network has been considered and analyzed by using the software COMBO and the results have been compared by the ones obtained from the analysis of the same case study with software EGO, namely a genetic algorithm. Finally in Chapter 6, the scheduling optimization of a case study carried-out with software COMBO, is presented. In this regard, a residential energy network has been investigated from both an energy and an economic point of view.

Acknowledgements

Nomenclature

Abbreviations

AB	Auxiliary Boiler
AC	Absorption Chiller
CC	Compression Chiller
CHP	Combined Heat and Power
DC	District Cooling
DCN	District Cooling Networks
DG	Distributed Generation
DGS	Distributed Generation System
DH	District Heating
DHN	District Heating Network
EES	Electrical Energy Storage
ESS	Energy Storage System
EGO	Energy Grid Optimizer
EV	Electric Vehicle
FA	Firefly Algorithm
FC	Fuel Cell
FF	Fitness Function
GA	Genetic Algorithm
GDH	Generation District Heating
HFC	HydroFluoroCarbons
HFE	HydroFluoroEthers
HP	Heat Pump
ICE	Internal Combustion Engine
ICT	Information and Communication Technology
IDN	Identification number of the Node
IDP	Identification number of the Pipe
IHENA	Intelligent Heat Network Analysis
LP	Linear Programming
MDO	Marine Diesel Oil
MGT	Micro Gas Turbine
MILP	Mixed Integer Linear Programming
MINLP	Mixed Integer Non Linear Programming
NZEB	Near Zero Energy Building
NZED	Near Zero Energy District
NG	Natural Gas
OF	Objective Function
ORC	Organic Rankine Cycle
P2G	Power To Gas
PHEV	Plug-in Hybrid Electric Vehicle
PM	Prime Mover
PSO	Particle Swarm Optimization
PV	Photovoltaic
RES	Renewable Energy Source
RG	Renewable Generator
SDC	Smart District Cooling
SDH	Smart District Heating
SDHN	Smart District Heating Network
SMES	Superconducting Magnetic Energy Storage
SNG	Synthetical Natural Gas
SNGN	Synthetical Natural Gas Network
ST	Solar Thermal
TES	Thermal Storage
V2G	Vehicle To Grid
WT	Wind Turbine
ZEB	Zero Energy Building

Symbols

C	Cost [€]
COP	Coefficient Of Performance [-]
ΔH	pressure losses [Pa]
D	diameter [m]
E	energy [kWh]
EER	Energy Efficiency Ratio [-]
f	drag coefficient
H	energy content of fluid [Pa]
ITER	iteration [-]
l	load [-]
L	length [m]
NC	number of combinations [-]
NPV	Net Present Value [€]
NS	number of systems
Q	thermal power
ROI	return of investment [y]
SC	system combinations [-]
T	temperature [°C]
U	global heat exchange coefficient [W/m^{2}K]

Greek symbols

α	convection coefficient [W/m^{2}K]
β	coeff. of concentrated pressure losses [-]
η	efficiency [-]
λ	conduction coefficient [W/mK]
ξ	specific cost [€/kW]
ρ	density [kg/m^3]
v	mean velocity [m/s]

Subscripts and superscripts

conc	concentrated
dis	distributed
disp	dissipated
e	electrical
E	electricity
ext	external
F	fictitious
in	at the inlet
ins	insulating
int	internal
L	low
M	maintenance
m	mean
max	maximum
min	minimum
opt	optimal
out	at the outlet
P	purchase
S	sale
th	thermal
u	user
UP	upper

1. Complex Energy Networks

A *complex energy network* can be defined as a network suitable for the production and/or distribution of electrical, thermal, cooling energies and fuel. Such networks represent a new challenge within the energy sector playing an important role for the achievement of the targets impose by the European and international policies related to environmental issues in order to reduce the greenhouse gases emissions associated to the employment of fossil fuels and to increase the energy conversion efficiency.

In particular, the main challenges related to the complex energy networks concern the definition of the optimal management criteria (such as the optimization of the energy systems scheduling) and the optimal energy systems design. Generally, these problems have been addressed by the researchers through the development and implementation of algorithms based on different mathematical methods.

In this context, in this chapter will be described the main distributed generation systems and technologies, the complex energy networks are presented, and the main algorithms adopted to address the aforementioned problem they have to face are presented.

1.1 Distributed generation and complex energy networks

One of the main reasons that led to the development of the complex energy networks is the emergence of the distributed generation systems (DGS). The increasing diffusion of the Distributed Generation Systems (*i.e.:* photovoltaic panels, wind turbine, energy storage devices, microturbines, etc.) due to the growing need of renewable energy sources exploitation and integration within the existing carbon-based energy production systems, along with the necessity of a great attention to the climate change and pollutant greenhouse gas emission due to the European targets related to this issue, led to a different paradigm for the energy production. In particular, over the years, the energy production paradigm shifted from a centralized generation – namely few huge power plants – to a growing deployment of distributed generation systems for the on-site production [1-3].

The employment of distributed generation systems, in fact, involves several advantages both from an economic and an operational point of view, such as a more flexibility of the network, the increase in the power quality and in the grid stability, the reduction of the energy losses due to the energy distribution, etc. [4,5]. Furthermore, the installation of a DGS at the user of a given network (regardless of whether it is electrical, thermal, cooling or natural gas) give the possibility of a bidirectional flow exchange between the network and the user itself. This involves a great participation of the users connected to the grid which can act both as producer – since the DGS provide to the fulfillment of the users itself and, in the event that the DGS production is greater that the user needs, it can feed the surplus into the energy network – ad as consumer – in the case of the DGS systems is not sufficient to supply all the user required energy – becoming *smart user* (or *prosumers*). An energy networks characterized by the aforementioned peculiarity is define as *smart energy network* [6-8].

On the other hand, the need to integrate such distributed generation system with the traditional fossil fuel-based generators led to an increase in the complexity of the existing grids both from the energy distribution and the network management points of view. This led to the so-called complex energy networks, namely the electrical thermal and cooling energies production and/or fuel distribution grids. As an example, a schematic representation of a complex energy network, is shown in Figure 1.1.
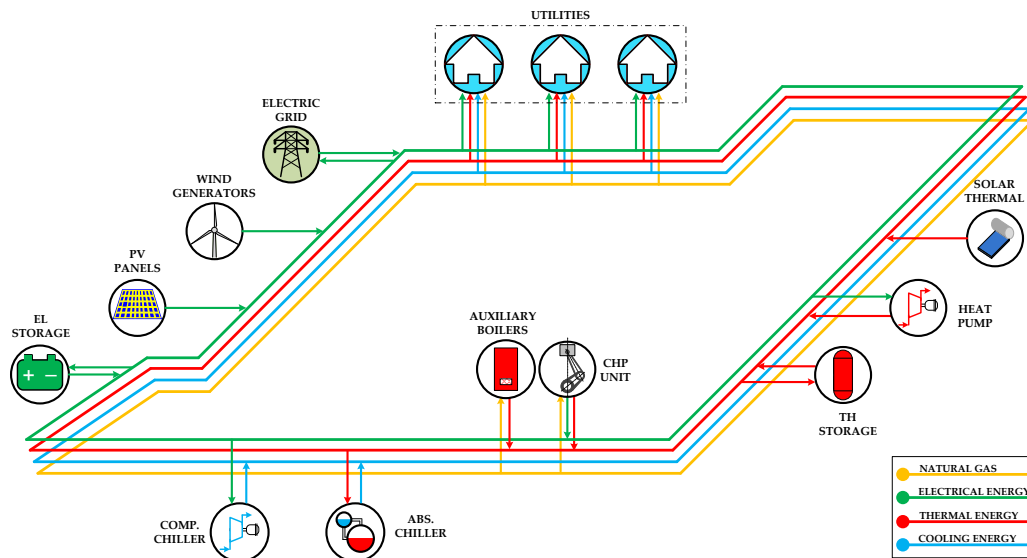

FIGURE 1.1: SCHEME OF A COMPLEX ENERGY NETWORK.

Before entering into the detail of the transition of the current energy grids into smart energy grid, the main distributed generation systems used within such networks are presented and described.

1.2 Distributed generation systems and innovative technologies for energy production

Within the complex energy networks, the distributed generation systems play an important role since they allow to decentralize the energy production. Different typology of DGS can be used to produce the electrical, thermal and cooling energy and fuel which can be introduced into the network for the users needs fulfilment.

To this respect, there are different technologies of DGS that can be adopted in the energy grid, for example the traditional generators such as the micro- turbines or the internal combustion engines, or the non-traditional generators such as the fuel cell. Furthermore, there are all those energy production systems which exploit the renewable energy sources such as the photovoltaic panels,

the solar panel, the wind turbines and so on. The latter, due to the non-programmability of the energy source, needs to be coupled with the energy storage devices to overcome these issues. In the following a briefly description of the main technologies used within the energy network are described.

Within the complex energy networks, the main available technologies for the distributed generation of electricity are: microturbines (MTG), internal combustion engines (ICEs), organic Rankine cycle (ORC), fuel cells (FC), photovoltaic panels (PV), wind turbines (WT), electrical energy storage devices (EES).

Microturbines

The microturbines are not a scale-down of the traditional gas turbines, but they are conceived as a new development for the energy production. Compared with the traditional gas turbines, the microturbines are characterized by limited compression rate values (typically in the range 3-5), a turbine inlet temperature lower than 900-950 °C and higher rotational speeds (50'000-120'000 rpm).

As for the maturity stage, the microturbines represent a well-established technology characterized by an electric power size lower than the traditional gas turbines, since they vary between 50 kWe and 200 kWe with an electrical efficiency up to about 30 %. Moreover, the higher rotational speeds, gives the possibility to be more flexible since they can vary depending on the load.

Another important aspect concerns the possibility to be employed as cogeneration topping cycle fort the combined production of electricity and heat by recovering the exhaust gases coming from the turbine since they are characterized by high temperatures in the range of 250-300 °C [9]. The use of microturbines as CHP units have higher cogenerative performances with a thermal efficiency that can reach a value up to 45-55 %.

As for the fuels, microturbines have originally design to be powered by the natural gas. However, several models can operate with different fuels such as fossil fuels (*i.e.:* liquefied petroleum gas, diesel, and kerosene) or renewable fuels (*i.e.:* biomass and biogas) [10].

One of the main advantages of the microturbines concerns the environmental impact since they are categorized as low emissions technology. In fact, with respect to the main pollutant emissions, they are characterized by a concentration of NO_x and CO emissions respectively lower that 15 ppm and 50 ppm. This implies the reduction of those efforts for the treatment of the exhaust gases. Another advantage concerns the limited dimensions and weight, and the low noise and vibration. Furthermore, the employment of the microturbines allows to obtain a greater reliability of operation, to use different fuels and the possibility of operating with partial load conditions. Finally, with respect to the economic aspect, the installation costs, as well as the maintenance costs are lower than other technologies.

Internal combustion engines

The internal combustion engines represent another well-established technology widely used within the complex energy networks frameworks for the electricity production [11].

As for the design electricity, this technology offers the possibility to be employed for different applications since they are available in a wide size range. In fact, they vary from small size, in the order of 1-5 kW of electric power (mainly used for residential application) to bigger size, in the order of the megawatt (around 10 MW) with an electrical efficiency that can reach high value up to 45 %.

The internal combustion engines can be categorized in two main operating cycles depending on the number of movements of the piston: the four-stroke cycle and the two-stroke cycle. In the case of cogenerative application, in which this technology can be used, the most employed cycle is the four-stroke one. The high temperature of the exhaust gases, which are equal to about 350-450 °C, in fact, make these systems very suitable for cogenerative applications.

Also as it concerns the fuel to be used, the internal combustion engines have a great flexibility. To this respect, the main employed fuels include gasoline, diesel, liquefied petroleum gas and natural gas, as for fossil fuels, hydrogen, acetylene, ethanol and biofuels as alternative fuels [12].

Among the different advantages, the internal combustion engines offer the possibility of a wide size range which make them suitable for different applications and a good flexibility of operation. Furthermore, it is a consolidate technology with a high reliability and great conversion efficiency also characterized by limited installation costs.

Organic Rankine cycle

The organic Rankine cycle (ORC) is a steam cycles using an organic fluid instead of water for their operation which can be used within the energy grid as distributed generation system [13]. To this respect, the ORCs are used for the energy production from solid biomass or using the waste heat from industrial process or from prime movers.

The ORC performances depend on the temperature of the thermal source and on the selected working fluid. As for the size, these systems vary from 30 kW to 1˙500 kW and allows to reach an electric efficiency around 18-20 %.

Furthermore, this technology is suitable to be coupled with other systems for the combines heat and power production. To this respect, in cogenerative applications, they allow to reach a thermal efficiency equal to about 75-80 %.

As for the organic fluids, they allow to exploit low temperature sources (in the range of 100-400 °C), low vaporization pressures, also in condition close to the critical ones and to obtain systems with small dimensions compared to the ones operating with water steam.

Fuel cells

Fuel cells are electrochemical systems able to convert the chemical energy of the fuel in electricity without a combustion process. In general, they use hydrogen as fuel but in some applications also natural gas converted into hydrogen can be used [14].

As for the maturity stage, fuel cells are an emerging technology that allows to obtain high electrical efficiencies also with smaller sizes. Typically, the size of these systems ranges between 5 W to 10 MW.

Depending on the nature of the electrolyte, the fuel cells are classified in:

- alkaline fuel cells;
- polymer membrane fuel cells;
- phosphoric acid fuel cells;
- fused carbonate fuel cells;
- direct methanol fuel cells.

These configurations are characterized by different working temperature which vary from 50 °C to 900 °C.

As for the previous technologies, the fuel cells can be used in cogenerative arrangement. To this respect, the electrical efficiency is characterized by high values, for example, in the case of hydrogen, the electrical efficiency ranges between 40-45 % for low temperature fuel cells and between 48-50 % in the case of high temperature fuel cells.

Photovoltaic panels

The photovoltaic panels are widely use within the complex energy networks for the electricity production from solar energy since they allow to exploit the energy coming from the solar radiation and converted it into electricity. For this reason, the photovoltaic panel represents a green technology for the electricity production. They can be installed both on the rooftop of a building for the self-consumption or to feed the electric grid.

The main typology of photovoltaic panel used in the energy networks are:

- monocrystalline and polycrystalline silicon photovoltaic cells;
- thin film photovoltaic cells (2nd generation);
- 3rd generation photovoltaic cells.

The monocrystalline PV are characterized by a purity level of silicon higher than the polycrystalline ones and are characterized by higher efficiency ranging between 14 % and 18 % compared to the ones of the polycrystalline PV which range between 12 % and 14 %.

The thin film PV represent an alternative to the use of the previous typology of PV since they are developed with the use of amorphous silicon. This technology is characterized by a lower efficiency compared to the crystalline one, equal to about 5-7 %.

The third generation of PV has been developed with the main purpose of taking advantages of the chemical-organic materials used for their realization. To this generation belong all those PV such as the organic photovoltaic, whose efficiency has been arisen up to a value equal to about 6 % and the luminescent solar concentrators, characterized by an efficiency around 7 % [15].

The main issue related to the photovoltaic panels is the non-programmability of the energy source which involves a non-continuous electricity production. However, this problem can be overcome by use electrical storage devices which allows to store the exceeding energy to use it when required.

Wind turbines

Wind turbines are another renewable technology installed within the energy networks for the distributed generation of electricity by eliminating the pollutant emissions such as NO_x, CO_2 and SO_x. The two main typologies of this technology are classified in vertical axis turbines and horizontal axis turbines.

As for the size of such energy systems ranges from few kilowatts (1-5 kW), typically used in residential applications or small wind plants, to few megawatts (about 5-10 MW), in the case of large-scale offshore wind farm.

As for the efficiency of these technologies, besides the theoretical Betz limits, they can reach an effective efficiency equal to about 35-40 % which can increase up to 50 % in the case of peak wind.

These systems are characterized by several advantages mainly from the environmental impact since they exploit the wind energy for electricity production. However, the installation of these technologies strongly depends on the condition of the site since they need a wind speed in the range of 3-25 m/s.

As well as the photovoltaic panels, the main problem related to the wind turbines technology is due to the non-programmability of the wind availability. Therefore, also this energy systems needs to be coupled with the electrical energy storage devices to guarantee a continuous electricity availability.

Electrical energy storage devices

The employment of the electrical storage devices within the complex energy networks has been increased as a consequence of the increasing diffusion of the distributed generation, especially the non-programmable renewable energy production systems such as the aforementioned photovoltaic panels and the wind turbines. The use of electrical storage devices within the energy network, in fac, allow to contribute to the stability and reliability of the grid and to overcome to the energy lack which can occur in the presence of non-programmable renewable generators.

In general, the electrical energy storage systems can be classified in (*i*) mechanical, (*ii*) electrochemical, (*iii*) electrical and (*iv*) chemical.

The mechanical storage devices include the pumped hydro storage, the compressed air energy storage and flywheel energy storage. These devices are mature technologies characterized by high efficiency (around 60-80 % the pumped hydro, about 70 % the compressed air systems). However, their use, in particular the pumped hydro and the compressed air devices, depended by the availability of the resource. Therefore, they can be considered only in those energy grid in which there are significant land for flooding or geological formations as storage reservoir.

The electrochemical storage technologies include the secondary and the flow batteries. To the first group belong the lead acid, Nickel-Cadmium, Li-ion, Nickel Metal Hydride and Sodium Sulphur batteries while the redox and hybrid batteries belong to the second group. All these devices are characterized by high efficiencies that, depending on the typology of the battery, can reach a value equal to 95 %. However, these devices are characterized by the limitation in terms of voltage and current that implies a series and/or parallel arrangement. In the field of the energy networks, these devices are widely use since, from the installation point of view, they can be easily installed both at the user side and along the network without any restriction.

The electrical storage devices include the capacitors and supercapacitors systems and the superconducting magnetic energy storage (SMES). The main advantages of these systems are the high lifecycles and the high efficiency which is equal to about 90 % in the case of capacitors and supercapacitors and about 98 % in the case of SMES. As for the complex energy networks, these devices are used within them, usually in hybrid arrangement combined with batteries.

The chemical energy storage systems include hydrogen and synthetical natural gas (SNG) which represents storable and transportable clean energy carrier characterized by high density. However, they involve high costs and energy losses during the single cycle. These technologies have been taken place in the energy networks fields since they allow to use the electricity surplus to be converted in hydrogen or SNG through specific process such as electrolysis or steam reforming for the hydrogen production, methanation or power to gas for the synthetic natural gas production that can be stored or introduced into the gas grid.

As it regards the distributed thermal power generation, in addition to the aforementioned microturbines, internal combustion engines, ORC and fuel cells, that can be used also for the combined heat and power generation, also the traditional auxiliary boilers (AB) and heat pump (HP) can be used within the energy networks as well as the renewable generators such as the solar thermal (ST) panels. Even in this case, thermal energy storage (TES) devices are used in the energy grid to store the exceeding energy and use it when required.

Auxiliary boilers

The auxiliary boilers represent a well-established technology widely used within the energy networks for the thermal power production. Among the different typology, the gas fired boilers are the most employed ones, mainly installed to support the thermal production coming from the cogenerative units. As for the performances of such devices, they are characterized by high efficiency around a value of 80 %.

Heat pumps

Heat pumps represent an alternative to the fossil fuel boilers for the decentralized production of thermal power. This technology is a mature technology widely used within the complex energy networks. As for the performances, these devices are characterized by a coefficient of performance between 3-6. The main advantages of the heat pumps consist in a lower electricity consumption compared to the traditional energy systems, lower maintenance costs and, from the environmental impact point of view, these devices avoid the use of the fossil fuels sine they are powered by electricity that can be also produced by renewable energy generators.

Solar thermal panels

The thermal solar panels are a mature technology which allows to produce thermal energy by exploit the solar energy. These renewable generators are widely diffuse within the energy networks for the distributed generation of thermal power. In fact, they are installed on the rooftop of each building to fulfill both the hot water and the space heating needs. This technology can be classified in: (*i*) low temperature, (*ii*) medium temperature and (*iii*) high temperature.

The low temperature devices are a mature and consolidate technology mainly used in residential application characterized by a temperature value up to 100 °C. The main typologies are flat plane collectors and the evacuated tube collectors. Both can be installed on the rooftop of the buildings. However, the evacuated tube collectors are characterized by a higher efficiency compared to the flat plane ones.

The medium temperature devices are characterized by an operating temperature from 100-150 °C to 350 °C. the main typologies are the compound parabolic concentrator and the mirror Fresnel collectors. This technology is mainly employed for industrial process applications.

The high temperature technologies allow to reach temperature also greater than 400 °C. these devices are mainly used in all those application for the electricity production of by a thermodynamic way.

The main advantages of this technology are the high efficiency, the renewable energy exploitation and the very low operating costs. However, they have high installation costs, low energy density and the non-programmability of the energy source.

Thermal energy storage devices

As for the electrical storage, the installation of the thermal energy storage devices within the energy grid is mainly used to overcome the non-programmability of the renewable energy sources and to store the thermal energy surplus to give it back when required. The main typologies of thermal storage systems are sensible heat, latent heat, and thermochemical.

The sensible heat thermal energy storage consists in the energy storage through the temperature variation of a liquid or solid medium without any phase change. The amount of energy stored is

proportional to the difference between the inlet and final temperature, to the mass and to the specific heat of the considered medium.

As it regards the latent heat thermal energy storage, it is based on the absorption and release of the heat during the phase change of the storage medium from solid to liquid or from liquid to gas and vice versa without significant temperature changes. For this reason, these materials are called phase change materials. This technology is a promising solution for the heat storage due to the high storage density and the small temperature variations.

The thermochemical energy storage is based on the absorption and released of energy during the breaking and formation of molecular bonds within a fully reversible chemical reaction. The amount of the heat that can be stored depends on the mass of the material and on the fraction of the converted reagents.

As it concerns the cooling power, the traditional energy systems used within the complex energy networks are the compression chillers (CC) and absorption chillers (AC). Actually, among the innovative energy systems, a new promising and green technology has been developed in recent years, the so-called magnetocaloric refrigerators.

The compression chillers are the most diffused and consolidate technology used for the cooling power production within the energy grids. Their operation required a certain amount of electricity to operate the compressor and use refrigerants such as hydrofluorocarbons (HFC) and hydrofluoroethers (HFE), that are characterized by a lower environmental impact compared to the already banned chlorofluorocarbons. With respect to the energy performances, these systems are characterized by an energy efficiency ratio in the range of 3.5-6. The two main typologies of compression chiller used within the energy networks are the chillers and the roof top. As it concerns the chillers, depending on the fluid used for compressor refrigeration, they can be divided in water chillers or air chiller. The size of the most used chillers varies between 100 kW to 500 kW. The main difference between chillers and roof tops lies in the fact that the latter use air on both the condenser and evaporator sides. Moreover, as it concerns the roof top chillers, depending on the size, they use a single hermetic reciprocating compressor with a single refrigerating circuit (size up to 30 kW); two hermetic compressors with two independent cooling circuits (size from 30 kW to 90 kW) or two semi-hermetic compressors using two independent cooling circuits (size over 90 kW).

The absorption chillers are more complex technologies compared to the compression ones but are suitable for cogenerative (and trigenerative) applications and, therefore, they are used within the complex energy networks. Differently from the compression chillers, the absorption chillers use a mixture of two fluid as refrigerants such as the most common water and ammonia or water and lithium-bromide. As it concerns the energy performance, the absorption chillers are characterized by an energy efficiency ratio lower than 1, typically ranges between 0.6-0.75.

The magnetocaloric refrigeration represents an environmentally friendly alternative to the compression chillers since they avoid the use of the traditional refrigerant fluid. Magnetic refrigeration is based on the magnetocaloric effect which has been discovered in 1881 by Warburg who observed that introducing an iron sample under a magnetic field, a temperature increase occurred, while removing the sample from the magnetic field, its temperature decreases [16-19].

Therefore, the magnetocaloric refrigeration is realized by using a varying magnetic field, a magnetocaloric material – such as gadolinium, gadolinium alloys or other typology of alloys – and a working fluid, such as water, water and glycol, helium and so on. This technology is still at the prototypal stage, only one device has been realized and commercialized in the world.

During the PhD, part of the research activities has been focused on the design and development of a magnetocaloric prototype [20]. Therefore, for reason of completeness, a detail description of the realized device is presented in Appendix A.

1.3 Energy grids transition into smart energy networks

The transition of the existing energy grids into smart networks have been taken place over the year and is still going on since, as aforementioned, they play an important role in the achievement of the European targets related to the pollutant and climate-change gas emission reduction. Therefore, a briefly description of the evolution of each energy grid – electrical, thermal, cooling and natural gas – is presented in order to better understand the main peculiarities of each one along with the main advantages they have entailed over the years.

Electricity networks

During the last decades the electricity demand has been increased mainly due to some factor such as the growth of the emerging economies, the challenges related to the environmental issue, and the improvement of the life quality [21]. According to the available data, this behavior is continuously growing (see Figure 1.2) and it has been expected that the global electricity demand will increase up to 57 % by 2050 [22,23].
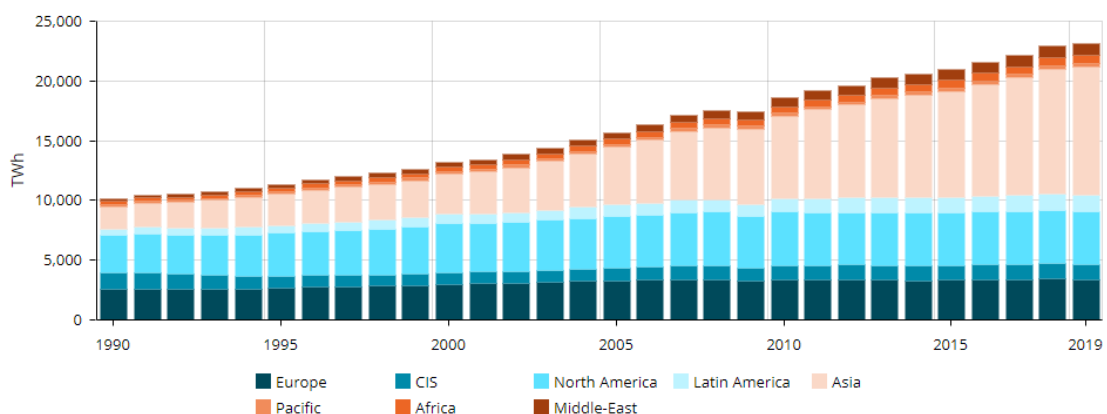
FIGURE 1.2: GLOBAL ELECTRICITY CONSUMPTION [22].

This involves some challenges from the electricity production and distribution viewpoints, leading to a growing complexity of the existing grids by increasing the needs of a major reliability, efficiency, security and issue related to the environmental and energy sustainability [24]. Thus, result in the development of the concept of *smart grid* which can be defined as an electricity network allowing a two-way flow of electrical energy and data – supported by the digital communications technologies – between the electric grid and the users connected to it [25].

By entering into the detail of the *smart grid*, it has to be pointed out that there isn't a univocal definition, however, the concept at the basis of its definition lies in the integration of distributed generation systems installed at the user for the electricity production which provide to the user partial or total fulfillment, allowing bidirectional energy fluxes between the electrical grid and the users connected to it. To this respect, an important role is covered by the Information and Communication Technologies (ICT) which are installed at any generation ad consumption point for the energy fluxes tracking [26-28]. As for the main distributed generation systems used within the smart grid, they include, for example, micro gas turbines, fuel cells, as well as generation systems based on renewable sources such as photovoltaic panels and wind turbines [29]. In addition, the smart grids are also integrated with energy storage systems (ESS) to face both the non-programmability of the renewable energy sources and the floating electricity demand of the user, by collecting the surplus of energy and introducing it into the grid when required, thus ensuring a continuing of electricity supply [30,31]. The transition to the smart grid paradigm involves a series of advantages such as the improvement electricity transmission, the increase on the grid security and reliability thanks also to the ESS, as well as a more flexibility of the networks.

However, the transition from the traditional electrical energy network to the smart grid is a long process which has been developed during the years. In fact, the development of the first electricity grids, dates back to the end of 19th century. In particular, in 1882 Thomas Edison opened the first steam electrical power station in New York. This station was used to supply electricity to about sixty different customers located near the power station. Later in the years, thanks to the development of infrastructure for the electricity distribution, the electricity supply companies developed central power stations to take advantage of economies of scale and moved to centralized power generation, distribution, and system management. In the early 21th century dates back the commercialization of the electric power when, the rapid growth of the electricity demand led to the development of an effective distribution system. At first, the energy supply to local industrial plants and private communities was made by small utility companies. Therefore, for reasons of a greater efficiency and distribution, the electricity utility companies began to share their resources and transmission lines creating the electrical networks.

In general, the traditional electricity networks were generally used to distribute the electricity produced by the central power station to a large number of users or customers. Hence, this paradigm was characterized by a centralized unidirectional system for the electricity generation, transmission and distribution from the power plant to the end users. Only during the recent years, with the diffusion of renewable based systems as well as the increase on the electrical energy demand, the existing electricity networks evolved towards a new electricity generation paradigm with a more distributed generation systems employment [24].

A further improvement in the smart grid development concerns the electric vehicle. With the electrification of the transportation sector occurring in the last few years, indeed, the smart grid has been further improved by including the plug-in hybrid electric vehicles (PHEVs) or electric vehicles

(EVs). This results in the so-called Vehicle to grid (V2G) concept which involves the use of the electric vehicles within the smart grid with the main aim of improving the power system operations. The V2G allows a bidirectional electricity flow exchange between an electric car (or an electric battery) and the smart grid. In fact, the electric vehicles can be as an electrical storage device able to store the low peak produced energy and return any exceeding quantity to the grid [32,33]. The introduction of EVs within a smart grid implies some efforts both from economic and operational viewpoints such as actions on the existing infrastructure and therefore high installation costs. On the other hand, the EVs technology can provide ancillary services – such as peak power shaving, voltage and frequency regulation etc. – whenever needed [34].

The integration of electrical vehicles within the smart grid represents a great potential for the smart grid development. The V2G implementation, indeed, can provide the frequency regulation as well as recover the power system failure during in case of blackout. The use of the V2G technology can involves different advantages such as the supply of the power from the EV to the grid for the auxiliary services, the use of the surplus energy to provide active power support to the grid, the reactive power compensation for the voltage regulation, etc. involving also a major flexibility of the grid [35-37].

However, on the other hand, the vehicle to grid technology led to some challenges also due to the non-maturity of the technology. For example, the continuous charging and discharging phases can led to a degradation of the battery, or even the high costs of investment which have to be supported to upgrade the current infrastructure to allow the use of EVs within the grids, as well as the social barriers [38,39].

District heating networks

As for the smart electric grid, even the district heating networks (DHNs) – namely the network suitable for the thermal power production and/or distribution from a thermal power station to an end user – have been developed over the years moving to the so-called _Smart District Heating_ (SDH).

The heating sector is play an important role since, according to the available data, in the European Union, it is responsible for about 50 % of the final energy demand contributing for about 40 % of the global CO_2 emissions [40]. Furthermore, with respect to the total heat production, about 46 % is used for the space heating and hot water needs fulfillment and about 50 % is used for the industrial process while the remaining percentage, indeed, is used in the agricultural sector [41].

In the heat supply, even if the fossil fuels continue to represent the most used fuels, renewables are covering a percentage equal to about 10 %. This percentage has been growth in the last few years and it is expected to further increase in the future, according to the European and international policies on this matter [41].

In this context, the establishment and diffusion of district heating network has been taken place in Europe as well as in the rest of the world. Nowadays, in the European Union, the district heating supplies about 30 % of the heat demand, 12 % of which is for domestic hot water and space heating in residential buildings [42]. Moreover, as it regards the enlargement of such networks, the total operating district heating pipelines has increased in the recent years as is shown in Figure 1.3 [43].
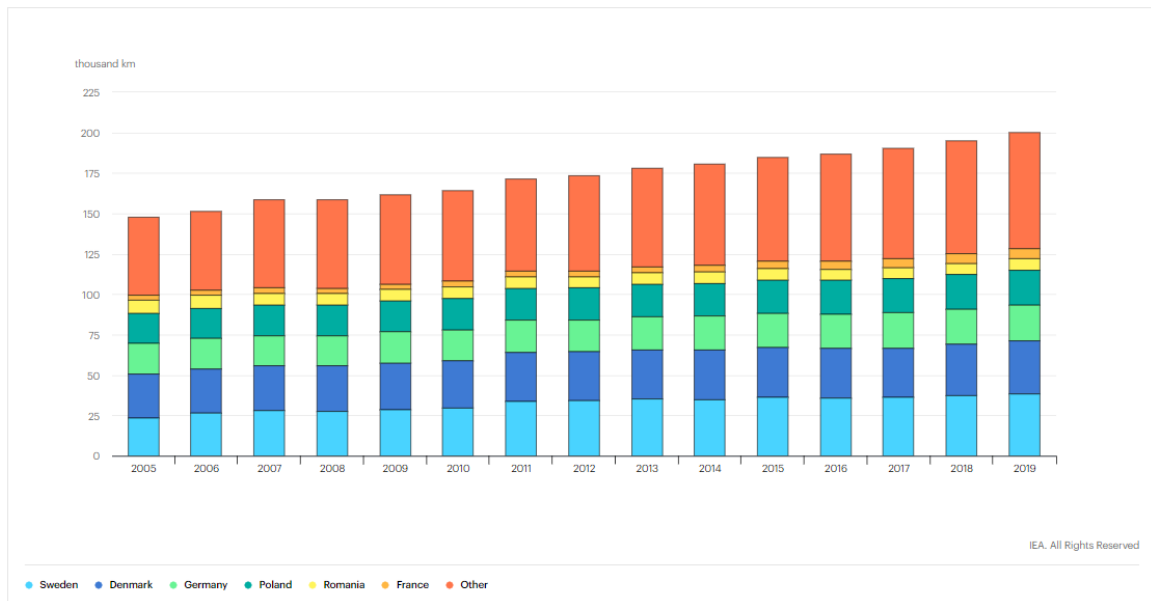
FIGURE 1

FIGURE 1.3: TOTAL OPERATING DISTRICT HEAT PIPELINES IN EUROPE, 2005-2019 [43].

The traditional district heating networks are characterized by a centralized power stations that produced the thermal power to fulfill the hot water and/or space heating needs of the user connected to heat. However, these networks have been evolved during the years towards a smart paradigm. In particular, the evolution of the DHNs can be categorized into five different generations [44-49].

The first generation district heating (1GDH), introduced for the first time in 1880s in the USA, is characterized by the use of pressurized steam, mainly coming from steam power plant or from boilers, as carrier fluid. Due to its high heat content (*i.e.:* the large enthalpy content), steam was considered a good transportation media. On the other hand, the high temperature of the steam-based DH, higher than 200 °C, can incur into network reliability and safety problems – such as corrosion and condensation or even explosion – as well as heat losses along the pipeline. In 1930, the second generation district heating was developed (2GDH) using pressurized hot water as carrier fluid. The use of water at a temperature above 100 °C, allowed to achieve some advantages in terms of increase in energy efficiency, increase in the reliability and safety of heat supply, reduction of the risk characterizing the first generation.

The development of the third generation district heating (3GDH) dates back to 1970 even if the first application was in 1980. Likewise, the second generation, even the 3GDH use hot water as transportation media, but operated at temperatures lower than 100 °C. Compared to the 2GDH, the development of 3GDH led to different advantages such as the reduction of the heat losses due to the lower temperature, the improvement of the network efficiency as well as the increase of the reliability, security and more flexibility.

The transition to the fourth generation district heating (4GDH) took place in the recent years with the main aim of integrating renewable energy sources, reducing the specific energy consumption in

buildings and improve the energy efficiency of the systems. To this purpose, in the 4GDH the temperature of the pressurized water reduces at a value around 50 -60 °C.

In recent years the district heating is moving to the fifth generation (5GDH) which is characterized by lower temperature of the carrier fluid which is reduced up to 15-20 °C. This peculiarity allows to further decrease the heat losses along the DH pipeline and to further increase the efficiency of the system.

Furthermore, the lats generation – which are also called low temperature district heating – encourages the so-called Smart District Heating (SDH), which consist in the possibility of bidirectionality of the energy transfer of the fluid between the district heating and the users connected to it. As a consequence, the user become *prosumer* (or *smart user*) since they act both as consumers and as producer.

District cooling networks

In European Union, cooling in buildings and industry accounts, together with heating, for about 50 % of the total final energy demand [50]. According to the available data, the energy demand for space cooling has been increase in the last few decades representing nowadays about 3 % of the total energy demand of heat and cooling [50-51]. Furthermore, since the largest part of the energy used in this sector is produced by the employment of non-renewable energy sources, it results in the contribution of CO_2 emissions.

In this context, in the same way as district heating networks, district cooling networks (DCNs) have started to develop and spread both in Europe Union and in other countries in the rest of the world within the main aim of providing cooling power in a more efficient and sustainable way. However, differently the development of district cooling networks is more recent compared to the development of the district heating ones.

District cooling (DC) is the centralized production of chilled water and its distribution to the end users for the fulfillment of the cooling need. This technology allows to replace the individual chillers installed at the user side and, consequently, to reduce the electricity consumption associated to it. Furthermore, it allows the integration of renewable generators with the fossil fuels-based energy systems.

As for the district heating, even district cooling has been evolved during the years towards the smart district cooling (SDC) paradigm [52].

The firsts district cooling networks have been introduced approximately at the end of the 19th century consisting of a central chiller plant which supply the cooling energy to the decentralized end users through a closed-loop pipeline. Such networks were characterized by the employment of mechanical chillers in the power plant and the use of cold water as carrier fluid.

Therefore, in the 1990s, in consequence of the Montreal protocol which have banned the use of the CFC refrigerants, a new generation of district cooling has been developed which included not only the mechanical chillers (with or without heat recovery) for the cooling energy production but also other devises such as absorption chillers, cooling energy storages devices, and so on.

The adoption of district cooling involves different advantages from different viewpoints. For example, from an economic point of view, it involves a reduction in the maintenance costs with respect to the use of the traditional systems for the air conditioning, as well as the reduction of the operating costs such as the one associated to the purchase of electricity due to a lower consumption of it. From an energy point of view, the district heating involves both the efficiency and the reliability increase and a more flexibility of air-conditioning loads with a longer lifetime of the power plant. Furthermore, it allows to significantly reduce the CO_2 emissions (up to 80 %) due to the increasing exploitation of renewable energy sources within the network.

However, there are few disadvantages associated to the district cooling networks mainly consisting in the higher capital cost of installation (compared with the costs associated to the installation of the chillers at each building). Moreover, this technology is characterized by the consumption of a great amount of water incurring, in some cases, in the availability problems.

Natural gas networks

The global consumption of natural gas (NG) is continuously increasing. In 2018, the NG consumption accounted for about 1˙611 Mtoe, mainly due to its employment in the residential and the industry sectors, representing respectively a percentage equal to about 29.9 % and 37 % of the total final consumption according to the scheme of Figure 1.4 [53].
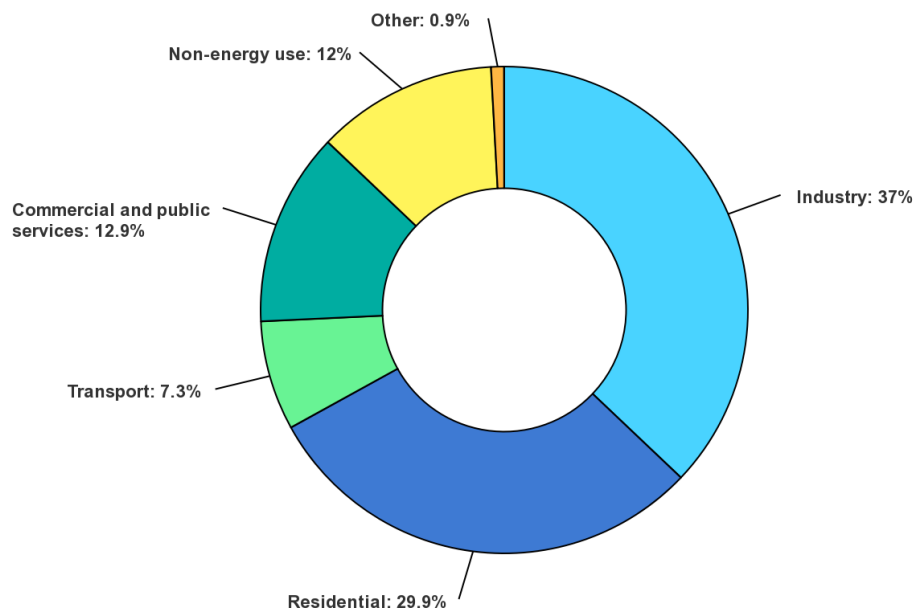
FIGURE 1.4: WORLD NATURAL GAS FINAL CONSUMPTION BY SECTOR [53].

The main issue related to the use of natural gas mainly consists in the greenhouses emission coming from its combustion, even if they are significantly lower than the ones resulting from the other fossil fuels. Moreover, in addition to the availability of the stock issues, the extraction and distribution of natural gas involves also problems associated to the environmental impact mainly due to the uncontrolled gas dissipations and/or the water and gasoline leakages which can be settle on the bottom of the pipelines.

In this context, the natural networks (NGNs) grids play an important role for the achievement of the greenhouses gas emissions targets imposed by the European Union, as well as other international countries, to face the climate change. This also reflect in the complex energy networks in which the distribution of the natural gas represents a great contribute since it is used to the direct use of the end user fort the fulfillment of its need or also to power the energy systems (auxiliary boilers and/or CHP units).

This led to a transition of the traditional natural gas networks into a smart paradigm. To this respect it has to be underlined that, differently from the aforementioned energy networks, the evolution of the gas grid into a smart network does not implies the presence of a distributed generation systems at each user of the grid but in a more decentralization of the energy production.

On the basis of the available literature, there is not a unique definition of *smart natural gas network* (SNGN) however, the main characteristics shared by the different definitions highlight that the smart gas grid is a network able to deal with the presence of non-conventional gases (for example hydrogen or biomethane which have a higher potential for the gas grid decarbonization) being a multi gas grid. Moreover, the smart gas grid is more flexible than the traditional one, being characterized by the presence of smart metering systems which also allow to reduce the operating as well as the management costs [54,55].

As aforementioned, the main peculiarities of the evolution of the traditional natural gas grid in smart networks consists in the decentralized production of the gas fuel and in the use of non-conventional gases. To this respect, within the complex energy grids the main decarbonized solutions are represented by the production, distribution and use of biomethane and hydrogen whose production also involves the exploitation of the renewable energy sources.

As for the biomethane, it is a low carbon gas deriving from the biogas through a refining and purification process whose methane concentration of CH_4 can exceed a percentage equal to 98 %. The characteristics of the biomethane are suitable to be introduced into the natural gas network pipelines.

As for the hydrogen, it can be produced through different process, for example the water electrolysis, which involves the use of electrical energy from renewable energy, or the steam reforming, namely a chemical transformation of the fossil fuels. Furthermore, it can be produced by the use of more recent technologies such as the so-called *Power to Gas* (P2G) systems which has been conceived in order to use the electricity surplus from non-programmable renewable energy sources to produce a green gas which can be therefore introduced into the natural gas network.

1.4 The role of smart energy networks

The evolution of the electrical, thermal, cooling, and natural gas grids into smart networks led to an increase in the complexity of such grids. In addition, thanks to a wide use of the information and communication technologies, the diffusion of the energy storage systems and the integration of the renewable energy sources, these infrastructures are currently undergoing a further transition towards a new paradigm which involves the integration between all these networks into a single *complex energy network*. Furthermore, this transition has been also extended to the current energy systems which have been evolved into *Smart Energy Systems*.

A *Smart Energy Systems* is conceived as an efficient, sustainable and safety systems characterized by the integration and coordination of the energy production systems, the infrastructures and the renewable energy sources by means of the energy services, user participation and the information and communication technologies. Therefore, the smart energy systems include both the aforementioned smart networks and the smart structures, namely the commercial or residential zero energy buildings (ZEBs) or near zero energy buildings (NZEBs), whose concept has been developed in recent years. According to the European directive, a nearly zero energy building is a structure in which the consumption of electrical, thermal and cooling consumption is very low and, in particular, quite equal to zero [56-58].

In this scenario arise the concept of the *Near Zero Energy District* (NZED) which represents, along with the aforementioned *prosumers*, one of the main the main stakeholders of this new paradigm. The near zero energy district extends the idea of the near zero energy principle characterizing the NZEB [59]. In detail, they represent a delimited portion of a city (or in any case an urban, industrial or rural area) characterized by a low energy demand mainly covered by the renewable source-based energy systems, and by a very high energy performance due to the energy efficiency improvement [60-61].

To this respect, one of the main challenges the research is facing today, consist in the energy district planning, management and diagnostics. This involves a decisional process aimed to optimize the design of the network (or of the energy district) and to find optimal criteria for its management [62]. In particular, the design optimization problem consists in the definition of the grid configuration in terms of number of energy systems, typology, size, number of energy storage devices, and so on. On the other hand, the network management consist in the optimization of its operational strategies (for example the energy systems scheduling optimization during the whole year of operation) [63-65]. However, both the design and the management optimization problems are aimed to achieve a twofold objective: one from the economic point of view – such as the minimization of the cost of energy production – and one from the energy point of view – as for example the reduction of the greenhouses gas emissions.

These processes are characterized by a high complexity due to multiple factors (such as the diversification of production systems, the presence of energy storage devices, the energy needs forecast, the dynamic demand, the presence of non-programmable renewable energy source generators, etc.) and for they represent a multi-objective problem [66].

This type of problem can be addressed by the implementation of different algorithms depending on the nature of the problem itself. To this respect, the main algorithm adopted for the design and/or management optimization will be presented.

1.5 Optimal design and management of the complex energy networks

As aforementioned, the design and the management optimization problem can be addressed by the development and implementation of different typology of algorithms which can be basically categorized as approximate or exact mathematical methods [67].

The approximate methods allow to face the nonlinearities of the objective function and of some constrains through the implementation of random search techniques providing a good solution of the problem with acceptable computational time [68,69]. The approximate methods include both the heuristic – such as the constructive and the local search algorithms – and the metaheuristic methods – such as the trajectory and the population-based algorithms [70-72]. Within the complex energy networks optimization, the main heuristic methods are represented by the *Genetic Algorithms* (GA) and by the *Firefly Algorithms* (FA) while the main implemented metaheuristic methods is the *Particle Swarm Optimization* (PSO). The basis of the *Genetic Algorithms* – which are widely used in the complex energy network optimization – consist in the genetic rules of the population evolution. This type of algorithms allows to find a good-quality solution by maintaining, at the same time, the non-linearity of the problem [73-75]. On the other hand, the *Firefly Algorithms* have been developed more recently compared to the genetic ones. Anyway, the FA represents a population-based technique which use a swarm intelligent approach for the research of the optimal solution of the problem [76]. As it concerns the *Particle Swarm Optimization*, instead, is a simple resolution method, whose development is based on the swarm behavior, that allows to find a good solution of the problem with a limited computational time and maintaining the nonlinearity of some constrain [77].

As it concerns the exact resolution methods, differently from the approximate methods, they allow to find the optimal solution (namely the exact solution) of the problems. However, in the event of the problem is characterized by a high complexity, its resolution will take a long computational time. The main algorithms belonging to this category are the enumerative algorithms, the branch and bound technique [78] and the linear programming (LP) [79]. Others resolution methods included into the exact resolution methods are the Mixed Integer Linear Programming (MILP) and Mixed Integer Non Linear Programming (MINLP) problems. In more detail, the MILP problems allow to find the exact solution, however, the nonlinearities of the problem are lost since they are defined by linear functions and discrete variables. [80,81]. With respect to the MINLP problems, instead, they are more complex methods with higher computational time, but they allow to find the exact solution by maintaining the nonlinearity of the problem [82,83].

As aforementioned, these algorithms are used within the complex energy networks planning process to address both the design and the management optimization problems. To this respect, the most suitable algorithms used for the resolution of the load allocation problem are the *genetic algorithms* [84] and the *firefly algorithms* [85] for what concern the approximated methods, and the MILP [86] for what concern the exact method. As it concerns the MINLP problems, they are considered an interesting resolution method for the optimization of the energy network management, but further efforts will be made to maintain the non-linearity nature of such problems and, at the same time, to reduce the computational time which is still too long for this kind of analysis. On the other side, as it regards the problem of energy network design optimization, it can be addressed by the implementation of *genetic algorithms* [87] or *particle swarm optimization* [88] as it concerns the

approximated methods. Otherwise, the most suitable exact methods for the resolution of this type of problems are both the MILP and MINLP methods [89,90].

References:

[1] Gharehpetian, G. B., & Agah, S. M. M. (Eds.). (2017). Distributed generation systems: design, operation and grid integration. Butterworth-Heinemann.

[2] Martín-Martínez, F., Sánchez-Miralles, A., Rivier, M., & Calvillo, C. F. (2017). Centralized vs distributed generation. A model to assess the relevance of some thermal and electric factors. Application to the Spanish case study. Energy, 134, 850-863.

[3] Strachan, N., & Farrell, A. (2006). Emissions from distributed vs. centralized generation: The importance of system performance. Energy Policy, 34(17), 2677-2689.

[4] Leithon, J., Werner, S., & Koivunen, V. (2020). Cost-aware renewable energy management: Centralized vs. distributed generation. Renewable Energy, 147, 1164-1179.

[5] El-Khattam, W., & Salama, M. M. (2004). Distributed generation technologies, definitions and benefits. Electric power systems research, 71(2), 119-128.

[6] Richter, A., van der Laan, E., Ketter, W., & Valogianni, K. (2012, December). Transitioning from the traditional to the smart grid: Lessons learned from closed-loop supply chains. In 2012 International Conference on Smart Grid Technology, Economics and Policies (SG-TEP) (pp. 1-7). IEEE.

[7] Ancona, M. A., Branchini, L., De Pascale, A., & Melino, F. (2015). Smart district heating: Distributed generation systems' effects on the network. Energy Procedia, 75, 1208-1213.

[8] Galatoulas, F., Frere, M., & Ioakimidis, C. S. (2018, March). An Overview of Renewable Smart District Heating and Cooling Applications with Thermal Storage in Europe. In SMARTGREENS (pp. 311-319).

[9] Noroozian, R., Asgharian, P., Gharehpetian, G. B., & Agah, S. M. (2017). Microturbine generation power systems. In Distributed Generation Systems (pp. 149-219). Butterworth-Heinemann.

[10] Lefebvre, A. H., & Ballal, D. R. (2010). Gas turbine combustion: alternative fuels and emissions. CRC press.

[11] Milewski, J., Szabłowski, Ł., & Kuta, J. (2012). Control strategy for an internal combustion engine fuelled by natural gas operating in distributed generation. Energy Procedia, 14, 1478-1483.

[12] Bae, C., & Kim, J. (2017). Alternative fuels for internal combustion engines. Proceedings of the Combustion Institute, 36(3), 3389-3413.

[13] Orosz, M., Quoilin, S., & Hemond, H. (2010). SORCE: A design tool for solar organic Rankine cycle systems in distributed generation applications.

[14] O'hayre, R., Cha, S. W., Colella, W., & Prinz, F. B. (2016). Fuel cell fundamentals. John Wiley & Sons.

[15] Castagna, D. (2014). il sole come fonte di energia: impianti fotovoltaici.

[16] A. Kitanovski and P. W. Egolf, "Thermodynamics of magnetic refrigeration," International Journal of Refrigeration, vol. 29, no. 1, pp. 3–21, 2006.

[17] V. K. Pecharsky and K. A. Gschneidner Jr, "Magnetocaloric effect and magnetic refrigeration," Journal of Magnetism and Magnetic Materials, vol. 200, no. 1, pp. 44–56, 1999.

[18] A. M. Aliev et al., "Magnetocaloric effect in some magnetic materials in alternating magnetic fields up to 22 hz," Journal of Alloys and Compounds, vol. 676, pp. 601–605, 2016.

[19] F. Shir, L. H. Bennett, E. Della Torre, C. Mavriplis, and R. D. Shull, "Transient response in magnetocaloric regeneration," IEEE transactions on magnetics, vol. 41, no. 6, pp. 2129–2133, 2005.

[20] Albertini, F., Bennati, C., Bianchi, M., Branchini, L., Cugini, F., De Pascale, A., ... & Rosati, J. (2017). Preliminary investigation on a rotary magnetocaloric refrigerator prototype. Energy Procedia, 142, 1288-1293.

[21] Aslam, S., Khalid, A., & Javaid, N. (2020). Towards efficient energy management in smart grids considering microgrids with day-ahead energy forecasting. Electric Power Systems Research, 182, 106232.

[22] https://yearbook.enerdata.net/

[23] IEA (2018), World Energy Outlook 2018, IEA, Paris https://www.iea.org/reports/world-energy-outlook-2018

[24] Butt, O. M., Zulqarnain, M., & Butt, T. M. (2020). Recent advancement in smart grid technology: Future prospects in the electrical power network. Ain Shams Engineering Journal.

[25] Bayod-Rújula, A. A. (2009). Future development of the electricity systems with distributed generation. Energy, 34(3), 377-383.

[26] Shabanzadeh, M., & Moghaddam, M. P. (2013, November). What is the smart grid? definitions, perspectives, and ultimate goals. In 28th International Power System Conference (PSC).

[27] El-Hawary, M. E. (2014). The smart grid—state-of-the-art and future trends. Electric Power Components and Systems, 42(3-4), 239-250.

[28] Specht, M., Rohjans, S., Trefke, J., Uslar, M., & González, J. M. (2013). International smart grid roadmaps and their assessment. EAI Endorsed Transactions on Energy Web, 1(1).

[29] Nur Asyik, H., Blagojce, S., & Akhtar, K. (2011). Analysis of distributed generation systems, smart grid technologies and future motivators influencing change in the electricity sector. Smart Grid and Renewable Energy, 2011.

[30] Nguyen, H. K., Song, J. B., & Han, Z. (2014). Distributed demand side management with energy storage in smart grid. IEEE Transactions on Parallel and Distributed Systems, 26(12), 3346-3357.

[31] Roberts, B. P., & Sandberg, C. (2011). The role of energy storage in development of smart grids. Proceedings of the IEEE, 99(6), 1139-1144.

[32] Mwasilu, F., Justo, J. J., Kim, E. K., Do, T. D., & Jung, J. W. (2014). Electric vehicles and smart grid interaction: A review on vehicle to grid and renewable energy sources integration. Renewable and sustainable energy reviews, 34, 501-516.

[33] Tan, K. M., Ramachandaramurthy, V. K., & Yong, J. Y. (2016). Integration of electric vehicles in smart grid: A review on vehicle to grid technologies and optimization techniques. Renewable and Sustainable Energy Reviews, 53, 720-732.

[34] Ehsani, M., Falahi, M., & Lotfifard, S. (2012). Vehicle to grid services: Potential and applications. Energies, 5(10), 4076-4090.

[35] Tan, K. M., Ramachandaramurthy, V. K., & Yong, J. Y. (2016). Integration of electric vehicles in smart grid: A review on vehicle to grid technologies and optimization techniques. Renewable and Sustainable Energy Reviews, 53, 720-732.

[36] Srivastava, A. K., Annabathina, B., & Kamalasadan, S. (2010). The challenges and policy options for integrating plug-in hybrid electric vehicle into the electric grid. The Electricity Journal, 23(3), 83-91.

[37] Wang, Z., & Wang, S. (2013). Grid power peak shaving and valley filling using vehicle-to-grid systems. IEEE Transactions on power delivery, 28(3), 1822-1829.

[38] Silvestre, C., Sousa, D. M., & Roque, A. (2012, October). Reactive power compensation using on board stored energy in Electric Vehicles. In IECON 2012-38th Annual Conference on IEEE Industrial Electronics Society (pp. 5227-5232). IEEE.

[39] Peterson, S. B., Apt, J., & Whitacre, J. F. (2010). Lithium-ion battery cell degradation resulting from realistic vehicle and vehicle-to-grid utilization. Journal of Power Sources, 195(8), 2385-2392.

[40] Dehaghani, E. S., & Williamson, S. S. (2012, June). On the inefficiency of vehicle-to-grid (V2G) power flow: Potential barriers and possible research directions. In 2012 IEEE Transportation Electrification Conference and Expo (ITEC) (pp. 1-5). IEEE.

[41] Kozarcanin, S., Andresen, G. B., & Staffell, I. (2019). Estimating country-specific space heating threshold temperatures from national gas and electricity consumption data. Energy and Buildings, 199, 368-380.

[42] IEA (2019), Renewables 2019, IEA, Paris https://www.iea.org/reports/renewables-2019

[43] Paardekooper, S., Søgaard Lund, R., Vad Mathiesen, B., Chang, M., Petersen, U. R., Grundahl, L., & Bertelsen, N. (2018). Heat Roadmap Europe 4: Quantifying the Impact of Low-Carbon Heating and Cooling Roadmaps: Deliverable 6.4.

[44] IEA, Total operating district heat pipelines in Europe, 2005-2019, IEA, Paris https://www.iea.org/data-and-statistics/charts/total-operating-district-heat-pipelines-in-europe-2005-2019

[45] Lund, H., Möller, B., Mathiesen, B. V., & Dyrelund, A. (2010). The role of district heating in future renewable energy systems. Energy, 35(3), 1381-1390.

[46] Thorsen, J. E., Lund, H., & Mathiesen, B. V. (2018). Progression of district heating–1st to 4th generation.

[47] Buffa, S., Cozzini, M., D'Antoni, M., Baratieri, M., & Fedrizzi, R. (2019). 5th generation district heating and cooling systems: A review of existing cases in Europe. Renewable and Sustainable Energy Reviews, 104, 504-522.

[48] von Rhein, J., Henze, G. P., Long, N., & Fu, Y. (2019). Development of a topology analysis tool for fifth-generation district heating and cooling networks. Energy conversion and management, 196, 705-716.

[49] Li, H., & Wang, S. J. (2014). Challenges in smart low-temperature district heating development. Energy Procedia, 61, 1472-1475.

[50] Lund, H., Werner, S., Wiltshire, R., Svendsen, S., Thorsen, J. E., Hvelplund, F., & Mathiesen, B. V. (2014). 4th Generation District Heating (4GDH): Integrating smart thermal grids into future sustainable energy systems. Energy, 68, 1-11.

[51] Möller, B., Wiechers, E., Persson, U., Grundahl, L., & Connolly, D. (2018). Heat Roadmap Europe: Identifying local heat demand and supply areas with a European thermal atlas. Energy, 158, 281-292.

[52] IEA (2020), Cooling, IEA, Paris https://www.iea.org/reports/cooling

[53] Werner, S. (2013). District heating and cooling.

[54] IEA, World natural gas final consumption by sector, 2018, IEA, Paris https://www.iea.org/data-and-statistics/charts/world-natural-gas-final-consumption-by-sector-2018

[55] Crisostomi, E., Raugi, M., Franco, A., & Giunta, G. (2013, October). The smart gas grid: State of the art and perspectives. In IEEE PES ISGT Europe 2013 (pp. 1-5). IEEE.

[56] Speirs, J., Balcombe, P., Johnson, E., Martin, J., Brandon, N., & Hawkes, A. (2018). A greener gas grid: What are the options. Energy Policy, 118, 291-297.

[57] D'Agostino, D., & Mazzarella, L. (2019). What is a Nearly zero energy building? Overview, implementation and comparison of definitions. Journal of Building Engineering, 21, 200-212.

[58] Marszal, A. J., Heiselberg, P., Bourrelle, J. S., Musall, E., Voss, K., Sartori, I., & Napolitano, A. (2011). Zero Energy Building–A review of definitions and calculation methodologies. Energy and buildings, 43(4), 971-979.

[59] Torcellini, P., Pless, S., Deru, M., & Crawley, D. (2006). Zero energy buildings: a critical look at the definition (No. NREL/CP-550-39833). National Renewable Energy Lab.(NREL), Golden, CO (United States).

[60] Amaral, A. R., Rodrigues, E., Gaspar, A. R., & Gomes, Á. (2018). Review on performance aspects of nearly zero-energy districts. Sustainable cities and society, 43, 406-420.

[61] Recast, E. P. B. D. (2010). Directive 2010/31/EU of the European Parliament and of the Council of 19 May 2010 on the energy performance of buildings (recast). Official Journal of the European Union, 18(06), 2010.

[62] Heendeniya, C. B., Sumper, A., & Eicker, U. (2020). The multi-energy system co-planning of nearly zero-energy districts–Status-quo and future research potential. Applied Energy, 267, 114953.

[63] Di Somma, M., Yan, B., Bianco, N., Graditi, G., Luh, P. B., Mongibello, L., & Naso, V. (2015). Operation optimization of a distributed energy system considering energy costs and exergy efficiency. Energy Conversion and Management, 103, 739-751.

[64] HA, M. P., Huy, P. D., & Ramachandaramurthy, V. K. (2017). A review of the optimal allocation of distributed generation: Objectives, constraints, methods, and algorithms. Renewable and Sustainable Energy Reviews, 75, 293-312.

[65] Luo, P., Wang, X., Jin, H., Li, Y., & Yang, X. (2018, December). Load management for multiple datacenters towards demand response in the smart grid integrating renewable energy. In Proceedings of the 2018 2nd International Conference on Computer Science and Artificial Intelligence (pp. 140-144).

[66] Marah, R., & El Hibaoui, A. (2018). Algorithms for smart grid management. Sustainable cities and society, 38, 627-635.

[67] Di Somma, M., Yan, B., Bianco, N., Luh, P. B., Graditi, G., Mongibello, L., & Naso, V. (2016). Multi-objective operation optimization of a Distributed Energy System for a large-scale utility customer. Applied Thermal Engineering, 101, 752-761.

[68] Festa, P. (2014, July). A brief introduction to exact, approximation, and heuristic algorithms for solving hard combinatorial optimization problems. In 2014 16th International Conference on Transparent Optical Networks (ICTON) (pp. 1-20). IEEE.

[69] Chen, Y. K., Wu, Y. C., Song, C. C., & Chen, Y. S. (2012). Design and implementation of energy management system with fuzzy control for DC microgrid systems. IEEE Transactions on power electronics, 28(4), 1563-1570.

[70] Lin, M. H., Tsai, J. F., & Yu, C. S. (2012). A review of deterministic optimization methods in engineering and management. Mathematical Problems in Engineering, 2012.

[71] Cooper, L. (1964). Heuristic methods for location-allocation problems. SIAM review, 6(1), 37-53.

[72] Javaid, N., Javaid, S., Abdul, W., Ahmed, I., Almogren, A., Alamri, A., & Niaz, I. A. (2017). A hybrid genetic wind driven heuristic optimization algorithm for demand side management in smart grid. Energies, 10(3), 319.

[73] Blum, C., & Roli, A. (2003). Metaheuristics in combinatorial optimization: Overview and conceptual comparison. ACM computing surveys (CSUR), 35(3), 268-308.

[74] Sivanandam, S. N., & Deepa, S. N. (2008). Genetic algorithms. In Introduction to genetic algorithms (pp. 15-37). Springer, Berlin, Heidelberg.

[75] Song, Y. H. (Ed.). (2013). Modern optimisation techniques in power systems (Vol. 20). Springer Science & Business Media.

[76] Yang, X. S. (2013). Multiobjective firefly algorithm for continuous optimization. Engineering with computers, 29(2), 175-184.

[77] Poli, R., Kennedy, J., & Blackwell, T. (2007). Particle swarm optimization. Swarm intelligence, 1(1), 33-57.

[78] Mitten, L.G. Branch-and-bound methods: General formulation and properties. Operations Research, 18(1) (1970) 24-34.

[79] Murty, K.G. (1983). Linear programming. Chichester.

[80] Arcuri, P., Florio, G., Fragiacomo, P. A mixed integer programming model for optimal design of trigeneration in a hospital complex. Energy, 32(8) (2007) 1430-1447.

[81] Polat, U., Gürtuna, F. A Review of Applications of Linear Programming and Mixed Integer Linear Programming in Energy Management: From Policy Makers/Producers to Consumers. European Journal of Engineering and Applied Sciences, 1(2) (2018) 84-89.

[82] Marzband, M., Sumper, A., Domínguez-García, J. L., Gumara-Ferret, R. Experimental validation of a real time energy management system for microgrids in islanded mode using a local day-ahead electricity market and MINLP. Energy Conversion and Management, 76 (2013) 314-322.

[83] Alipour, M., Zare, K., Abapour, M. MINLP probabilistic scheduling model for demand response programs integrated energy hubs. IEEE Transactions on Industrial Informatics, 14(1) (2017) 79-88.

[84] Miranda, V., Ranito, J. V., & Proenca, L. M. (1994). Genetic algorithms in optimal multistage distribution network planning. IEEE Transactions on Power Systems, 9(4), 1927-1933.

[85] Chaurasia, G.S., Singh, A.K., Agrawal, S., Sharma, N.K. A meta-heuristic firefly algorithm based smart control strategy and analysis of a grid connected hybrid photovoltaic/wind distributed generation system. Solar Energy, 150 (2017) 265-274.

[86] Wang, H., Meng, K., Dong, Z. Y., Xu, Z., Luo, F., & Wong, K. P. (2015, July). Efficient real-time residential energy management through MILP based rolling horizon optimization. In 2015 IEEE Power & Energy Society General Meeting (pp. 1-6). IEEE.

[87] Hajela, P., & Lin, C. Y. (1992). Genetic search strategies in multicriterion optimal design. Structural optimization, 4(2), 99-107.

[88] Kornelakis, A. (2010). Multiobjective particle swarm optimization for the optimal design of photovoltaic grid-connected systems. Solar Energy, 84(12), 2022-2033.

[89] Mehleri, E. D., Sarimveis, H., Markatos, N. C., & Papageorgiou, L. G. (2012). A mathematical programming approach for optimal design of distributed energy systems at the neighbourhood level. Energy, 44(1), 96-104.

[90] Arcuri, P., Beraldi, P., Florio, G., & Fragiacomo, P. (2015). Optimal design of a small size trigeneration plant in civil users: A MINLP (Mixed Integer Non Linear Programming Model). Energy, 80, 628-641.

2. Smart District Heating Networks

The idea of the Smart District Heating (SDH) represents the enlargement of the traditional district heating (DH) concept. A SDH network, differently from the traditional one, involves the possibility of realizing a bidirectional exchange of thermal energy between the district heating network and one or more users composing it. This is realized by the installation of a distributed generation (DG) system at the user side and, thus, involving the presence of one or more smart user (or thermal prosumer) within the network [1]. To this respect, the smart user (which can be defined as a user who can act both as a consumer and as a producer) plays a key role in the smart district heating [2,3]. One of the main issues related to the smart users, indeed, is the regulation and optimization of their thermal exchange with the network in order to improve the efficiency and the reliability of both the user itself and the entire DHN [4]. To this respect, both the typology (configuration) and the position of the smart user substation represent two key aspects. In this context, the already developed software IHENA (Intelligent Heat Energy Network Analysis) has been modified by the development of an additional tool aimed to find out the optimal allocation of the smart user for a given district heating network. The tool is then validated by investigating a branched and a ring district heating network designed in order to be representative of the two main typology of DHN. Finally, an existing DH network has been analyzed by the implementation of the additional tools of the software.

2.1 Smart user substations

A smart user (or thermal prosumer) is a customer who can both consume and produce thermal energy by the on-site installation of a distributed generation system able to produce a part, the total or more than the thermal needs of the user itself. This means that the thermal need of the user (for the domestic hot water and/or space heating) can be in part or completely fulfilled by the self-consumption and, in the case of the thermal energy produced by the DG exceed the user needs, the surplus can be stored or feed into the district heating network. This involves a continuous interaction between the smart user and the district heating network which provides for the energy balance.

The presence of one or more smart user within a smart district heating network allows the possibility of realizing a bidirectional thermal energy exchange between the district heating network and the smart user itself (namely the distributed generation system). This implies a modification of the traditional user substation in order to allow the energy fluxes bidirectionality. To this respect, four different configurations of smart user substation have been considered [5], respectively presented from Figure2.1 to Figure 2.4:

- Scheme 1 (*feed to return*): a mass flow rate is extracted from the feed line of the network, heated from the distributed generator and reintroduced into the return line (see Figure 2.1);
- Scheme 2 (*feed to feed*): the thermal energy transfer from the decentralized production systems and the district heating network affects only the feed line (see Figure 2.2);
- Scheme 3 (*return to return*): the thermal energy transfer from the decentralized production systems and the district heating network affects only the return line (see Figure 2.3);
- Scheme 4 (*return to feed*): a mass flow rate is taken from the return line of the DHN, heated from the decentralized generator and reintroduced into the feed line (see Figure 2.4).
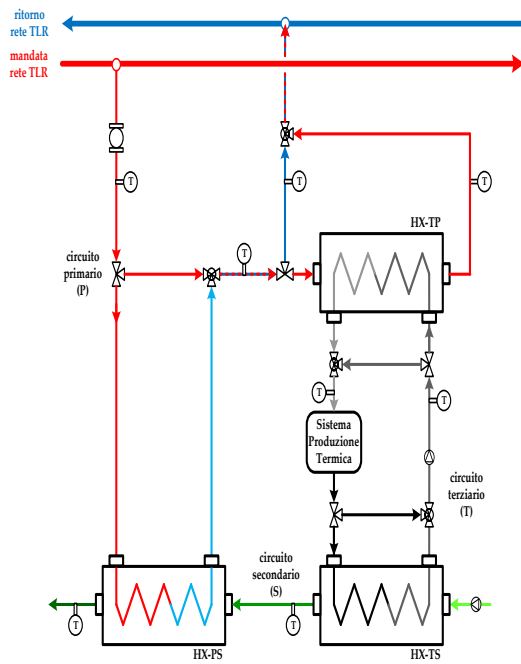
FIGURE 2.2: SCHEME 1, *FEED TO RETURN.*
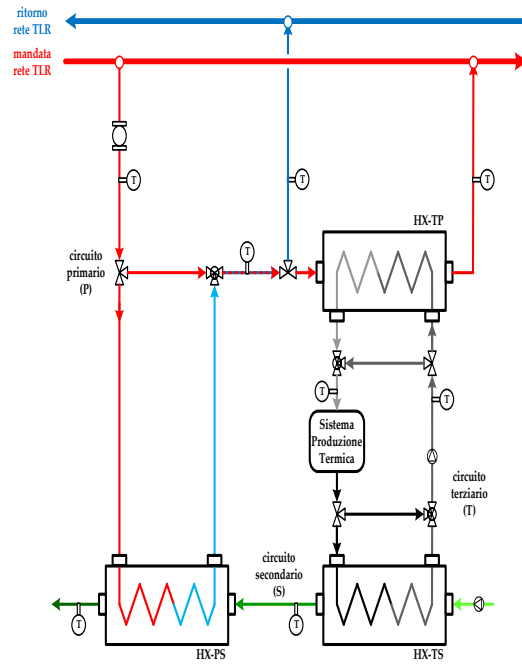
FIGURE 2.2: SCHEME 2, *FEED TO FEED.*
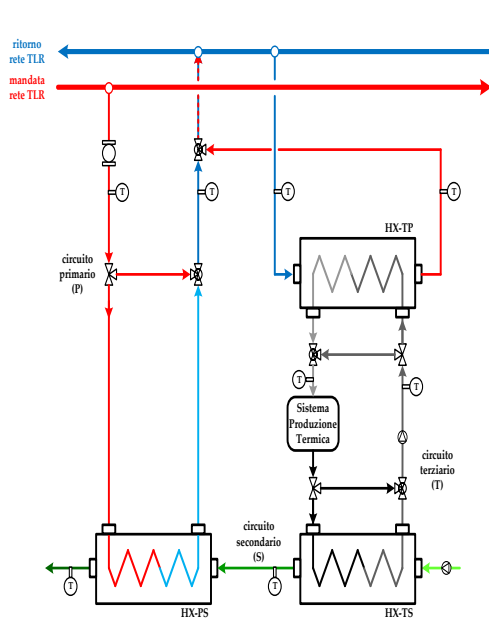
FIGURE 2.3: SCHEME 3, *RETURN TO RETURN.*
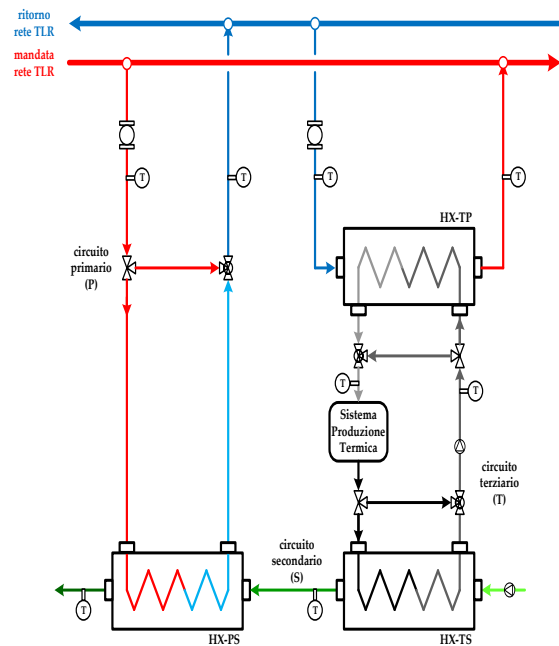
FIGURE 2.4: SCHEME 4, *RETURN TO FEED.*

These schemes represent four alternatives of smart user substation. It has to be highlighted that they differ each other depending on the energy system installed at the user side for the thermal power production and on the temperature levels of the network (in terms of feed and return temperatures). Furthermore, it has to be underlined that the choice between these for schemes for the conversion from traditional district heating into SDH represents an important aspect and it is made with the

33

main purpose of optimizing the thermal exchange between the decentralized energy production systems and the district heating network. For this reason, the main characteristics of each of them are highlighted in the following [5,6].

A first consideration concerns the Scheme 1 (*feed to return*). This scheme provides that the thermal power produced by the energy systems is used for the user fulfilment. However, in the case of the thermal power generated by the DGS is not sufficient to cover the whole user demand, the DHN provides to supply the remaining part. Conversely, if the produced thermal power is greater than the user need, the exceeding quantity is feed into the network by extracting a mass flow rate from the feed line and reintroduced it into the return line. Furthermore, it has to be observed that, from the management point of view this scheme is not appreciable since the temperature become higher in the DH network return line, and, consequently also in the return line at the inlet of the thermal power station. This leads to a reduction in the efficiency of the centralized production system connected to the network. On the other side, this scheme is the simplest one since its choice does not affect the network flows. Therefore, the network regulation will be easier from the management viewpoint.

As it regards the Scheme 2, it has to be pointed out that, differently from the previous scheme, in case of power surplus produced by the decentralized energy system, this amount is introduced into the feed line (not to the return line as it for the Scheme 1). Therefore, the increase in the temperature involves the feed line of the DHN. For this reason, in the case of the network management is able to predict an optimal control of the local heat production, the feed temperature of the thermal power station can be adapted each time to the new network conditions. On the contrary, it can occur that if the feed temperature is kept constant, the users located subsequent to the smart user are fed by a fluid with a higher temperature. This represents an undesired situation because these users may necessitate a constant temperature, or – if they are smart users too – they could be excluded from further introduction of thermal power into the network.

As it regards the Scheme 1 and the Scheme 2, it has to be pointed out that an opportune distributed generator is needed both for Scheme 1 and Scheme 2 in order to produce the thermal power at the opportune temperature for the exchange with the network feed line. To his respect, it has to be observed that these two schemes can be considered only in the case of given energy production systems and at certain network temperatures, namely in all those cases in which, after the heat exchange with the user, the temperatures of the fluid circulating within the energy systems circuit are higher than the feed temperature.

The Scheme 3 provides that the distributed generation systems installed at the user side can transfer the thermal power to a mass flow rate which is both extracted and reintroduced from/to the return line. This involves that the presence of a smart user affects the only return line of the DHN starting from the smart user itself. Therefore, also in this case, as for the Scheme 1, there is an increase in the return line temperature which make this configuration not appreciated from the point of view of the network management. In addition, the management of the mass flow rate extracted from the return line to the distributed generators is more difficult in this configuration.

The last considerations concern the Scheme 4 which is the most complex among all. This scheme, in fact, provide the extraction of a mass flow rate from the return line and the reintroduction into the feed line, leading to an increase of temperature already from the feed line in correspondence of the smart user. Moreover, in this scheme the management of the mass flow rate become a very important issue. However, with this configuration the feed and the return line temperature levels can be kept constant by heating the mass flow rate extracted from the return line up to the feed line temperature level (and not beyond). This implies that, from the management point of view, this

scheme represents the most appreciated among all the considered configurations. Overall, the main advantage of this scheme is that it allows to introduce the thermal power into the network without affecting the feed temperatures. On the other hand, this scheme involves a variation in the mass flow rates circulating within the pipelines and it implies some intervention by the thermal power station. Finally, since this scheme does not necessary implies an increase in the feed temperature, it allows to avoid particular regulation problems in terms of temperature profiles. Thus, Scheme 4 is widely adopted in the existing smart district heating networks.

2.2 Software IHENA

The software IHENA (Intelligent Heat Energy Network Analysis), is a software developed by the Energy Systems research group of University of Bologna with the main purpose of investigating the behavior of a district heating network, in traditional or in smart configuration. In particular, the software IHENA allows to analyze the DHN from both a hydraulic and a thermodynamic point of view respectively for the calculation of the mass flow rates and pressure drops and for the evaluation of the heat exchange and, therefore, the heat dissipations.

Hydraulic resolution

The hydraulic resolution of the problem at the basis of the software IHENA is based on the Todini-Pilati algorithm generalized by the Darcy-Weisbach equation [7,8]. This choice is mainly due to the convergence speed and to the reliability of the resolution method.

Generally, a hydraulic district heating (or cooling) network can be represented as a subsequence of a certain number of pipes (NP) and nodes (NN). To this respect, an example of a portion of district heating network is represented in Figure 2.5 [9]. Each node can be identified as a source (namely the thermal power station or the smart user), a mixer (a nodes in which the balance between the inlet and outlet mass flow rate is equal to zero) and a user (namely the end user).
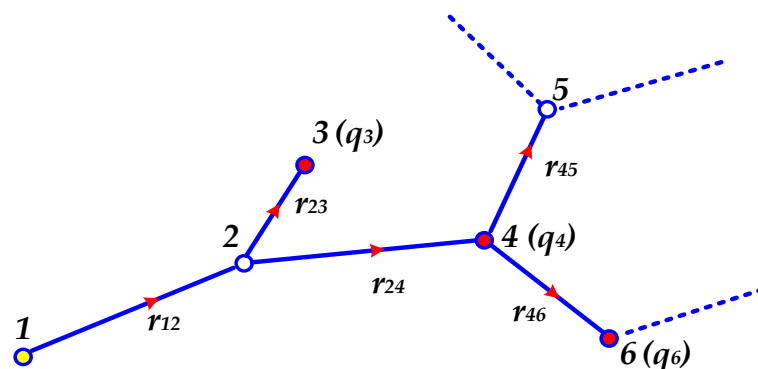
FIGURE 2.5: PORTION'S EXAMPLE OF A DISTRICT HEATING NETWORK.

By considering a generic pipe, and denoting the upstream and downstream nodes respectively with i and j, for each pipe p_{ij} the energy balance can be written as follows:

$$\Delta H_{p_{ij}} - \left(H_i - H_j \right) = 0 \qquad\qquad \text{Eq.2.1}$$

where $\Delta H_{p_{ij}}$ represents the total pressure drops which occur in the pipe p_{ij}. The terms H_i and H_j, instead, respectively represents the energy content of the fluid at the ith and j^{th} nodes.

The total pressure drop along the entire pipelines can be written as the sum of the distributed and the concentrated pressure drops. The first ones (ΔH_{dis}, expressed in Pa) can be calculated according to the Darcy-Weisbach equation as follows:

$$\Delta H_{dis} = f \frac{L}{D} \rho \frac{v^2}{2} \qquad [\text{Pa}] \qquad\qquad \text{Eq.2.2}$$

in which f indicates the Darcy friction factor, while L and D are respectively two terms representing the length and the diameter of the pipe. The ρ, instead, denotes the fluid density while v is the fluid average speed.

On the other hand, instead, the concentrated pressure drops ΔH_{con} (expressed in Pa) are evaluated by the equation:

$$\Delta H_{con} = \beta \rho \frac{v^2}{2} \qquad [\text{Pa}] \qquad\qquad \text{Eq.2.3}$$

being β the coefficient representative of the friction losses, which can be found in literature depending on the geometry of the pipe.

Furthermore, for each node of the DHN it can be written the following mass flow rates balance:

$$\sum_{in} Q_{in} - \sum_{out} Q_{out} - \sum_{u} q_u = 0 \qquad\qquad \text{Eq.2.4}$$

where, for a given node, $\sum_{in} Q_{in}$ represent the sum of the inlet mass flow rate, while $\sum_{out} Q_{out}$ represent the outlet ones. The terms $\sum_{u} q_u$, instead, denotes the sum of the mass flow rate required by the user, if present.

It follows that, by considering a generic DHN composed by *NN* nodes and *NP* pipes, it will be obtained *NP* equation related to the energy balance and *NN* equation of mass flow rate balance. These can be written in a matrix form. The equation systems will be formulated as follows:

$$\begin{cases} F_P(Q, H) = A_{11} \cdot Q + A_{12} \cdot H = 0 \\ F_Q(Q, H) = A_{21} \cdot Q - q = 0 \end{cases}$$

Eq.2.5

where Q and H, which are the mass flow rates and the energy content of the liquid, represents the unknown parameters. As can be noted, it consists of a system composed by *NN+NR* equations.

With respect to the equation Eq.2.5, the terms A_{11} represents the diagonal matrix $A_{11} = [NP \times NP]$ whose non-zero elements (in the diagonal) can be expressed as follows:

$$A_{11}(j, j) = \frac{\partial F_{Pj}}{\partial Q_j} = \frac{\partial \Delta H_j}{\partial Q_j}$$

Eq.2.6

The terms A_{21} of Eq.2.5, instead represents a topological matrix $A_{21} = [NN \times NP]$ whose rows represent the DHN nodes and the column represent the DHN pipes.

Considering the relation between a generic node i and a generic pipe j, and considering the direction of the flow, each of the A_{21} matrix elements can be equal to:

- +1 if the mass flow rate q_{ij} through the pipe j is entering into the node i (in the case of downstream nodes i with respect to the pipe j);

- -1 if the mass flow rate q_{ij} through the pipe j is outgoing from the node i (in the case of upstream nodes i with respect to the pipe j);

- 0 if there is no correlation between the node i and pipe j.

Finally, the matrix $A_{12} = [NP \times NN]$ represents the transpose matrix of A_{21}.

Then, by an iterative procedure based on the Newton-Raphson method generalized in matrix form by Todini-Pilati, the algorithm calculated the equation system. This procedure starts by assuming a mass flow rate and energy content initial values, together with the direction of the flow in each pipe.

The procedure continues with the calculation of the three aforementioned matrixes. At each iteration *m* the equation systems will be the following:

$$\begin{cases} F_P(Q, H) = A_{11} \cdot Q^{(m)} + A_{12} \cdot H^{(m)} = 0 \\ F_Q(Q, H) = A_{21} \cdot Q^{(m)} - q = 0 \end{cases}$$

Eq.2.7

By applying the Newton-Rapson method it will results:

$$\begin{cases} F_P(Q,H) = A_{11} \cdot \Delta Q^{(m)} + A_{12} \cdot \Delta H^{(m)} = -dE \\ F_Q(Q,H) = A_{21} \cdot \Delta Q^{(m)} = -dq \end{cases}$$

Eq.2.8

in which dE and dq denotes the residual of the energy and mass flow rate balances at the *m-1* iteration.

The resolution of the systems consists in the definition of $\Delta Q^{(m)}$ and $\Delta H^{(m)}$.

The iterative procedure ends when the convergence is reached. It occurs when $|dq_i|$ and $|dE_i|$ are lower than 10^{-9}.

Thermodynamic resolution

The thermal resolution is carried out on the basis of the forced convection heat exchange by considering the thermal exchange within a cylindric pipe. To this respect, the software calculates the thermal dissipation along the pipelines according to the following equation:

$$Q_{th,dis} = \sum_{i=1}^{NP} U_i L_i (T_{m,i} - T_{ext}) \qquad [\text{W}]$$

Eq.2.9

being U_i the global heat exchange coefficient [W/mK], L_i the length of the ith pipe while the terms $T_{m,i}$ and T_{ext} [K] represent respectively the mean temperature of the fluid flowing in the ith pipe and the external temperature (namely the ambient air).

As it concerns the global heat exchange coefficient, it is evaluated, for a horizontal pipe characterized by a circular section and insulation, as follows:

$$U = \frac{\pi}{\frac{1}{\alpha_1 D_{int}} + \frac{1}{2\lambda_1}\ln\left(\frac{D_{ext}}{D_{int}}\right) + \frac{1}{2\lambda_2}\ln\left(\frac{D_{ins}}{D_{ext}}\right) + \frac{1}{\alpha_2 D_{ins}}} \qquad [\text{W/mK}]$$

Eq.2.10

in which the terms D_{int}, D_{ext} and D_{ins} respectively represent the internal and external pipe diameters and the diameter of the insulating material. The coefficients α_1 and α_2, instead, refer respectively to the internal and external convection thermal exchange while λ_1 and λ_2 denote the conduction coefficient respectively for the pipe and the insulating material.

With the main purpose of investigating the choice of the smart user within a district heating network, during the PhD activities which led to the results presented in this Thesis, the software IHENA has been modified by integrating an additional tool. A schematic flow chart of the developed additional tool is presented in Figure 2.6.

More in detail, starting from the DHN input, such as the main geometric, users and power station characteristics, the developed tool firstly identified the number of users N_u composing the network. On the basis of this information, the developed tool allows to find all the possible combinations N_{com} in which one user is converted into a smart user and, consequently, evaluate the number of iterations $ITER_{max}$ to be processed. Therefore, at each ith iteration, the jth combination $N_{j,com}$ is evaluated by the network resolution. This means that the district heating network in presence of a smart user is evaluated from both the hydraulic and thermodynamic points of view according to the aforementioned equations (namely by the application of the Todini-Pilati algorithm and the forced heat convection laws). Once the evaluation of the ith iteration has been done, the developed tool carries-out a series of check aimed to verify the value of the minimum pressure drop ΔP_{min} at the heat exchanger at the users. To this respect, in the case of the ΔP_{min} is different from 0.50 bar – which is set as reference value $\Delta P_{min,ref}$ – the additional tool starts a check procedure, always at the ith iteration, to properly modify both the thermal power station P_{tps} and the smart user P_{su} pressures and to evaluate the DHN performances. Once the ΔP_{min} value is equal to the one reference one $\Delta P_{min,ref}$, the procedure restart with the ith+1 iteration.

The calculation ends when all the smart user combinations are evaluated, namely when the number of iterations analyzed are equal to $ITER_{max}$. Therefore, the software provides all the main performances parameters of each configuration of smart users, such as the total mass flow rate, the total supplied thermal power (both for the power plant and the smart user), the heat losses, the pumping power expenditure, the minimum pressure drop, the critical users (corresponding to the users with the minimum pressure drop) etc.
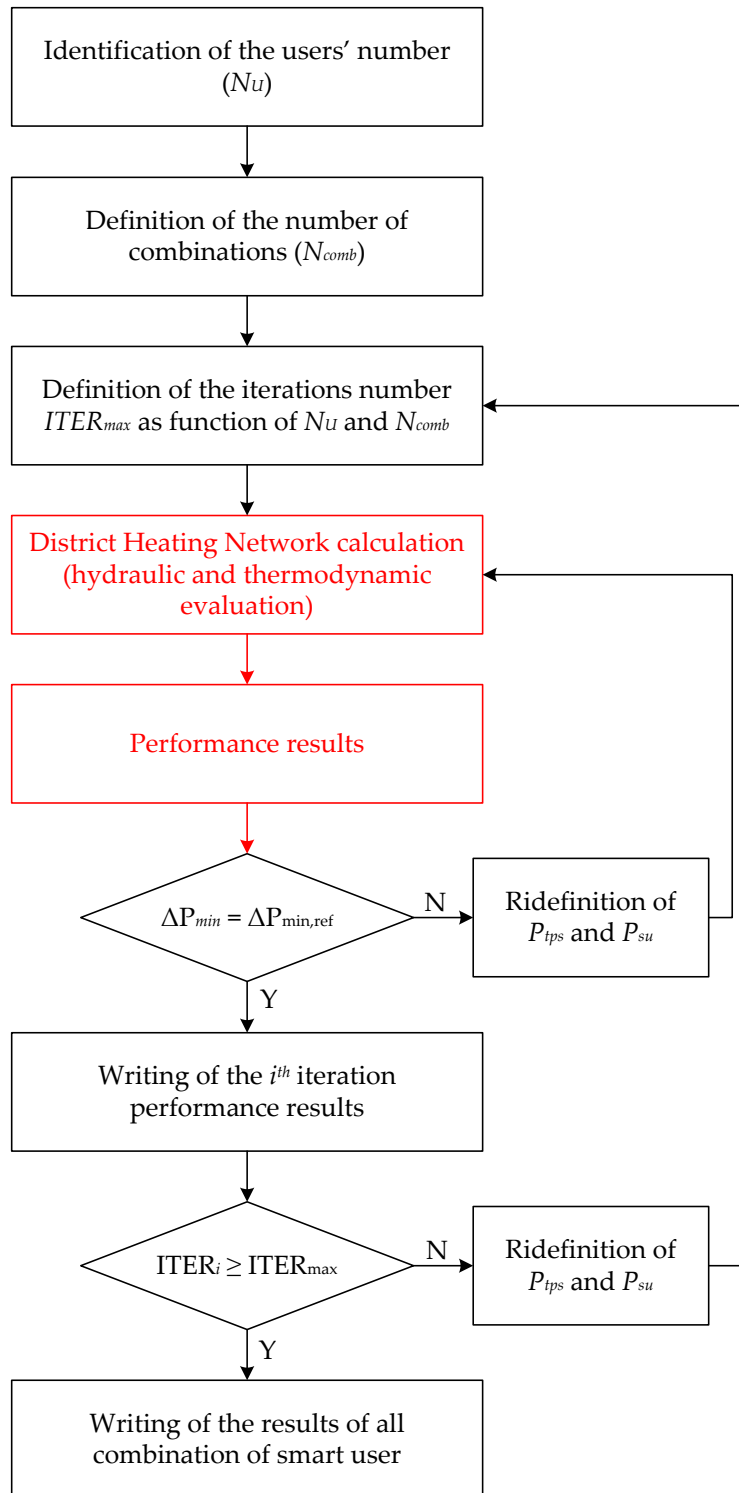
FIGURE 2.6: SCHEMATIC FLOW CHART OF THE DEVELOPED TOOL.

2.3 Optimal allocation of smart user within the DHN: test DHNs case studies

With the main purpose of investigating which user belonging to a district heating network is more suitable to be chosen for the conversion into a smart user and how the choice of its position will affect the performances of the whole network, two different case studies have been defined representative of the two main typologies: a branched and a ring DHN. More in detail, once the branched and the ring networks have been defined and analyzed on three different levels in order to investigate (*i*) the design operation; (*ii*) the smart user evaluation and the (*iii*) district heating network management in the presence of the smart user.

In order to evaluate how the choice of the smart user position affect the performances of a district heating networks, and to investigate if the typology of the network affect this choice, a general branched network and a general ring network have been defined and analyzed. In detail, as a starting point, a branched and a ring DHN have been designed with the main aim to be representative of the two main typologies of the DH networks. To this respect, these two networks – represented respectively in Figure 2.7 and in Figure 2.8 – are two small size networks which have been designed in such a way as to be composed by the same number of users located in the same position (in terms of geometric coordinates), by the same number of pipelines (with the exception of the additional pipe of the ring DHN). In particular, as can be noted from the figures, the branched DHN is composed by a total of 17 nodes – a thermal power station (in yellow), 5 users (in red) and 11 mixers (in white) – and 16 pipes.
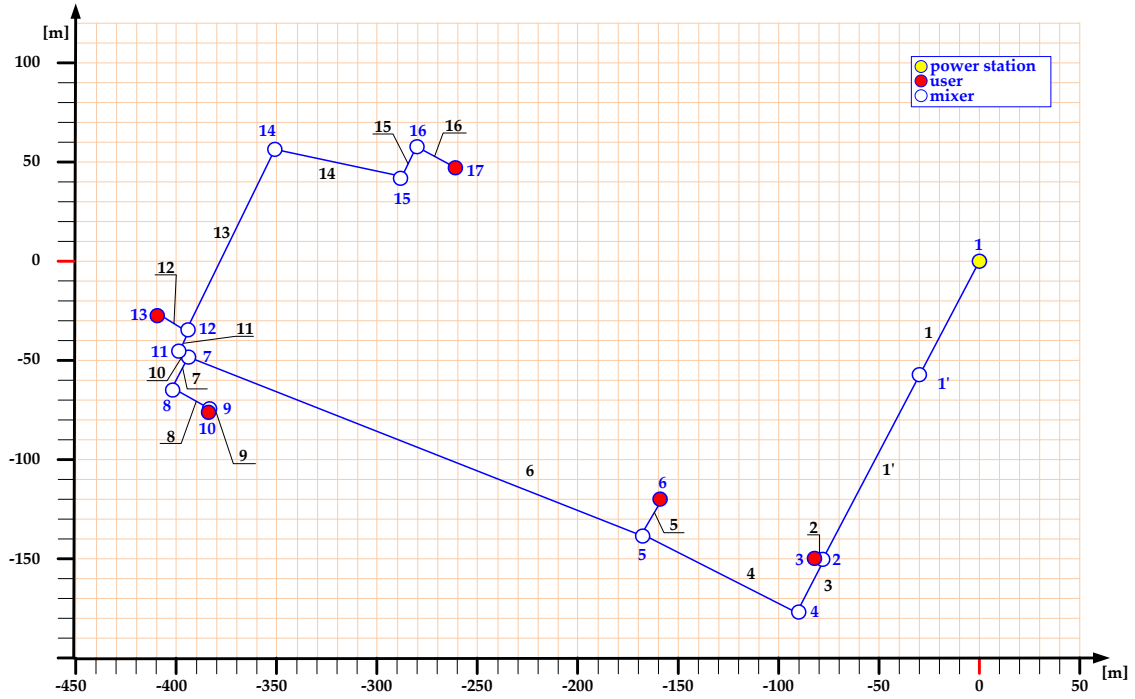
FIGURE 2.7: SCHEMATIC OF THE BRANCHED DISTRICT HEATING NETWORK.
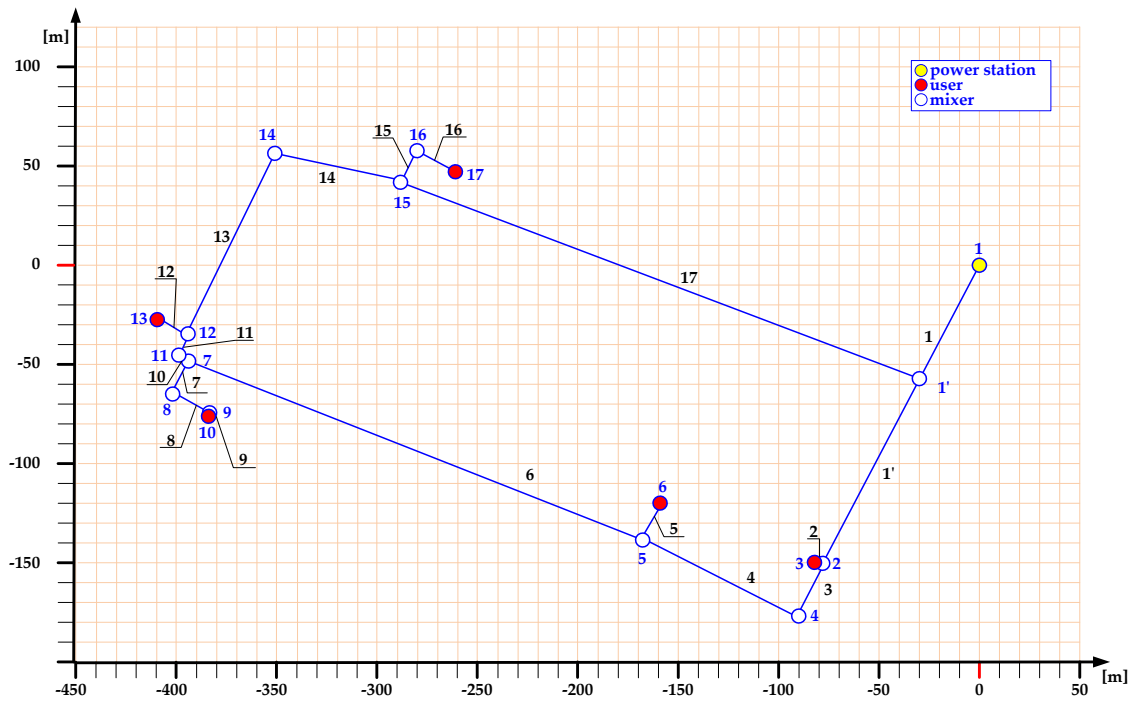
FIGURE 2.8: SCHEMATIC IF THE RING DISTRICT HEATING NETWORK.

2.3.1 Hypothesizes and assumptions

In this section the main hypotheses at the basis of the carried-out analysis are presented. A first point concerns the design thermal needs of the users composing the network which have been assumed as is represented in Figure 2.9. According to this figure, it has to be pointed out that the user characterized by the lower thermal demand is the one identified with the IDN3 (equal to 250 kW) which is also the nearest to the thermal power station in both the branched and ring case, while the user characterized by the higher thermal need is the one identified with IDN6 (equal to 825 kW).
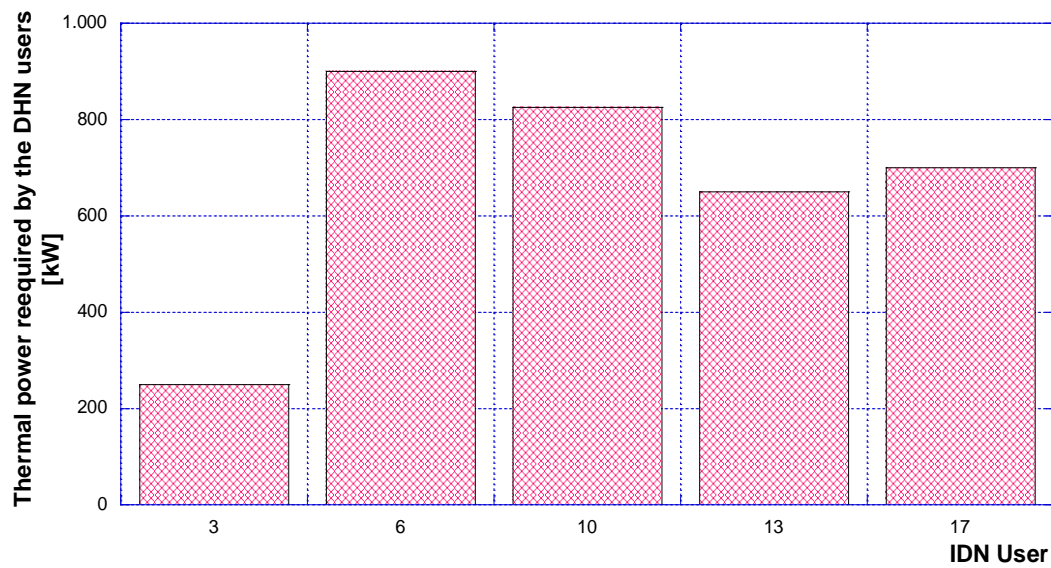
FIGURE 2.9: DESIGN THERMAL NEEDS OF THE DHN USERS.

Moreover, with respect to the user substation, it has been assumed that the feed temperature of the primary circuit (*i.e.:* network side) is equal to 80 °C and the return temperature is equal to 60°C. On the other hand, as it regards the secondary circuit (*i.e.:* user side), the inlet temperature has been assumed equal to 40 °C and the outlet temperature equal to 55 °C. The temperature parameters are summarized in Table 2.1.

TABLE 2.1: INLET AND OUTLET TEMPERATURE OF THE PRIMARY AND SECONDARY CIRCUITS.

Parameter	Units	Value
Inlet temperature of the primary circuit	[°C]	80
Outlet temperature of the primary circuit	[°C]	60
Inlet temperature of the secondary circuit	[°C]	40
Outlet temperature of the secondary circuit	[°C]	55

In order to perform the evaluation of the most suitable smart user within the considered district heating networks, it has been assumed to convert only one user into a smart one. Furthermore, it has been hypothesized that both the thermal power station and the smart user are characterized by the same supply pressure which is defined in order to keep the pressure drop at the critical user equal to a minimum value of 0.5 bar. The pressure of the expansion vessel, instead, is kept constant at a value equal to 4 bar. Finally, as it regards the smart substation, with respect to the scheme presented in the previous Section 2.1, the simulation has been carried out by considering the *return to feed* scheme, namely the extraction of a mass flow rate from the return line of the DHN and, after the heat exchange with the decentralized production system, the reintroduction into the feed line. The choice of adopting the Scheme 4 has been mainly made on the basis of the fact that this configuration does not involves particular regulation problem in terms of temperature profiles and because it represents the most used in the SDHNs.

In the following section the results of the branched and ring district heating networks analysis are presented. As aforementioned, the carried-out analysis has been conducted by firstly investigating the design operation of both the test networks and then by the evaluation of the best smart user and the management of the entire district heating network in the presence of smart user.

2.3.2 Design operation

The design operation of the defined branched and ring district heating networks has been carried-out by the implementation of both networks within the software IHENA. A first result concerns the total thermal power produced and consumed within the considered DH networks. To this respect, the results of the branched DHN design investigation show that the total thermal power supplied by thermal power station is equal to about 3˙387 kW which is due in part to the fulfillment of the users of the DHN (for an amount equal to about 3˙325 kW) and in part to the heat losses along the DHN pipelines (about 68 kW) for the energy distribution.

As it regards the ring network, instead, under the same thermal needs of the users (equal to 3˙325 kW), the thermal power station produces a total thermal power equal to about 3˙402 kW which is slightly higher than in the branched case due to the higher heat dissipation along the pipelines (which amounts to about 77 kW).

It means that in the case of branched DHN the heat losses represent about 2.0 % of the total produced thermal power, while in the ring network they represent about 2.3 % of the total heat production.

Moreover, as it regards the pumping power, from the evaluation it results that the value obtained in the branched case differs from the one obtained from the ring case. In detail, the pumping power resulting from the design operation analysis of the branched networks – which is equal to about 5.68 kW – is slightly higher than in the ring case – which is equal to about 5.19 kW.

Another result concerns the mass flow rate circulating in the district heating networks. To this respect, the results show that in both cases – branched and ring DHN – the total mass flow rate circulating into the network pipelines is equal to about 40 kg/s. However, the distribution of this mass flow rate within each pipe of the network varies depending on the considered DHN typology. The partitions among each pipe of the mass flow rates are presented in Figure 2.10 for both the DH networks. As can be observed from the figure, the results show that, whit the exception of the pipe identified with IDP17, in all the other pipes the circulating mass flow rate in the case of branched

network is always greater than or at least equal to the one resulting from the ring network evaluation. As aforementioned, the only exception consists in the pipe IDN17, in fact, this pipe has been defined only in the ring network in order to obtain a closed structure with respect to the branched one.
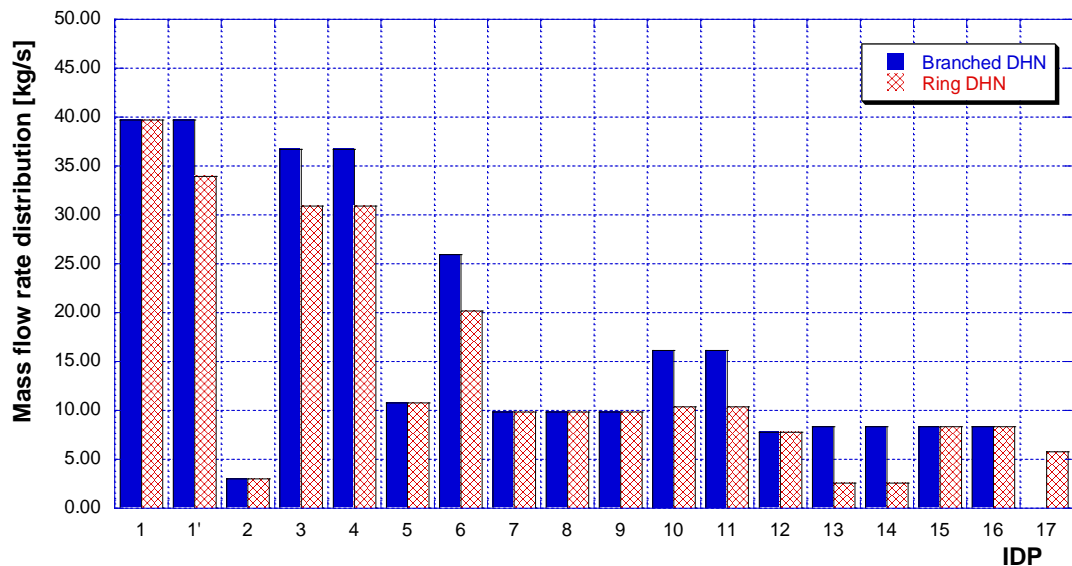
FIGURE 2.10: DISTRIBUTION OF THE MASS FLOW RATE WITHIN THE DHN PIPELINES FOR THE BRANCHED AND RING CASES.

In addition, another important result from the design evaluation is represented by the pressure drops that occur at each user substation. To this respect, the results for both the branched and ring networks are shown respectively in Figure 2.11a and in Figure 2.11b. The results show that, even in this case, the typology of the DH network affect the consider parameter. In fact, as can be noted from the figure, the values of pressure drops obtained from the branched DHN design analysis are different from the ones resulting from the ring DHN evaluation although the trend is quite similar. In particular, with the exception of the users identified with IDN10 and IDN17, in all the other cases, the pressure drops occurring at each user substation are slightly higher in the branched network case. Moreover, as it concerns the user defined with IDN10, it results that both for the branched and ring networks the pressure drops value are equal to about 0.5 bar representing in both cases the minimum value. From this result it follows that the user IDN10 can be considered as the critical user being characterized by the minimum pressure drop.

The corresponding critical paths – namely the sequence of pipes from the thermal power station to the critical user – are represented in Figure 2.12 and in Figure 2.13 (in red color) respectively for the branched and ring district heating network case.
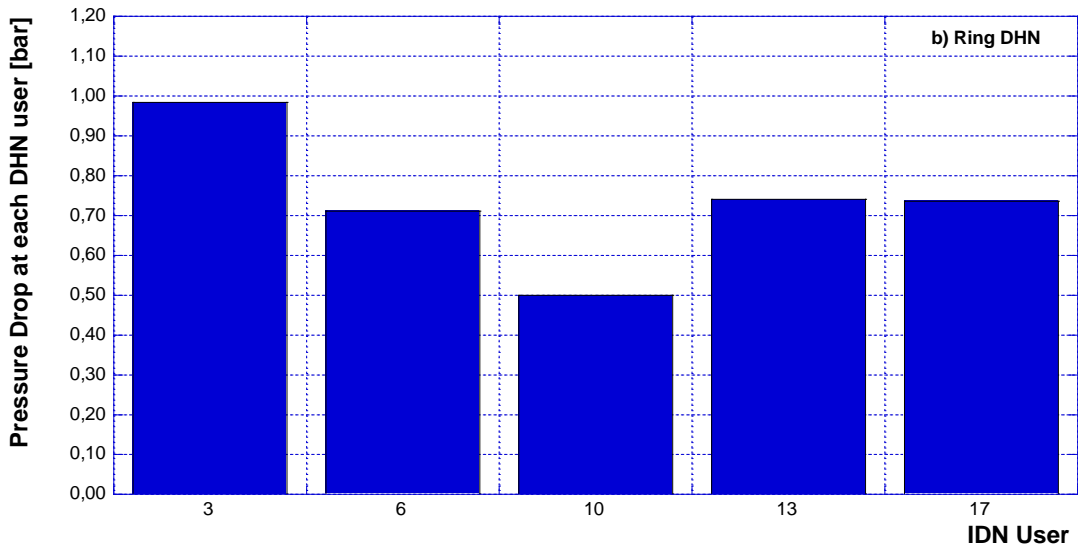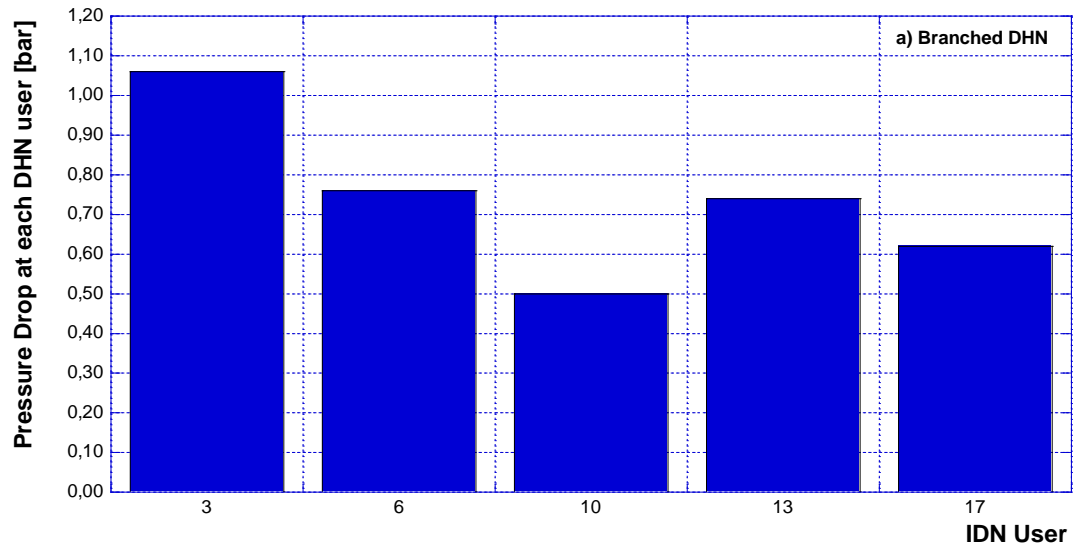
FIGURE 2.11: PRESSURE DROP AT EACH USER FOR THE (A) BRANCHED AND (B) RING DHNs.

FIGURE 2.12: CRITICAL PATH RESULTING FROM THE DESIGN ANALYSIS IN THE CASE OF BRANCHED DHN.

FIGURE 2.13: CRITICAL PATH RESULTING FROM THE DESIGN ANALYSIS IN THE CASE OF RING DHN.

At least, in Table 2.2Table 2. the main parameters resulting from the design operation simulation of the branched and ring district heating networks are summarized.

TABLE 2.2: MAIN RESULTS OF THE DESIGN OPERATION ANALYSIS.

Parameter	Units	Branched DHN	Ring DHN
Inlet mass flow rate	[kg/s]	40	40
Thermal power from the power station	[kW]	3˙387	3˙402
Thermal power supplied to the users	[kW]	3˙325	3˙325
Heat losses	[kW]	62	77
Pumping power	[kW]	5.68	5.19
Supply pressure	[bar]	5.26	5.15
Expansion vessel pressure	[bar]	4.00	4.00

2.3.3 Smart user evaluation

As aforementioned, the second level of the carried-out analysis concerns the evaluation of the district heating network behavior in order to define which of the connected users is more suitable for the conversion into a smart user. In particular, this analysis has been conducted by applying the developed additional tool of the software IHENA for each of the considered typologies of district heating network (branched and ring), on the basis of the main assumption described in the previous section.

The results, normalized with respect to the design operation, have been shown from Figure 2.14 to Figure 2.16 for both the branched and ring district heating networks. Furthermore, according to the aforementioned assumptions and the Todini-Pilati algorithm, at the basis of the software IHENA, these results refer to the optimal hydraulic equilibrium operation of the network – which is defined as the optimized operational point of the network – for given smart user.

A first result, shown in Figure 2.14, concerns the pumping power change for each configuration of smart user. This result shown that, regardless of the district heating network typology, all the configurations including the presence of a smart user, involve a variation – and in particular a reduction – of the pumping power consumption with respect to the design (traditional) operation. Moreover, it can be noted from the figure that in the case of branched district heating network the pumping power reduction is greater than in the case of the ring network. In fact, the installation of a distributed generation systems at the user side – for the conversion into a smart user – results in a reduction of the thermal power (*i.e.:* of the total mass flow rate) introduced into the district heating network with a consequent decrease of the pressure drops along the networks pipelines and of the pumping power. In particular, in the case of branched district heating network, the pumping power variation ranges between a minimum value equal to 50 % (corresponding to the smart user IDN10) to a maximum value equal to about 83 % (corresponding to smart user IDN3). The same trend occurs also in the case of branched DHN, in which the pumping power consumption varies from a minimum value equal to 52 % (in correspondence of smart user IDN10) to a maximum value equal to 85 % (in correspondence of smart user IDN3). Therefore, in both cases, the minimum pumping power consumption occurs when the user identified with IDN10 – which has been already identified as the critical one in the design operation analysis – is converted into a smart user.
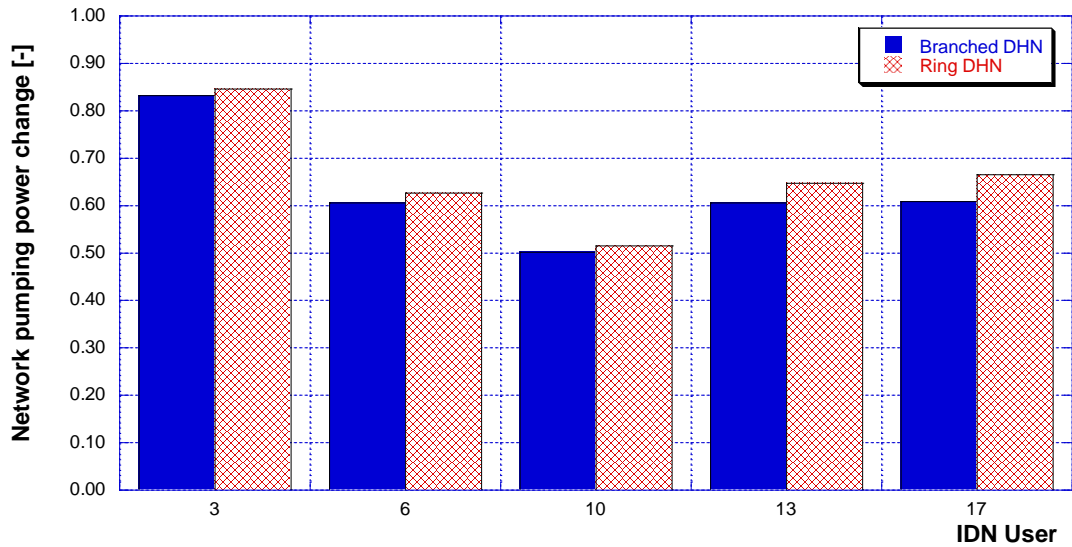
FIGURE 2.14: VARIATION OF THE PUMPING POWER FOR THE BRANCHED AND RING DISTRICT HEATING NETWORKS.

Another result, shown in Figure 2.15Figure 2., concerns the variation of the mass flow rate circulating in the district heating network with respect to the design operation.
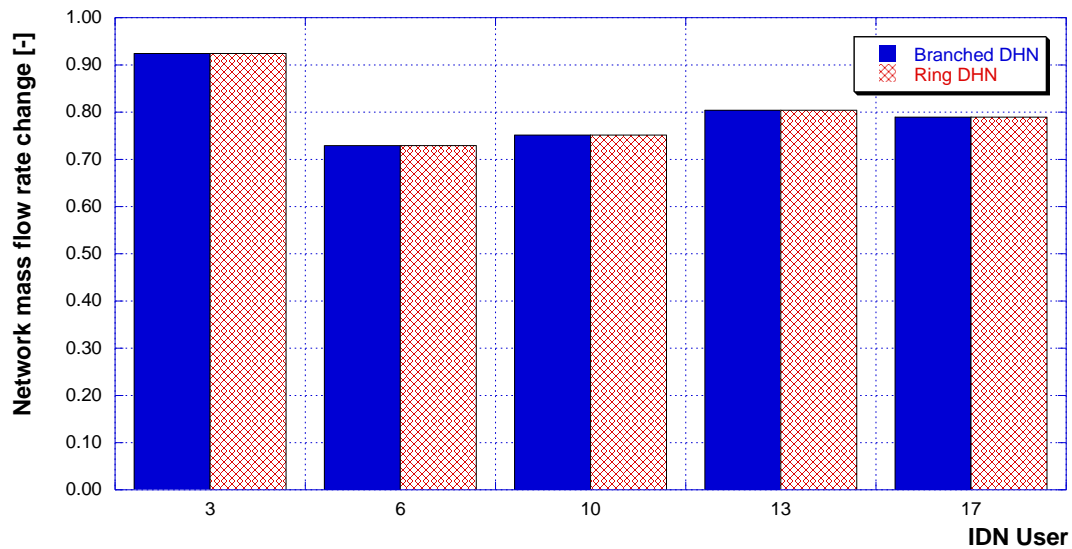
FIGURE 2.15: VARIATION OF THE MASS FLOW RATE FOR THE BRANCHED AND RING DISTRICT HEATING NETWORKS.

As well as for the pumping power change, even in this case there is a reduction in the mass flow rate with respect to the design operation in each configuration of smart user, both in the case of branched DHN and ring DHN. In fact, the conversion of a user into a smart user leads to a reduction

and to a redistribution of the total mass flow rate circulating within the pipelines of the network. In detail, as can be observed from Figure 2.15Figure 2., each configuration providing the presence of a smart user involves a reduction in the total mass flow rate both in the case of branched and ring district heating networks. However, differently from the previous results (namely the pumping power), the total mass flow rate variation is not affected by the district heating network typology, being characterized by the same value in each configuration of smart user both in the branched and ring DHN case. In particular, the minimum value of the total mass flow rate, equal to about 73 % of the design value, occurs in the case of smart user IDN6 – which is also the user characterized by the higher thermal need. Actually, even in the case of smart user IDN10 – which is the critical user according to the result of the design evaluation – the mass flow rate assumes one of the lower values (*i.e.:* it is equal to about 75 % of the design value). On the contrary, instead, the minimum value of the mass flow rate variation occurs when the user IDN3 – which is the one with the lower thermal need – is converted into smart user, since in this case the total mass flow rate is equal to about 80 % of the design value.

Furthermore, another interesting result of the smart user evaluation concerns the distribution efficiency – which is defined as the ratio between the thermal power totally required by the district heating network users and the total thermal power introduced into the network – represented in Figure 2.16 for each case of smart user as the variation with respect to the design operation.
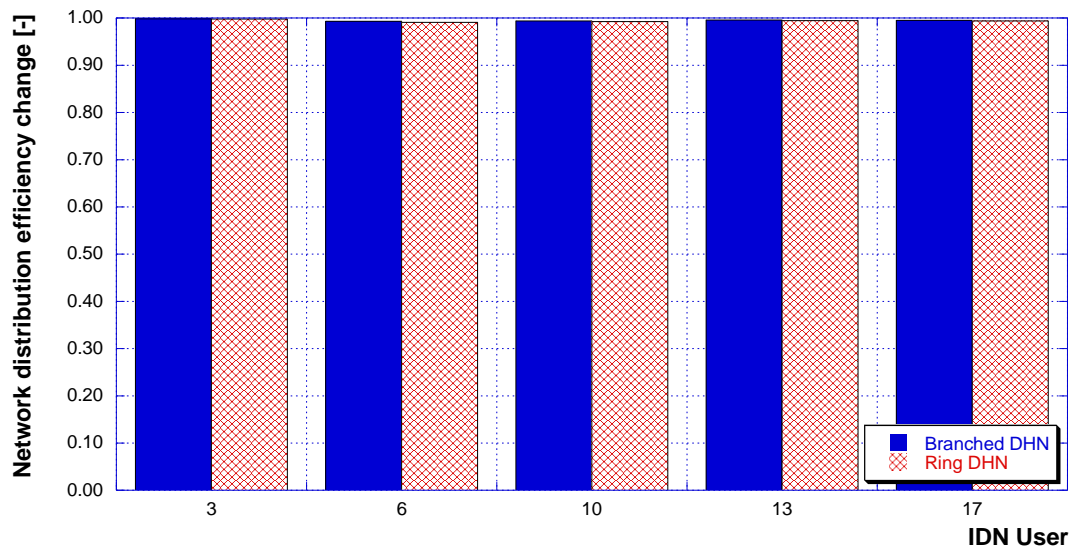
FIGURE 2.16: VARIATION OF THE DISTRIBUTION EFFICIENCY FOR THE BRANCHED AND RING DISTRICT HEATING NETWORKS.

The results show that there is not a significant variation in the distribution efficiency in the presence of a smart user in both case of DHN. In fact, in the case of branched district heating network, the distribution efficiency ranges between a minimum value – with respect to the design value – equal to about 99.3 % to a maximum value equal to about 99.9 % respectively for the configuration of smart user IDN6 and smart user IDN3. The same trend occurs for the ring district heating network

case being the minimum value, equal to about 99.2 % of the design value, in correspondence of smart user IDN6 and the maximum value, equal to about 99.8% of the design value in the case of smart user IDN6. According to Figure 2.9, the user IDN3 and IDN6 respectively represent the user characterized by the lower and the higher thermal needs.

Finally, the last result of the smart user evaluation, show in Figure 2.17, regards the variation of the supply pressure, which represents the feed-in pressure of the thermal power station. As can be observed from the figure, with respect to the design operation, there is a very low reduction in the supply pressure both in the case of the branched DHN and in the case of ring DHN. In particular, for each typology of DHN, the supply pressure reduces in each configuration of smart user, and this reduction is always greater in the case of branched district heating network. In fact, in the case of branched network, the supply pressure varies from a minimum value equal to about 92 % of the design value in correspondence od smart user IDN10 to a maximum value slightly less than 98 % of the design value in the case of smart user IDN3. On the other hand, the ring DHN values of the supply pressure ranges between a minimum value equal to about 93 % of the design value in the case of smart user IDN10 to a maximum value equal to about 98 % of the design value in correspondence of smart user IDN3. Anyway, both for the branched and ring district heating network cases the minimum value occurs in the case of the critical user is converted into a smart one.
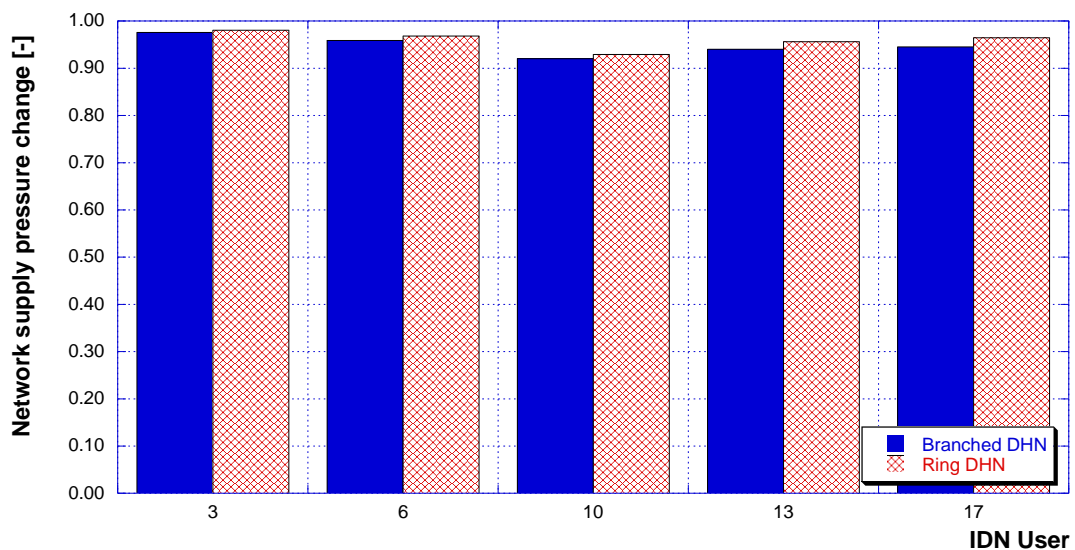
FIGURE 2.17: VARIATION OF THE SUPPLY PRESSURE FOR THE BRANCHED AND RING DISTRICT HEATING NETWORKS.

2.3.4 Management of the smart district heating networks

The third and last level of the carried-out analysis concerns the management of the district heating network in the presence of smart user. In fact, the installation of a given distributed generation systems located at the user side, in particular the size and typology, affects the behavior of the entire

DH network. To this respect, this evaluation is aimed to investigate how the main performance parameters varies depending on the thermal power feed into the network by the smart user. To this purpose, a parametric analysis has been carried-out for each typology of considered network by varying – in each configuration of smart user – the total thermal power supplied from the distributed generation systems installed at the smart user in each configuration of smart user. Therefore, without entering into the detail of the characteristics of the distributed generation system (*i.e.:* typology, number, size, etc.), all the five configurations of smart user have been analyzed. It has to be underlined that each configuration of smart user represents a specific setup of the district heating network. Nevertheless, for the analysis have been defined seven different cases which differ each other depending on the amount of the thermal power produced by the smart user (namely by the distributed generation system). These seven cases, which characterizes each configuration of smart user, are defined as follows:

- Case 1 (*design*): this scenario corresponds to the design operation of the network presented in the previous Section 2.3.2 in which the only heat source is the thermal power station (namely there is no distributed production). For this reason, the results of this case coincide for each of the considered configurations;

- Case 2 (*traditional DH*): in this scenario the thermal energy produced by the distributed generation systems for each of the considered configuration of smart user is always lower than the need of the user itself. Therefore, the thermal energy produced by the distributed generation system (DGS) is entirely used to fulfill only a part of the smart user need;

- Case 3 (*self-consumption*): this case represents the point in which the thermal power produced by the distributed generation systems is equal to the thermal power required to the considered smart user. It means that the user need is completely fulfilled by the distributed generation system;

- Case 4 (*smart DH, $Q_{th}<Q_{th,hy.eq.}$*): this scenario represents the case in which the thermal energy produced by the DGS exceeds the user needs and, consequently, the surplus is introduced into the network. Therefore, the DHN become a smart district heating network. However, the thermal energy feed into the network (Q_{th}) is lower than the one resulting from the hydraulic equilibrium point ($Q_{th,hy.eq.}$);

- Case 5 (*hydraulic equilibrium*): this scenario corresponds to the DH network optimal hydraulic equilibrium point which represents, as aforementioned, the optimized operational point of the network. Therefore, the results of this case are the same of the one presented in the previous Section 2.3.2;

- Case 6 (*smart DH, $Q_{th}>Q_{th,hy.eq.}$*): as well as for Case 4, in this scenario the thermal power produced by the DGS at the smart user is more than the user need and then an amount of thermal energy is feed into the network. However, in this case, the thermal energy introduced by the distributed generation system exceeds the one of the hydraulic equilibrium (Case 5);

- Case 7 (*smart user only*): in this case, the entire thermal energy needs of the DHN is fulfilled by the heat produced via the generation system installed at the smart user. It follows that the thermal power station does not contribute to the user fulfillment.

An example of the schematic representation of the different cases for a generic performance parameter is represented in Figure 2.18. According to the figure, the parametric analysis aims to understand how the curves of the main performance parameters vary for each of the five configurations of smart user, starting from the design point (Case 1) which is the same to each of them. This means to find the different points, representative of the aforementioned cases, each of which is representative of a given setup of the district heating network. Before entering into the detail of the results of the investigation, it has to be said that it is expected that each case will occur at a different value of the thermal power produced by the distributed generation system depending on the configuration of smart user. As a consequence, for this reason the results presented in the figure must be intended as an example of how the performance will be shown and discussed.
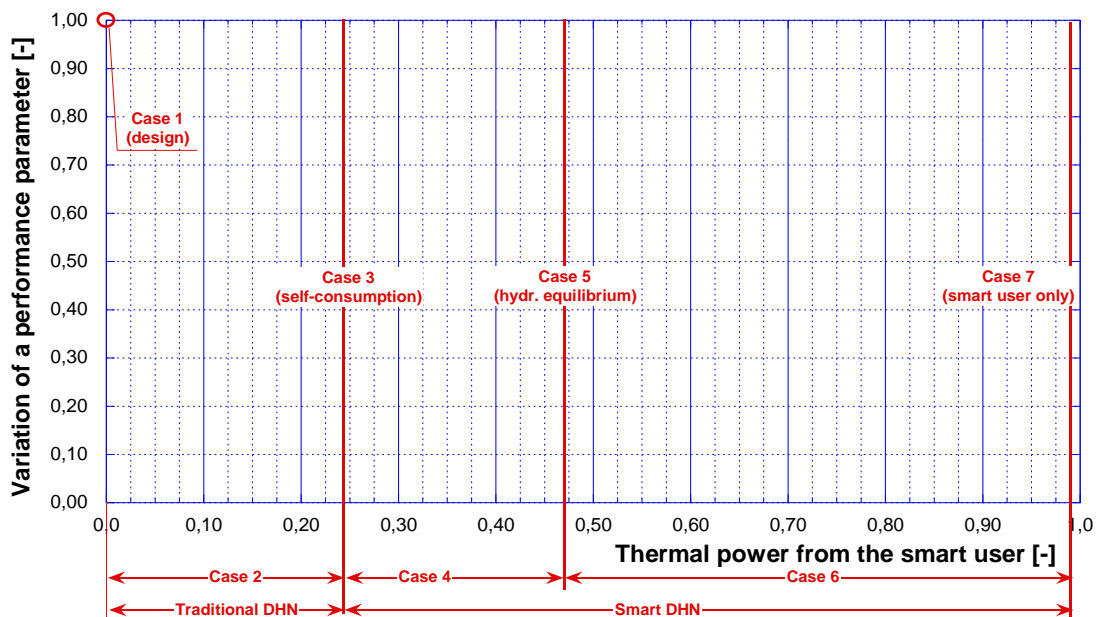
FIGURE 2.1: SCHEMATIC REPRESENTATION OF THE SEVEN CASES CHARACTERIZING THE DHN MANAGEMENT INVESTIGATION.

The results of the investigation will be firstly presented for the branched district heating network and then for the ring one. Moreover, it has to be highlighted that the results are normalized with respect to the design operation (*Case 1*) that is the configuration in which there is no heat production from the distributed generation system.

Branched DHN

A first result of the branched district heating network concerns the pumping power change which is represented in Figure 2.19 for each configuration of smart user. As can be observed from the figure, the pumping power consumption has an initially decreasing behavior (with respect to the design point) with the increase in the thermal power produced by the DGS. This trend is the same, even if with different values, for each of the smart user configurations. The decrease in the pumping

power occurs until a minimum value is reached. This point represents the hydraulic equilibrium of the network and then corresponds to the *Case 5*. Therefore, according to the definition of the hydraulic equilibrium operation and to the results of the smart user evaluation (Section 2.3.3), it represents the minimum value of pumping power consumption for each one of the considered configurations. Moreover, according to the results of Figure 2.14, it can be noted that the minimum value of pumping power results in the case of smart user IDN10 (which is the critical user resulting from the design operation). The opposite behavior, instead, occurs when the user identified with IDN3 – which represents the user characterized by the lower thermal needs and, at the same time, the closest one to the power station – is converted into a smart user. In this case, in fact, the minimum value (at the hydraulic equilibrium, *Case 5*) of the pumping power consumption is equal to about 83 %, namely it consists in a reduction of only 17 % with respect to the design operation (*Case 1*).

As it regards the other cases, it can be noted from the figure that, from the hydraulic equilibrium (*Case 5*) the trend of the pumping power increases in each considered configuration of smart user up to the case in which the smart user is set as the only thermal energy source (namely the *Case 7*). In this case, for each of the considered configurations of smart user, it results that the pumping power consumption is higher than the one of the design case. Moreover, among all, the higher values of pumping power variation equal to about 214 % and 216 % take place respectively in the case of smart user IDN10 and smart user IDN17, namely the critical user and the further user, are set as the only heat source. The opposite case, instead, occurs in the case of smart user IDN3 (which is, as already said, the closest user and the one with the lower thermal need).
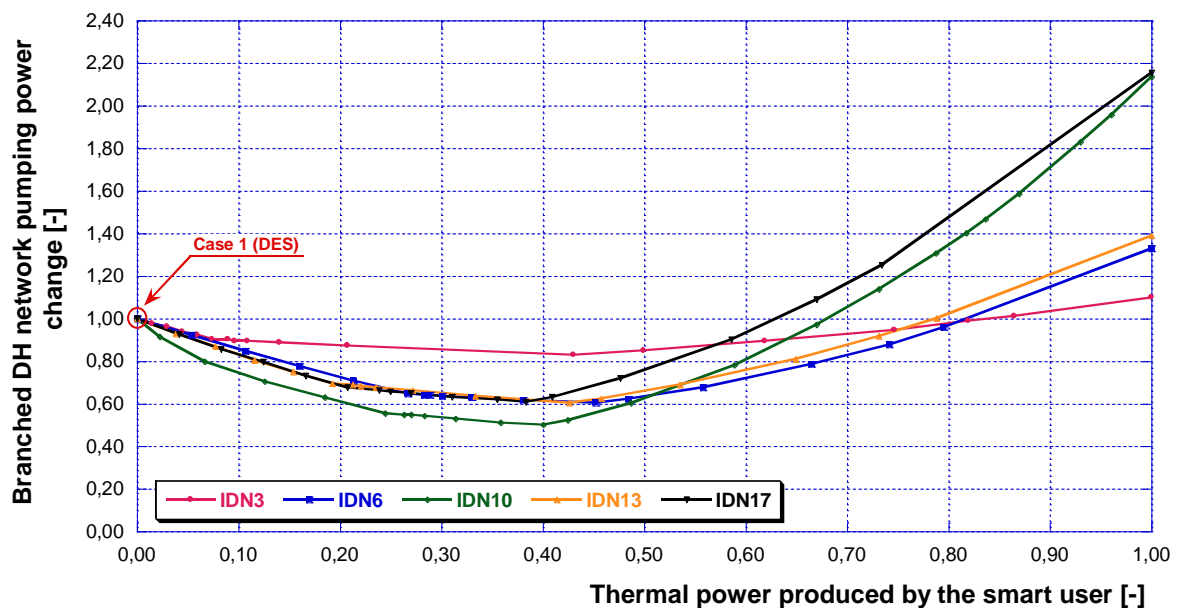
FIGURE 2.19: PUMPING POWER CHANGE AS FUNCTION OF THE THERMAL POWER PRODUCED BY THE SMART USER IN THE CASE OF BRANCHED DHN.

Another result, shown in Figure 2.20, concerns the variation of the mass flow rate circulating within the district heating network. The conversion of one user into a smart one, involves a reallocation of the mass flow rate and in particular, as can be noted from the figure, it implies a reduction of this parameter which occurs for all the configuration of smart user. In detail, with respect to the case of

the design operation (*Case 1*), the mass flow rate has a decreasing behavior as the thermal power produced by the distributed generation systems increases. However, for all the considered configurations of smart user, the decreasing trend occurs only in *Case 2*, namely the scenario in which the DGS heat production is lower than the thermal need of the user at which it is installed. In fact, in the self-consumption scenario (*Case 3*) the mass flow rate reaches its minimum value for each configuration of smart user. From this point on (*Case 4*), the distributed generator allows to fulfill the entire needs of the user also producing a further amount of thermal power that will feed into the SDHN. At the same time, as can be noted from Figure 2.20Figure 2., the variation of the mass flow rate remains constant as the network become a smart district heating network, namely up to the *Case 7*. As is shown in the figure, this behavior is common to all the configuration of smart user. The main difference concerns the point – in terms of amount of thermal power produced by the smart user – in which occur the transition from a traditional to a smart district heating network since this depends on the thermal need of each user. To this respect, according to the design thermal needs presented in Figure 2.9, from Figure 2.20 results that the lower variation in the circulating mass flow rate, namely a reduction equal to about 7.5 %, occurs when the user identified with IDN3 – which is the one characterized by the lower thermal need – is converted into a smart user. Furthermore, in this case, the conversion into a smart DHN occurs for the lower value of thermal power produced by the DGS installed in correspondence of the smart user. On the contrary, the opposite case occurs in the case of user IDN6 – namely the one characterized by the higher thermal need – is converted into a smart user. In this case, as can be noted from the figure, the mass flow rate variation decreases by reaching a minimum value equal to about 73 % with respect to the design value. This is the maximum decrease among all the considered configuration of smart user.

In general, the reduction of the mass flow rate circulating within the DHN of each configuration of smart user (calculated with respect to the design operation) increase with the increase in the thermal need of the user itself.
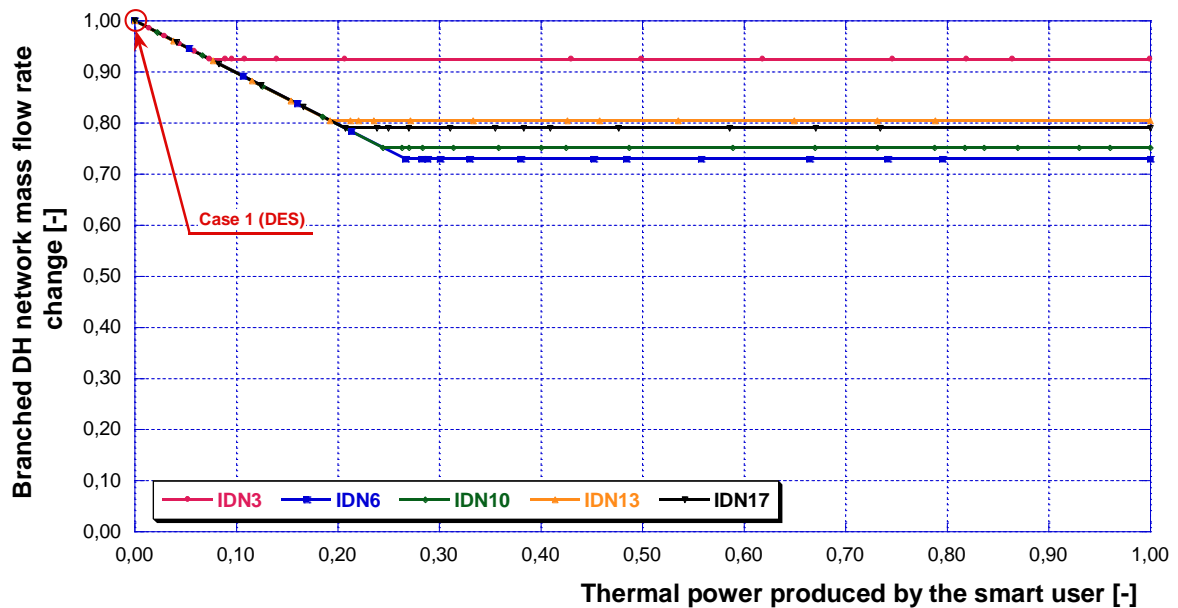
FIGURE 2.20: MASS FLOW RATE CHANGE AS FUNCTION OF THE THERMAL POWER PRODUCED BY THE SMART USER IN THE CASE OF BRANCHED DHN.

With respect to the ring district heating network, a first result, presented in Figure 2.21Figure 2., concerns the variation in the pumping power resulting from the management analysis with respect to each considered configuration of smart user. From these results it can be noted that, similarly to the branched case, the pumping power is initially characterized by a decreasing behavior (with respect to the design case) with the increase of the thermal power produced by the distributed generation system. This decrease reaches the minimum value in correspondence to the hydraulic equilibrium operation of the network, namely *Case 5*. This point represents the minimum value for each considered configuration of smart user, according to both the definition of hydraulic equilibrium point and the results presented in the previous section. Furthermore, from the figure, it can be noted that the minimum value between the different considered configurations occur when the critical user (namely the one identified with IDN10) is converted into smart user, that is equal to about 52 %. On the other hand, even in this case, the lower decrease which results in the higher value in correspondence of *Case 5* is in the case of smart user IDN3 (which is the user characterized by the lower thermal need). In this case, in fact, the minimum value (at the hydraulic equilibrium, *Case 5*) of the pumping power consumption is equal to about 85 % with respect to the design operation (*Case 1*). As it regards the other configuration – smart user IDN6, IDN13 and IDN17 – the minimum value is quite similar being respectively equal to about 63 %, 65 % and 67 %. Therefore, by increasing the thermal power produced by the distributed generation system, the pumping power increase up to the case in which the thermal need of the entire DHN is fulfilled only by the smart user (*Case 7*). This behavior characterizes all the smart user configuration, however, depending on each configuration, the increase differs case by case. In fact, while in the case of smart user IDN3 the pumping power slightly increase by reaching its maximum value in the *Case 7* equal to about 115 % with respect to the design case, on the other case this value is higher. To this respect, the maximum value is reached in the case of smart user IDN10 (namely the critical user resulting from the design evaluation) being the pumping power equal to about 235 %.
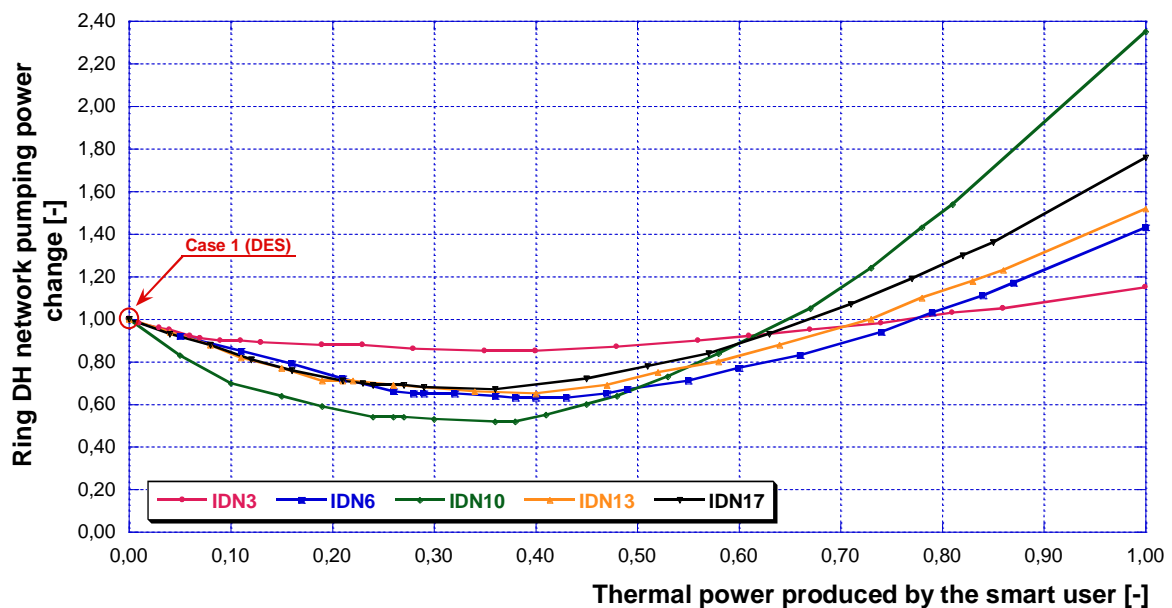
FIGURE 2.21: PUMPING POWER CHANGE AS FUNCTION OF THE THERMAL POWER PRODUCED BY THE SMART USER IN THE CASE OF RING DHN.

The last result of the district heating management, shown in Figure 2.22 is represented by the mass flow rate variation of each considered configuration, with respect to the design operation. To this respect it has to highlighted that the results obtained from the ring district heating network investigation are similar to the results of the branched one. In fact, the mass flow rate variation initially decreases for all the considered configuration by reaching the minimum value in correspondence of *Case 2* From this case to the last *Case 7* (in which there is only the smart user that concur to the DHN fulfillment) the mass flow rate of each configuration is kept constant. In particular, the higher is the design thermal power required by the user converted into smart user (Figure 2.9), the greater is the reduction in the mass flow rate circulating within the DH network. To this respect, it can be observed from the figure that the mass flow rate change ranges from a minimum value equal to about 73 % to a maximum value equal to about 92 % respectively in correspondence of the smart user IDN6 and IDN3. In the case of the critical user (IDN10) is converted into smart user, instead, the minimum value of the mass flow rate is equal to about 75 %.
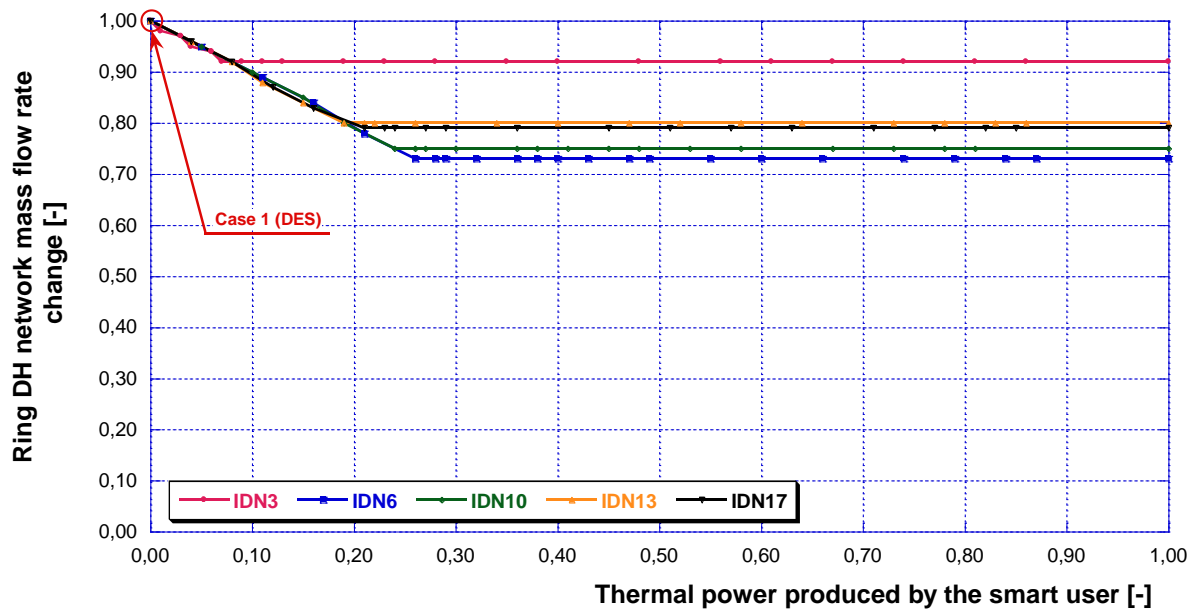
FIGURE 2.22: MASS FLOW RATE CHANGE AS FUNCTION OF THE THERMAL POWER PRODUCED BY THE SMART USER IN THE CASE OF RING DHN.

2.3.5 Critical user as smart user

To better understand the results presented in the previous section in terms of variation of pumping power (Figure 2.19Figure 2 and Figure2.21) and mass flow rate (Figure2.20 and Figure2.22Figure 2.), and to highlight the different analyzed scenarios (from *Case 1* to *Case 7*), the management of the DHN when the critical user (IDN10) is converted into smart user is presented this section. In particular, the network management is presented for both the branched and ring DHNs.

For reasons of completeness, the variation in both the pumping power and mass flow rate of all the other configurations of smart user are presented in the Appendix B.

As it concerns the branched DHN, the variation in the pumping power consumption and in the circulating mass flow rate are shown respectively Figure2.23 and in Figure2.24.

As already said, the presence of the smart user consists in the installation of a distributed generation systems at the user side. As the DGS starts to produce a certain amount of thermal power (*Case 2*) the mass flow rate circulating into the network decreases (see Figure2.24) and, as a consequence, the pumping power consumption decreases (see Figure2.23). Therefore, the pumping power consumption it reduces from the design point (*Case 1*) down to reaching the minimum value – equal to about 50 % – at the hydraulic equilibrium point (*Case 5*) which occurs when the thermal production is equal to 1˙350 kW. From this case, the pumping power trend increases with the increase in the DGS thermal production up to reach its maximum value, equal to about 214 % with respect to the design point, in *Case 7* (namely the configuration in which the smart user IDN10 fulfill the entire thermal needs of the network). On the other hand, instead, the mass flow rate has a decreasing trend with the increase in the heat production which occurs in *Case 2* up to *Case 3* in which the minimum value, consisting in a decrease of about 25 %, is reached. As aforementioned, from the *Case 3* (corresponding to the self-consumption configuration of the network), the value of the mass flow rate circulating within the DHN is kept constant with the increase of the heat production, up to the *Case 7*.

FIGURE 2.23: VARIATION OF THE DHN PUMPING POWER IN THE CASE OF SMART USER IDN10 FOR THE BRANCHED DHN.

FIGURE 2.24: VARIATION OF THE DHN MASS FLOW RATE IN THE CASE OF SMART USER IDN10 FOR THE BRANCHED DHN.

Finally, as was previously highlighted, each case defined and analyzes represents a specific setting of the district heating network. Therefore, to better understand these differences, the scheme related to each one of the seven cases will be presented in the following.

First of all, as it concerns the Case 1, namely the design configuration of the DHN, it has to be highlighted that the corresponding network setting is the one presented in the previous Figure2.12.

With respect to the Case 2, the network setting is the one show in Figure2.25. As can be noted from the figure, the main differences with the Case 1 consists in the critical user. In fact, in Case 2, the new critical user is the one identified with the IDN17, and the corresponding critical path is the one show in red color in the figure. Furthermore, the direction of the flow within the DHN pipelines has been highlighted in order to better understand the differences between each case.

As it concerns the Case 3, whose network setting is presented in Figure2.26, it can be observed that, some pipes are considered virtually closed (in black color). In this configuration, in fact, the thermal power produced by the distributed generation systems at the smart user side is equal to the thermal need of the user itself. It means that there is no introduction of thermal power into the DHN.

The network setting of the Case 4, which represents the SDHN in the case of the thermal power introduced into the network by the smart user is lower than the one of the hydraulic equilibrium point, is shown in Figure2.27Figure 2.. As can be noted from the figure, there is a pipes subsequence (in green color) in which a reverse flow occurs. This is due to the fact that, from this case, the smart user starts to feed the DHN. Furthermore, it has to be observed that this network setting corresponds also to the one of Case 5, namely the hydraulic equilibrium in the presence of the smart user. The thermal power produced by the smart user IDN10 in Case 4 and in Case 5, in fact, is sufficient, in

addition to the self-consumption, to fulfill only a small part of the network demand. In these two cases, the major contribute is due to the thermal power station production.

A quite different situation occurs in Case 6, whose network setting is presented in Figure2.28Figure 2.. As can be noted from the figure, in fact, due to the greater amount of thermal power produced by the smart user, the reverse flow pipes are more than in the previous cases. It means that the smart user IDN10 further contributes to the DHN need fulfillment.

The last network setting, related to the Case 7, is presented in Figure2.29. In this case the only energy source is represented by the smart user and, therefore, the thermal power station is shutdown. This involves that the pipes from the thermal power station to the district heating network are considered as closed (in black color) and, as a consequence, since only the smart user provide for the need fulfillment, some other reverse flow occur with respect to the design case (pipes in green color).
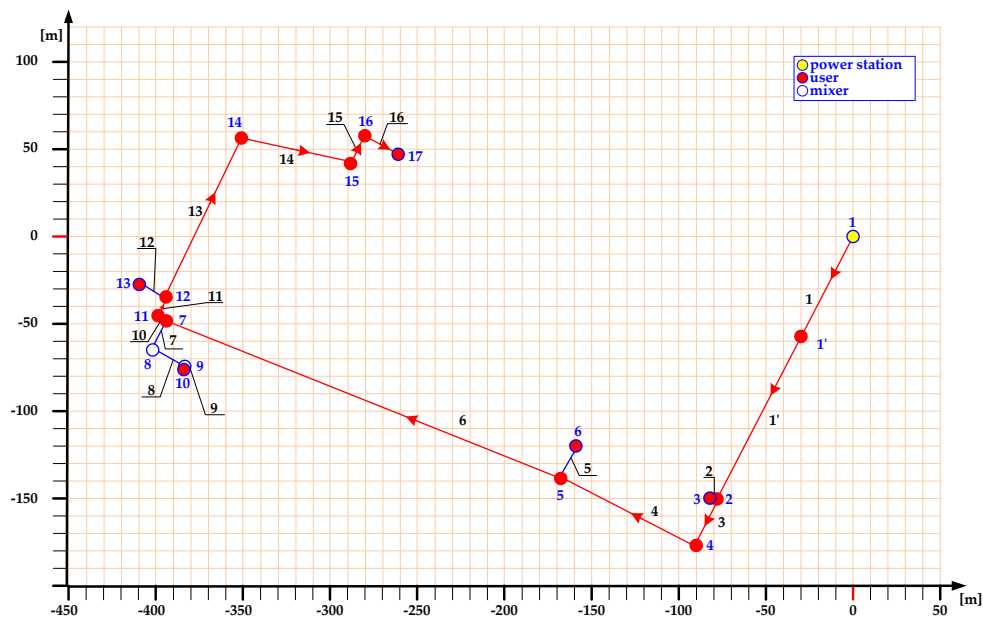
FIGURE 2.25: NETWORK SETTING OF THE BRANCHED DHN IN CASE 2 (IN RED COLOR THE CRITICAL PATH).
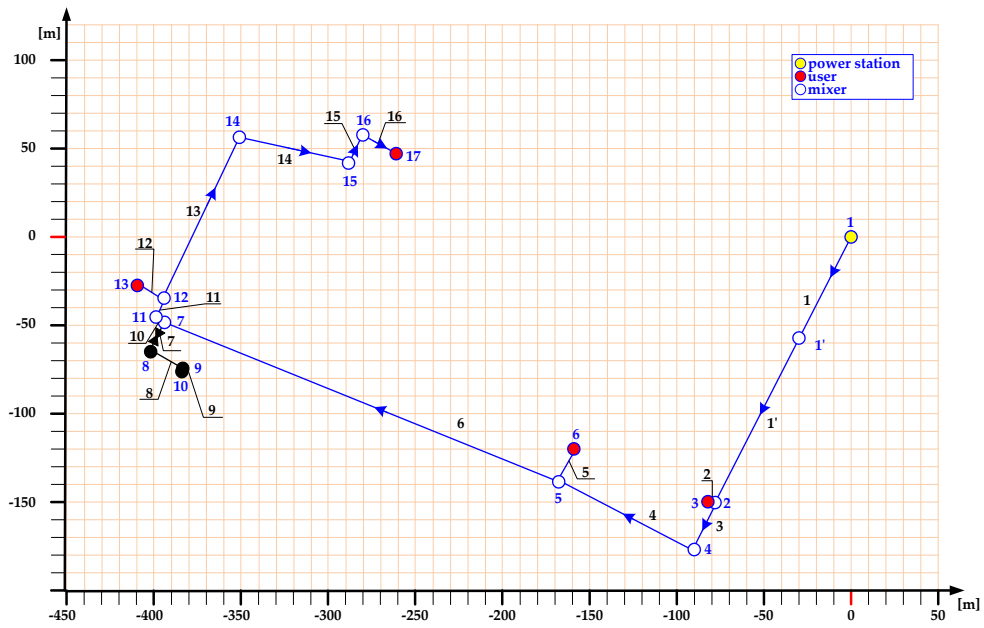
FIGURE 2.26: NETWORK SETTING OF THE BRANCHED DHN IN CASE 3 (IN BLACK COLOR THE CLOSED PIPES).
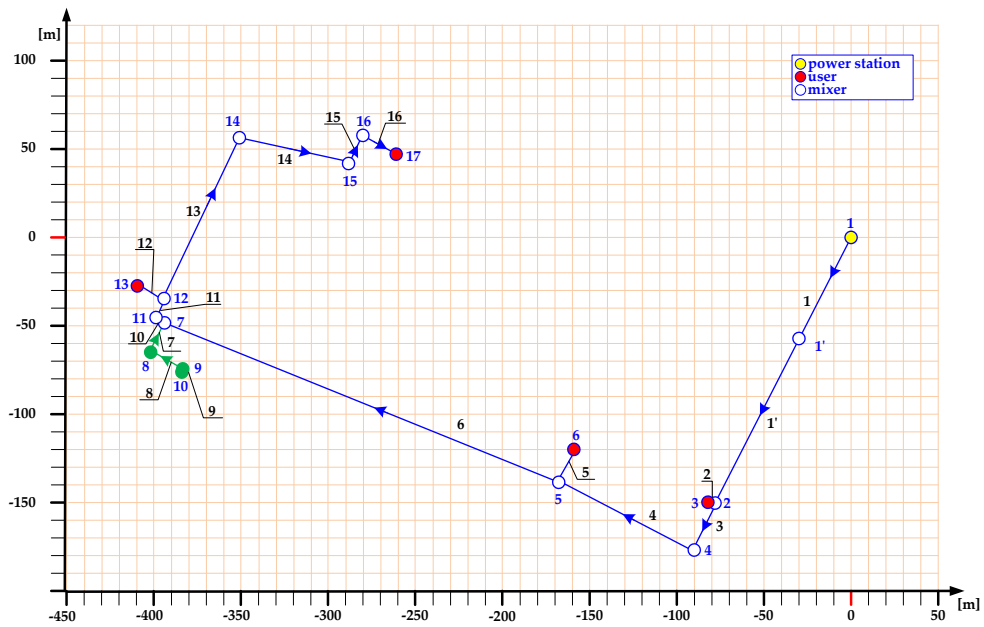
FIGURE 2.27: NETWORK SETTING OF THE BRANCHED DHN IN CASE 4 AND CASE 5 (IN GREEN COLOR THE REVERSE FLOW PIPES WITH RESPECT TO THE DESIGN CASE).
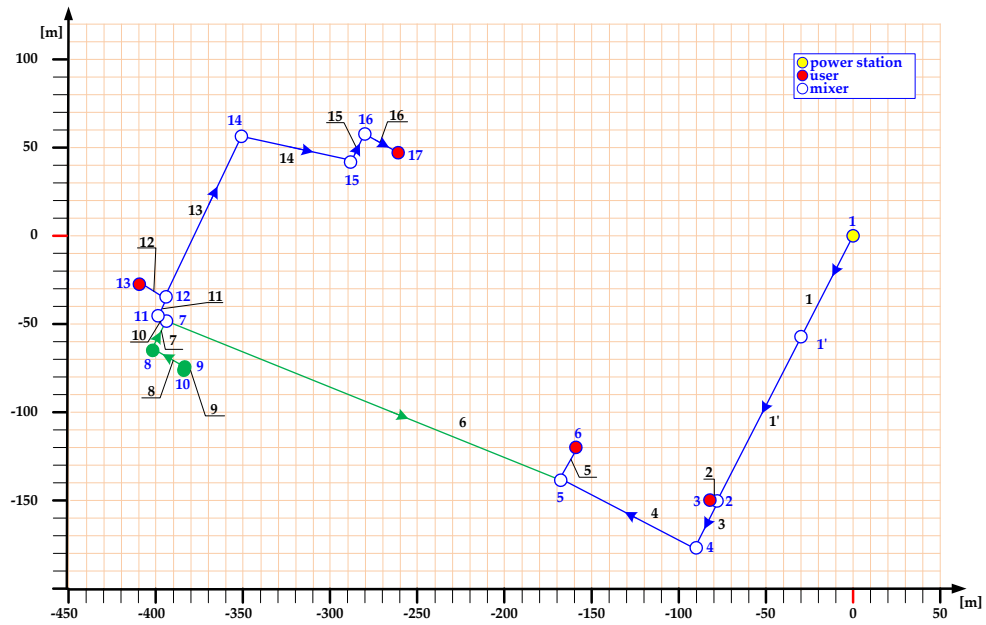
FIGURE 2.28: NETWORK SETTING OF THE BRANCHED DHN IN CASE 6 (IN GREEN COLOR THE REVERSE FLOW PIPES WITH RESPECT TO THE DESIGN CASE).
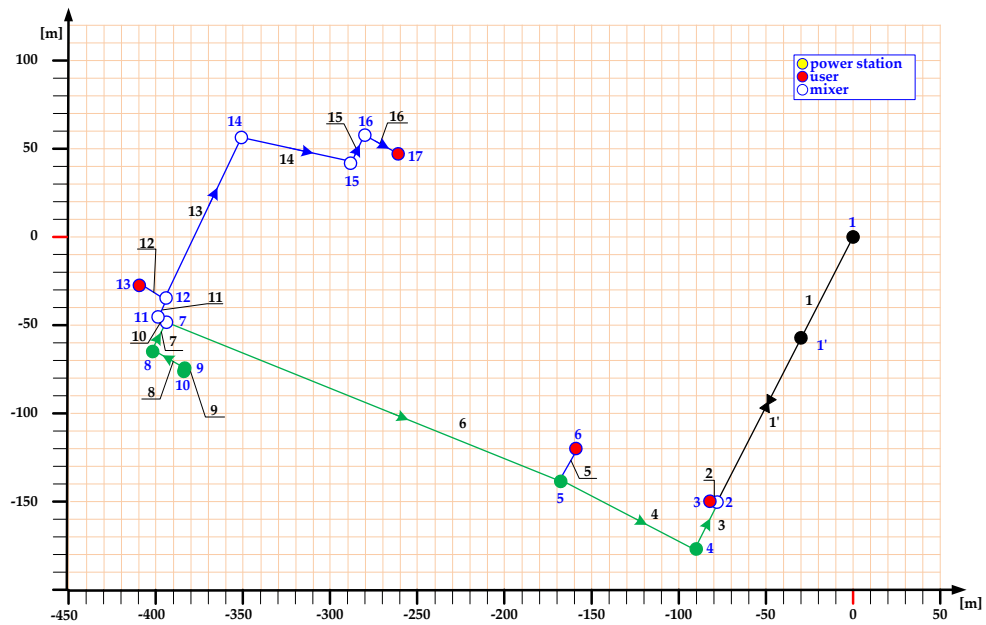
FIGURE 2.29: NETWORK SETTING OF THE BRANCHED DHN IN CASE 7 (IN GREEN COLOR THE REVERSE FLOW PIPES WITH RESPECT TO THE DESIGN CASE, IN BLACK COLOR THE CLOSED PIPES).

The results of the ring DHN management in the case of smart user IDN10 in terms of pumping power and mass flow rate changes are presented respectively in Figure 2.30Figure 2. and in Figure 2.31. From the figures, it can be observed that, starting from the design operation (*Case 1*), the self-consumption point (*Case 3*) – which determines the transition from the traditional to the smart district heating network – occurs for a value of the total thermal power produced by the smart user equal to 825 kW, according to the thermal design needs of the considered users (see Figure 2.9). In this case, the pumping power and the mass flow rate values are respectively equal to about 54 % with respect to the design operation. From this case, the mass flow rate circulating within the networks pipelines remain constant while the pumping power further decrease reaching the minimum value, equal to about 52 %, in correspondence hydraulic equilibrium point (*Case 5*) in which the produced thermal power is equal to 1'290 kW. Therefore, the pumping power increases reaching a maximum value, equal to about 235 % with respect to the design case, when the smart user is the only heat source for the entire DHN fulfillment.
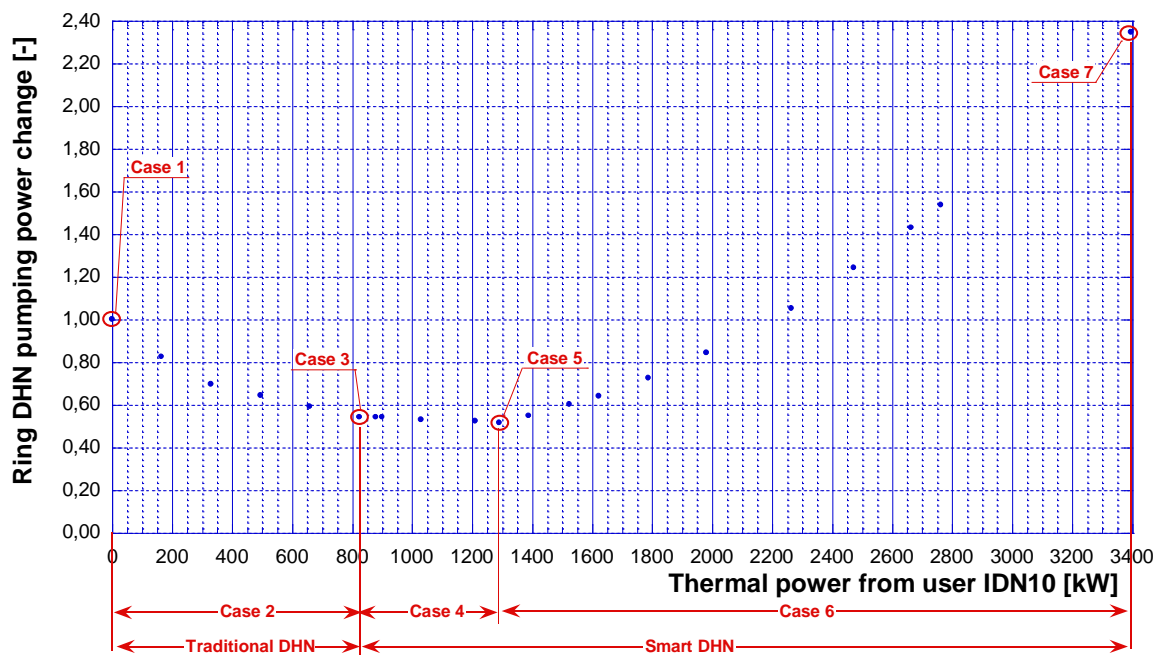
FIGURE 2.30: VARIATION OF THE DHN PUMPING POWER IN THE CASE OF SMART USER IDN10 FOR THE RING DHN.
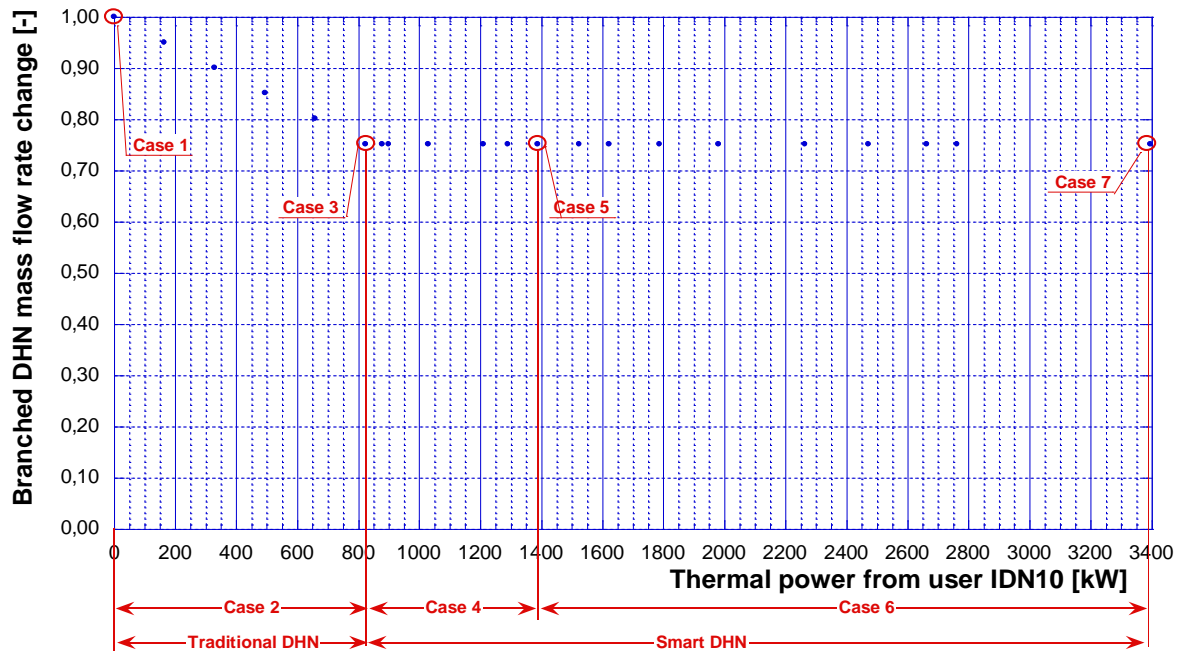
FIGURE 2.31: VARIATION OF THE DHN MASS FLOW RATE IN THE CASE OF SMART USER IDN10 FOR THE RING DHN.

The results of the carried-out analysis, in terms of design and prosumer evaluation and management of the DHN, together with the main characteristics of the developed district heating networks in terms of geometry and thermal energy users' needs, show that in both the branched and the ring network the critical user is the same (identified with the IDN10). Moreover, a further consideration resulting from the analysis concerns the fact that – in the ring network – the smart user IDN10 correspond also to the further one with respect to the thermal power station. In the case of branched district heating network, instead, the further user is the one identified with the IDN17. Finally, in both cases, the critical user differs from the one characterized by the higher thermal need which corresponds, according to the input presented in Figure 2.9, with the node IDN6.

As for the branched DHN, the network settings are presented also for the ring network with respect to each defined case.

As it concerns the Case 1, even in this case, the setting of the network is the one presented in Figure 2.13 since it represents the design operation of the DHN.

As it regards the Case 2, the redistribution of the mass flow rate, along with the presence of the smart user (IDN10) involves a different setting of the network. In detail, as can be noted from Figure 2.32, this led to a different critical user, with respect to the design case, which is individuated by the user IDN6. The corresponding critical path is shown (in red color) in the figure.

The network setting of Case 3, indeed, is presented in Figure 2.33. In this case, representing the self-consumption point, the smart user does not provide to fulfill the district heating network needs but only that of itself. therefore, it follows that the pipelines from the smart user to the network (in black color in the figure) can be considered closed.

As it concerns the Case 4, as for the previous case of branched DHN, even in this case the corresponding network setting is the same of the Case 5. To this respect, as is shown in Figure 2.34, a reversion in the flow direction occurs in some pipes (in green color) due to the fact that the smart user starts to introduce a given quantity of thermal power into the network. However, the thermal power station contributes for the greater part to the users needs fulfillment.

In the Case 6, whose corresponding network setting is presented in Figure 2.35, due to the higher quantity of thermal power produced by the smart user, the reverse flow pipes increase (in green color) and it means that the smart user further contributes to the fulfilment of the user demand.

The last Case 7, indeed, which represents the case of the smart user as only thermal power sources, corresponds to the network setting presented in Figure 2.36. In this case, the thermal power station is completely shut down since the entire demand of the network is covered by the thermal power produced by the smart user. It follows that the pipe from the power station to the closer node (namely to the DHN) can be considered closed.
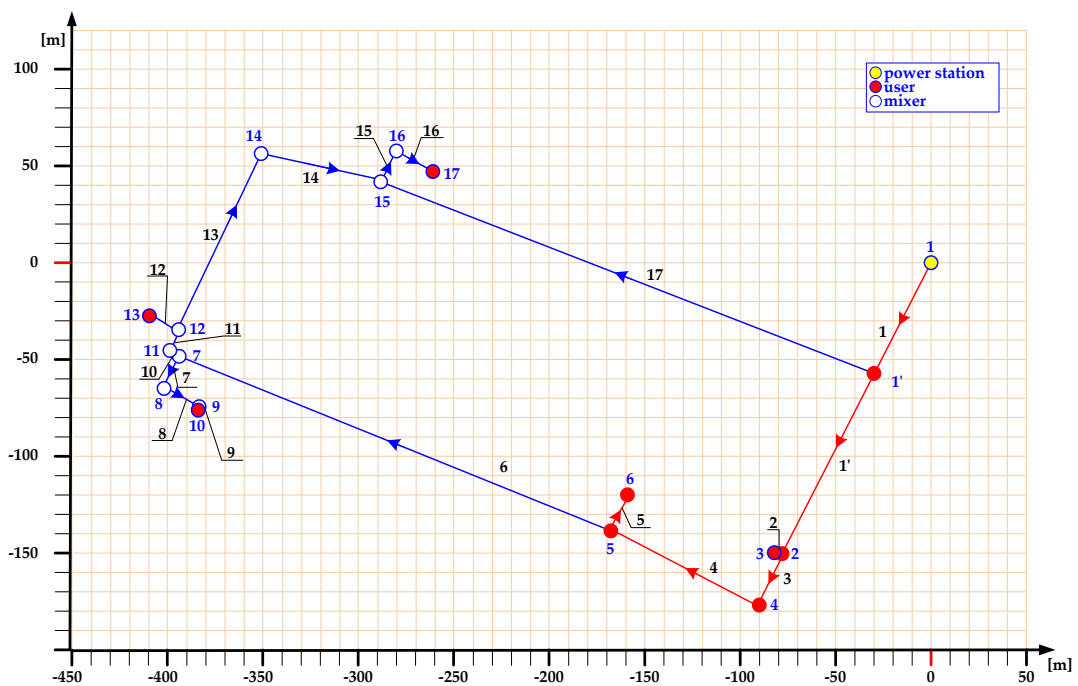
FIGURE 2.32: NETWORK SETTING OF THE RING DHN IN CASE 2 (IN RED COLOR THE CRITICAL PATH).
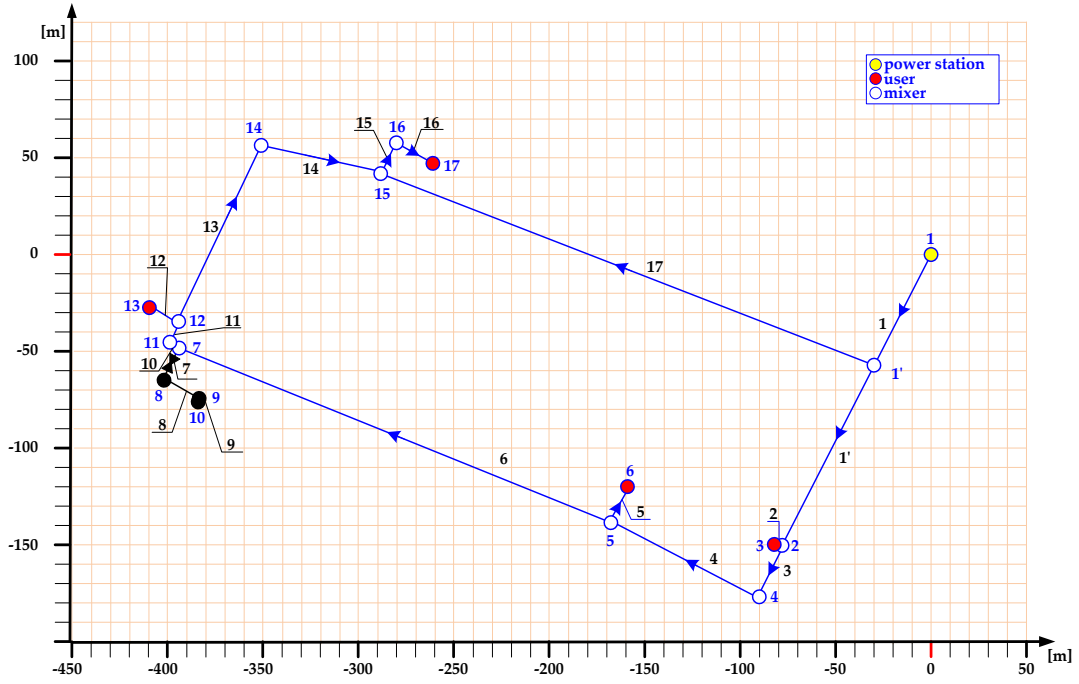
FIGURE 2.33: NETWORK SETTING OF THE RING DHN IN CASE 3 (IN BLACK COLOR THE CLOSED PIPES).
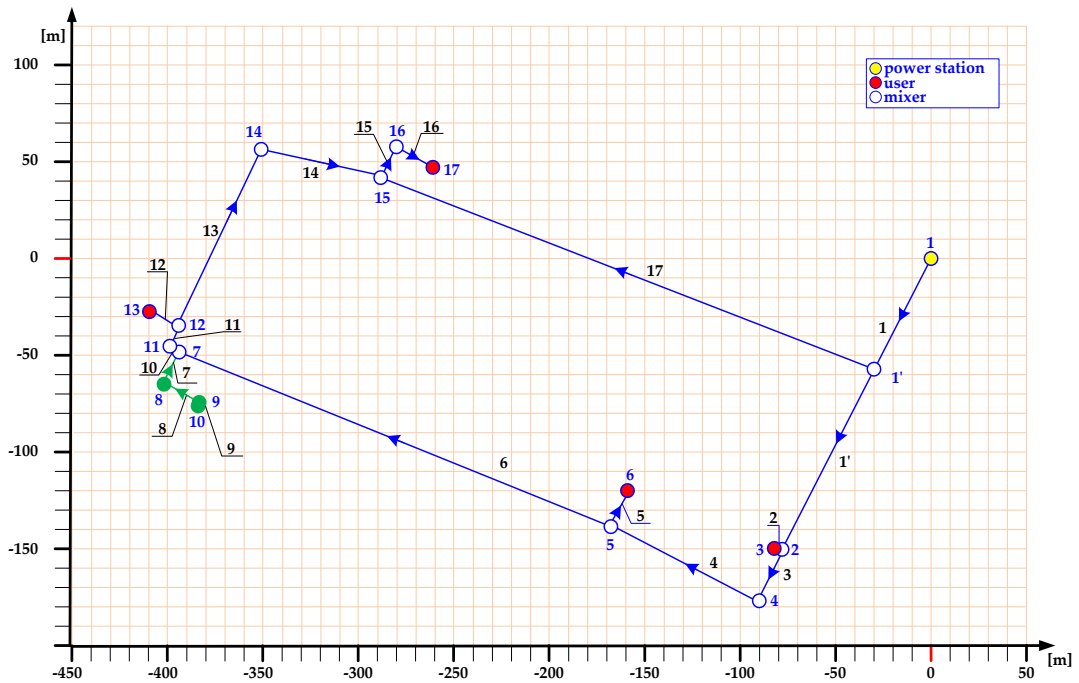
FIGURE 2.34: NETWORK SETTING OF THE RING DHN IN CASE 4 AND IN CASE 5(IN GREEN COLOR THE REVERSE FLOW PIPES WITH RESPECT TO THE DESIGN CASE).
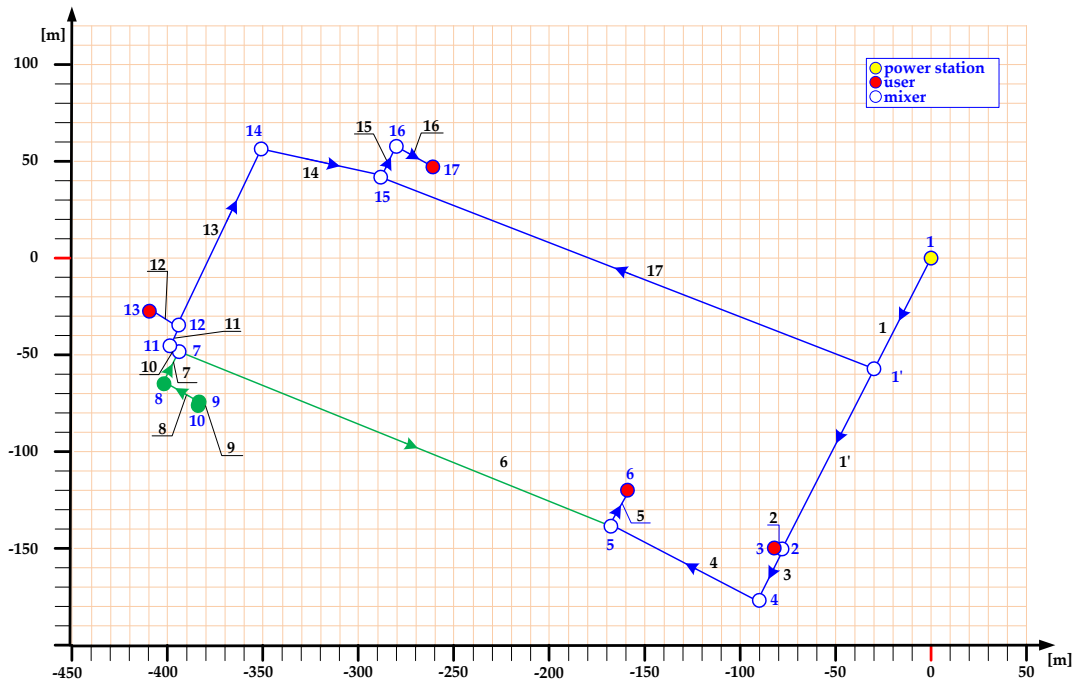
FIGURE 2.35: NETWORK SETTING OF THE RING DHN IN CASE 6 (IN GREEN COLOR THE REVERSE FLOW PIPES WITH RESPECT TO THE DESIGN CASE).
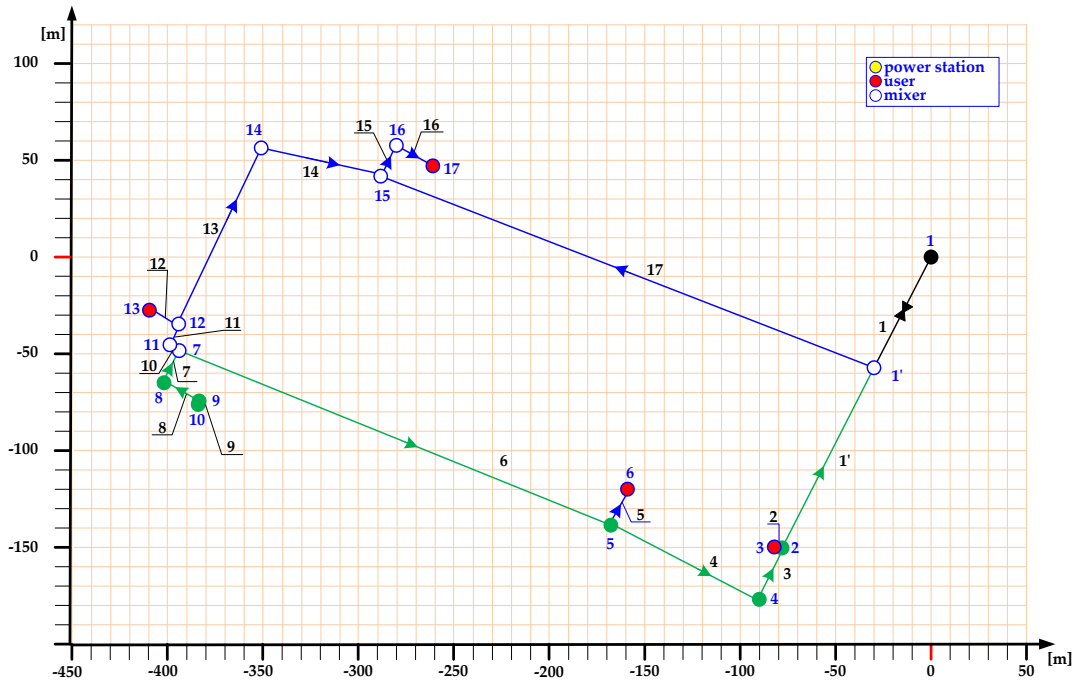
FIGURE 2.36: NETWORK SETTING OF THE RING DHN IN CASE 7 (IN GREEN COLOR THE REVERSE FLOW PIPES WITH RESPECT TO THE DESIGN CASE, IN BLACK COLOR THE CLOSED PIPES).

The carried-out analysis has highlighted the management of the two considered small district heating networks for all the cases in which a user is converted into a smart user. To this respect the main performance parameters – namely the pumping power and mass flow rate – have been considered and analyzed to understand how they vary with the variation of the thermal power produced by the smart user. The results show that the most significant reduction in the pumping power occurs in the case of the critical user – so defined on the basis of the design operation analysis – is converted into smart user. In particular, this is verified for the hydraulic equilibrium configuration, that is the optimized operation of the network, in both the considered test cases. On the other hand, the mass flow rate maximum decrease occurs in the case of the smart user characterized by the higher thermal need, however a good result is reached also in the case of the critical user chosen as smart user. In the light of these results, the critical user can be identified as the more suitable user to be converted into a smart one.

In support of the results obtained with this analysis, in the next and last paragraph of this chapter, the developed tool has been also used to analyze a medium size district heating network.

2.4 Case study: university campus

The results of the analysis presented in the previous section by considering two simplified district heating networks representative of the two typologies, led to the conclusion that the critical user is the one more suitable to be converted into a smart user.

With the main purpose of validating this result, a further investigation, similar to the one presented in the previous section, has been done. To this respect, a small/medium size network, consisting in a portion of and exiting network located within a university campus in the North of Italy has been considered. The district heating network provides to the fulfilment of the users thermal demand for the only space heating. The layout of the considered network, in which the users typology are represented along with their identification number, is shown in Figure 2.37.
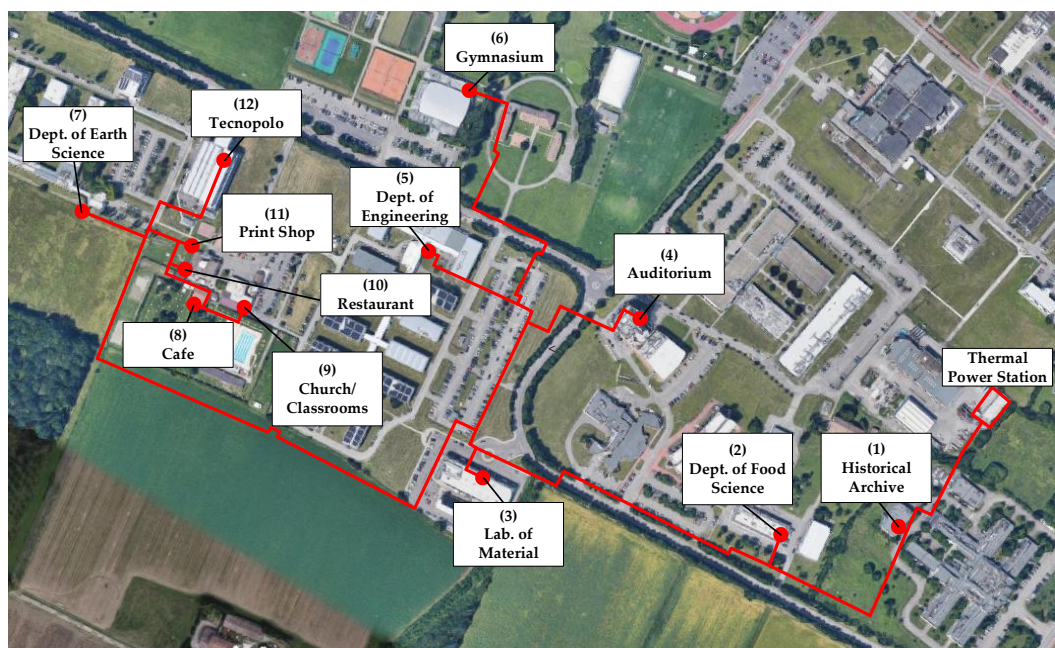
FIGURE 2.37: SCHEME OF THE DH NETWORK WITHIN THE UNIVERSITY CAMPUS.

2.4.1 Hypothesis and assumptions

Before entering into the detail of the carried-out analysis, in this section the main hypotheses and assumptions are presented.

First of all, as aforementioned, the considered district heating network is composed by twelve users each one characterized by a design thermal need, as shown in Figure 2.38. As can be noted from the figure, the thermal needs in the design condition are very different depending on the user, varying from a minimum value equal to about 25 kW, in correspondence of the user ID8, to a maximum value equal to about 4˙500 kW, in correspondence of the user ID5. The total thermal power required by the DHN user is equal to 11˙511 kW.
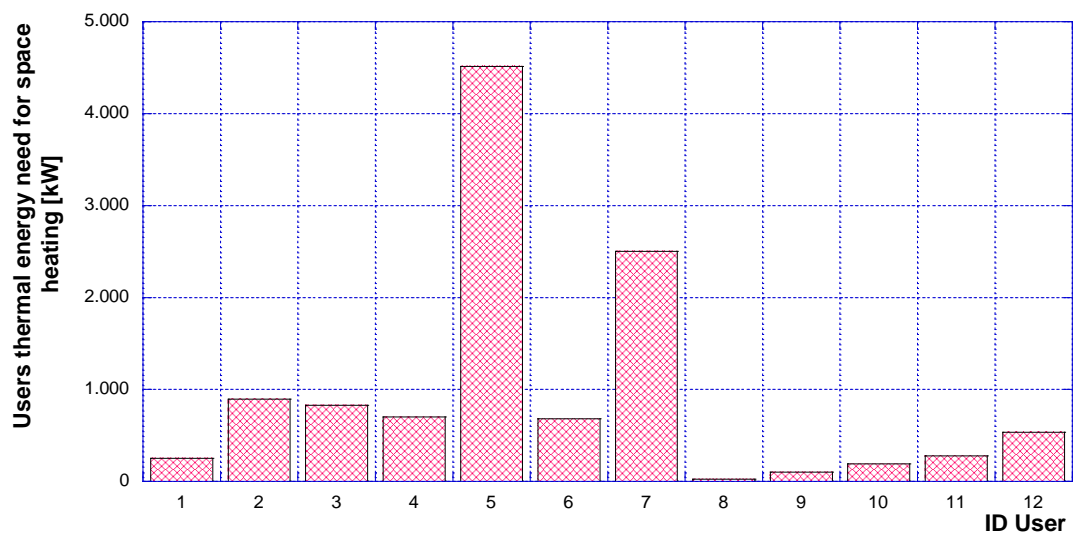
FIGURE 2.38: DESIGN THERMAL NEEDS OF THE DHN USERS.

As it concerns the thermal power station at the service of the whole district heating network, it is composed by a total of five boilers. More in detail, the total installed thermal power, equal to 17˙500 kW, is almost equally shared between the five boilers. To this respect, each boiler is characterized by a design thermal power equal to about 3˙500 kW. As it regards the design thermal efficiency, instead, it is not the same for each boiler. In fact, it ranges between a minimum value equal to 90.4 % to a maximum value equal to 95.4 %. In more detail the design thermal power and the design thermal efficiency values of each boiler are listed in Table 2.3.

TABLE 2.3: DESIGN PARAMETERS OF EACH BOILERS.

Boiler	Thermal power	Thermal efficiency
Boiler #1	3˙500 kW	95.4 %
Boiler #2	3˙500 kW	95.4 %
Boiler #3	3˙520 kW	92.4 %
Boiler #4	3˙520 kW	92.4 %
Boiler #5	3˙489 kW	90.4 %

Furthermore, the thermal power station is also equipped with a pumping power station which is composed by three identical pumps arranged in parallel. A schematic representation of the thermal power station is presented in Figure 2.39.
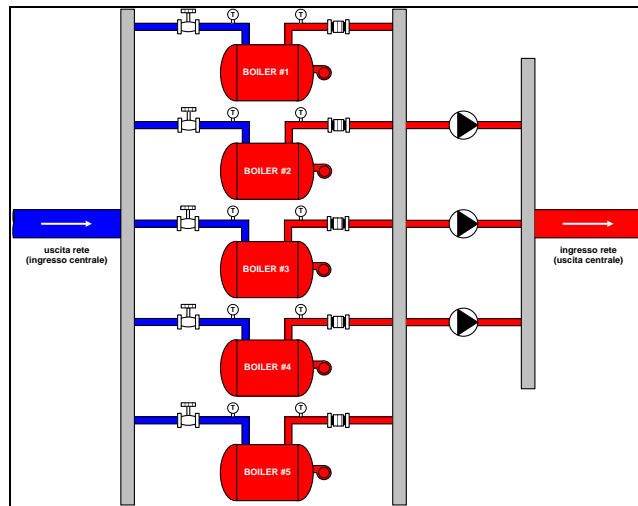
FIGURE 2.39: SCHEMATIC OF THE THERMAL POWER STATION SERVING THE DHN.

As for the previous analysis, even in this case the investigation of the considered network has been done with the software IHENA. The geometric representation of the network within the software IHENA is shown in Figure 2.40.
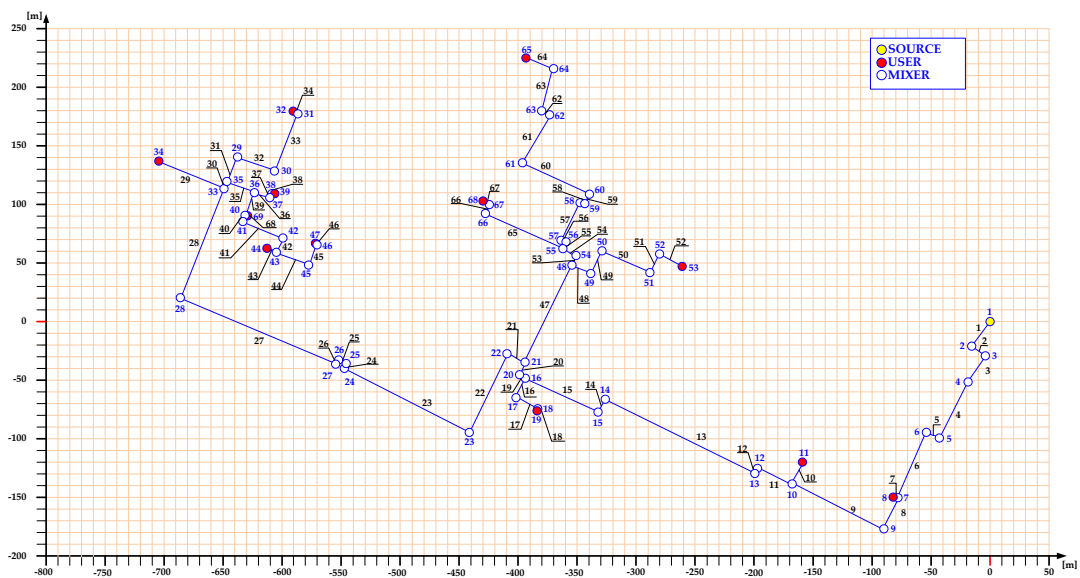
FIGURE 2.40: UNIVERSITY CAMPUS DHN IMPLEMENTATION WITH SOFTWARE IHENA.

As can be observed from the figure, the university campus district heating network consist of a total of 69 nodes and of 68 pipes. As it regards the nodes, they consist of a source, namely the thermal power station (in yellow), 12 users (in red) and 56 mixers (in white). The correspondence between the identification number of the user shown in Figure 2.37 and the identification number of each node shown in Figure 2.40 is listed in Table 2.4Table 2. along with the user name.

TABLE 2.4: USERS ID AND IDN IHENA.

User typology	ID User	IDN IHENA
Historical archive	1	8
Dept. of Food Science	2	11
Lab. of Material	3	19
Auditorium	4	53
Dept. of Engineering	5	68
Gymnasium	6	65
Dept. of Earth Science	7	34
Cafe	8	44
Church / classrooms	9	47
Restaurant	10	69
Print shop	11	39
Tecnopolo	12	32

Moreover, among the main assumptions, in Table 2.5 are listed the inlet and outlet temperature of both the primary and secondary circuits of the user substation. In particular, as for the primary circuits, it has been assumed a feed temperature equal to 80 °C and a return temperature equal to 60°C. Conversely, as it regards the secondary circuit, the feed temperature has been hypothesized equal to 40 °C and the return temperature equal to 55 °C.

TABLE 2.5: INLET AND OUTLET TEMPERATURE OF THE PRIMARY AND SECONDARY **CIRCUITS.**

Parameter	Units	Value
Inlet temperature of the primary circuit	[°C]	80
Outlet temperature of the primary circuit	[°C]	60
Inlet temperature of the secondary circuit	[°C]	40
Outlet temperature of the secondary circuit	[°C]	55

Finally, with respect to the smart user evaluation, the main hypotheses at the basis of the analysis are:

- only one smart user is considered at a time;
- along the DHN pipelines have not been considered additional pumps and/or valves, with the exception of the additional pumping systems at each substation of the considered smart user;

- both the thermal power station and the considered smart user are characterized by the same supply pressure which is set in order to keep constant the minimum pressure drop at the user substation at a value equal to 0.50 bar;

In the following section the results of the analysis will be presented and discussed. According to the previous analysis, even in this case, the results are presented for the three level of investigation: (*i*) design operation, (*ii*) smart user evaluation and (*iii*) network management in the presence of a smart user.

2.4.2 Design operation

The first level of the analysis concerns the investigation of the design operation of the whole network. To this respect, the results of the analysis show that in design condition the total thermal power produced by the thermal power station is equal to 11˙657 kW, 11˙511 kW of which are produced for the DHN users fulfilment and the remaining 146 kW are due to the heat dissipations along the networks pipelines.

As it regards the mass flow rate circulating within the DH network, it is equal to about 137 kg/s. This amount is distributed among the DHN users as presented in Figure 2.41. From the figure it can be observed that, according to the thermal needs assumed and presented in Figure 2.38, the minimum value, equal to about 0.30 kg/s corresponds to the user identified with IDN44. On the other hand, the maximum value of the mass flow rate in design condition equal to about 54 kg/s occurs in correspondence of the user IDN68.
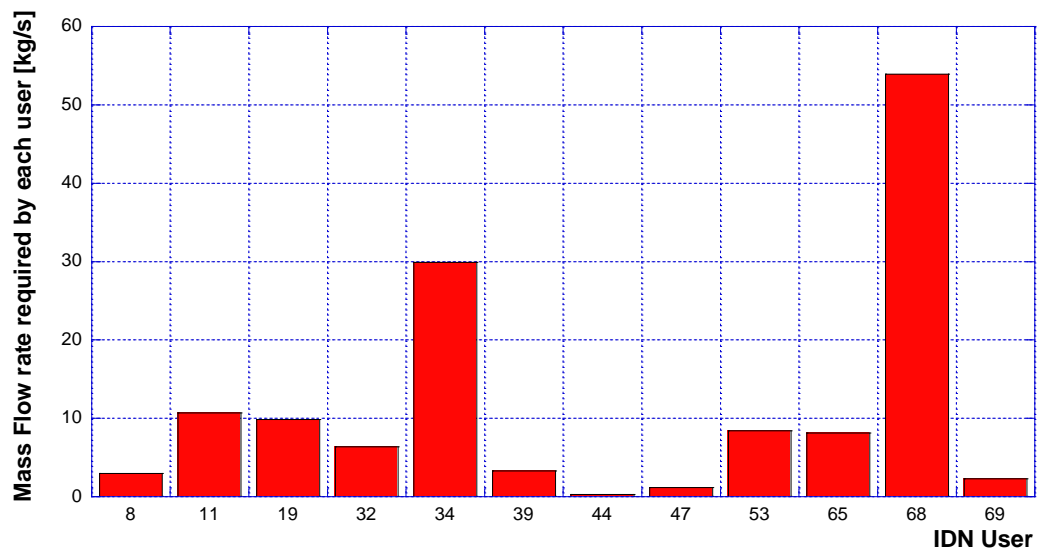
FIGURE 2.41: MASS FLOW RATE DISTRIBUTION BETWEEN THE DHN USERS.

Moreover, another result concerns the pressure drops of each user of the DH network presented in Figure 2.42. To this respect, it can be observed that, in design condition, the minimum pressure drop, equal to about 0.50 bar, occur in correspondence of the user IDN68. For this reason, the user identified with the IDN68 results to be the critical user of the considered district heating network.

The corresponding critical path, from the thermal power station to the critical user for the considered DHN is shown in Figure 2.43 together with the flow direction of the water within the DHN feed line.
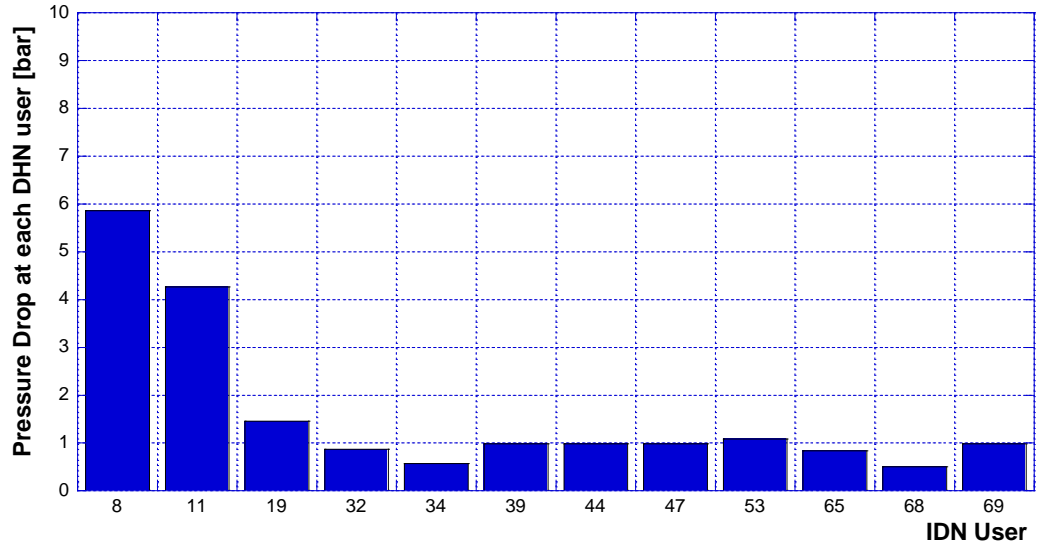
FIGURE 2.42: PUMPING POWER CONSUMPTION OF EACH DHN USERS.
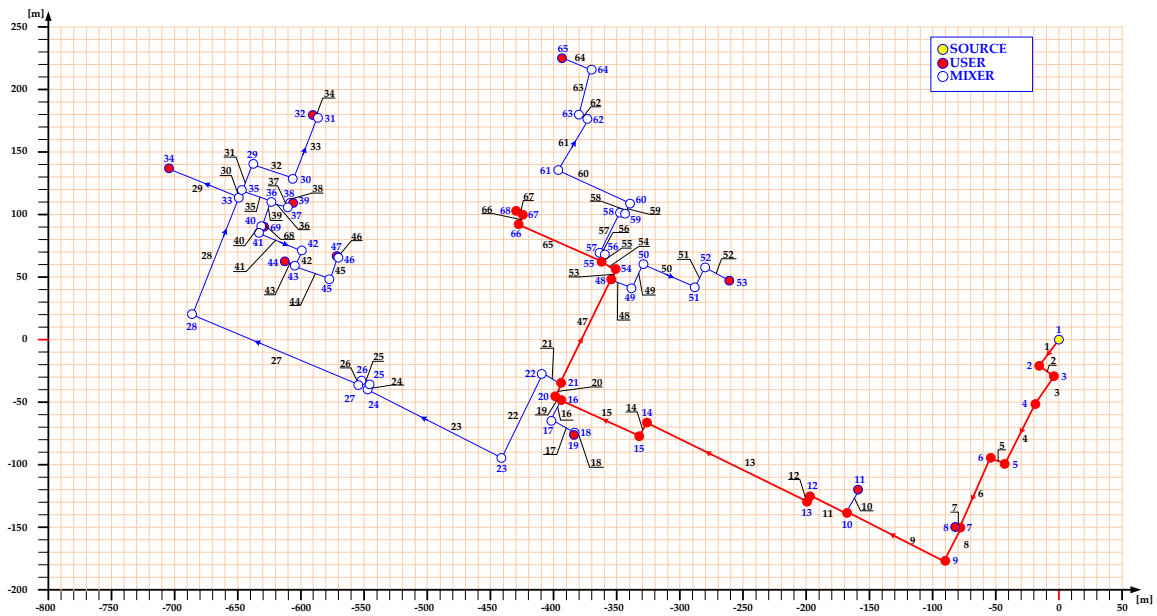
FIGURE 2.43: CRITICAL PATH AND FLOW DIRECTION OF THE WATER WITHIN THE SUPPLY LINE OF THE NETWORK.

In addition, another result concerns the pumping power consumption, which results to be equal to about 130 kW in the design operation.

Finally, as it concerns the thermal power station, the results of the DHN design operation shown that the supply pressure is equal to 12.32 bar while the expansion vessel pressure is equal to 4.00 bar.

The main performances parameters resulting from the design investigation are summarized in Table 2.6.

TABLE 2.6: MAIN PARAMETERS OF THE DESIGN ANALYSIS.

Parameter	Units	Value
Inlet mass flow rate	[kg/s]	137
Thermal power supplied to the users	[kW]	11˙511
Thermal power from the power station	[kW]	11˙657
Heat losses	[kW]	146
Pumping power	[kW]	130
Supply pressure	[bar]	12.32
Expansion vessel pressure	[bar]	4.00

2.4.3 Smart user evaluation

Within the main aim to identify which one of the users belonging to the DHN is more suitable to be converted into smart user, and consequently how the choice of the position affects the performances of the whole network, the second level of the carried-out investigation concerns the evaluation of the smart user.

The analysis has been conducted by implementing the network within the software IHENA including the specifically developed additional tool and, therefore, the obtained results are related to the optimal hydraulic equilibrium of the DHN. This means that the both the mass flow rates circulating within the network and the pressures distribution depend only on the geometry of the network itself.

A first result concerns the variation of the pumping power consumption which is shown in Figure 2.44 with respect to the design operation. The results show that, with respect to the design operation, the pumping power is reduced for all the considered configurations of smart user. To this respect, the minimum reduction, equal to about 20 %, occurs in the case the user identified with IDN8 is converted into smart user. The maximum pumping power reduction, instead, occurs in the case of smart user IDN68 (namely the critical user). In this case, the pumping power is equal to about the 15 % of the design value.

Moreover, as was expected, the presence of a smart user within the DHN involves a reallocation of the circulating mass flow rate and, as a consequence, of the direction of the water flow within the networks pipelines. This reallocation depends on the choice of the user converted into a smart user.

To this respect, the variation of the mass flow rate resulting from the smart user evaluation is presented in Figure 2.45. As it can be noted from the figure, in the case of smart user IDN47, the

mass flow rate reduction is very low being equal to about 1 %. On the other hand, even in this case, the smart user who minimizes the mass low rate is the one identified with IDN68, namely the critical user. In this configuration, in fact, the mass flow rate is equal to about 60.8 % of the design value.
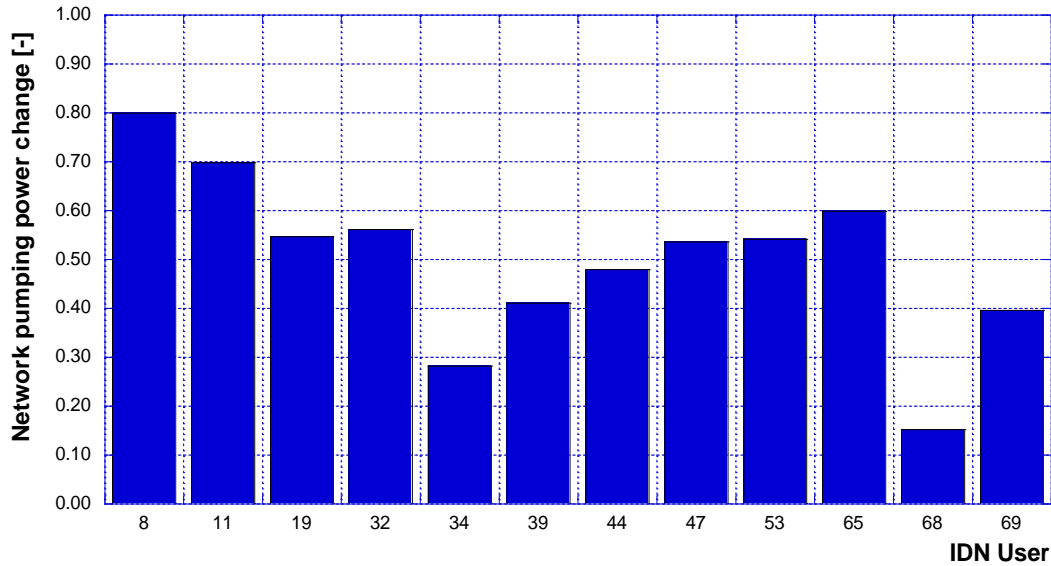
FIGURE 2.44: DHN PUMPING POWER CHANGE FOR EACH SMART USER CONFIGURATION.
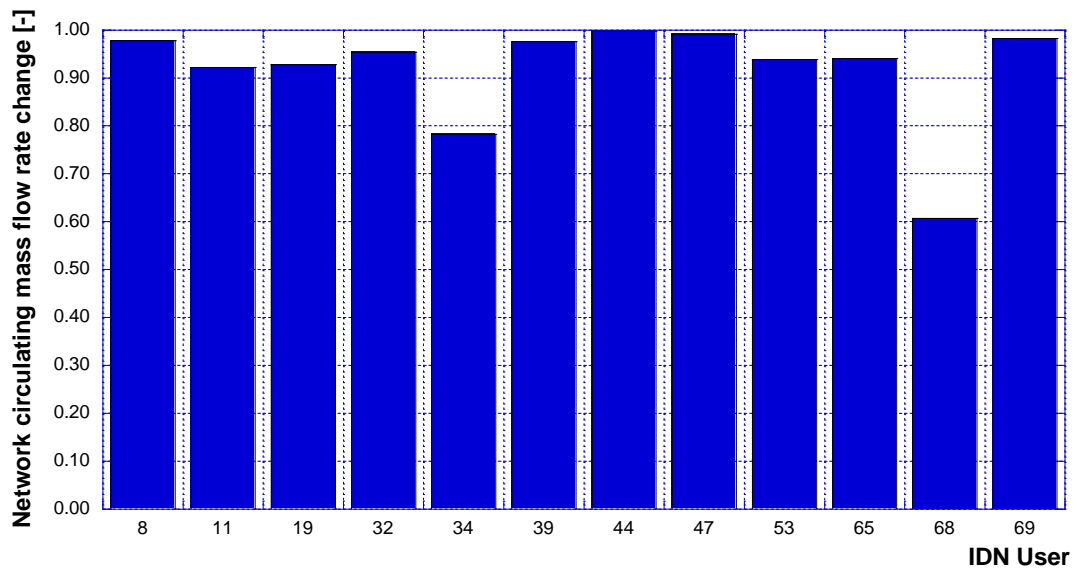
FIGURE 2.45: DHN MASS FLOW RATE CHANGE FOR EACH SMART USER CONFIGURATION.

Another result, presented in Figure 2.46, regards the variation of the supply pressure of each configuration of smart user with respect to the design configuration. On this regard, according to the assumption described in the previous section, it results that the supply pressure of each configuration is lower than the one of the design operations. In particular, as can be noted from the figure, it varies from a minimum value equal to about 49 % of the design value in correspondence of the critical user (IDN68), to a maximum value equal to about 88 % of the design value, in correspondence of the smart user IDN8.
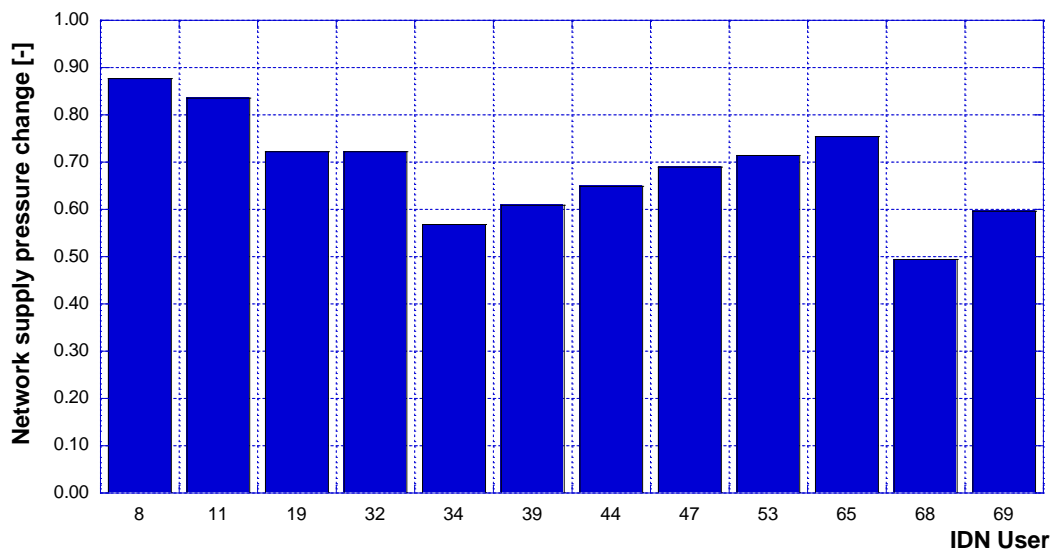
FIGURE 2.46: DHN SUPPLY PRESSURE CHANGE FOR EACH SMART USER CONFIGURATION.

The last result of the smart user analysis concerns the distribution efficiency of each configuration, namely the ratio between the thermal power required by the user and the thermal power provided by the thermal power station, again presented with respect with the design point. The values obtained from the investigation are shown in Figure 2.47. As can be noted from the figure, the distribution efficiency of the network remains very close to the one resulting from the design operation. In fact, it ranges between a minimum value equal to about 99.20 % – in the case of smart use IDN68 – to a maximum value equal to about 99.99 % in the case of smart user IDN44.
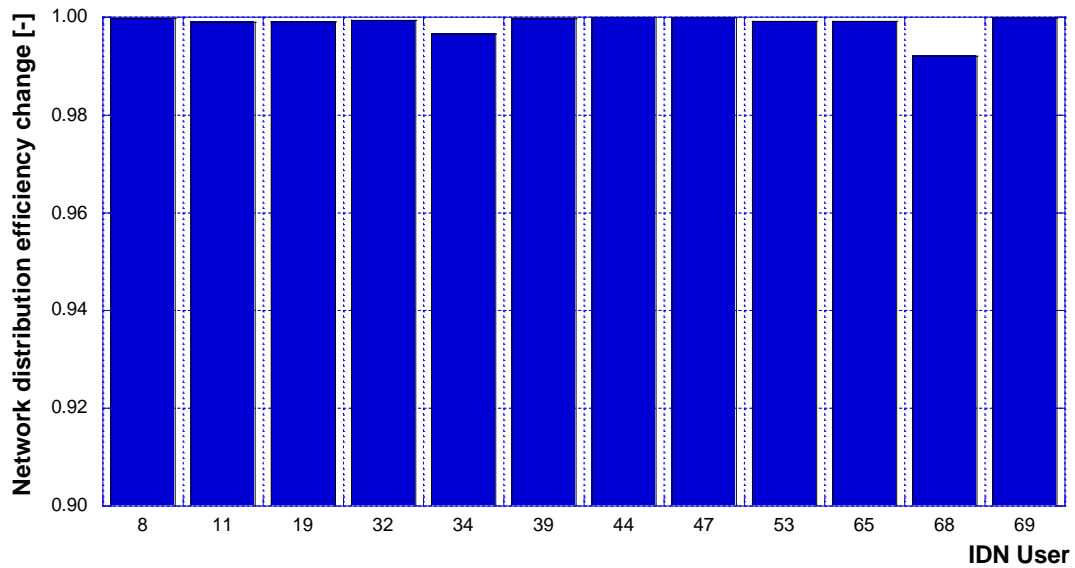
FIGURE 2.47: DHN DISTRIBUTION EFFICIENCY CHANGE FOR EACH SMART USER
CONFIGURATION.

2.4.4 Management of the Smart District Heating Network

From the joint analysis of the results obtained from the analysis of the branched and ring DHNs presented in the previous Section 2.4.2 and of the results obtained from both the design operation and smart user investigations, it can be deduced that the critical user is the most suitable to be converted into smart user. To this respect, in fact, the convenience of this choice can be seen under different point of views which can be summarized as follows:

- in all the analyzed cases the conversion of the critical user into smart user allows to reduce the pumping power consumption of the district heating network. In detail, the maximum reduction occurs at the hydraulic equilibrium point which is defined as the optimized operation of the whole network;
- the conversion of the critical user into smart user allows to minimize (in the case of the university campus DHN) the mass flow rate circulating within the district heating network;
- in the event of the critical user upgrade into smart user, the supply pressure can drop to a minimum value which is also implies in the maintenance costs.

For all the aforementioned considerations, for this case study the management of the district heating network will be presented for the only configuration of smart user IDN68, namely the critical user.

To this respect, the main performance parameters are presented from Figure 2.48 to Figure 2.50 respectively representing the variation – with respect to the design point – of the pumping power consumption, mass flow rate and supply pressure as function of the thermal power produced by the distributed generation system.
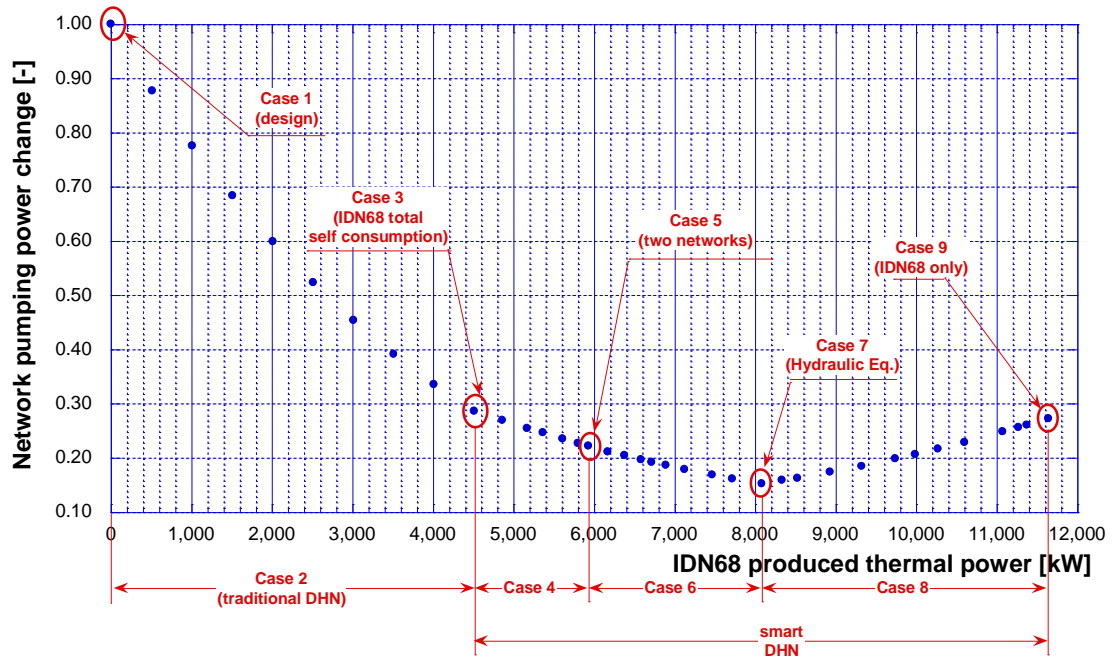
FIGURE 2.48: DHN PUMPING POWER CHANGE IN CASE OF SMART USER IDN68.
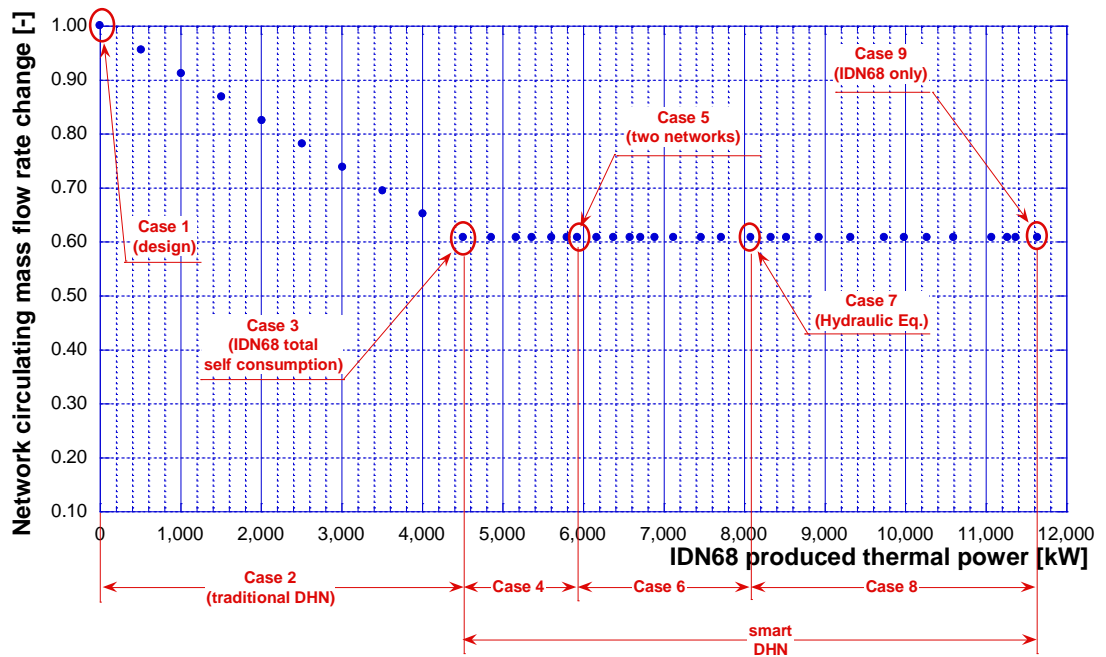
FIGURE 2.49: DHN MASS FLOW RATE CHANGE IN CASE OF SMART USER IDN68.
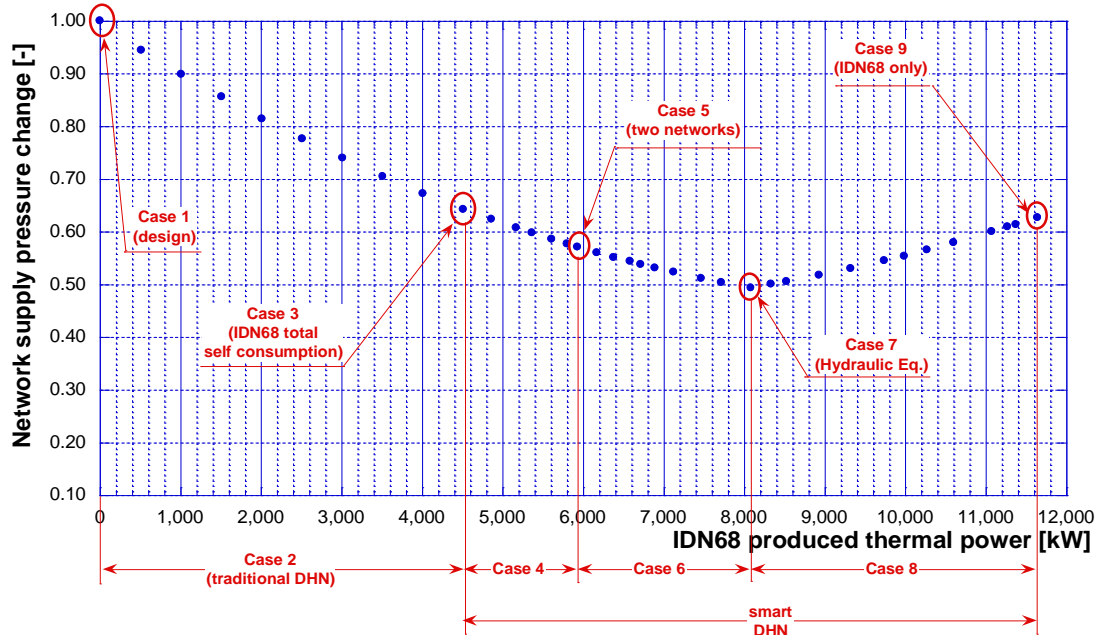
FIGURE 2.50: DHN SUPPLY PRESSURE CHANGE IN CASE OF SMART USER IDN68.

As represented in the figures, from the results can be pointed out nine different cases each of which representing a particular configuration of the district heating network, and therefore, a different management approach. These nine cases, which differs each other on the basis of the thermal power produced by the smart user, are defined as follows:

- Case 1 ($P_{th}68 = 0\ kW$): this configuration represents the design operation of the network as presented in the previous Section 2.4.2, and then the starting point of the evaluation.

- Case 2 ($0\ kW < P_{th}68 < 4515\ kW$): in this scenario, the heat produced by the distributed generator is always lower than the one required by the user itself, namely it consist on the traditional DHN case. However, the distributed generation allows to reduce the thermal power introduced by the thermal power station which results in a reduction of the pumping power (see Figure 2.48), of the mass flow rate circulating within the DHN pipelines (see Figure 2.49) and of the supply pressure (see Figure 2.50).

- Case 3 ($P_{th}68 = 4\dot{}515\ kW$): this configuration represents the self-consumption point, namely the DHN setup in which the heat produced by the DGS is equal to the one required by the user. In this case, the pumping power reduces down to a value equal to about 28.6 %. As it regards the mass flow rate, it has to be underlined that in this configuration, the variation reaches its minimum value, equal to about 60.7 %. From this point on, according to the results presented for the previous cases studies, this value is kept constant with the increase of the thermal power produced by the smart user. The supply pressure, instead, similarly to the pumping power behavior, further decreases reaching a minimum value equal to about 64.3 % of the design value.

79

- Case 4 ($4\dot{}515\ kW < P_{th}68 < 5\dot{}931\ kW$): in this case the thermal production of the distributed generation system exceeds the thermal needs of the user itself. It follows that a certain amount of heat is feed into the network. Therefore, the network become a smart DHN. As expected, as the thermal power introduced into the network increases, the production of the thermal power station decreases. In this case, as aforementioned, the mass flow rate remains constant (see Figure 2.49) while both the pumping power consumption and the supply pressure (respectively in Figure 2.48 and Figure 2.50) decrease with the increase in the thermal power produced by the smart user.

- Case 5 ($P_{th}68 = 5\dot{}931\ kW$): this scenario represents a particular configuration of the network since the thermal power produced by the user IDN68 allows to fulfill the needs of the users IDN68, IDN65 and IDN53. By considering the DHN layout of Figure 2.40, this configuration consists in the closure of the pipe identified with the IDP47 and therefore it is as if there were two different networks, one served by the smart user and one served by the thermal power station.

- Case 6 ($5\dot{}931\ kW < P_{th}68 < 8\dot{}084\ kW$): in this case the thermal power produced by the smart user increases by allowing to fulfill a greater number of users. This configuration, however, involves a change in the flow direction is some pipes of the network.

- Case 7 ($P_{th}68 = 8\dot{}084\ kW$): this scenario represents the hydraulic equilibrium point of the DHN. As defined before, this consists in the optimized operation of the whole network. Furthermore, according to the results presented in the previous section, in this case, the pumping power and the supply pressure reach their minimum values, respectively equal to 15.3 % and 49.4 % of the design value.

- Case 8 ($8\dot{}084\ kW < P_{th}68 < 11\dot{}641\ kW$): in this configuration, the thermal power produced by the smart user further increases as the thermal power station contribution decreases. Therefore, with respect to the hydraulic equilibrium, this specific setting represents a modification leading to an increase in the pumping power and in the supply pressure.

- Case 9 ($P_{th}68 = 11\dot{}641\ kW$): this last case represents the configuration in which the only heat source is represented by the smart user. As a result, the pumping power has further increase with respect to the previous case assuming a value equal to about 27.3 % of the design value. The same behavior occurs also for the supply pressure which increases reaching the value of 62.7 % of the design value.

Each of the presented case involves a different setup of the district heating network. To this respect, for reasons of completeness, the schematic representation of the DHN in each of the presented case are presented in the Appendix C.

In conclusion, the analysis carried-out in this Chapter has been pointed out that, in the conversion of a traditional smart district heating network, the most suitable user to be upgraded into a smart one is the critical user. This choice, in fact, allows to reduce and/or minimized (in the case of optimal operation of the network) the main performance parameters such as the pumping power, mass flow rate, supply pressure and distribution efficiency.

References

[1] Ancona, M. A., Branchini, L., De Pascale, A., & Melino, F. (2015). Smart district heating: Distributed generation systems' effects on the network. Energy Procedia, 75, 1208-1213.

[2] Postnikov, I., Stennikov, V., & Penkovskii, A. (2019). Prosumer in the District Heating Systems: Operating and Reliability Modeling. Energy Procedia, 158, 2530-2535.

[3] Mathiesen, B. V., Lund, H., Connolly, D., Wenzel, H., Østergaard, P. A., Möller, B., ... & Hvelplund, F. K. (2015). Smart Energy Systems for coherent 100% renewable energy and transport solutions. Applied Energy, 145, 139-154.

[4] Brand, L., Calvén, A., Englund, J., Landersjö, H., & Lauenburg, P. (2014). Smart district heating networks–A simulation study of prosumers' impact on technical parameters in distribution networks. Applied Energy, 129, 39-48.

[5] Ancona, M. A., Branchini, L., Di Pietra, B., Melino, F., Puglisi, G., & Zanghirella, F. (2015). Utilities substations in Smart District heating networks. Energy Procedia, 81, 597-605.

[6] Ancona, M. A., & Melino, F. (2013). Analisi di soluzioni tecniche e gestionali che favoriscano l'implementazione di nuovi servizi energetici nelle reti termiche in presenza di sistemi di generazione distribuita. Report Ricerca di Sistema Elettrico, Accordo di Programma Ministero dello Sviluppo Economico–ENEA, Piano Annuale di Realizzazione.

[7] Todini, E. (2008). On the convergence properties of the different pipe network algorithms. In Water Distribution Systems Analysis Symposium 2006 (pp. 1-16).

[8] Todini, E. (2008). Towards realistic extended period simulations (EPS) in looped pipe network. In Water Distribution Systems Analysis Symposium 2006 (pp. 1-16).

[9] Ancona, M. A., Bianchi, M., Branchini, L., & Melino, F. (2014). District heating network design and analysis. Energy Procedia, 45, 1225-1234.

3. Optimal Design of Complex Energy Networks

The simultaneous production of electrical and thermal energy (cogeneration) represents one of the most effective methods for the achievement of the energy efficiency improvement and energy savings targets in a perspective of attention for the environmental preservation [1, 2]. For this reason, the combined heat and power (CHP) systems are largely employed in the context of the complex energy networks, both in commercial and industrial areas as well as in the residential sector. With respect to the residential applications, different typologies of CHP systems can be adopted, such as the internal combustion engines (ICEs), the micro gas turbine (MGT), fuel cell, Stirling engines and micro Organic Ranking Cycle (μORC). However, whatever the type of the system, one of the main issues of the complex energy networks is the definition of the optimal design [3-5]. Among the different criteria which can be adopted for the research of the optimal design of a given complex energy network, as described in detail in Chapter 1, in the following section the focus is on the genetic algorithm and on its application for the investigation of a case study, including cogeneration systems.

3.1 Software EGO

The software EGO (Energy Grid Optimizer) has been already developed by the Energy Systems research group of the University of Bologna with the main purpose of defining both the optimal design and the scheduling of a number of energy systems belonging to a complex energy network by minimizing the total cost of energy production [6]. To this respect, the software EGO is implemented for the optimal design of a complex energy network while, in the next chapter, it will be used for the optimization of the load allocation problem. With respect to the calculation core of the software, it is based on the resolution of a genetic algorithm. More in detail, the software EGO allows to simulate a given energy network composed by:

- an arbitrary number of prime movers (PM), also in CHP application;
- generators from renewable source (for the thermal energy production (RGt) such as the solar thermal panels or fort the electricity production (RGe) such as the wind turbines and photovoltaic panels;
- electrical and/or energy storage devices (ES);
- thermal generators, such as auxiliary boilers (AB) and heat pumps (HP);
- cooling machines (compressor – CC – and absorption chillers – AC);

which are used to fulfill the electrical, thermal and cooling needs of one (or more) user belonging to the network which can be also connected to the national electrical grid and with the gas distribution network.

The input section of the software consists in the definition of the main characteristics of the whole network such as:

- the electrical, thermal and cooling power required by each user of the network and, in case, even the gas demand for the direct use of the users;
- the number, typology and main peculiarities of (*i*) prime movers, (*i.e.:* electrical and thermal design power output, efficiency, off-design behavior, etc.); (*ii*) renewable sources generators (*i.e.:* peak power, performance, etc.); (*iii*) heating and cooling systems (*i.e.:* size, performance, off-design behavior, etc.) and (*iv*) electric and thermal energy storage devices (*i.e.:* maximum storable energy);
- the tariff scenario;
- a series of characteristic parameters related to the genetic algorithm.

The main output of the software EGO, instead, is represented by the optimal load of each energy systems composing the network which allows, as aforementioned, to minimize the total cost of the energy production for the users fulfillment.

Therefore, the genetic algorithm is based on the minimization of a cost-based fitness function FF (€) which is defined as follow:

$$FF = C_\lambda + C_M + C_E + C_F \qquad \text{Eq.3.1}$$

being C_λ the total cost of the fuel, C_M the total cost for the maintenance, C_E the total cost of the electricity purchase and C_F the so-called *fictitious costs*.

In more detail:

- C_λ, which represents the total cost due to the use of the fuel for the operation of some energy systems, is evaluated according to the equation:

$$C_\lambda = \left[\sum_{i=1}^{n_{PM}} f_{\lambda,i}^{PM}\left(L_{PM,i}\right) + \sum_{i=1}^{n_{AB}} f_{\lambda,i}^{AB}\left(L_{AB,i}\right) \right] \cdot \lambda_{fuel} \qquad \text{Eq.3.2}$$

  in which the terms $f_{\lambda,i}^{PM}$ and $f_{\lambda,i}^{AB}$ indicates the total power introduced with the fuel to the ith generation systems (respectively for the prime mover and auxiliary boilers) as function of the load of the system itself ($L_{PM,i}$ and $L_{AB,i}$). The term λ_{fuel}, instead, denotes the specific cost of the fuel (€/kW) used to feed the energy production system.

- C_M is the parameter which represents the total cost for the energy systems maintenance and is evaluated by taking into in account the specific maintenance cost μ_i (expressed in €/kW). The calculation of C_M is done as function of the electrical (EL), thermal (TH) or cooling (FR) power produced by each energy system as follows:

$$C_M = \sum_{i=1}^{n_{PM}+n_{RGe}} P_{EL,i} \cdot \mu_{EL,i} + \sum_{i=1}^{n_{RGt}+n_{AB}+n_{BB}+n_{HP}} P_{TH,i} \cdot \mu_{TH,i} + \sum_{i=1}^{n_{CC}+n_{AC}} P_{FR,i} \cdot \mu_{FR,i}$$

Eq.3.3

where P_i (expressed in kW) indicates the electrical, thermal or cooling power produced by the corresponding energy systems, expressed as function of the load $P_i = f(L_i)$.

- C_E represents the total cost due to the purchase of electricity from the electric grid. This parameter is calculated on the basis of the following equation:

$$C_E = P_{EL,P} \cdot \xi_{EL,P}$$

Eq.3.4

in which $P_{EL,P}$ is the total electric power from the electric grid to the users and $\xi_{EL,P}$ is the specific cost of the electricity purchased from the national grid. With respect to the electric power $P_{EL,P}$, it has to be highlighted that, in the event it is greater than zero, it can be calculated as follows:

$$P_{EL,P} = \sum_{i=1}^{n_U} P_{EL,i}^U + \sum_{i=1}^{n_{CC}} \frac{P_{FR,i}^{CC}}{f_{EER,i}^{CC}(L_{CC,i})} + \sum_{i=1}^{n_{HP}} \frac{P_{TH,i}^{HP}}{f_{COP,i}^{HP}(L_{HP,i})} - \sum_{i=1}^{n_{RGe}} f_{EL,i}^{RGe}(L_{RGe,i}) - \sum_{i=1}^{n_{PM}} f_{EL,i}^{PM}(L_{PM,i}) - \sum_{i=1}^{n_{ES}} P_{EL,i}^{ES}$$

Eq.3.5

The equation Eq.3.5 takes into account the sum of the electricity required by the users (U), the compressor chillers (CC) and the heat pumps (HP). From this amount, it has to be subtracted, if present, the electrical power produced by the renewable generators (RGe), prime movers (PM) and the power recovered from the electrical storage devices (ES).

In addition, the functions represented by the terms $f_{EER,i}^{CC}$ and $f_{COP,i}^{HP}$ respectively indicate the Energy Efficiency Ratio (EER) and the Coefficient of Performance (COP) of the cooling devises the first one and of the heat pumps the second one. These parameters are expressed as function of the load of the corresponding energy system ($L_{CC,i}$ and $L_{HP,i}$).

The last term $f_{EL,i}^{PM}$, instead, represent the total power produced by the ith prime mover as function of the load ($L_{PM,i}$).

- C_F, instead, represents the so-called fictitious costs. The main purpose of this term is to force the regulation strategy of the entire energy network to account for aspects related to environmental issues and grid stability. In particular, the regulation strategies are:

  - *thermal priority*: in this case, the main purpose is to minimize the environmental impact due to the heat dissipations through the stack. To this respect, a fictitious cost is considered, which takes into account the thermal power discharged from the prime movers and not used for the users fulfillment. If the electrical power production exceeds both the users' needs and the storage devices capability, this regulation strategy provides that the surplus can be sold to the electrical grid. In this case, the fictitious costs are calculated with the following equation:

  $$C_F = \sum_{i=1}^{n_{PM}} \frac{Q_{disp,i}}{\eta_{AB,av}} \cdot \lambda_{fuel} \cdot p_T - P_{EL,S} \cdot \xi_{EL,S} \qquad \text{Eq.3.6}$$

  where the thermal energy dispersed to the stack $Q_{disp,i}$ is considered as a cost evaluated as a multiple p_T of the fuel cost to generate the same amount of thermal power in a traditional natural gas boiler. At the same time, the revenue related to the electricity sold to the grid is calculated, by taking into account the specific cost $\xi_{EL,S}$ (expressed in €/kW).

  - *electrical priority*: contrary to the previous case, in this regulation strategy, the electricity sold to the electric grid represents a cost in order to discourage this option, while no penalization is given to the heat dissipations to the stack. This is a typical strategy that is adopted in the case of isolated network or in the case of a limited connection (in terms of capacity) with the national grid. In this case, the fictitious costs are calculated as:

  $$C_F = P_{EL,S} \cdot \xi_{EL,S} \cdot p_E \qquad \text{Eq.3.7}$$

  Being, as aforementioned, the term $P_{EL,S}$ representative of the electricity sold to the grid which is converted into a cost by the multiplier factor p_E and the specific costs of the sold electricity $\xi_{EL,S}$ (€/kW).

  - *combined priority*: this last regulation strategy corresponds to a mix between the two previous strategies. In this case, the fictitious costs are calculated as follow:

  $$C_F = \sum_{i=1}^{n_{PM}} \frac{Q_{disp,i}}{\eta_{AB,av}} \cdot \lambda_{fuel} \cdot p_T + P_{EL,S} \cdot \xi_{EL,S} \cdot p_E \qquad \text{Eq.3.8}$$

whose terms have been already explained in the previous equations Eq.3.6 and Eq.3.7. This equation points out that both the dissipations to the stack and the sale of electricity to the grid are discouraged with this approach.

Whether the adopted regulation strategy, the *genetic algorithm*, which is aimed to minimize the fitness function FF of Eq.3.1, generates, for each iteration, a population of candidate solutions each one represented by a possible scheduling of the considered energy systems. To this regard, each system's load L_i represents the chromosome of each individual of the population and then allows to define the FF with the aforementioned equations. As usual for the genetic algorithm, the evolution of the population starts with a first generation which is created in a random way.

It has to be said that the size of the population p_S (namely the number of individuals of each generation) is evaluated as function of the total number of generation systems n_{tot} of the energy network as follows:

$$p_S = P_{FM} \cdot (L_{UP} - L_{LO}) \cdot n_{tot}$$
<div align="right">Eq.3.9</div>

being the terms L_{UP} and L_{LO} respectively representing the upper and lower limits of the variation range of L_i. The term P_{FM}, instead is an integer multiplicative parameter, greater than 1, which affects the velocity of the convergence of the algorithm. Lower values of P_{FM} correspond to a small population and therefore to a large number of iterations.

After the first generation is created, the fitness function is calculated for each individual and a FF rank is created. To this respect, the individuals are categorized as a high rank solution in case of lower values of energy production cost which implies lower values of FF. Conversely, individuals characterized by higher energy production cost, and then high value of FF, are representative of the low rank solutions. A certain percentage of the low rank solution – usually representing a percentage equal to about 25 % of the whole population – is then eliminated from the generation and it results in a new generation of individuals. This generation process follows the crossover method without mutation, namely, the new generation is created by two parent individuals of the previous generation. The selection of the parent individuals is implemented through the application of a *roulette method* aimed to guarantee a higher probability to those individuals characterized by a higher rank. The highest rank solution $FFR\#1(i)$ of each generation (excepted the first one) is compared with the corresponding of the previous generation, $FFR\#1(i-1)$. The iterative procedure ends when the difference between these two quantities is lower than a given tolerance value TOL according to the following equation:

$$|FFR\#1(i) - FFR\#1(i-1)| < TOL$$
<div align="right">Eq.3.10</div>

3.2 Combined heat and power generation systems design: a case study

Within the main purpose of defining a general methodology aimed to identify the optimal size of different power generation systems composing a complex energy network, the annual operation of a residential neighborhood has been investigated [7]. In detail, starting from a small residential neighborhood composed by a total of 100 households, a parametric analysis has been carried-out by varying the total number of the considered households up to 1000 units, in order to define the optimal design of each energy system suitable for the network users fulfillment as function of the number of the users connected to the network itself. For each scenario, the annual operation has been analyzed considering three typical days, representative of wintertime, middle season and summertime. Furthermore, among the various technologies for CHP applications, in this study Internal Combustion Engines (ICE) have been considered due to their higher efficiency and technological maturity. The analysis has been carried-out considering both the energy and cost saving with respect to a Reference Case.

For what concern the energy results, the daily and annual electrical, thermal and cooling demand sharing between the various energy systems will be shown for the analyzed scenarios, taking into account the sizing of the ICE as CHP units with respect of the electric peak. In addition, to find the optimal size of the considered energy systems, an economic evaluation has been done.

As results, the energy systems that better meets the electrical, thermal and cooling demand for a given number of residential units have been pointed out and mapped.

In the following sections the main assumptions, in terms of energy loads, season partition, energy systems and economic parameters, will be deeply described and the results will be presented.

3.2.1 Hypothesis and assumptions

The first assumption concerns the energy loads in terms of electrical, thermal and cooling demand which characterize the single household. To this respect, the typical demand of a residential unit is characterized by electrical energy (for lighting, computer side, cold and/or hot appliance, etc.), thermal energy (for hot water and – in winter season – space heating) and cooling energy (for air conditioning in summer season). Therefore, to find the typical energy load profiles, the electrical [8], thermal [9] and cooling [10] dimensionless load curves available from the literature have been taken into account.

With respect to the electrical loads, it has to be highlighted that, due to the electricity consumption of the cold appliances, the electrical energy demand will be different in relation to the considered season. Therefore, it involves three different profiles for the summertime, wintertime and middle season. On the other hand, as it regards the thermal demand, it is due to two main components: the space heating and the hot water needs for each of which a dimensionless load curve is considered. Furthermore, while the hot water demand occurs in wintertime, summertime and middle season, the space heating is considered only for the winter season. Finally, as it regards the cooling demand, as is known, it is characterizing the only summer season.

On the basis of the aforementioned considerations, it follows those three typical days – each of which characterized by the electrical, thermal and cooling demand defined according to the previous considerations – can be defined respectively representative of wintertime, middle season and summertime. In addition, in order to evaluate the hourly based load profiles for a household unit, the considered specific electrical, thermal and cooling peaks for a squared meter in a year are listed in Table 3.1[9-11].

TABLE 3.1. SPECIFIC PEAK LOADS [9-11].

Peak loads	Units	Value
Electricity	[kWh/m2 y]	30
Hot water	[kWh/m2 y]	30
Space Heating	[kWh/m2 y]	220
Cooling	[kWh/m2 y]	44

Therefore, by considering the surface of a single household equal to $80 \, m^2$ – which is representative of a typical apartment – the resulting electrical, thermal and cooling hourly load curves, each representative of the typical winter, middle season and summer days, are respectively presented in Figure 3.1, Figure 3.2 and Figure 3.3. These values are hourly average powers corresponding to a single residential unit with reference to Italy's typical values.

In addition, with reference to Italians' regulations, the following seasons' partition during the year has been hypothesized:

- winter: 183 days;
- middle season: 90 days;
- summer: 92 days.
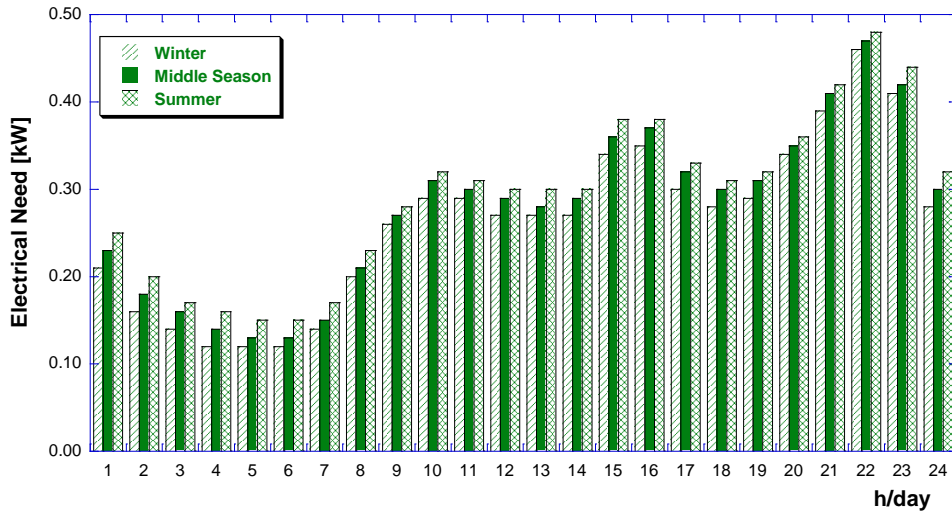
FIGURE 3.1: HOURLY ELECTRICAL PROFILE OF A SINGLE RESIDENTIAL UNIT.
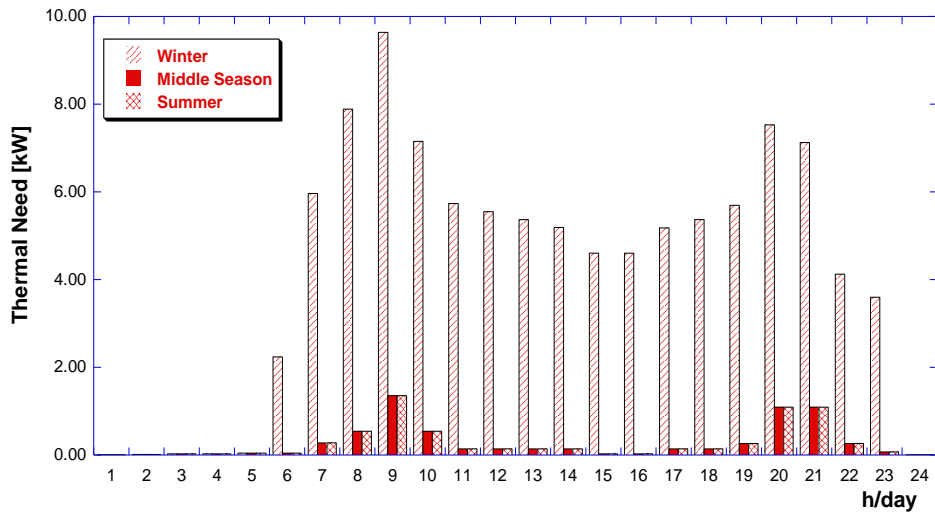
FIGURE 3.2: HOURLY THERMAL PROFILE OF A SINGLE RESIDENTIAL UNIT.
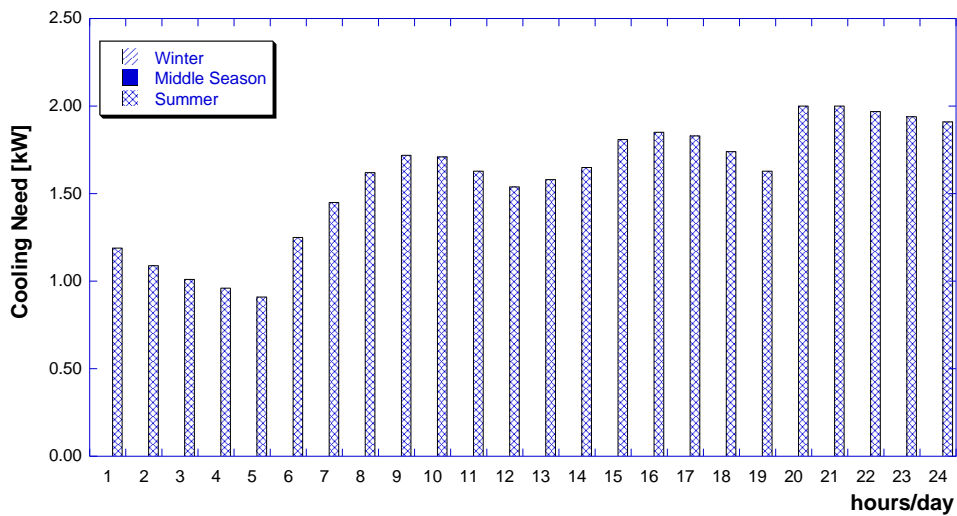
FIGURE 3.3: HOURLY COOLING PROFILE OF A SINGLE RESIDENTIAL UNIT.

Another assumption concerns the energy systems. To this respect, in order to satisfy the electrical, thermal and cooling demand of a certain number of households, the possibility to exploit different energy systems has been evaluated.

In detail, for the electrical and thermal production have been considered the cogeneration systems, as well as heat pumps and natural gas auxiliary boilers – for thermal needs – and the electrical grid connection – for electrical needs. As it regards the cooling need, it is supposed to be fulfilled by the employment of absorption and/or compression chillers. Furthermore, as previously mentioned, as it concerns cogeneration systems, the internal combustion engines (ICE) have been considered in this analysis due to their higher efficiency and commercial availability with respect to micro-gas turbines.

In particular, the software EGO contains an internal database of commercial CHP systems, including the ICE, on the market. Starting from this database and in order to select the best ICE size for the analyzed case, the ratio between the rated electrical and thermal powers and the electrical efficiency have been plotted as function of rated electrical power, respectively in Figure 3.4 and in Figure 3.5.

The logarithm curves presented in these figures, have been used to choose the correct CHP size for the analysis and represent the design parameters of the main commercial CHP. As it will be shown in the results section, the size of these systems has been selected – for given number of considered residential units – on the basis of the electrical peak need.
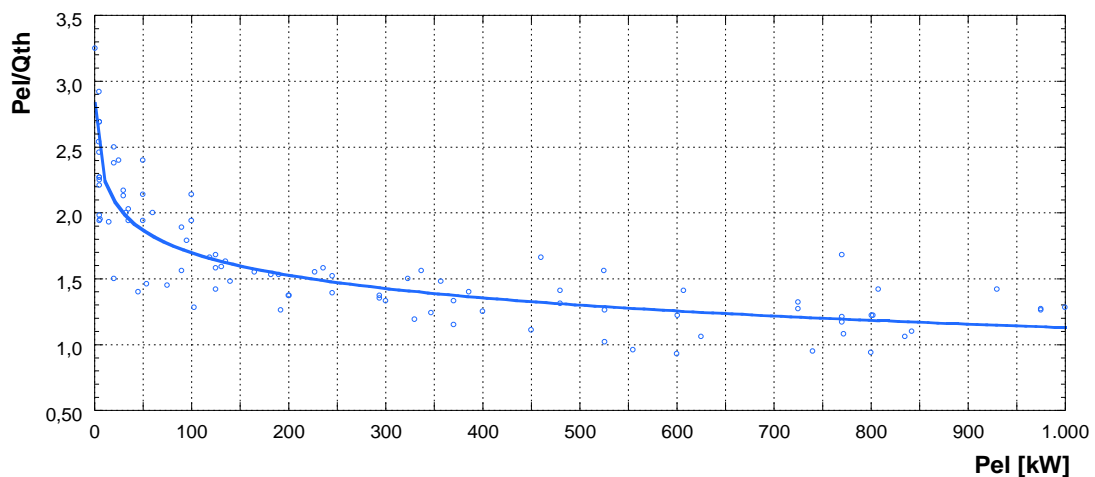
FIGURE 3.4: COMMERCIAL INTERNAL COMBUSTION ENGINES P_{EL}/Q_{TH} TREND AS FUNCTION OF P_{EL}.
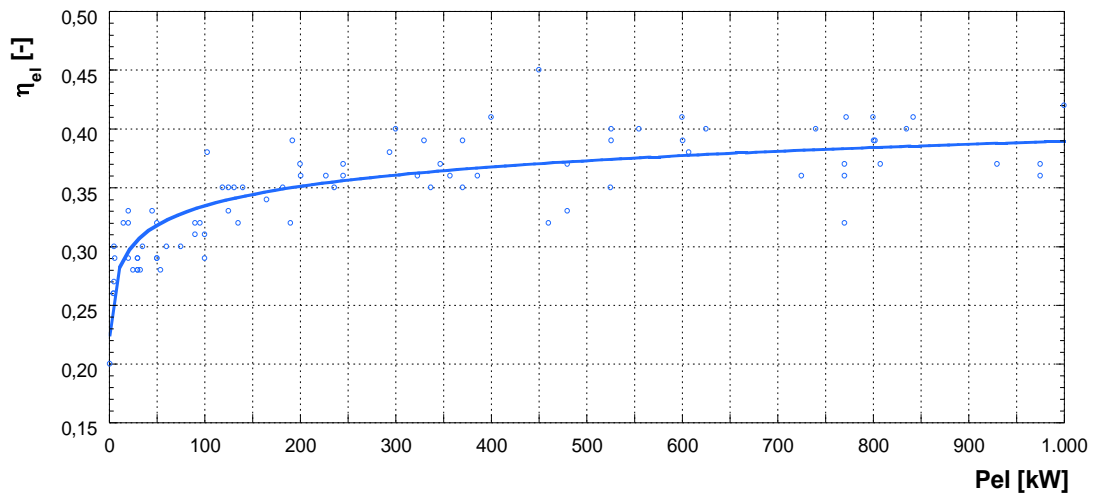
FIGURE 3.5: COMMERCIAL INTERNAL COMBUSTION ENGINES ELECTRICAL EFFICIENCY
TREND AS FUNCTION OF P_{EL}.

Furthermore, the software EGO requires the off-design curves for each energy system. With this purpose, the off-design behavior of the ICEs has been modeled and the electrical and cooling efficiencies are evaluated starting from the non-dimensional (with respect to the rated values) curves presented in Figure 3.6. More details related to the calculation methodology of the curves can be found in [12].
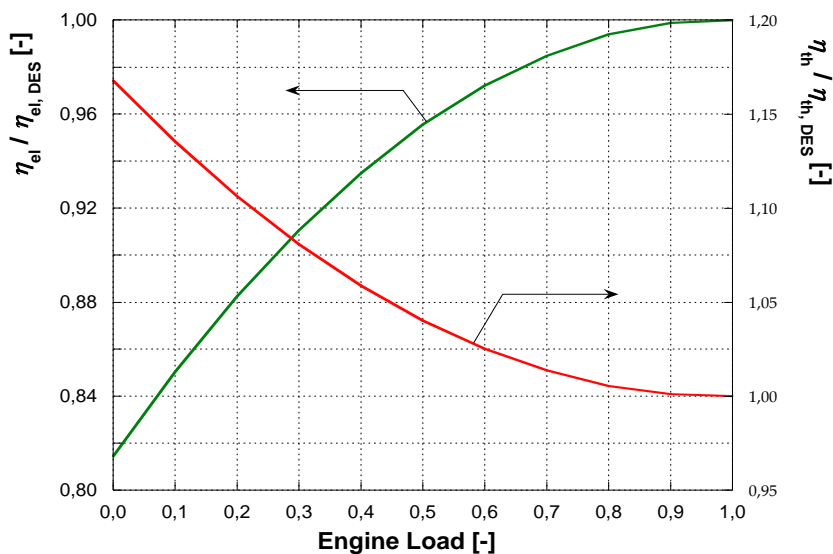
FIGURE 3.6: NON-DIMENSIONAL CURVES FOR ICE OFF DESIGN BEHAVIOR CALCULATION OF
ELECTRICAL AND THERMAL EFFICIENCY.

However, a complex energy network is not composed only by combined heat and power technologies. To guarantee the fulfillment of the electrical, thermal and cooling demand, in fact, they are usually integrated with other systems. In particular, in this study, in addition to the internal combustion engines, for what concern the thermal demand, auxiliary boilers and heat pumps have been considered. On the other hand, compression and/or absorption chillers have been integrated into the network to satisfy the cooling demand. Furthermore, it has to be said that the complex energy network is connected with the electrical grid to pick up or feed into the electrical energy. To this respect, the performance parameters for the heat pump, auxiliary boilers and cooling machines – assumed for the whole analysis – are listed in Table 3.2 [13]. All these design parameters have been considered as constants for the parametric analysis, also for the off-design behavior and with the variation of the size. On the other hand, the definition of the size for each production system, instead, is the object of the carried-out study.

TABLE 3.2: PERFORMANCE DESIGN PARAMETERS CONSTANT FOR THE WHOLE ANALYSIS [13].

Parameter	Units	Value
Heat Pump COP	[-]	4.00
Auxiliary Boilers Efficiency	[-]	0.85
Compressor Chiller EER	[-]	3.50
Absorption Chiller EER	[-]	0.67

The last hypotheses concern the economic analysis. To this respect, in fact, an economic evaluation has been carried-out with the main purpose of giving a complete analysis and to compare the obtained optimal setup of the energy systems with a more traditional generation setup in residential sector. To this respect, for each considered number of households, a Reference Case has been defined in which it has been assumed that the energy demand is fulfilled only by the natural gas boilers and by the electricity purchase from the national electric grid. Furthermore, the economic analysis has been done according to the differential Net Present Value (NPV) methods, calculated with respect to the Reference Case, and considering a time horizon of 10 years. The Net present value calculation has been made according to the following equation:

$$NPV = -I_0 + \sum_i \frac{F_i}{(1+r)^i} \qquad \text{Eq.3.11}$$

in which the terms I_0 and F_i respectively represent the investment cost, which is done at the year zero (namely at the beginning of the considered time horizon) and the cash flow. Furthermore, r represents the opportunity cost and the subscript i denotes the considered year.

To this purpose, the considered specific investment costs of the energy systems are listed in Table 3.3 along with the assumed maintenance costs [7].

TABLE 3.3: INVESTMENT AND MAINTENANCE COSTS OF EACH GENERATION SYSTEM.

Generation system	Investment costs	Maintenance costs
CHP unit	500 €/kW$_e$	0.020 €/kWh$_e$
Heat Pump	200 €/kW$_{th}$	0.010 €/kWh$_{th}$
Auxiliary Boilers	50 €/kW$_{th}$	0.005 €/kWh$_{th}$
Compressor Chiller	350 €/kW$_{fr}$	0.006 €/kWh$_{fr}$
Absorption Chiller	350 €/kW$_{fr}$	0.002 €/kWh$_{fr}$

At least, with respect to the operational costs assumed for the analysis, the electricity purchase cost has been set equal to 0.180 €/kWh$_e$ and the natural gas cost has been assumed equal to 0.824 €/Sm^3. Finally, on the basis of the NPV analysis, for each case the return on investment (ROI) has been evaluated.

3.2.2 Results and discussion

In this section the results of the carried-out simulation will be deeply presented and described. A first result concerns the design parameters of the internal combustion engines set as CHP units, which have been chosen from the internal database of the software EGO (namely they correspond to commercial machine).

To this respect the selection of the ICEs for each case has been done according to the electrical peak needs of the user. In addition, this choice has also been done with the purpose of minimizing (or avoiding) the introduction of electrical energy into the network. These design parameters are listed in Table 3.4. It can be observed that all the selected machines employ the Natural Gas (NG) as fuel.

Another observation concerns the electrical and thermal design efficiencies that, as can be noted from the table, varies in relation of both the ICEs model and size. As expected, this will affect the results related to the internal combustion engines operation. As it regards the others energy systems, their optimal size, will be discussed later in the chapter, since it is a result of the optimization analysis.

TABLE 3.4: DESIGN PARAMETERS OF THE CHP UNITS.

# Households	100	200	300	400	500	600*	700	800	900	1000
Manufacturer	EMD	Energifera	Ecogen	EMD	Stone Power	Ecogen	MDE	MDE	EMD	Caterpillar
Model	EMD 45	TEMA 100	EG140	EMD 200	2230	EG140	ME 3042 L	ME 3042 Z	EMD 400	G3508 LE
Fuel	NG	NG	NG	NG	NG	NG	NG	NG	NG	NG
Design Electrical Power [kW]	45	95	140	190	236	140	337	386	400	480
Design Thermal Power [kW]	63	170	207	290	372	207	525	541	500	631
Design Electrical Efficiency [-]	0.325	0.321	0.351	0.319	0.354	0.351	0.350	0.364	0.414	0.369
Design Thermal Efficiency [-]	0.455	0.574	0.519	0.487	0.558	0.519	0.545	0.510	0.518	0.485

*Two ICEs of this model have been considered for this case.

In the second place, the starting case is presented, namely the one in which 100 households have been considered.

To this respect, in Figure 3.7 the hourly electrical, thermal and cooling demands with highlighted the energy generation mix obtained for their fulfillment have been presented. As can be noted from the figure, the daily results have been shown with respect to the three typical days representative of wintertime, middle season and summertime. In particular, for each representative day, the electrical and thermal energy required by the users have been shown along with the generation mix. Obviously, the cooling energy load allocation has been instead represented only with reference to summertime. To this respect, from the figure it can be observed that the cooling demand is fulfilled by mostly employing the compressor chillers while only during the central hours of the day – between 9 a.m. to 8 p.m. – the cooling demand is also fulfilled by the use of the absorption chillers. In addition, the electricity production mix – composed by the ICE production and the electricity purchase from the national grid – changes depending on the considered season. To this respect, the results show that during the wintertime and summertime, the electrical demand is mainly satisfied by the internal combustion engine. The electricity purchased, in fact, occurs during the nighttime and, in particular, from 11 p.m. to 6 a.m. and from 9 p.m. 7 a.m. respectively for the winter and summer season. The opposite results, instead, occur for the middle season representative day in which the electricity purchase from the grid is preferred to the ICE production which occurs only from 7 a.m. to 11 a.m. and from 7 p.m. to 10 p.m.. These results become evident considering the whole energy needs: indeed, during the summer season a low thermal need is registered (only for domestic hot water) and no cooling needs are present (thus, no thermal and electrical energies are required respectively for absorption and compression chillers). As a consequence, the CHP operation is not convenient being low the efficiency of these systems at partial load. For what concerns the thermal demand, as aforementioned and presented in Figure 3.2 and in Figure 3.3, the middle season and the summertime are characterized by the same daily profile. However, even in this case, the energy production mix is different. To this respect, from the figure it results that in both cases during the nighttime – namely from 11 p.m. to 6 a.m. the thermal needs is fulfilled by the only use of the auxiliary boilers. For the rest of the day, in the case of middle season, the peak powers are fulfilled by the ICE, heat pump and auxiliary boilers while the central hours only the auxiliary boilers are employed. In the case of summertime, instead, for the same reason explained for the electrical needs, the ICE covers the major demand and only in the peak hours also the auxiliary boilers are used. A different situation occurs during the wintertime representative day. In this case, in fact, since the thermal needs are very high, the auxiliary boilers fulfill the most of the users' needs while both the ICE and the heat pump give a minor contribution.

For completeness, the results in terms of hourly electrical, thermal and cooling demands along with the generation mix for the other cases are presented in the Appendix D.

(a) Winter
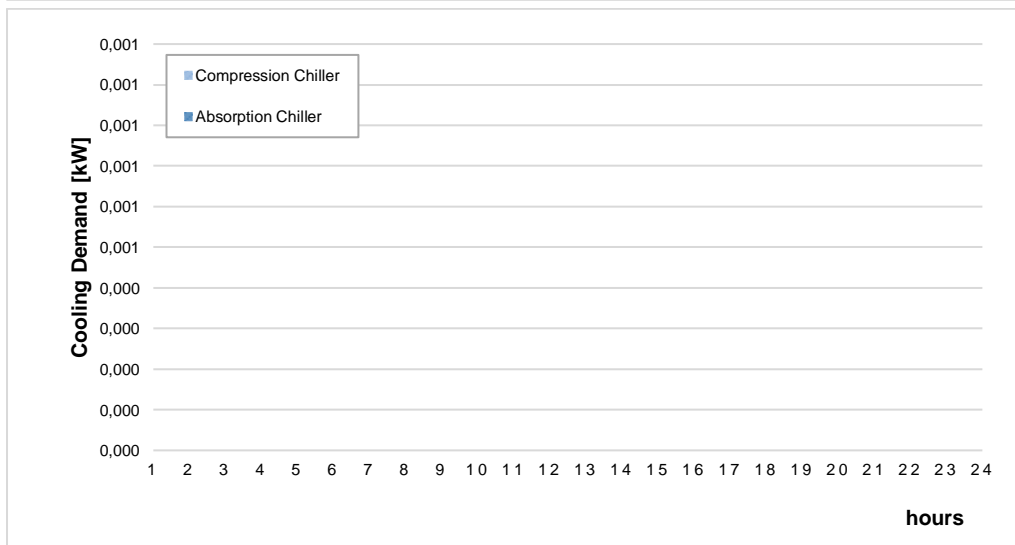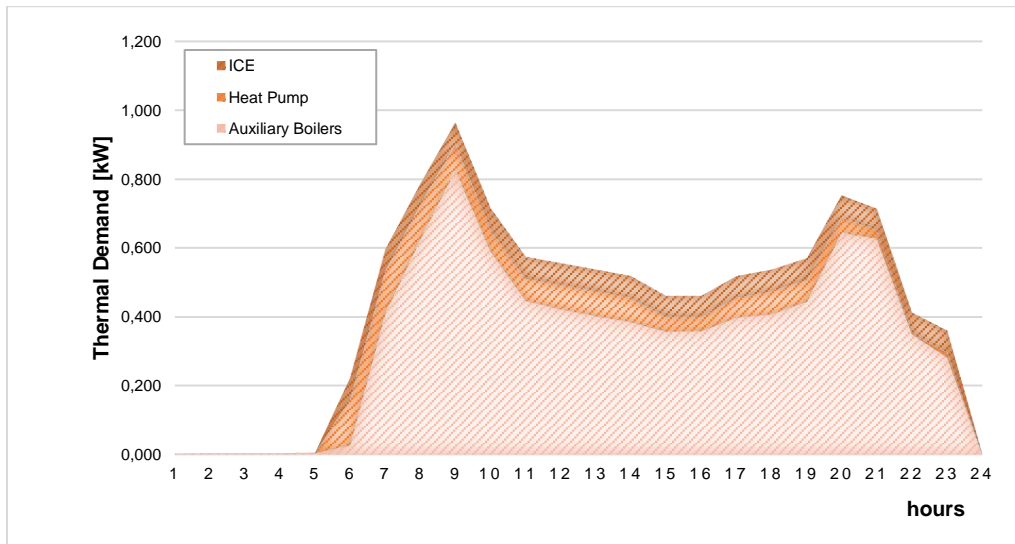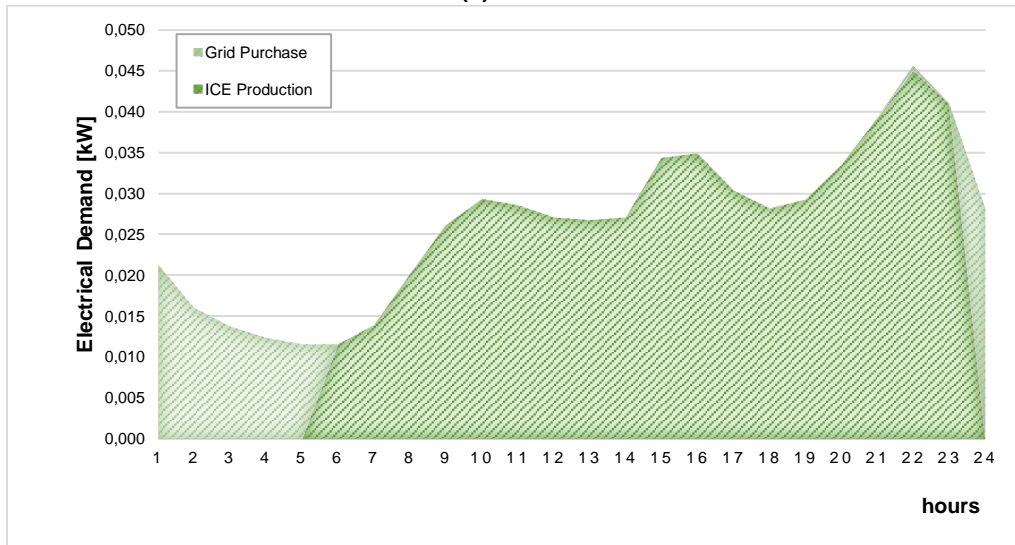
(b) Middle season
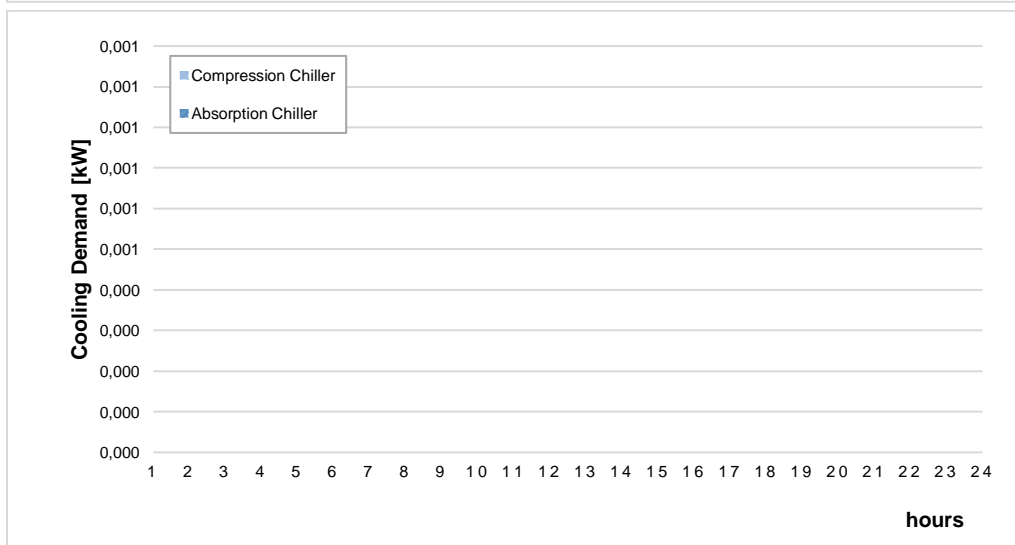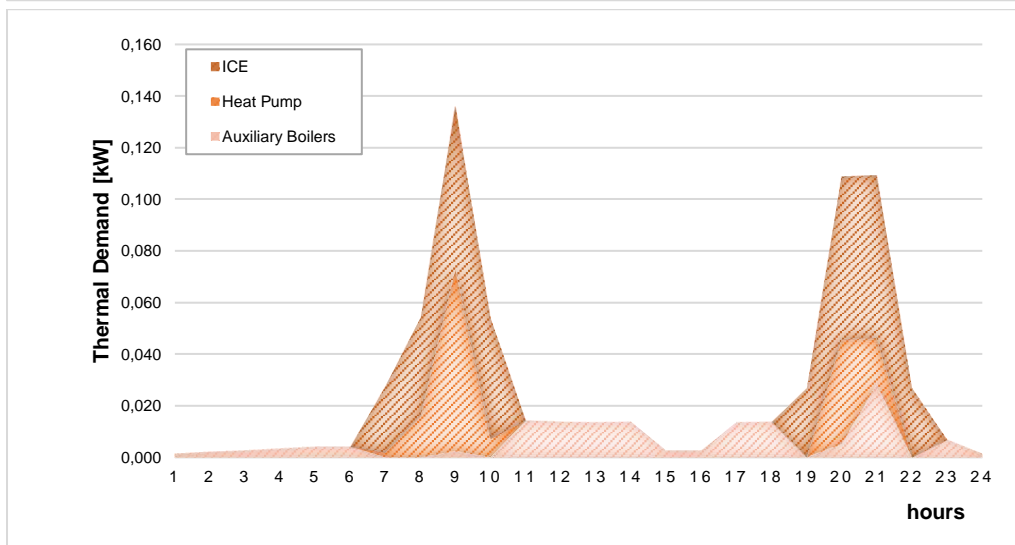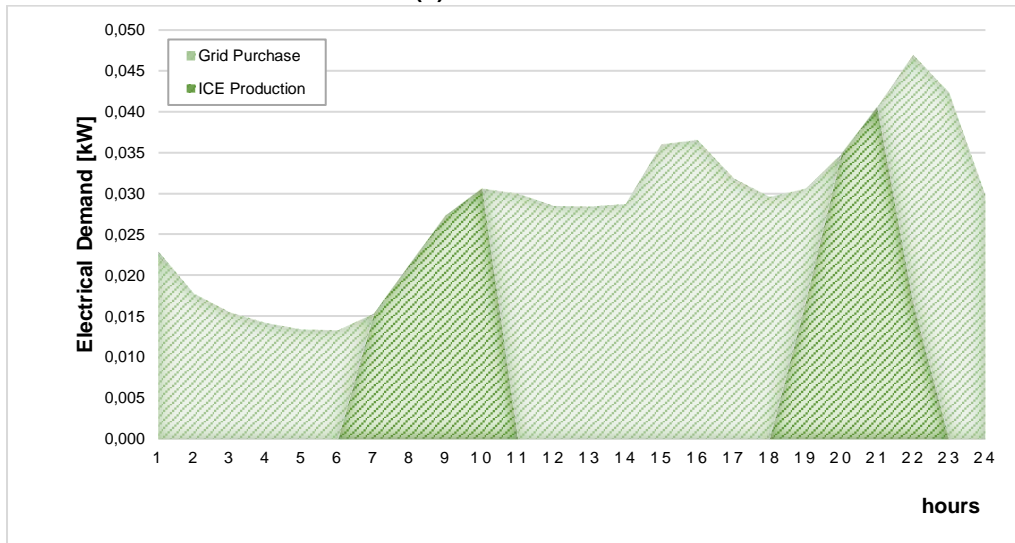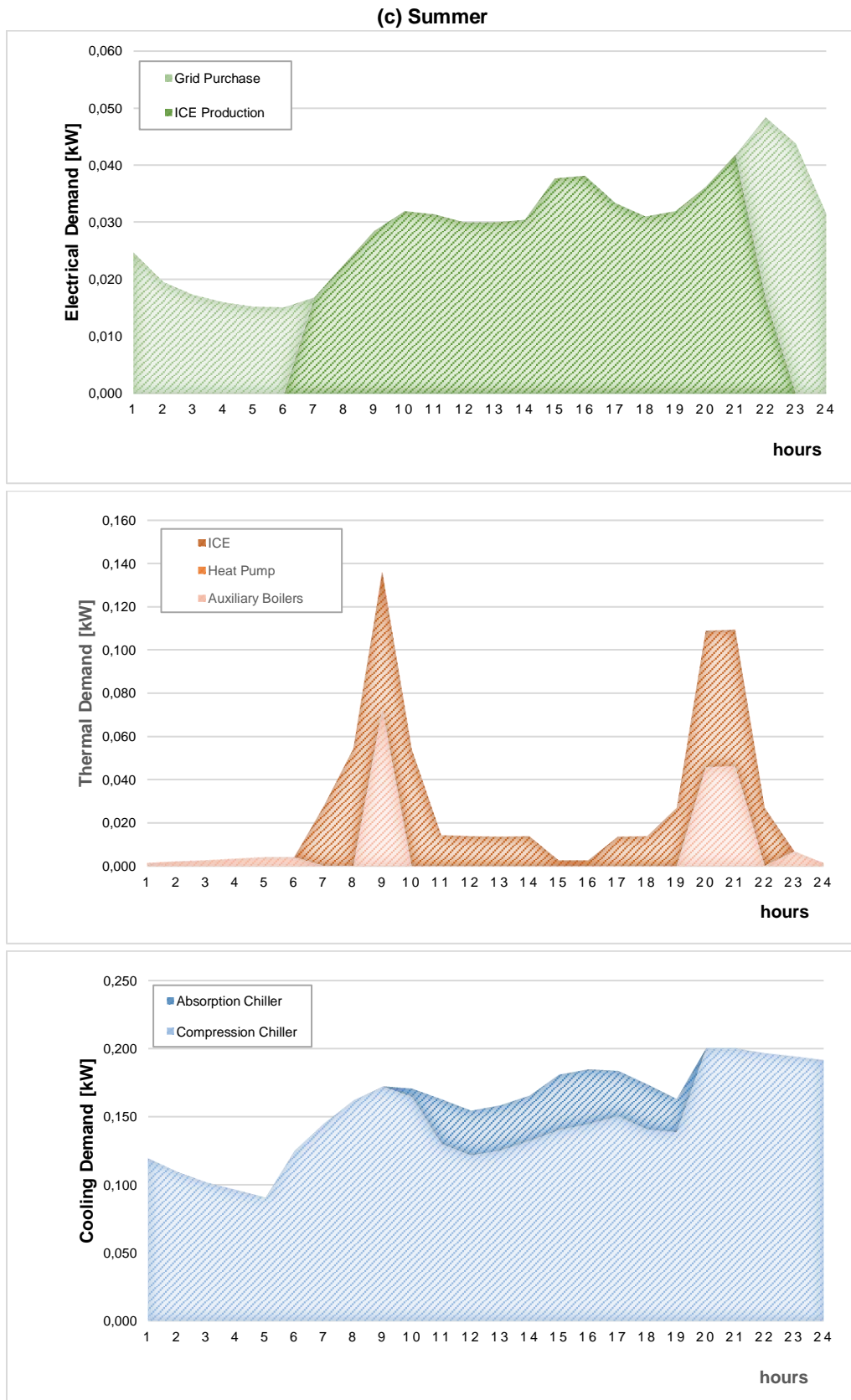
(c) Summer

FIGURE 3.7: HOURLY LOAD PROFILE AMONG THE GENERATION SYSTEMS OF (*a*) WINTERTIME, (*b*) MIDDLE SEASON AND (*c*) SUMMERTIME FOR THE CASE OF 100 HOUSEHOLDS.

Starting from the internal combustion engines of Table 3.4, from the application of the software EGO the optimal size of the other energy systems and the optimal scheduling related to the entire operational year can be evaluated.

In addition, the yearly percentage repartition of the electrical, thermal and cooling needs of the users are shown respectively in Figure 3.8, Figure 3.9 and Figure 3.10 with respect to the number of considered households and by highlighting the generation mix. In more detail, as it concerns the yearly electrical needs, from Figure 3.8 it can be observed that in all the considered cases of residential units, the greater contribution for the user fulfillment is due to the internal combustion engine operation. To this respect, in fact, the results show that the ICE production ranges between a minimum value equal to about 64.40 % in correspondence of the case of 200 residential units, to a maximum value equal to about 68.90 % in the case of 900 residential units. It follows that the remaining demand is provided by the electricity purchase from the national grid. A different generation mix results for the yearly thermal users needs shown in Figure 3.9. In this case, in fact, it can be observed that the internal combustion engine contributes for a very low amount to the fulfillment of the thermal need. In fact, in the different cases, the ICE production varies from a minimum value equal to about 12.70 % to a maximum value equal to about 17.90 % which occurs respectively in the case of 900 and 200 considered households. This result is evidently due to the high amount of thermal energy required by the users (which results greater than the electrical need) and to the choice of sizing the CHP units on the basis of the users' electrical needs in order to limit (or avoid) the introduction of electricity into the national grid. A similar trend results for the heat pump: indeed, the heat production in this case ranges from a minimum value equal to about 10.70 % corresponding to 900 considered residential units to a maximum value equal to about 13.30 % corresponding to 800 considered residential units. As a consequence, the higher percentage of the users demand is provided by the auxiliary boilers whose operation covers a demand range from a minimum value equal to about 69.50 % to a maximum value equal to about 76.60 % respectively in the case of 200 and 900 considered households. Finally, as it concerns the yearly cooling demand of each case of considered households, from Figure 3.10 it results that, according to the summertime cooling daily profile of Figure 3.7, it is almost entirely fulfilled by employment of the compressor chiller. Indeed, the compressor chillers fulfill an amount of the cooling demand which ranges from a minimum value equal to about 87.90 % for the case of 200 residential units to a maximum value equal to about 91.90 % for the case of 100 residential units. The remaining small percentage of the cooling demand (varies from 8.10 % to 12.10 %) is fulfilled by the use of the absorption chiller. This is mainly due to the fact that, according to the priority of the software EGO, the absorption chiller can be powered only by the heat produced by the ICE.
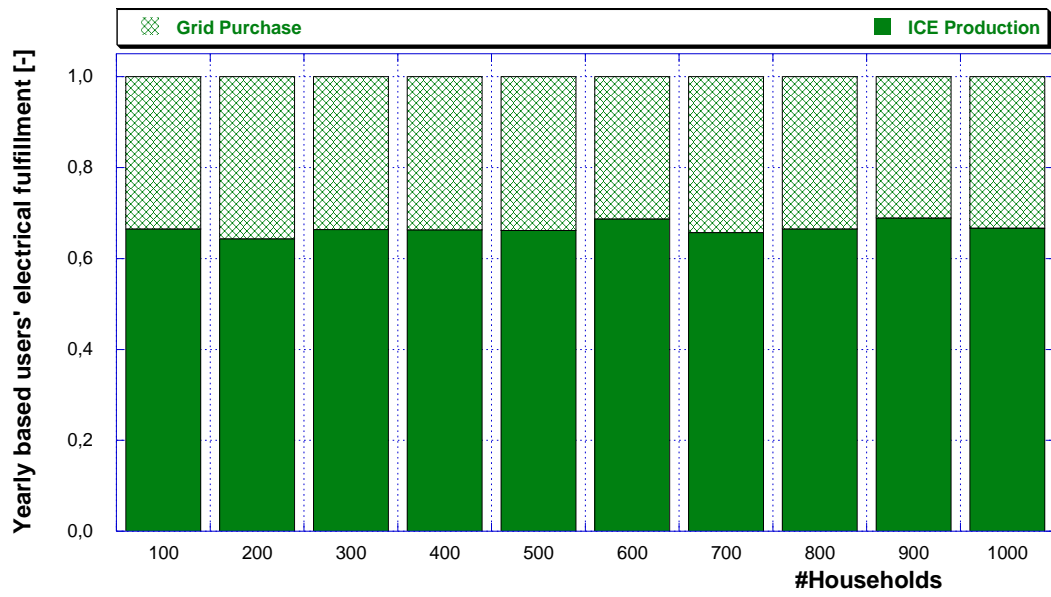
FIGURE 3.8: NON-DIMENSIONAL USERS' ELECTRICAL NEEDS, ALONG WITH THE GENERATION MIX CONSIDERING A YEAR OF OPERATION.
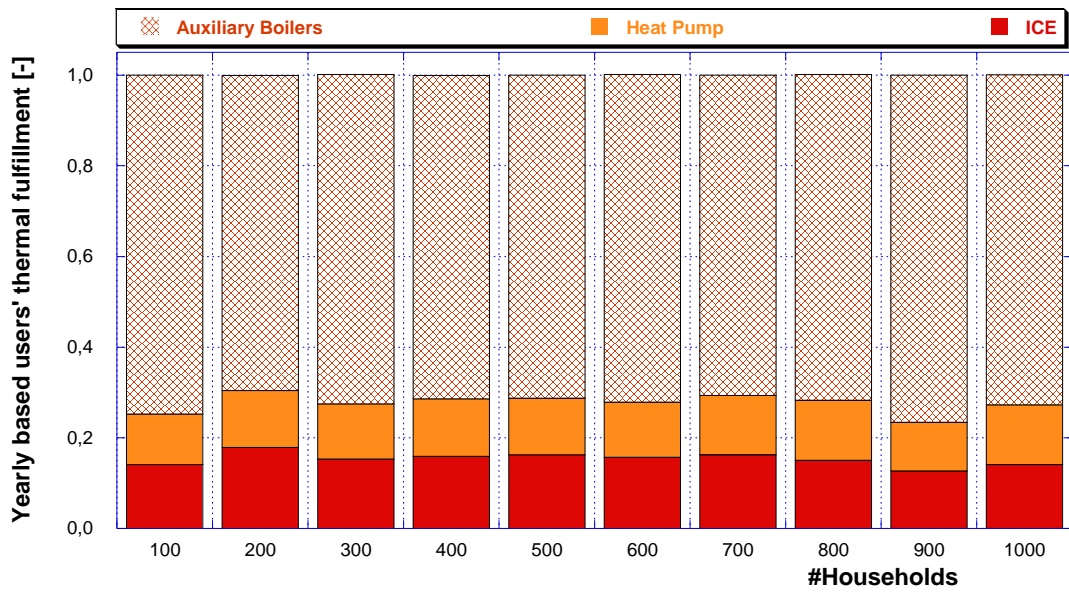
FIGURE 3.9: NON-DIMENSIONAL USERS' THERMAL NEEDS, ALONG WITH THE GENERATION MIX CONSIDERING A YEAR OF OPERATION.
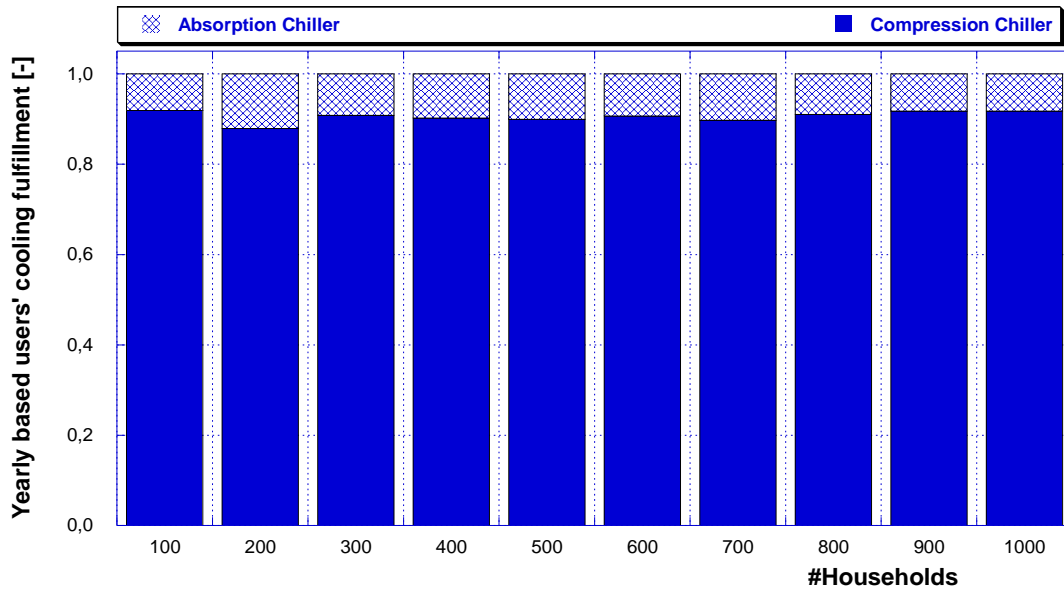
FIGURE 3.10: NON-DIMENSIONAL USERS' COOLING NEEDS, ALONG WITH THE GENERATION MIX CONSIDERING A YEAR OF OPERATION.

The results obtained from the carried-out simulations relating to the optimal size of each energy systems are presented in Figure 3.11Figure 3. for all the considered cases of residential units. As might be expected, both the auxiliary boilers and the compressor chillers optimal size has a linear increasing trend with the growing number of considered households. As it concerns the other energy systems, as for example the heat pumps and the absorption chillers, it can be noted from the figure that they have a different trend. In fact, their optimal size trend does not follow a proportional trend with the increase of the considered number of residential units. This result is a consequence of the adoption of the genetic algorithm for the analysis of the case study.
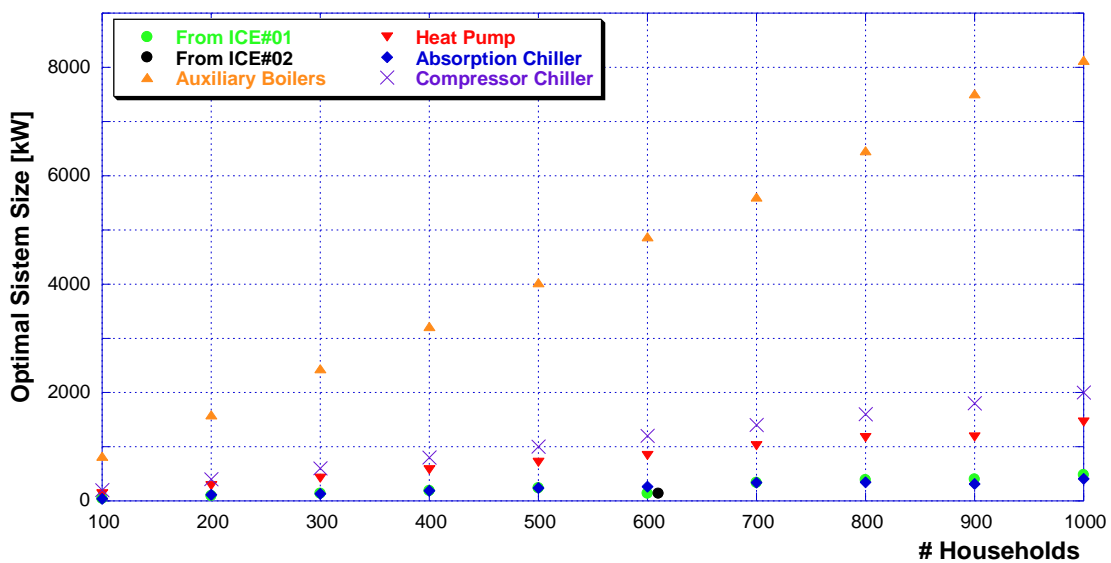
FIGURE 3.11: OPTIMAL SIZE OF EACH ENERGY SYSTEM.

The last result concern the economic analysis. To this respect, the differential net present value and the return of investment resulting from the analysis have been evaluated and presented, for each considered case of households number, in Table 3.5Table 3.1 by taking into account a time horizon equal to 10 years for the NPV calculation. From the results listed in the table, it follows that there is not a univocal correlation between the NPV and the ROI parameters with respect to the number of residential units.

More in detail, from the results of the economic analysis it can be noted that the worst case is represented by 100 households since it is characterized by the minimum value of the net present value and a return on investment equal to 10 years. Conversely, the best case is represented by 900 households being characterized by the maximum net present value and a return on investment equal to 4 years. These results are the consequence of different factors connected to the optimization methods such as the fuel consumption, the electricity purchase and the heat recovery, and to the equivalent hours of operation of each energy system. It follows that the best case resulting from the simulation is the one that better exploit the ICE and the absorption chiller (namely the maximum value of equivalent hours of operation for each of them).

At least, with respect to the other energy system, it can be noted from the results that their behavior (in terms of employment) is almost the same in each one of the considered cases of residential units.

TABLE 3.1: DIFFERENTIAL NET PRESENT VALUE FOR A TIME HORIZON EQUAL TO 10 YEARS AND RETURN OF INVESTMENT FOR EACH CASE.

#Households	NPV [€]	ROI [y]
100	1˙407	10
200	179˙901	5
300	223˙705	5
400	134˙713	7
500	520˙243	4
600	471˙053	5
700	703˙402	4
800	733˙026	5
900	869˙025	4
1000	787˙781	5

In conclusion, on the basis of the results obtained from the carried-out analysis, the optimal range of the specific size of each energy system can be defined, being the specific size intended with respect to the number of households and to the peak load. It follows that, for the scenario considered for the analysis, the resulting specific values, listed in the following Table 3.6, can be considered as reference parameters for the energy systems optimal design in residential applications.

TABLE 3.6: OPTIMAL SIZE RANGE FOR EACH ENERGY SYSTEM.

Energy system	kW/household	kW/kW$_{peak}$
ICE	0.4-0.5 kW$_e$/household	0.5-1.0 kW$_e$/kW$_{peak}$
Heat Pump	1.3-1.5 kW$_{th}$/household	0.1-0.2 kW$_{th}$/kW$_{peak}$
Auxiliary Boilers	7.9-8.4 kW$_{th}$/household	0.8-0.9 kW$_{th}$/kW$_{peak}$
Compressor Chiller	2.0 kW$_{fr}$/household	1.0 kW$_{fr}$/kW$_{peak}$
Absorption Chiller	0.3-0.6 kW$_{fr}$/household	0.2-0.3 kW$_{fr}$/kW$_{peak}$

References

[1] Orlando JA. Cogeneration design guide. USA: ASHRAE, Inc; 1996.

[2] Fuentes-Cortés, L. F., Santibañez-Aguilar, J. E., & Ponce-Ortega, J. M. (2016). Optimal design of residential cogeneration systems under uncertainty. Computers & Chemical Engineering, 88, 86-102.

[3] Onovwiona, H. I., & Ugursal, V. I. (2006). Residential cogeneration systems: review of the current technology. Renewable and sustainable energy reviews, 10(5), 389-431.

[4] Milcarek, R. J., Ahn, J., & Zhang, J. (2017). Review and analysis of fuel cell-based, micro-cogeneration for residential applications: Current state and future opportunities. Science and Technology for the Built Environment, 23(8), 1224-1243.

[5] Pereiraa, J. S., Ribeiroa, J. B., Mendesa, R., Vazb, G. C., Andréa, J. C. (2018) ORC based micro-cogeneration systems for residential application – A state of the art review and current challenges. Renewable and Sustainable Energy Reviews, Vol. 92, September 2018, Pages 728–743.

[6] Ancona, M. A., Bianchi, M., Branchini, L., De Pascale, A., Melino, F., Orlandini, V., Peretto, A., "Generation Side Management in Smart Grid", Proceedings of ASME-ATI-UIT 2015 Conference on Thermal Energy Systems: Production, Storage, Utilization and the Environment, 17 – 20 May 2015, Napoli, Italy – ISBN 978-88-98273-17-1.

[7] Ancona, M. A., Bianchi, M., Branchini, L., De Pascale, A., Melino, F., Peretto, A., & Rosati, J. (2019). Combined Heat and Power Generation Systems Design for Residential Houses. Energy Procedia, 158, 2768-2773.

[8] Commission of the European Communities. DEMAND-SIDE MANAGEMENT – end-use metering Campaign in 400 households of the European Community Assessment of the Potential Electricity Savings – Project EURECO; January 2002.

[9] Macchi E., Campanari S., Silva P., "La microcogenerazione e gas naturale", 2005, Polipress, Milano.

[10] UNI EN ISO 10349 – Italian Legislation.

[11] Bianchi, M., Ferrari, C., Melino, F., & Peretto, A. (2012). Feasibility study of a Thermo-Photo-Voltaic system for CHP application in residential buildings. Applied energy, 97, 704-713.

[12] Baldi, F., Ahlgren, F., Melino, F., Gabrielii, C., & Andersson, K. (2016). Optimal load allocation of complex ship power plants. Energy Conversion and Management, 124, 344-356.

[13] Ancona, M. A.; Bianchi, M.; Biserni, C.; Melino, F.; Salvigni, S.; Valdiserri, P., Optimum Sizing of Cogeneration for a Hospital Facility: Multi-Objective Analysis Applied to a Case Study, in: Proceedings SET Conference 2017, Bologna, 2017, pp. 1 – 10.

4. Optimal Scheduling of Complex Energy Networks

The previous chapter focused on one of the two main issue related the complex energy networks and in particular on the design optimization. In this chapter, indeed, the scheduling optimization problem is addressed, since it represents another key aspect of such networks. To this purpose, a case study, consisting in an isolated grid (namely a cruise ship), is presented and further investigated. In particular, the operation of the vessel has been simulated by the implementation within the software EGO, which has been presented in detail in the previous chapter. The analysis has been carried-out by investigating the energy, economic and environmental aspects.

4.1 Case study: cruise ship

The case study considered for the scheduling optimization analysis with the software EGO is represented by an existing medium size cruise ship characterized by a capacity of about 1˙800 passengers. It consists in a vessel characterized by a length of 177 meters and a width of 28 meters which sails with a design speed equal to 21 knots. Moreover, the cruise ship, which operates in the Baltic Sea, has a two ways route between Stockholm (in Swedish mainland) and Mariehamn (in the Åland islands). Furthermore, it is equipped with restaurants, clubs and bars, as well as saunas and pools [1].
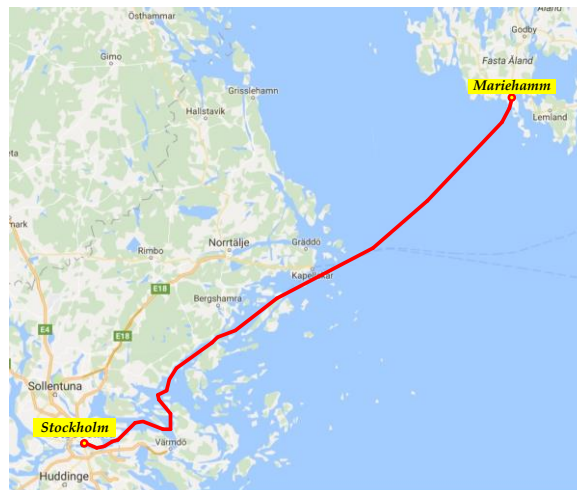
FIGURE 4.1: SCHEME OF THE CRUISE SHIP DAILY ROUTE.

The daily route of the ship, repeated every day during the whole year (365 days/year), is shown in Figure 4.1. On the basis of this route and according to the available information, it is possible to define the yearly operation of the ship which can be divided, as is presented in Figure 4.2, between the (*i*) sea going, (*ii*) port and sea stay and (*iii*) maneuvering (when the ship is entering or leaving

the port). In particular, each one of these three operation phases accounts for a different percentage, respectively equal to 59 %, 33 % and 8%. Therefore, it can be observed that on one hand, the sea going represents the phase characterized by the greater percentage of the ship operation, but an important contribution is given also by the port stays phase, accounting for about one third of the total operational profile.
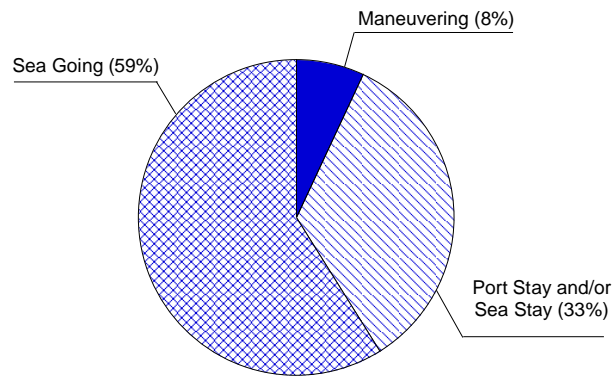
FIGURE 4.2: OPERATION PHASES OF THE SHIP.

4.2 Methodology and assumptions

In this section the main assumptions at the basis of the carried-out analysis are presented and described in detail.

4.2.1 Energy demand

The first assumption regards the energy demand of the considered ship, which consists of (*i*) mechanical energy (for propulsion), (*ii*) electrical energy (for lighting, cold appliances, hot appliances, auxiliary systems, etc.), (*iii*) thermal energy (mainly for space heating and hot water production) and (*iv*) cooling energy (for air conditioning, it occurs only during the summer period). To this respect, it has to be highlighted that, as will be shown in detail in the following, the energy needs vary depending on both the operation of the ship and the considered season.

As aforementioned, the cruise ship operates the same route every day, therefore it is characterized by the same daily typical operational profile in which at 6:00 p.m. is scheduled the departure from Stockholm, then the ship reaches the open sea, where it stays for a few hours during the night before leaving to reach the port of Mariehamn in the early morning hours. Then, at 9:00 a.m., the ship leaves Mariehamn to go back to Stockholm where it arrives at 4:00 p.m..

Considering the energy needs, both the thermal and cooling demand varies in relation to the considered season since they are affected by the variation of the weather conditions. A different situation, indeed, is represented by the mechanical demand, which depends on the travelling conditions, and it is assumed that no variation occurs during the year.

The characterization of the energy needs of the ship could be done by taking into account the aforementioned operational modes and the following considerations:

- during the *port stay* and the *sea stay*, the energy demand consists of the electrical and thermal needs (and, during the summertime, also cooling need is accounted), in order to guarantee all those services for the boarding and alighting procedures of the passengers (during the *port stay*) and for their comfort on board (during the *sea stay*);

- during the navigation (*sea going*) the mechanical demand reaches its maximum value;

- when the ship enters or leaves the port (namely during the *maneuvering* phase) the mechanical demand is intermediate between the ones of the *sea going* and the *port stay/sea stay*;

- the electrical and thermal demand (for space heating and/or hot water production) are affected by the season but not by the operational profiles of the ship.

Another consideration regards the season partition which has been assumed for the analysis. To this respect, according to the average temperatures occurring in Sweden [2], it has been supposed the following partition:

- winter: 182 days (from 1st of January to 15th of April and from 16th of October to 31st of December);
- middle season: 121 days (from 16th of April to 30th of June and from 1st of September to 15th of October);
- summer: 62 days (from 1st of July to 31st of August).

From the previous considerations and the experimental data collected on board [3], the hourly load profile curves – in terms of mechanical, thermal, electrical and cooling powers – have been estimated with respect to each representative day (namely wintertime, middle season and summertime), as presented in Figure 4.3.

From the figure it can be noted that the mechanical demand (for the propulsion) and the electrical demand hourly profiles do not change with the considered season. In addition, as it concerns the mechanical power, it can be noted that there is no request during the sea stay and port stay operation phases. This is mainly due to the fact that when the mechanical power for the propellers is not necessary for the ship movement, the request is equal to zero.

With respect to the thermal power, instead, it has to be highlighted that during the summertime it accounts for only the hot water need while during the wintertime and middle season also the space heating need is taken into account, which also represents a major part of the thermal need. The peak of the thermal power, which occurs in wintertime at around 7:00 a.m., is equal to about 7 MW.

The electrical and thermal powers are always present since the continued operation of safety systems (smoke detectors, gas detectors, fixed fire-fighting equipment, alarms, emergency lights, etc.) and minimum comfort on-board (lighting, entertainment, space heating, hot water, etc.) have to be always guaranteed. Furthermore, due to the fact that the considered ship is used for the passengers transportation, both the electrical power (in addition to lighting, also for equipment for the preservation and preparation of food, refrigerators, etc.) and thermal power (for example for the

heating of the cabins) must be guaranteed also during the phase of the port stay. On the other hand, as can be noted from the figure, during the summer it is accounted also the cooling power which trend is almost constant with an average value equal to about 1˙000 kW.
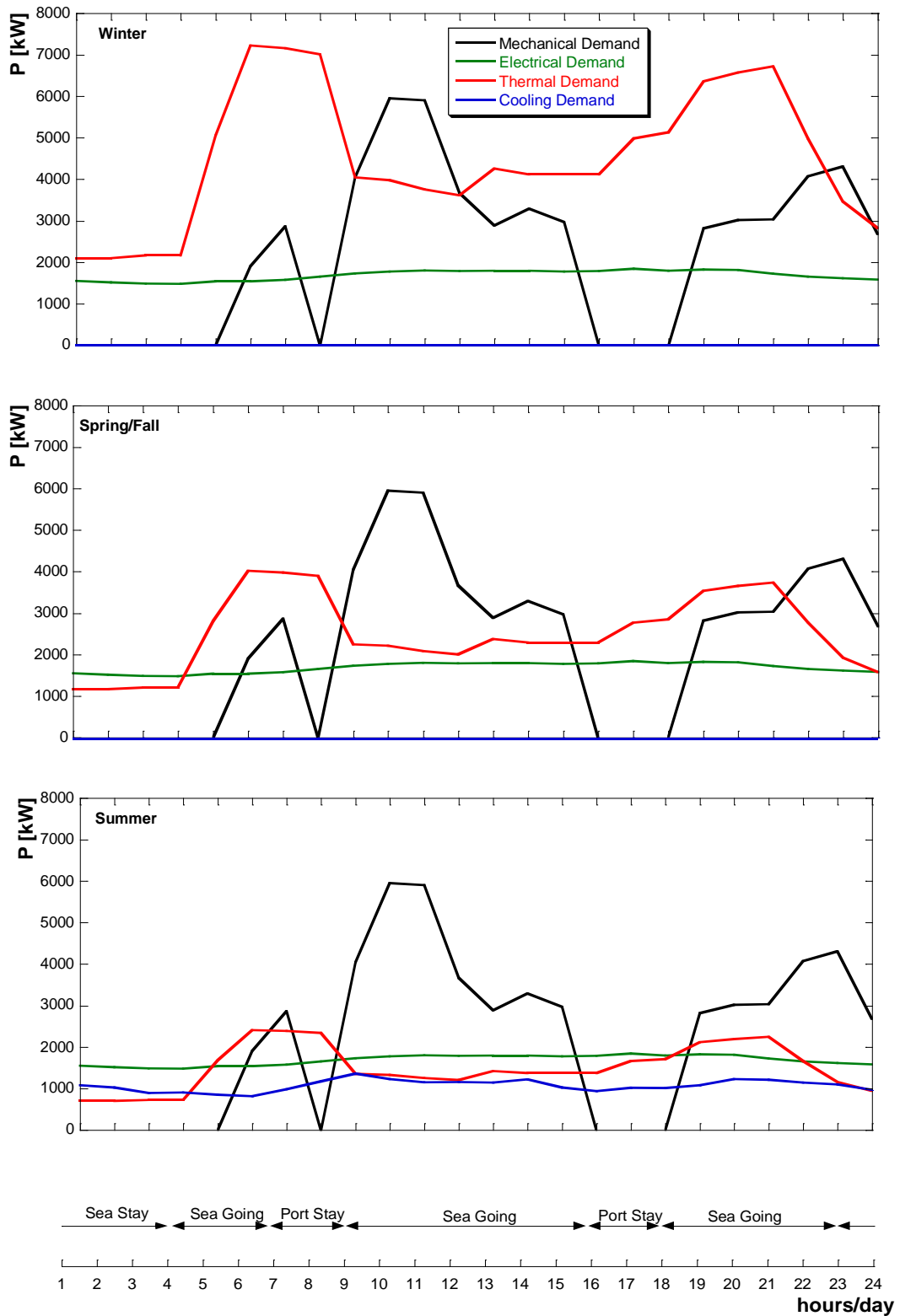
FIGURE 4.3: HOURLY LOAD CURVES FOR EACH REPRESENTATIVE DAY.

4.2.2 Developed strategies

The energy systems installed on board for the fulfillment of the electrical, thermal, cooling and mechanical energy needs are shown in Figure 4.4 and have been set as the Base Case *BC* configuration for the carried-out optimization analysis. In detail, the considered ship is equipped with a total of eight engines: four main engines for the mechanical power production (4× Wärtsilä 6L46 – from PM#01 to PM#04) and four auxiliary engines for the electrical power production (4× Wärtsilä 6L32 – from PM#05 to PM#08). All of the eight engines can operate as cogeneration units by recovering the discharged heat.
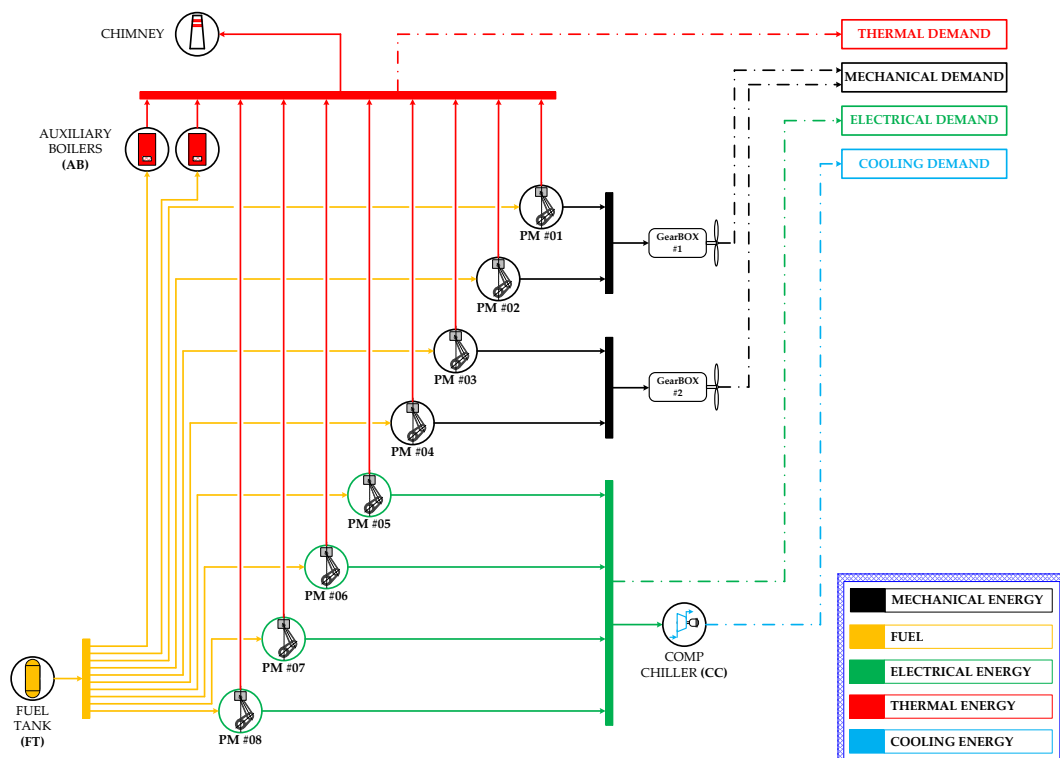
FIGURE 4.4: BASE CASE (BC) LAYOUT.

As can be noted from the figure, the four main engines are divided in two different groups (gearbox), each one responsible for the energy need for only one propeller. Thus, the mechanical load is equally shared between the two propellers. As a consequence, in the case of the mechanical demand is present, at least two main engines are involved.

The installed engines are medium speed engines [4,54] characterized by 500 RPM and 750 RPM, respectively in case of main and auxiliary engines. The design performance parameters of the primary movers are listed in Table 4.1[6,7].

TABLE 4.1: DESIGN PARAMETERS OF THE INTERNAL COMBUSTION ENGINES [5,6].

Main engine	
Model	Wärtsilä 6L46
Mechanical Power [kW]	5850
Thermal Power [kW]	6081
Mechanical Efficiency [-]	0.44
Thermal Efficiency [-]	0.46
Auxiliary engine	
Model	Wärtsilä 6L32
Electrical Power [kW]	2760
Thermal Power [kW]	3049
Electrical Efficiency [-]	0.43
Thermal Efficiency [-]	0.47

As it regards the thermal energy request, two auxiliary boilers concur, together with the eight engines, to its fulfillment. The maximum thermal power produced by each auxiliary boiler is equal to 4˙500 kW while the design thermal efficiency is equal to 80 %. On the other hand, for the cooling need fulfillment, the ship is equipped with a compression chiller which is characterized by a maximum cooling power output equal to 2˙000 kW and by a design EER equal to 3.5.

In order to evaluate the optimal way to fulfill the ship energy needs, besides the energy systems scheduling, another important aspect concerns the energy systems configuration. To this respect, in addition to the already presented base case (BC), five different configurations have been defined and analyzed with the main aim to determine both the optimal configuration and optimal scheduling of the energy systems. These configurations can be divided into two main groups, on the basis of the operational strategy performed by the engines: on one hand, the base case and the first two proposed strategies are based on the standard configuration which is typical for this typology of ships; on the other hand, the remaining three strategies are characterized by a hybrid configuration of the engines, which is mainly adopted on the military ships.

More in detail, the developed configuration are the following ones:

- Base Case (BC): this strategy, whose energy systems layout is presented in Figure 4.4, represents the current configuration of the ship. In this case, the mechanical and electrical powers fulfillment is made by equally sharing the production among the corresponding engines.

- Optimized Load (OL): even in this case, the setup of the energy systems is the one represented in Figure 4.4Figure 4.. However, differently from the BC case, in this configuration the load of each engine is optimized by the software EGO, based on the minimization of the fuel consumption and the wasted thermal energy.

- Optimized Load with Storage (OL-S): in this configuration, shown in Figure 4.5, a thermal storage device has been considered in addition to the previous energy systems setup. Furthermore, as for the previous OL configuration, even in this case the engines load scheduling is operated according to the software optimization.

- Hybrid (HY): this configuration, shown in Figure 4.6, is characterized by a different operational mode of the engines. In this case, in fact, has been assumed a hybrid configuration in which all the engines concur to the electricity production while the mechanical power for the propulsion is realized by two electrical engines instead of the two gearboxes.

- Hybrid with Storage (HY-S): this configuration, shown in Figure 4.7 is the same of the HY one with the only difference of an additional thermal storage tank.

- Hybrid with Storage and Absorption Chiller (HY-S-AC): this configuration, which is presented in Figure 4.8, has been developed on the basis of the HY and HY-S, but an absorption chiller has been further considered.

The investigation of each one of the defined configurations has been done by them implementation within the software EGO. This evaluation has been made by considering the energy profiles presented in Figure 4.3 of each representative day (wintertime, middle season and summertime).

Moreover, as it concerns the OL-S, HY-S and HY-S-AC configurations – which involves the addition of a storage device – it has to be highlighted that the thermal storage volume represents a part of the optimization analysis. The storage volume, in fact, has been evaluated with the main purpose of minimizing both the fuel consumption of the auxiliary boilers and the thermal energy discharged by the internal combustion engines and dispersed through the chimney.
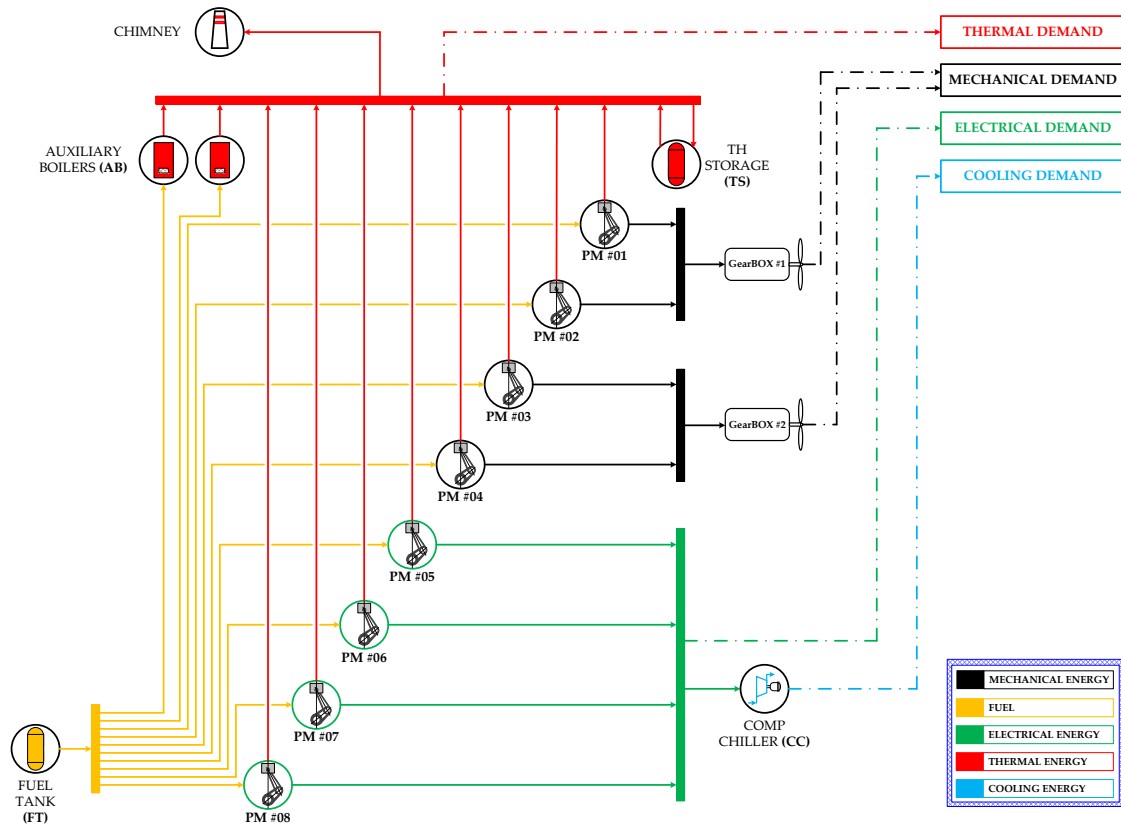
FIGURE 4.5: OPTIMIZED LOAD WITH STORAGE (OL-S) LAYOUT.
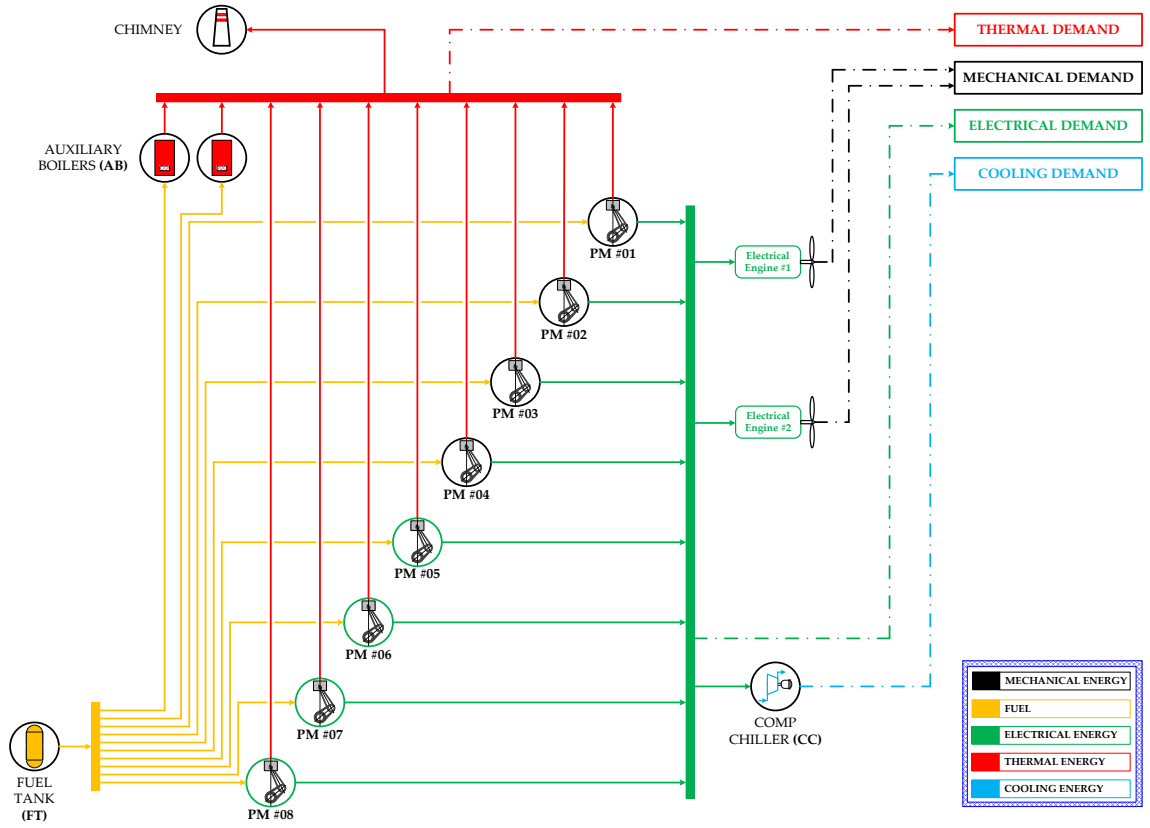
FIGURE 4.6: HYBRID (HY) LAYOUT.
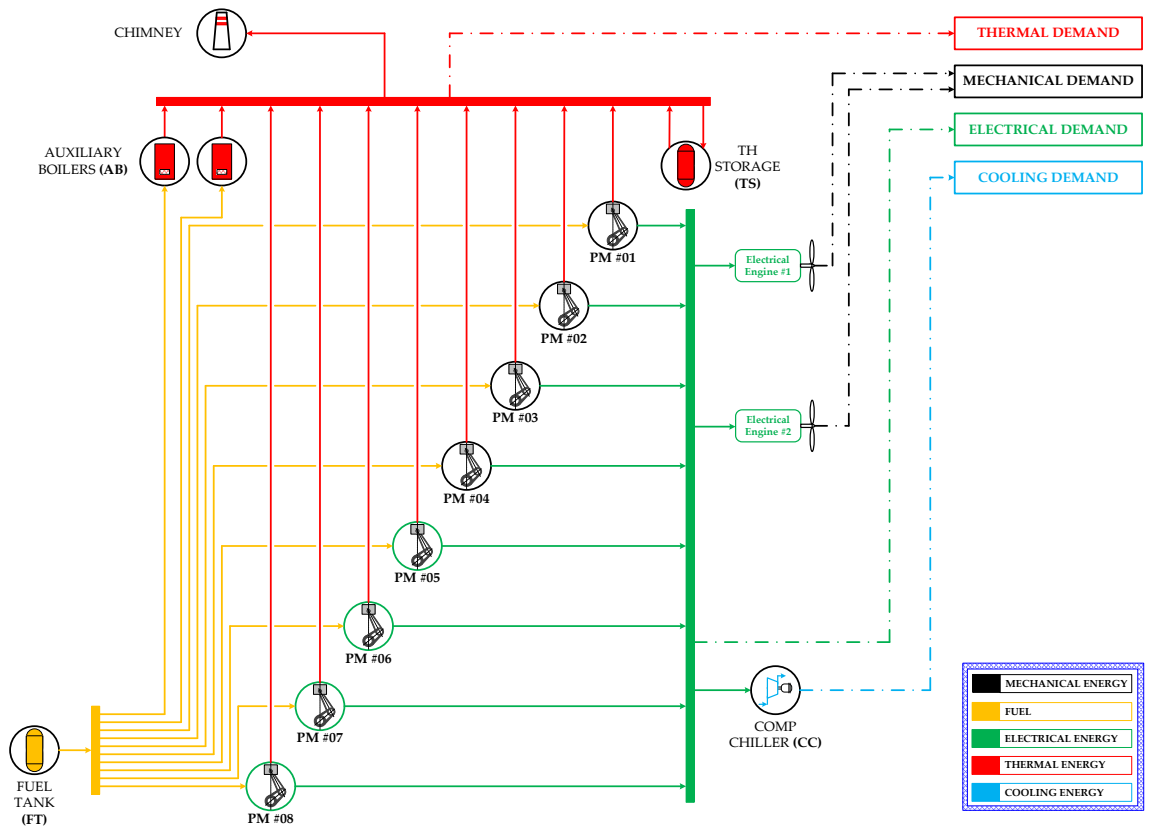
FIGURE 4.7: HYBRID WITH STORAGE (HY-S) LAYOUT.
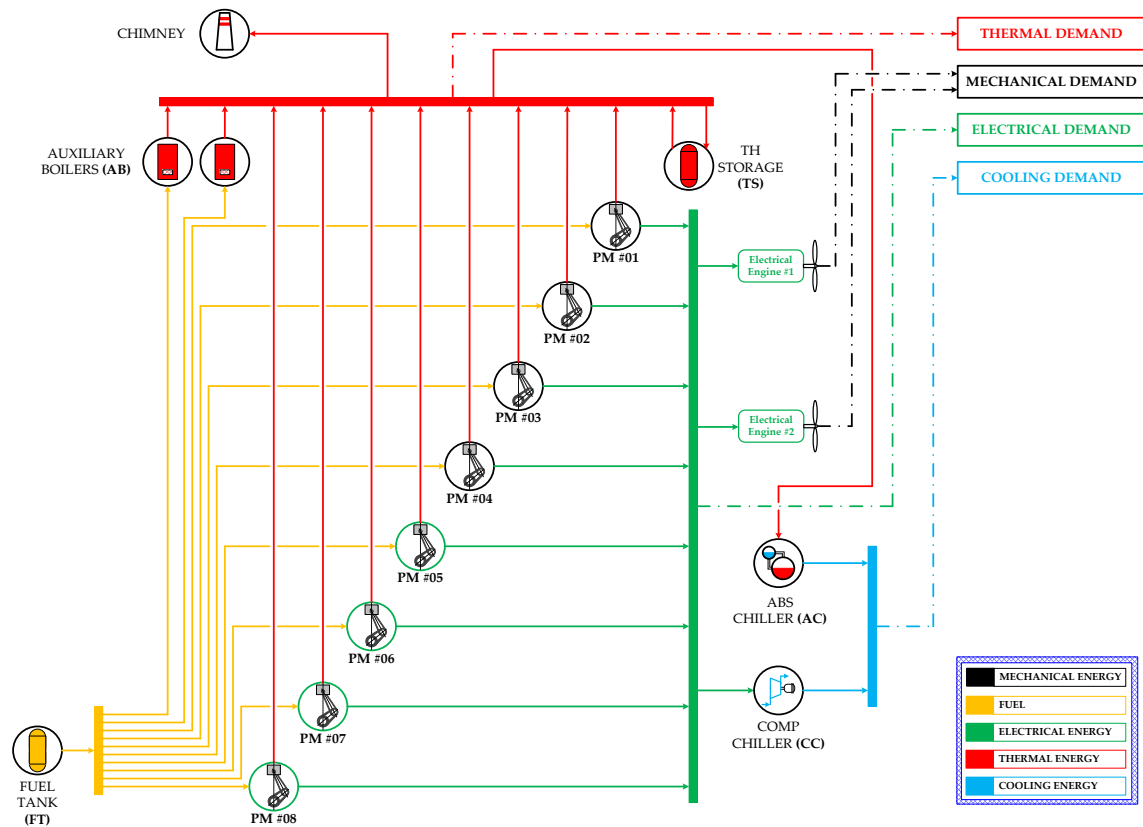
FIGURE 4.8: HYBRID WITH STORAGE AND ABSORBER CHILLER (HY-S-AC) LAYOUT.

4.2.3 Energy systems off-design

The lasts assumptions concern the off-design behavior of the energy systems. As it regards the main and auxiliary engines, the off-design behavior has been evaluated by considering the curves shown respectively in Figure 4.9 and in Figure 4.10.

From Figure 4.9 it can be observed that, on one hand, in correspondence of the engine's load equal to 80 % the mechanical efficiency assumes its maximum value (equal to about 44.7 %); on the other hand, at the same engine's load the thermal efficiency reaches its minimum value (equal to about 45.3 %).

Conversely, according to the Figure 4.10, the auxiliary engines are characterized by a maximum value of the electrical efficiency (equal to about 42.8 %) and a minimum value of thermal efficiency (equal to about 47.2 %) in correspondence of the full load.

The off-design of the auxiliary boilers, instead, is evaluated by means of the thermal efficiency is shown in Figure 4.11 as a function of the load. As can be observed from the figure, the maximum value of the thermal efficiency is equal to 80 % and occurs for a load equal to 30 %. This curve has been evaluated according to the evidence that generally – for marine applications – boilers are characterized by high performance, even at very low loads [8].

Moreover, the off-design of the compression chiller, in terms of EER, is shown in Figure 4.12 as function of the energy system load. The off-design behavior has been estimated according to the

literature [9] on the topic. Finally, as it concerns the absorption chiller, a constant value of EER equal to 0.67 has been assumed for the analysis.
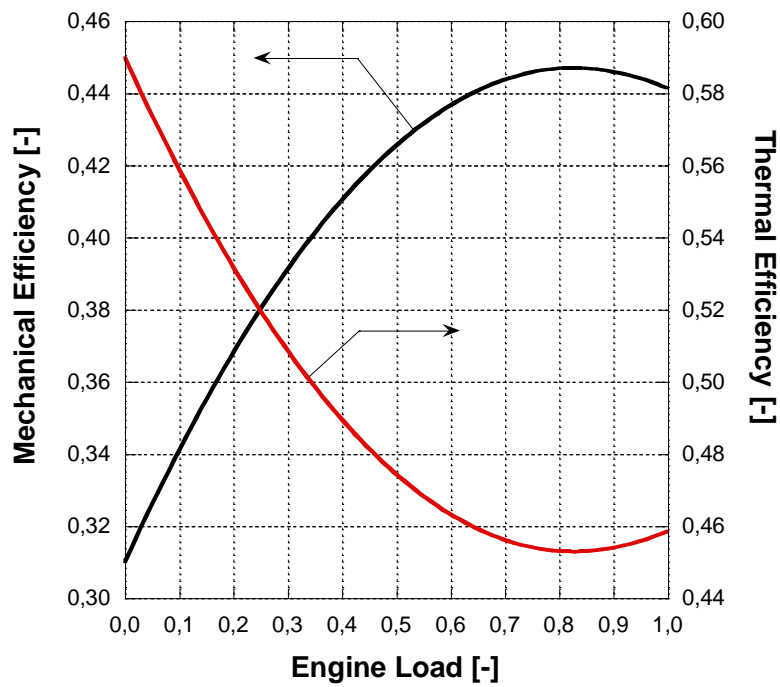
FIGURE 4.9: MECHANICAL AND THERMAL EFFICIENCY AS FUNCTION OF THE LOAD OF THE MAIN ENGINES.
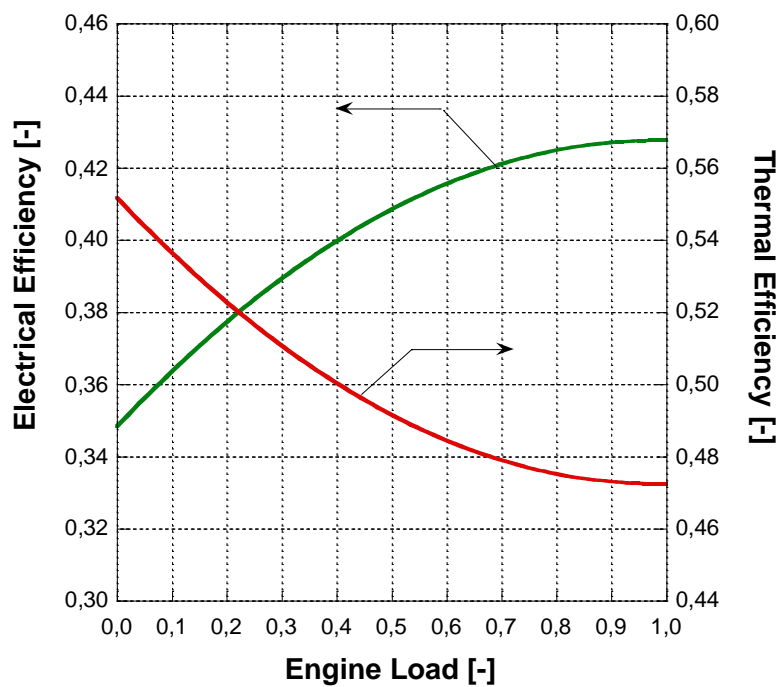
FIGURE 4.10: ELECTRICAL AND THERMAL EFFICIENCY AS FUNCTION OF THE LOAD OF THE AUXILIARY ENGINES.
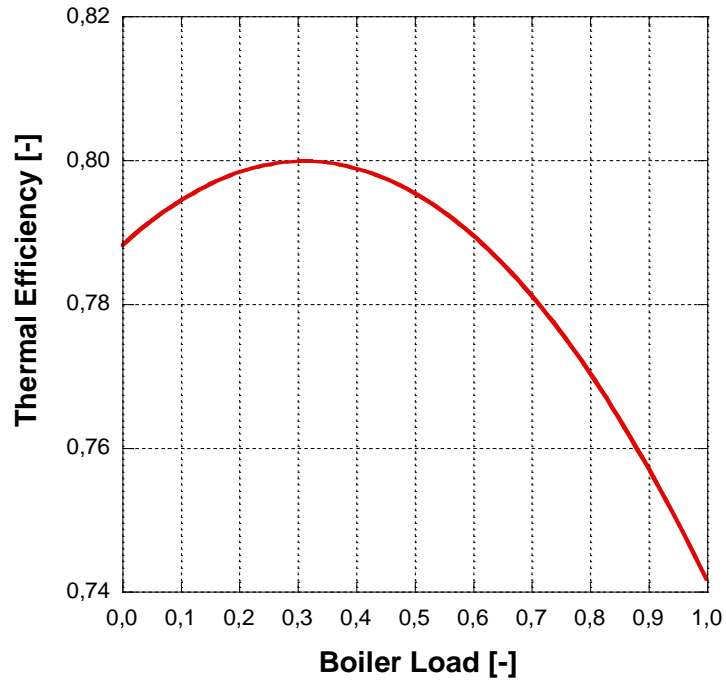
FIGURE 4.11: THERMAL EFFICIENCY OF THE AUXILIARY BOILER AS FUNCTION OF THE LOAD.
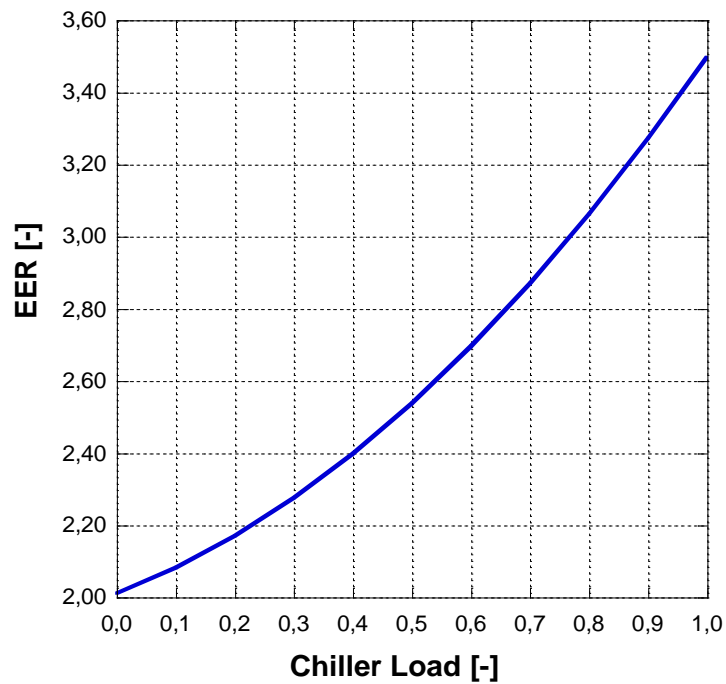
FIGURE 4.12: EER OF THE COMPRESSOR CHILLER AS FUNCTION OF THE LOAD.

Relating to the thermal storage required assumptions, an insulated tank with a global heat exchange coefficient equal to 0.5 W/m²K has been considered [10]. In addition, as it concerns the storage

116

temperature, it has been assumed that it ranges between a minimum value equal to about 100 °C and a maximum value equal to 300 °C. Instead, as previously mentioned, the choice of the optimal volume of the storage tank is a result of the analysis.

Furthermore, it has been assumed that all those auxiliary components (*i.e.:* gearbox, frequency converters and so on), which for simplicity have not represented in the configurations layout, are characterized by constant values of efficiencies, as listed in Table4.2 [11-13]. Moreover, a value equal to 0.97 has been supposed for the efficiency of the thermal and cooling energy distribution from the production systems to the user.

TABLE 4.2: EFFICIENCY OF THE AUXILIARY COMPONENTS [11-13].

Component	η_{des}
Gearbox	0.98
Generator	0.97
Electrical Engine	0.96
Frequency converter	0.98
Shaft	0.98

4.2.4 Economic and environmental analysis

For the sake of completeness, also an economic analysis has been also carried-out. To this respect, in order to evaluate the annual operational costs for each proposed configuration, the specific costs assumed for the fuel consumption and for the energy systems maintenance are listed in Table 4.3 [14, 15].

TABLE 4.3 SPECIFIC VARIABLE COSTS FOR FUEL AND MAINTENANCE [14, 15].

Energy system	Costs [€/kWh]
Fuel consumption	0.0843
Main Engines maintenance	0.0150
Auxiliary Engines maintenance	0.0150
Auxiliary Boilers maintenance	0.0060
Compression Chiller maintenance	0.0050
Absorption Chiller maintenance	0.0025

Another important aspect to be considered concerns the environmental evaluation. In fact, the environmental aspect represents a key point in the naval sector due to the actual high pollutant emissions. Indeed, it has to be highlighted that the shipping industry, even if represents only the 3 % of the whole CO_2 emissions [16], more than the 40 % of the total shipping costs is attributable to the fuel consumption. Furthermore, the regulation introduced by the International Maritime Organization (IMO) to continuously improve the standards of ship energy saving and emission reduction [17, 18]. These represents a challenge for the development of the shipping technology. To this respect, the goal is the reduction of CO_2 pollutant emissions from 40 % to 50 % [16]. For these reasons, a preliminary environmental investigation has performed.

With this purpose, the assumed emission factors are listed in Table 4.4 for the main pollutants, which – according to the Third IMO Greenhouse Gases study [17] – are Carbon Oxide (CO),

Carbon Dioxide (CO_2), Nitrogen Oxides (NO_X), Sulphur Oxides (SO_X), Particulate Matter (PM) and Non-Methane Volatile Organic Compounds (NMVOC). It has to be highlighted that these values represent the average emissions related to the specific naval sector with respect to the marine diesel oil (MDO) used as fuel for both the engines and auxiliary boilers. Finally, it has to be highlighted that these values depend on the engines speed: in this case, as aforementioned, the engines can be classified as medium-speed engines.

TABLE 4.1: EMISSION FACTORS FOR THE MDO FUEL [17].

Emission substance	Emission Factor [kg/kg fuel]
CO	0.00277
CO_2	3.20600
NO_x	0.08725
SO_x	0.00264
PMs	0.00102
NMVOC	0.00308

4.3 Results and discussion

In this section the energy results of the carried-out analysis are presented along with the economic and environmental ones.

Energy results

The main aspects of the energy production and management optimization of the cruise ship are represented by the fuel consumption and the thermal losses through the chimney. Thus, within the main purpose of investigating these two quantities, the cruise ship operation has been analyzed by varying the volume of the thermal storage tank. The results in terms of annual auxiliary boilers fuel consumption and thermal dissipations are shown respectively in Figure 4.13 and in Figure 4.14. These results have been presented for both the standard (BC, OL and OL-S) and the hybrid (HY, HY-S and HY-S-AC) configurations.

As obvious, since BC, OL and HY scenarios do not include the presence of a thermal storage, the corresponding results are represented by three points individuated in the y-axis. On the other side, the optimal volume of the other three strategies (OL-S, HY-S and HY-S-AC) is represented by the volume that avoid the operation of the auxiliary boilers and, at the same time, minimized the heat dissipations. As can be noted from the figures, the optimal volume resulting from the OL-S scenario is equal to about 61 m^3 while in the case of HY-S and HY-S-AC configurations, it is equal to about 69 m^3. These values represent a very big device. Thus, before the installation of the thermal storage devises on board, an important aspect is the evaluation of the space availability on the vessel.

To this regard, it has to be highlighted that, as can be noted from Figure 4.13, the yearly trend of the fuel consumption of OL and HY strategies are higher than the one of the Base Case configurations. However, with the introduction of the thermal storage (namely the OL-S, HY-S and HY-S-AC configurations) the yearly fuel consumption decreases by reaching values lower than the BC scenario. In particular, a decrease in the annual fuel consumption can be achieved starting from

a storage tank volume equal to about 12 m^3 for the OL-S configuration and equal to about 23 m^3 for HY-S and HY-S-AC configurations.

As it concerns the thermal dissipations (see Figure 4.14), indeed, it can be observed that all the proposed scenarios involve their reduction with the increase in the storage tank volume. To this regard, the HY-S-AC configuration results the best case, with the optimal storage volume equal to 69 m^3.
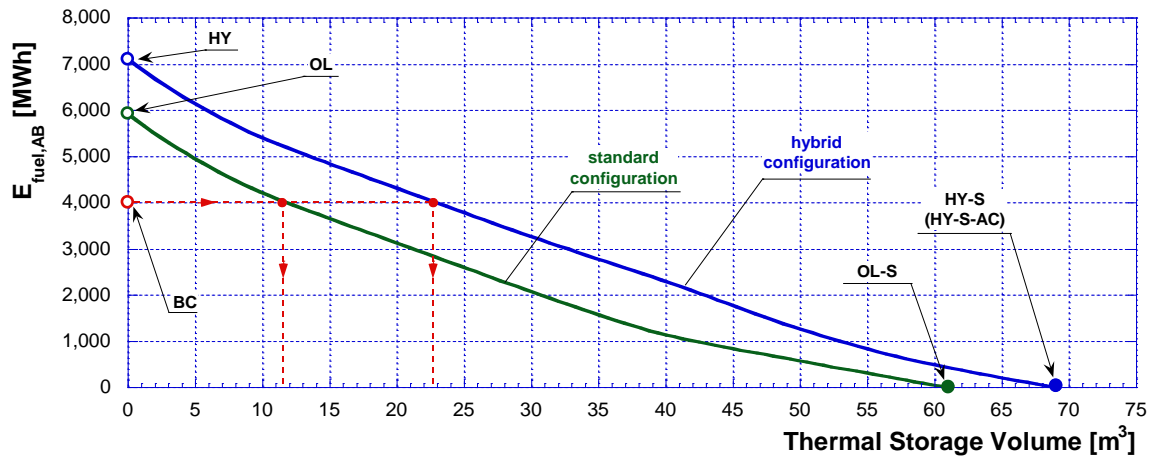
FIGURE 4.13: YEARLY AUXILIARY BOILERS FUEL CONSUMPTION AS FUNCTION OF THE STORAGE VOLUME.
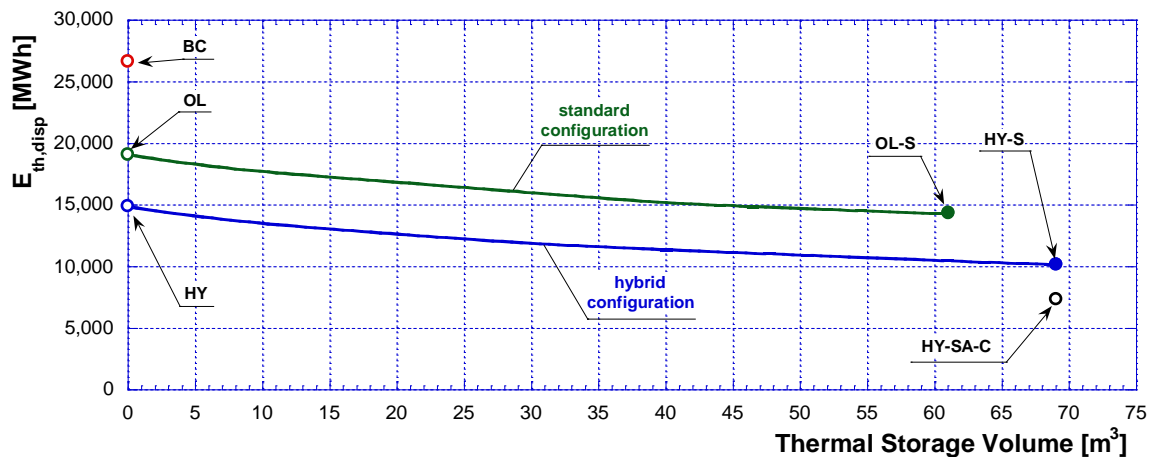
FIGURE 4.14: YEARLY THERMAL DISSIPATIONS AS FUNCTION OF THE STORAGE VOLUME.

On the basis of the aforementioned considerations, it is possible to point out both the minimum (to obtain a fuel consumption reduction with respect to the base case) and the optimal volumes of the storage device for each considered strategy. To this respect, as it concerns the standard configurations, they correspond respectively to 11.5 m^3 and 61 m^3. As it concerns the hybrid configurations, instead, the minimum volume is equal to 22.7 m^3 while the optimal one is equal to 69 m^3. In detail, the optimal thermal storage volumes – which are the ones that nullify the fuel consumption within the auxiliary boilers – correspond to the maximum volumes that allow to recover all the heat discharged from the engines. It does not imply that the maximum value of the thermal storage is the one that nullify the heat losses.

From Figure 4.13, it can be also noted that both the auxiliary boilers fuel consumption behavior and the optimal storage volume resulting from the hybrid configurations analysis are always higher that the ones resulting from the standard configurations and the Base Case evaluation. Therefore, it can be deduced that the standard configurations allow to obtain better performances than the hybrid ones. However, a deeper investigation, including the operation analysis of the other installed energy generation systems depending on the considered scenario, must be done for a complete evaluation of the proposed strategies. To this purpose, the yearly total fuel consumption (with highlighted the contribution of both the auxiliary boilers and the engines) and the yearly thermal losses have been evaluated and shown respectively in Figure 4.15 and in Figure 4.16.

These results for the OL-S, HY-S and HY-S-AC cases are represented with respect to the optimal volume of the storage tank. As can be noted from the figure, in these scenarios the employment of the boilers is completely avoided during the whole year.

Furthermore, from the fuel consumption results it can be observed that the maximum value equal to about 104˙000 MWh/y occurs for the Base Case configuration. On the other hand, in this case the heat losses (see Figure 4.16) amount to about 26˙000 MWh/y. However, with the OL scenario these values decrease. In particular, the fuel consumption and the heat losses reduction are respectively equal to about 8 % and to quite less than 29 %. As it concerns the fuel consumption reduction from BC to OL case, it can be observed that it is mainly due to an increase in the auxiliary boiler consumption for an amount equal to about 47 % coupled with a decrease of about 10 % in the engines fuel consumption. This result can be explained by considering that the optimal engines operation (which results in a different load allocation with respect to the BC) involves an increase in the conversion efficiency. As a consequence, being the total produced energy (mechanical, electrical, thermal and cooling energy) equal for each configuration, the thermal energy available from the engines decreases. Moreover, with the introduction of the thermal storage (OL-S) the fuel consumption further reduces down to completely shut down the auxiliary boilers by keeping the same the main and auxiliary engines operations. As expected, the optimal volume of thermal storage allows to reduce the thermal dissipations up to a value slightly higher than 14˙000 MWh for the standard configuration (OL-S strategy), corresponding to a reduction of about 57 % with respect to the BC strategy.

By considering the hybrid configurations, as for the OL case, even in the HY scenario the total fuel consumption is reduced with respect to the BC, since, on one hand, the auxiliary boilers consumption increases but, on the other hand, the engines fuel consumption decreases. However, the total amount of both fuel consumption and thermal dissipations is slightly higher than the ones of the OL-S configuration. Anyway, the hybrid configurations allow a greater flexibility for the engines load allocation: it follows that the engines fuel consumption from OL-S to HY reduces from more than 90˙000 MWh/y to 84˙400 MWh/y, even if an increase in dispersed thermal energy occurs (equal to about the 4%). It has to be highlighted that, moving from standard to hybrid strategy, the increase in the thermal losses occurs only when the thermal storage is not considered. In fact, the absence of the thermal storage involves the auxiliary boiler operation which results in a fuel consumption equal to about 7˙100 MWh in the HY case which represents the highest value among all the considered configurations. This result confirms that the load allocation optimization involves a fuel consumption reduction as it concerns the engines and, at the same time, a fuel consumption increases as it concerns the auxiliary boilers. Consequently, the adoption of the thermal storage, by considering the HY-S strategy, allows to nullify the fuel consumption of the auxiliary boilers and to reduce the thermal dissipations up to about 10˙000 MWh/y. Moreover, moving from HY to HY-S strategy, the adoption of a thermal storage device allows to completely shut down the boilers, but it does not affect the load allocation of the engines. Finally, the introduction of the absorption chiller (namely the HY-S-AC configuration), allows to reach a further reduction of the thermal dissipations (with a decrease of about the 72 % and the 27 % compared to

BC and HY-S respectively). In addition, with respect to the fuel consumption, with the HY-S-AC strategy it can be noted that there is a slight reduction with respect to HY-S, mainly due to the lower electrical demand of the compression chiller.
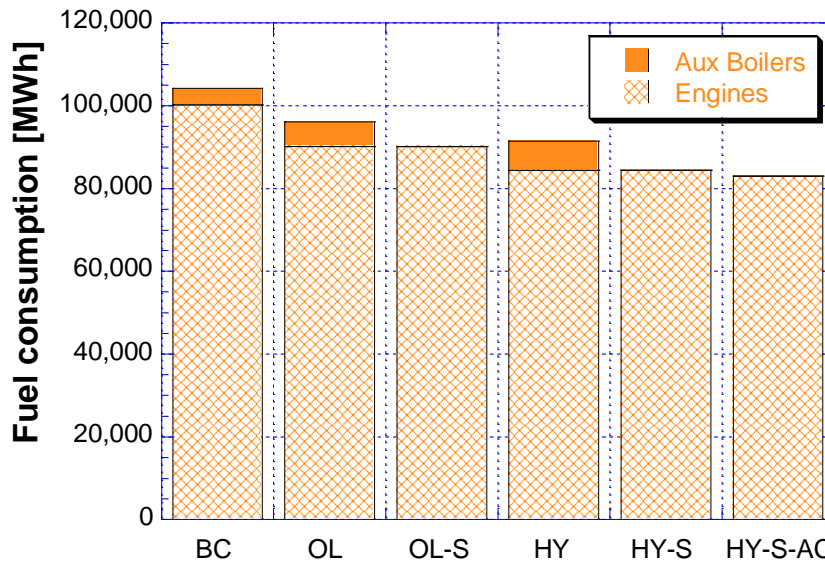
FIGURE 4.15: YEARLY TOTAL FUEL CONSUMPTION, DIVIDED BETWEEN AUXILIARY BOILERS AND ENGINES CONTRIBUTIONS.
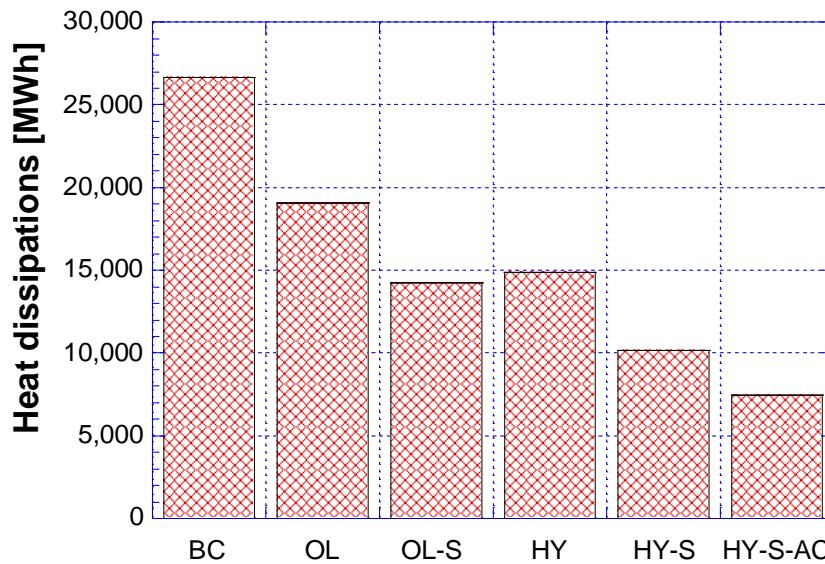
FIGURE 4.16: YEARLY TOTAL THERMAL DISSIPATIONS THROUGH THE CHIMNEY.

The last results of the energy analysis, shown in Figure 4.17, concerns the yearly operational equivalent hours – defined as the ratio between the annual produced energy and the design power

– which have been presented for each energy system (main engines from PM#01 to PM#04, auxiliary engines, from PM#05 to PM#08, auxiliary boilers, compression chiller and absorption chiller) and for each defined scenario. It has to be pointed out that the decrease in the operational equivalent hours of a given energy system means a reduction in the corresponding maintenance costs. Another consideration about the results of Figure 4.17 concerns the fact that there are no variations in the main engines, the auxiliary engines and the compression chiller operational equivalent hours by moving from BC to OL and OL-S strategies. The only difference between the OL and OL-S strategies stands in the equivalent hours of operation of the auxiliary boilers. In the same way, the HY and HY-S strategies are characterized by the same amount of operational equivalent hours for both the main and auxiliary engines. Furthermore, by comparing the HY and HY-S cases with the standard configurations results, it can be noted that an increase in the operational equivalent hours of the main engines and a decrease in the auxiliary engines occur. This result is due to the application of the optimization software which prefers the engines with the greater conversion efficiency. In addition, the HY scenario allows to increase the operating hours of the auxiliary boilers compared with the BC, while in the HY-S this value is equal to zero. As it regards the operational equivalent hours of the compressor chiller it does not varies with the strategies (namely from BC to HY-S), while with the HY-S-AC a reduction occurs due to the use of the absorption chiller. This clearly results in a reduction of the electrical load, with a consequent decrease in the operation of auxiliary engines. Finally, a slight increase in the equivalent hours of the main engines can be noted.
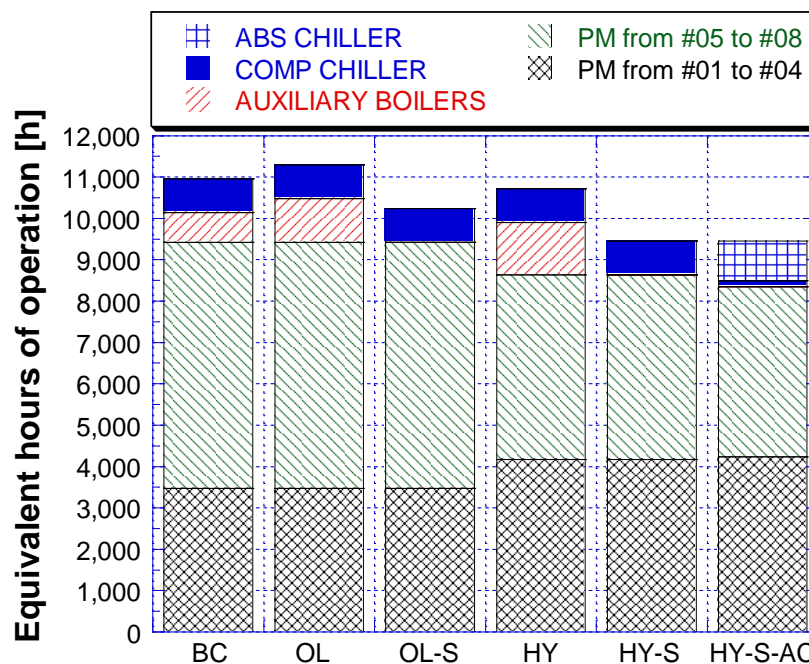
FIGURE 4.17: YEARLY EQUIVALENT HOURS OF OPERATION FOR EACH STRATEGY AND EACH ENERGY SYSTEM.

A first result obtained from the economic analysis concerns the yearly variable costs which are presented in Figure 4.18 for each considered scenario. From the figure it can be observed that the fuel costs represent the main contribution to the total variable costs. On the other hand, instead, the contribution of the maintenance costs represents the smaller percentage (around 7 %) of the total variable costs varying between a minimum value equal to about 550˙000 € to a maximum value equal to about 580˙000 €. Thus, the maintenance costs can be approximately considered constant.
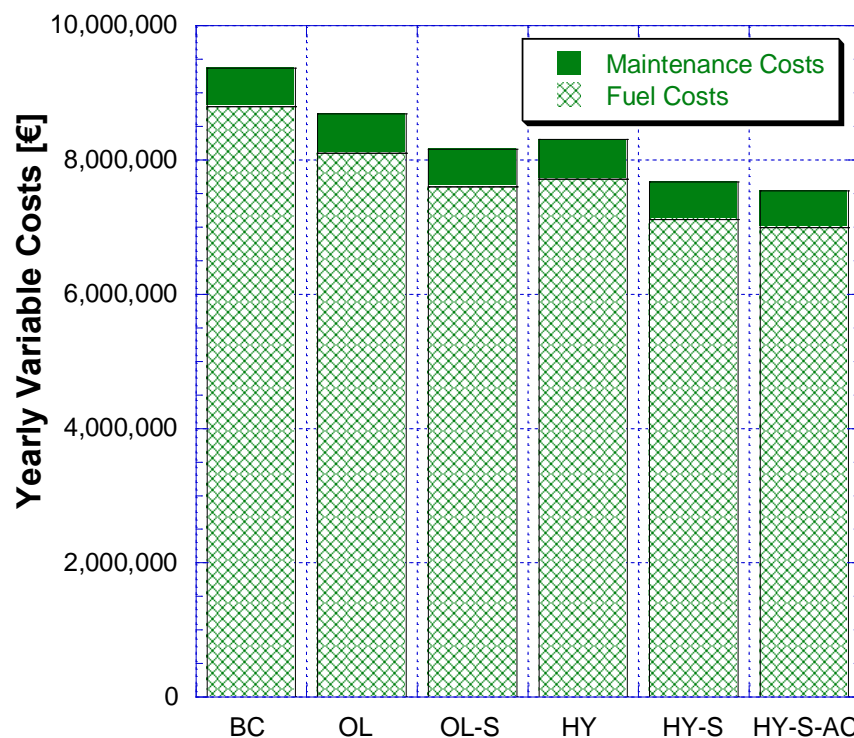
FIGURE 4.18: YEARLY FUEL CONSUMPTION AND MAINTENANCE COSTS.

Moreover, it can be also observed that the OL-S strategy allows to reduce the total variable costs, with respect to the BC, of about 13 %. It can be deduced that the increase in the investment cost due to the addition of the storage tank, can be considered moderate with respect to the decrease of the variable cost. With respect to the current layout (BC) of the ship, in the OL-S configuration, the engines setup is the same, the only difference stands in the thermal storage device.

As it for the HY-S and HY-S-AC cases, the yearly variable costs further decrease by reaching a percentage respectively equal to about 18 % and 20 %. The adoption of the thermal storage, in these cases involves a reconfiguration of the engines from the traditional to the hybrid operation. Moreover, with the HY-S-AC scenario, is also considered the installation of the absorption chiller, representing an additional cost.

On the basis if the results presented in Figure 4.18, it is possible to evaluate the annual money saving for each developed strategy with respect to the Base Case, as well as the maximum investment cost sustainable to pay back the expenditure in 2 years and in 5 years, as presented in Figure 4.19. It has to be highlighted that the worst case in terms of maximum viable investment cost occurs for the OL-S configuration, corresponding to a maximum viable investment cost ranging from a value slightly higher than 2˙000˙000 € to a value equal to about 5˙000˙000 €. By increasing the complexity of the strategy and of the setup, the value of the maximum investment cost increases up to 7˙000˙000 € in the HY-S-AC configuration. It has to be noted that this configuration is also the one that involves the installation of the greater numbers of components. Furthermore, it can be also observed that the investment costs resulting from the OL strategy have to be considered as a money saving, since the OL strategy does not change the energy systems setup but involves only the optimization of the energy systems operation. Anyway, this saving is relatively low, ranging from around 1˙000˙000 € to around 3˙000˙000 € respectively considering 2 and 5 years for the return of the investment.
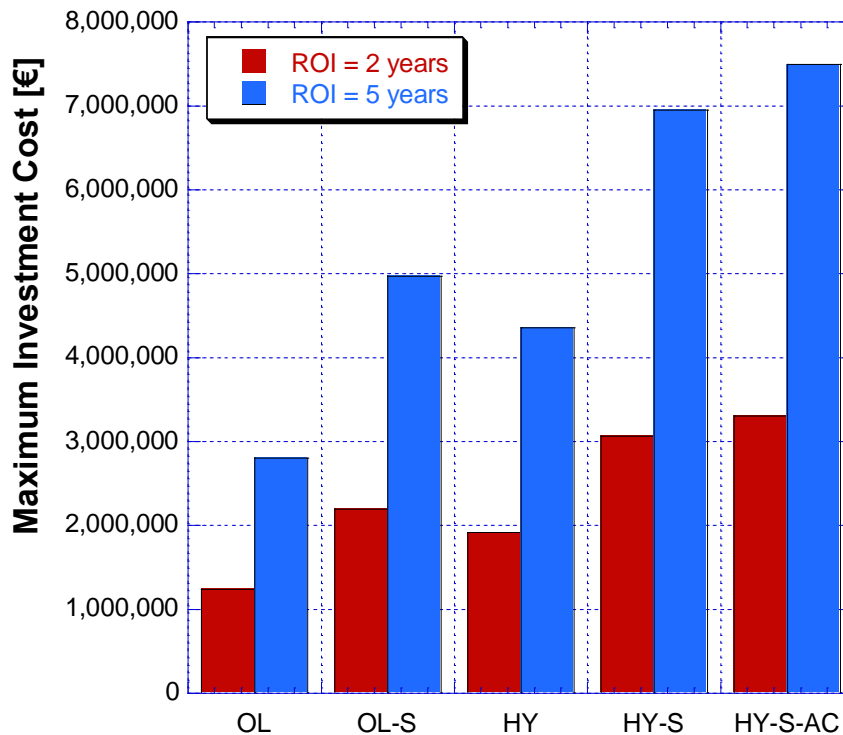
FIGURE 4.19: MAXIMUM VIABLE INVESTMENT COSTS IN ORDER TO HAVE A RETURN OF THE INVESTMENT IN 2 YEARS (RED BARS) OR 5 YEARS (BLUE BAR), FOR EACH STRATEGY.

As it concerns the environmental analysis, starting from the emissions factor listed in Table 4.6, the corresponding emissions quantities have been calculated for each of the developed configurations. The results are shown in Figure 4.20a, Figure 4.20b and Figure 4.20c.

As it regards the annual emissions of CO_2 (see Figure 4.20a), it can be observed that the values range between a minimum value equal to about 24˙000 $tons_{CO2}$/y corresponding to the HY-S-AC

scenario, to a maximum value equal to about 30˙000 tons$_{CO2}$/y for the Base Case. Due to these high values, the CO_2 represents the main pollutant.

As it concerns the Nitrogen Oxides NO_X (see Figure 4.20b), instead, it can be noted that the values range between a minimum value equal to about 650 tons/y (corresponding to the HY-S-AC case) to a maximum value equal to about 800 tons/y (corresponding to the BC).

Finally, the last result related the environmental analysis, concerns the other minor pollutant emissions (such as PMs, CO, NMVOC and SO_X) which have been presented in Figure 4.20c. With respect to the Particulate Matter (PM), from the figure it can be noted that it varies from 10 tons/y to around 8 tons/y.

As it regards the SO_X emissions, instead, it can be observed that they range from about 20 tons/y (corresponding to HY-S and HY-S-AC cases) to 25 tons/y (corresponding to the Base Case). The CO emissions, instead, vary from 21 tons/y to 26 tons/y, respectively in correspondence of the HY-S and HY-S-AC strategies and the Base Case. Finally, the NMVOC emissions vary from 23 tons/y (HY-S and HY-S-AC) to 29 tons/y (BC).

Generally, these results show that with the standard configurations (OL and OL-S) it is possible to reach a maximum decrease of the pollutant emissions equal to 14% with respect to the Base Case. On the other hand, with the hybrid configurations the emissions decrease has a further reduction for a total value equal to 20 % (from BC to HY-S-AC).

In conclusion, the hybrid configurations seem to be the most promising solutions for this kind of applications from both the energy and economic and environmental point of views. This also results in a decrease of the fuel consumption and maintenance costs, as well as the pollutant emissions, due to an increase in the global systems conversion efficiency.
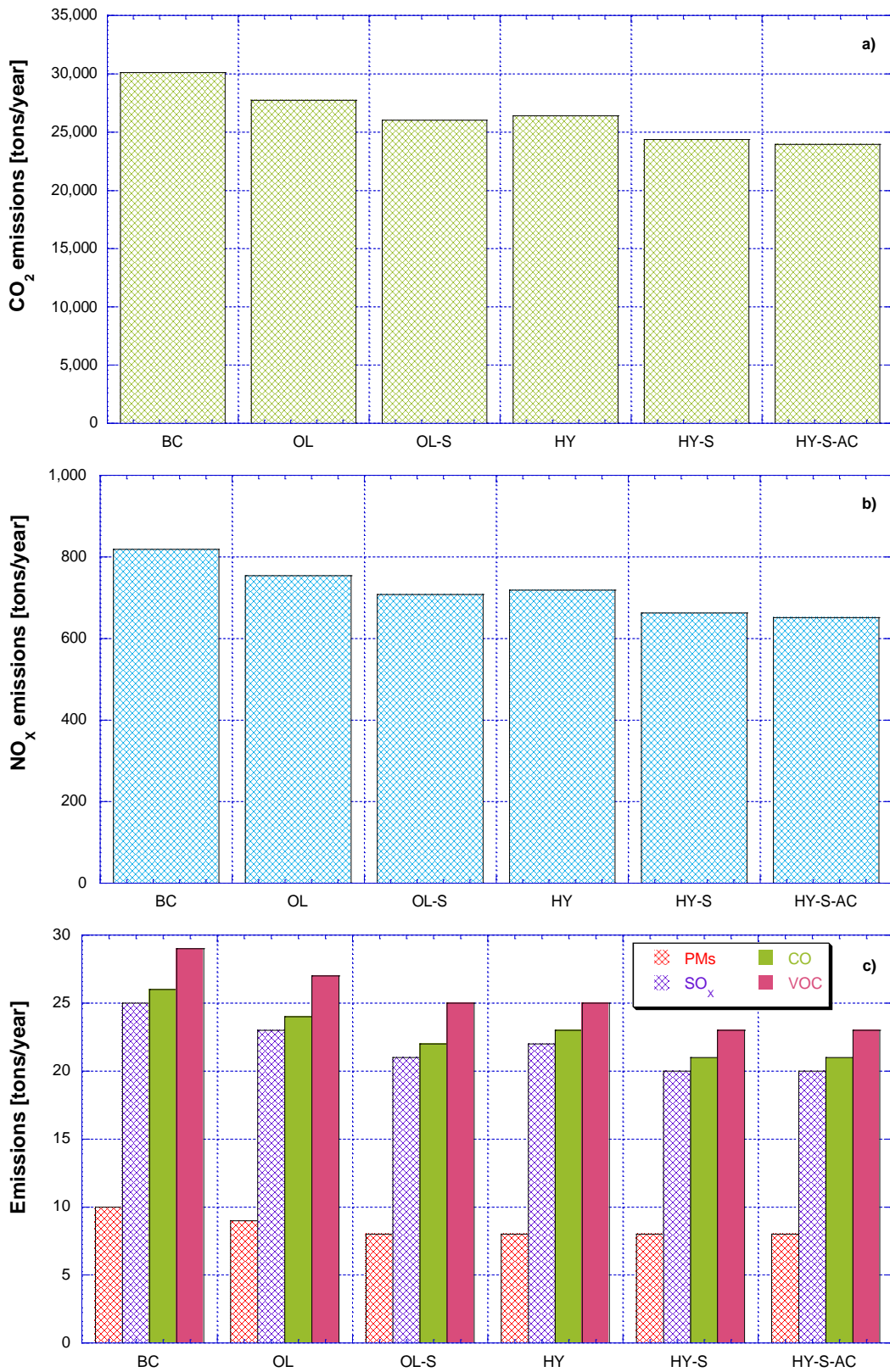
FIGURE 4.20: MAIN POLLUTANT EMISSIONS: (A) CO_2, (B) NO_X AND (C) CO, PMs, SO_X, AND VOC.

References

[1]   Ancona, M. A., Baldi, F., Bianchi, M., Branchini, L., Melino, F., Peretto, A., & Rosati, J. (2018). Efficiency improvement on a cruise ship: Load allocation optimization. Energy Conversion and Management, 164, 42-58.

[2]   Climate Change Knowledge Portal – http://sdwebx.worldbank.org/climateportal/

[3]   Baldi F, Ahlgren F, Melino F, Gabrielii C, Andersson K. Optimal load allocation of complex ship power plants. Energy Conversion and Management, 124 (2016) 344-356.

[4]   Ntziachristos L, Saukko E, Lehtoranta K, Rönkkö T, Timonen H, Simonen P, Keskinen J. Particle emissions characterization from a medium-speed marine diesel engine with two fuels at different sampling conditions. Fuel, 186 (2016) 456-465.

[5]   Andersson K, Brynolf S, Lindgren JF, Wilewska-Bien M. Shipping and the Environment: Improving Environmental Performance in Marine Transportation. Springer (2016).

[6]   Ntziachristos L, Saukko E, Lehtoranta K, Rönkkö T, Timonen H, Simonen P, Keskinen J. Particle emissions characterization from a medium-speed marine diesel engine with two fuels at different sampling conditions. Fuel, 186 (2016) 456-465.

[7]   Andersson K, Brynolf S, Lindgren JF, Wilewska-Bien M. Shipping and the Environment: Improving Environmental Performance in Marine Transportation. Springer (2016).

[8]   Cohen L, Fritz WA. Efficiency determination of marine boilers: input-output versus heat-loss method. J Eng Power 1962:39–43.

[9]   Macchi E, Campanari S, Silva P. La microcogenerazione a gas naturale. Polipress (2005) p.304. ISBN: 8873980163.

[10]   Ancona MA, Bianchi M, Diolaiti E, Giannuzzi A, Marano B, Melino F, Peretto A. A novel solar concentrator system for combined heat and power application in residential sector. Applied Energy, 185 (2017) 1199-1209.

[11]   Shi W, Stapersma D, Grimmelius HT. Analysis of energy conversion in ship propulsion system in off-design operation conditions. WIT Trans Econogy Environ, 121 (2009) 461-72.

[12]   Dedes E, Hudson DA, Turnock SR. Assessing the potential of hybrid energy technology to reduce exhaust emissions from global shipping. Energy Policy, 40 (2012) 204-18.

[13]   Ådanes, A.K. Maritime electrical installations and diesel electric propulsion. ABB AS Marine 2003.

[14]   Andreoni V, Miola A, Perujo A. Cost effectiveness analysis of the emission abatement in the shipping sector emissions. European Commission Joint Research Centre Institute for Environment and Sustainability, Luxembourg (2008).

[15] Gunnarsson G, Skúlason JB, Sigurbjarnarson Á, Enge S. Regenerative electric/hybrid drive train for ships – RENSEA II, Nordic innovation publication (2016).

[16] Johnson H, Styhre L. Increased energy efficiency in short sea shipping through decreased time in port. Transportation Research Part A: Policy and Practice, 71 (2015) 167-178.

[17] Anderson K, Bows A. Executing a Scharnow turn: reconciling shipping emissions with international commitments on climate change. Carbon Manage, 3 (2012) 615-628.

[18] Lindstad HE, Eskeland GS. Environmental regulations in shipping: Policies leaning towards globalization of scrubbers deserve scrutiny. Transportation Research Part D: Transport and Environment, 47 (2016) 67-76.

[19] European Commission (EC). Roadmap to a single European transport area – towards a competitive and resource efficient transport system. Brussels, Belgium; 2011.

5. Software COMBO

Among the different techniques adopted within the complex energy networks field for the definition of optimal management criteria (such as the optimization of the energy systems scheduling during the whole year of operation), in this chapter the non-heuristics algorithms are considered [1-3]. To this respect, in this Chapter 5 is presented a new software, called COMBO, based on a non-heuristic algorithm and able to solve the non-linear problem of systems scheduling is presented and validated. In detail, software COMBO has been developed in order to create all the possible combinations of the energy systems loads and to evaluate each one of them with the main purpose of finding the optimal solution, namely the configuration that minimizes the fitness function consisting in the total cost of the energy production. Therefore, the software validation is presented by considering a case study consisting in a residential neighborhood. The results of the implementation of the case study have been then compared with the results obtained by applying the same case study within the genetic algorithm-based software EGO, presented in Chapter 3.

The mathematical model of the software COMBO is presented in detail in the following, along with its validation.

5.1 Mathematical model

The software COMBO has been realized with the main aim to evaluate the optimal scheduling of the energy systems composing a complex energy network characterized by electrical, thermal cooling energies and fuel distribution [4,5]. In more detail, the software COMBO allows to determine the optimal load of each generation systems composing an energy grid by simulating the entire network. To this respect, different energy systems can be taken into account for the network fulfillment such as (*i*) prime movers for both the combined heat and power (CHP) application or electrical engines, (*ii*) thermal energy production systems (namely auxiliary boilers and heat pumps), (*iii*) cooling systems (*i.e.:* compressor chillers and/or absorption chillers) and (*iv*) non-programmable renewable energy sources generators (as, for example, the photovoltaic panels, the solar thermal panels, wind turbines).Furthermore, a connection with the national electric grid can be taken into account as well as the inclusion of the gas distribution network. The definition of the optimal load allocation of each energy systems – aimed to completely fulfill the electrical, thermal and cooling demand of the users connected to the network – is done in order to minimize the total cost of energy production.

To better understand the operation of the developed software, a schematic flow chart is represented in Figure 5.1. From the figure it can be pointed out that the core of the calculation of the software COMBO relies on a non-heuristic algorithm. In particular, to this respect, it can be noted that the algorithm consists in an iterative procedure which involves the creation and the evaluation of (potentially) all the possible loads combinations in order to point out the optimal one (namely the one representing the optimal solution in terms of the load allocation combination among the energy systems that minimizes the objective function).

More in detail, according to Figure 5.1, the input section of the algorithm consists in the definition of:

- energy demand of the users (namely the electrical, thermal, cooling and mechanical needs of the users within the network);
- prime movers (number, typology, size and main characteristics, such as the electrical and thermal design power output, off-design behavior, electrical and thermal design efficiency, etc.);
- heating systems (number, typology, size, efficiency, etc.);
- cooling systems (number, typology size, efficiency etc.);
- renewable energy sources generators (performances, peak power, etc.);
- tariff scenario (cost of the fuel, cost of purchased and sold electricity, etc.);
- internal parameters of the algorithm (number of iterations, tolerance value, etc.)

As it regards the output section, instead, it consists in the optimal scheduling of each generation systems composing the energy network along with the minimized total cost of energy production.
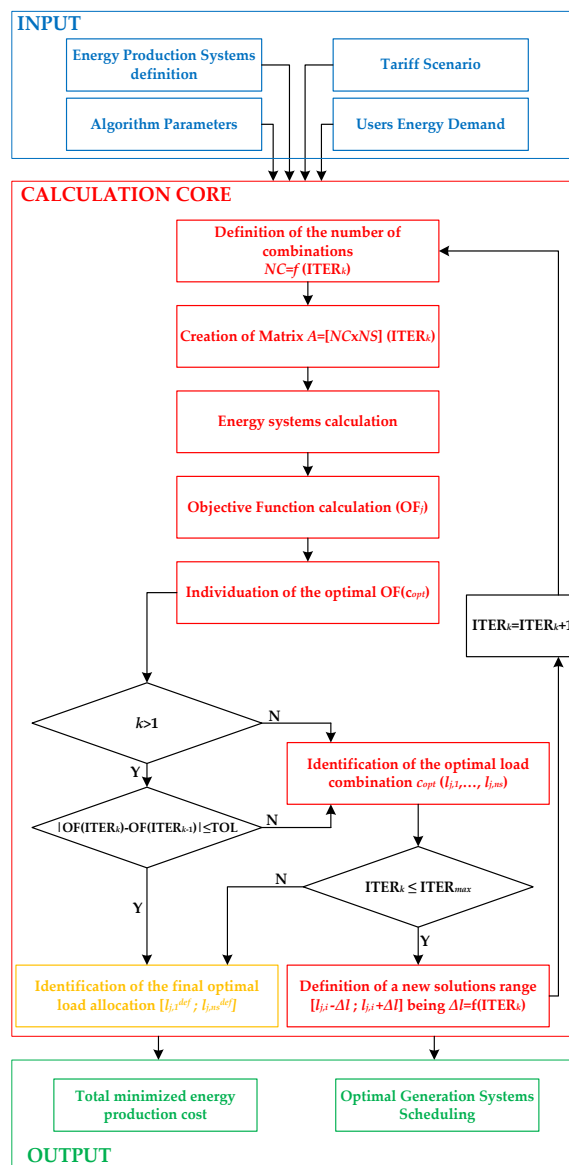
FIGURE 5.1: SCHEMATIC FLOW CHART OF THE SOFTWARE COMBO.

With respect to the calculation core of the software COMBO, instead, for a better understanding, it will be described in the following sections according to main blocks of the flow chart of Figure 5.1.

Creation of the load combinations

As aforementioned, the optimization methods at the basis of the software COMBO consists in an iterative process for the creation and investigation of (potentially) all the possible combinations of the energy systems load aimed to point out the optimal solution, namely the optimal load combination which minimizes the objective function based on the total cost of energy production.

The starting point consists in the definition, at each kth iteration (ITER$_k$) of the total number of combinations to be analyzed according to the following equation:

$$NC_k = SC^{NS}$$

<div style="text-align: right">Eq.5.1</div>

being NC (j=1,…,NC) the total number of loads combinations, NS (i=1,…,NS) the parameter indicating the total number of energy systems included in the analyzed network and SC the terms representing the total number of combinations created for a single energy system. In particular, the parameter SC can be expressed as follows:

$$SC_{i,k} = \left[1 + \frac{\left(L_{high_{i,k}} - L_{low_{i,k}} \right)}{L_{step}} \right]$$

<div style="text-align: right">Eq.5.2</div>

where the terms L_{high} and L_{low} respectively denote the higher and lower limits defining the load range while the term L_{step} indicates the step for the exploration of the range solution. All these parameters are defined at the beginning within the input section.

Once the total number of combinations NC has been calculated, the developed algorithm creates the matrix load $A = [NC \times NS]$, consisting in the list of all the load combination, defined as follows:

$$A_k = \begin{bmatrix} l_{1,1} & l_{1,2} & \cdots & l_{1,NS} \\ \vdots & \ddots & l_{j,i} & \vdots \\ \vdots & \cdots & \ddots & \vdots \\ l_{NC,1} & l_{NC,2} & \cdots & l_{NC,NS} \end{bmatrix} \Big|k$$

in which the general element $l_{j,i}$ is calculated, at each kth iteration according to the following equation:

$$l_{j,i_k} = l_{i,min} + \left[(l_{i,max} + l_{i,min}) \cdot \frac{\left\{ 1 + \left[\left[\alpha - \left(\beta \cdot \left[\frac{\alpha}{\beta} \right] \right) \right] \right] \right\} \cdot \varphi_1 \cdot \varphi_2}{l_{step}} \right] \qquad \text{Eq.5.3}$$

where the terms $l_{i,min}$ and $l_{i,max}$ respectively represents the minimum and the maximum value of the load referred to the ith system, while the term l_{step} indicates the load solution investigation step. Furthermore, the parameter β denotes the combinations generated for a single system (as well as the parameters SC of Eq.5.2) while the parameter α is defined as follows:

$$\alpha = \left\lfloor \frac{j-1}{SC^{i-1}} \right\rfloor \qquad \text{Eq.5.4}$$

being i and j representative respectively of the ith energy systems and of the jth combination considered.

As it concerns the terms φ_1 and φ_2 of Eq.5.3, instead, they represent the corrective factors for the definition of the matrix load and can be expressed with the following equations:

$$\varphi_1 = \frac{\left(L_{high_{i,k}} - L_{low_{i,k}} \right)}{NC - 1} \qquad \text{Eq.5.5}$$

$$\varphi_2 = L_{low_{i,k}} - \varphi_1 \qquad \text{Eq.5.6}$$

When the matrix load has been defined, the developed software proceeds with the investigation of each combination with the main purpose of evaluating the optimal one indicated, according to the flow chart of Figure 5.1, with the term $c_{opt_k}(l_{i,opt_k})$. However, in order to find out a more accurate solution, once the optimal combination of the kth iteration has been pointed out, at the next $k^{th}+1$ iteration, a new load range is defined for each considered energy system around the optimal solution of the previous iteration. This involves the creation of a novel load matrix A_{k+1}. To this respect, a new range of solution is calculated by redefining new higher and lower limits of the ITER$_{k+1}$. The new range limits are calculated according to the following equations:

$$l_{i,up_{k+1}} = l_{i,opt_k} + \Delta l \qquad \text{Eq.5.7}$$

$$l_{i,down_{k+1}} = l_{i,opt_k} - \Delta l \qquad\qquad\qquad \text{Eq.5.8}$$

in which the term Δl is a parameter that allows to define the upper and lower limits aimed to refine the optimal solution at the kth+1 iteration. On this regard, it has to be highlighted that the interval Δl decreases at each iteration since, as it can be noted from the previous equations, it is calculated each time as function of the considered iteration in order to make the investigation range, and consequently the research of the optimal solution, more accurate. It follows that, at each kth iteration (ITER$_k$) all the combination within the load matrix is investigated by the calculation of the objective function OF_{opt}^k as is represented in Figure 5.1. A detailed description of the objective function will be presented in the following sections.

To conclude, the iterative procedure ends in the case of all the iteration (ITER$_{max}$) defined at the beginning of the calculation have been processed and analyzed, or in the case of the absolute value of the difference between the optimal objective functions of the kth iteration and of the *k-1* iteration is lower than a given tolerance value (TOL), according to the following expression:

$$\left|OF_{opt}^k - OF_{opt}^{k-1}\right| \leq TOL \qquad\qquad\qquad \text{Eq.5.9}$$

Modelling of the energy systems

The calculation of the energy systems involves the determination of the power generated by each energy production system. On this regard, the realized software allows to model all the energy systems characterized by nonlinear efficiency curves – as a function of the load – that can be defined at the beginning of the calculation within the input section.

Starting from the performance curves, the algorithm evaluates the energy systems operation, allowing to determine – for each of the considered solutions in terms of load allocation – the electrical, thermal and cooling power produced by each energy system together with the fuel introduced into the prime movers and/or auxiliary boilers. Therefore, the total power production is compared with the energy needs of the users connected to the network, in order to find out the eventual non-production of power – which involves the non-complete fulfillment of the users – or, conversely, the eventual power surplus (in the case of the energy produced by the energy systems exceeds the one required by the users), which involves the fulfillment of the whole needs of the network but with a certain amount of energy dissipations. To this respect, the algorithm behind the software COMBO allows to find the optimal solution by minimizing and/or nullifying the non-production energy quantities. This will be show in the following in the section dedicated to the objective function.

Before entering into the detail of the definition of the objective function, it has to be highlighted that, due to its nature, the software COMBO allows to maintain the nonlinearity of the problems as well as it allows to potentially explore all the possible loads combination. This means that the developed software can find out the exact solution of the problem. Obviously, the exploration of all the possible combination will reflect on the computational time that will be higher, for example

with respect to a genetic algorithm. Furthermore, it has to be highlighted that, by analyzing a noticeable number of combinations, the developed algorithm allows to find out the optimal solution, with respect to a heuristic algorithm, with an acceptable computational time.

Objective function

After all the possible combinations of energy systems loads have been defined and listed in the load matrix A, for each iteration (ITER$_k$), each one of them is analyzed on the basis of an objective function OF in order to find out the optimal one. More in detail, the objective function – which consists in the total cost for the energy production – is calculated with the following expression:

$$OF = C_\lambda + C_M + C_E + C_F \qquad\qquad\qquad \text{Eq.5.10}$$

in which C_λ represents the total cost due to the fuel introduction into the prime movers and/or into the auxiliary boilers, C_M indicates the total cost of maintenance evaluated as the sum of the maintenance costs of each energy system, C_E represents the total cost resulting by the electricity purchase from the national electric grid and C_F is a term representing the so-called fictitious costs. It has to be highlighted that the objective function of Eq.5.10 is characterized by the same contributions – namely the maintenance, fuel, electricity purchase ad fictitious costs – which can be find in the definition of the fitness function of the software EGO presented in Chapter 3. However, the two objective functions differ in the definition of the fictitious costs C_F.

To this respect, in fact, the definition of the fictitious costs in the software EGO takes into account both the thermal dissipation through the chimney and the introduction of electricity into the grid. On the other hand, the fictitious costs of the software COMBO are defined with the main aim to avoid the non-production of electrical, thermal, cooling and, if present, mechanical energy for the users' needs fulfillment.

It follows that the surplus energy – that, due to the combinatorial nature of the algorithm, can characterize some solutions – is not taken into account within the fictitious costs but within the other contributions of the objective function and in particular in the C_λ or C_E and in the term C_M depending on the fact that the surplus is due to the employment of the prime movers, auxiliary boilers or other energy systems. More in detail, in the case of the energy surplus is resulting from the operation of the prime movers and/or the auxiliary boilers, it will be accounted as an increase in the costs of the fuel introduced within such energy systems (namely the term C_λ of Eq.5.10). In the case of the energy surplus is the result of the use of the heat pump or of the compressor chiller, it will be accounted as an increase in the electricity purchase cost (namely the term C_E of the Eq.5.10). However, whatever the nature of the surplus in terms of energy systems employed, it will also affect the maintenance costs C_M.

By entering into the detail of the fictitious costs of the software COMBO, they are calculated as follows:

$$C_F = C_{th,NP} + C_{c,NP} + C_{mec,NP} \qquad \text{Eq.5.11}$$

in which the terms $C_{th,NP}$, $C_{c,NP}$ and $C_{mec,NP}$ respectively represent the total costs due to the thermal, cooling and mechanical energy non-production.

In order to evaluate these fictitious costs, three virtual machines have been defined, consisting in an electric engine, a heat pump and a compressor chiller (respectively for mechanical, thermal and cooling energies non-production). In addition, the virtual machines have been supposed to be fed only by the electricity purchase from the national grid and do not contribute to the fulfillment of the users need. Indeed, their purpose is to evaluate the amount of mechanical, thermal and cooling energies non-production and considering this as a cost by converting these amounts into the equivalent amounts of electricity to be purchased from the national grid to move the corresponding virtual machine. In more detail, each term of the fictitious costs of Eq.5.11 can be further explicated by taking into account the specific costs of the electrical energy purchased from the national grid $\xi_{E,pur}$ for the virtual machines operation. To this respect, indeed, the cost associated to the non-produced thermal energy can be evaluated as follows:

$$C_{th,NP} = \frac{Q_{th,NP}}{COP^*} \cdot \xi_{E,pur} \qquad \text{Eq.5.12}$$

in which $Q_{th,NP}$ represents the non-produced thermal power and the term COP^*, instead, represents the Coefficient of Performance of the virtual heat pump.

Moreover, the cost of the non-production of cooling energy is accounted by the following expression:

$$C_{c,NP} = \frac{P_{c,NP}}{EER^*} \cdot \xi_{E,pur} \qquad \text{Eq.5.13}$$

being $P_{c,NP}$ representative of the cooling energy non-production and EER^* representative of the Energy Efficiency Ratio of the virtual compressor chiller.

The last terms of the Eq.5.11, which represents the non-production of mechanical power, is evaluated by the software with the following equation:

$$C_{mec,NP} = \frac{P_{mec,NP}}{\eta_{EM}^*} \cdot \xi_{E,pur} \qquad \text{Eq.5.14}$$

where the term $P_{mec,NP}$ indicates the non-produced mechanical power while η^*_{EM} indicates the electromechanical efficiency of the virtual electric engine.

At least, it has to be highlighted that the electrical energy non-production is not accounted, since the electrical needs are always satisfied by the purchase from the national grid, if the installed energy systems are not able by themselves to fulfill the whole network electricity request. As a consequence, the non-produced electrical energy ($P_{EL,NP}$) corresponds to the electrical energy purchased from the grid (with $P_{EL,pur} = P_{EL,NP}$). To this respect, taking into account the specific cost of the electricity purchase $\xi_{E,pur}$ already presented in the previous equations, the total cost due to the electricity purchase (namely the term C_E of the objective function in Eq.5.10) is expressed as follows:

$$C_E = P_{EL,NP} \cdot \xi_{E,pur} \qquad\qquad\qquad \text{Eq.5.15}$$

According to the previous consideration about the developed algorithm, after the evaluation of the fitness function, the software COMBO proceeds with the identification of the optimal solution as a starting point for the successive iteration.

5.2 Software validation

In order to validate the software COMBO, a residential neighborhood energy network has been considered as a case study. To this respect, three typical days in terms of energy needs have been individuated and taken into account for the simulation, in order to analyze a whole year of the network operation. Therefore, the results obtained with the developed software COMBO have been compared with the ones obtained by the implementation of the same case study within the software EGO (described in Chapter 3), based on a genetic algorithm. In the following section the case study is presented along with the results of the carried-out analysis.

5.2.1 Case study: residential network

The residential grid considered as case study consists in a small-medium size network composed by a total of 17 users, 13 of which are residential buildings (which includes 960 households) and 4 of which are tertiary users (divided between two schools, a day-hospital structure and a supermarket) [6]. The panoramic view highlighting the area of the considered energy network is shown in Figure 5.2.

FIGURE 5.2: AREA OF THE CONSIDERED ENERGY NETWORK.

For the investigation of the considered network three typical days have been identified representative of wintertime, middle season and summertime. The considered electrical, thermal and cooling hourly profiles (in terms of energy required by network) are presented respectively in Figure 5.3, Figure 5.4 and Figure 5.5.

These curves have been obtained starting from the non-dimensional electrical, thermal and cooling energy profiles of each users, available in literature as a function of the user typology and of the season. Then, based on the peaks of electrical, thermal and cooling demand characterizing each user, the corresponding dimensional profiles (and, consequently, also the profiles of the whole network) have been determined. To this respect, it has to be highlighted that the network thermal energy profiles account, in addition to the users thermal needs, also the heat dissipations occurring along the district heating network pipelines, while the electrical and the cooling profiles are simply determined as the sum of the contribution of each user.

In more detail, as it concerns the electrical hourly profiles, it can be observed from Figure 5.3 that it is similar for each representative day. In fact, it takes into account the electricity needs for the lighting, cold and/or hot appliances, computer side, etc., which are not so influenced by the seasonality.

In particular, the electrical demand ranges between a minimum value (that reach its absolute minimum, equal to about 520 kW, in wintertime) which occurs around 5 a.m. and by two peaks of request – which occur around 9 a.m. and 9 p.m. respectively – the higher of which is equal to about 1˙479 kW and occurs in the middle season.

With respect to the thermal needs of Figure 5.4, indeed, it can be observed that the profile of the middle season is almost the same of the one of summertime being both characterized by the only

domestic hot water request. To this regard, the thermal demand ranges between a minimum value equal to 68 kW and 80 kW to a maximum value equal to 803 kW and 836 kW, respectively during summertime and mid-season. A different profile, instead, occurs in wintertime since also the space heating is accounted. In fact, the thermal need is much higher varying between a minimum value equal to 300 kW to a maximum value equal to about 11 MW which occur respectively at 1 a.m. and at 9 a.m.

Finally, with respect to the cooling demand of Figure 5.5, which is obviously presented only for the summer season (since it accounts only for the air conditioning needs), it ranges from a minimum value equal to 875 kW to a maximum value equal to 2˙115 kW (occurring respectively at 5 a.m. and at 8 p.m.).
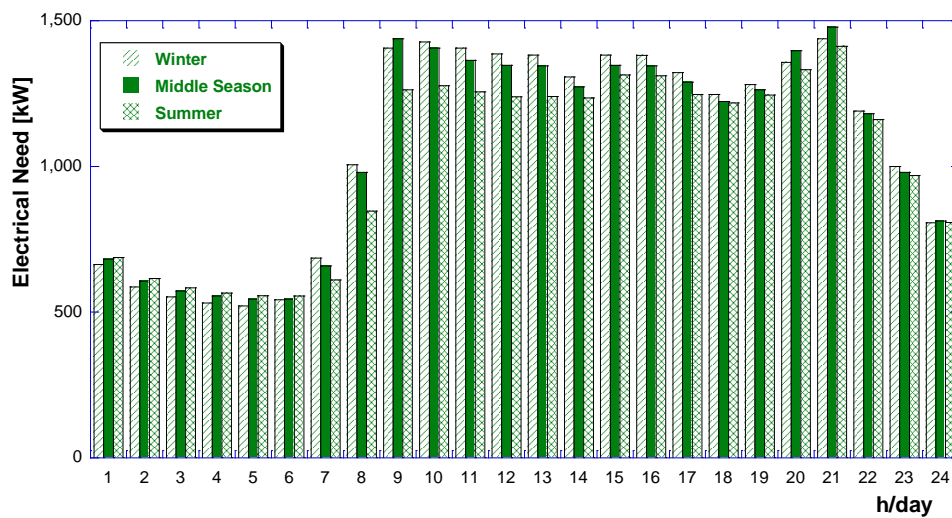
FIGURE 5.3: HOURLY ELECTRICAL PROFILES OF THE NETWORK FOR THE THREE TYPICAL DAYS.
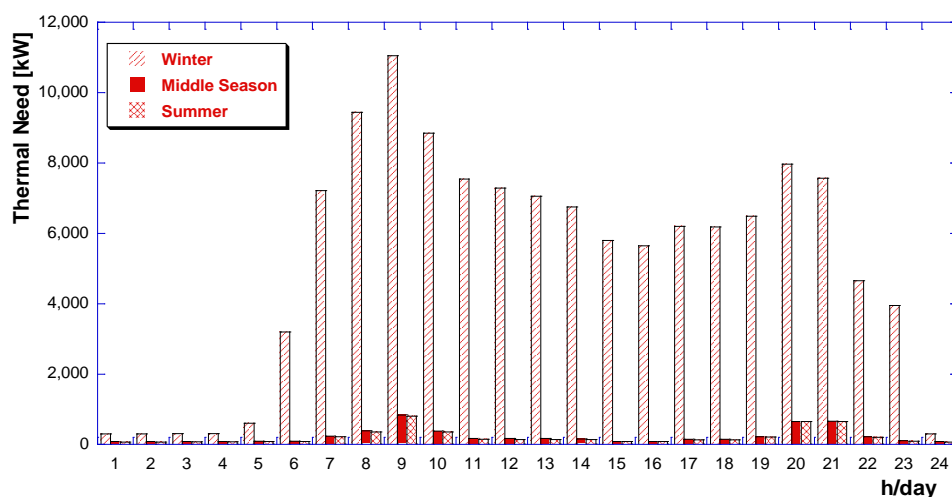
FIGURE 5.4: HOURLY THERMAL PROFILES OF THE NETWORK FOR THE THREE TYPICAL DAYS.
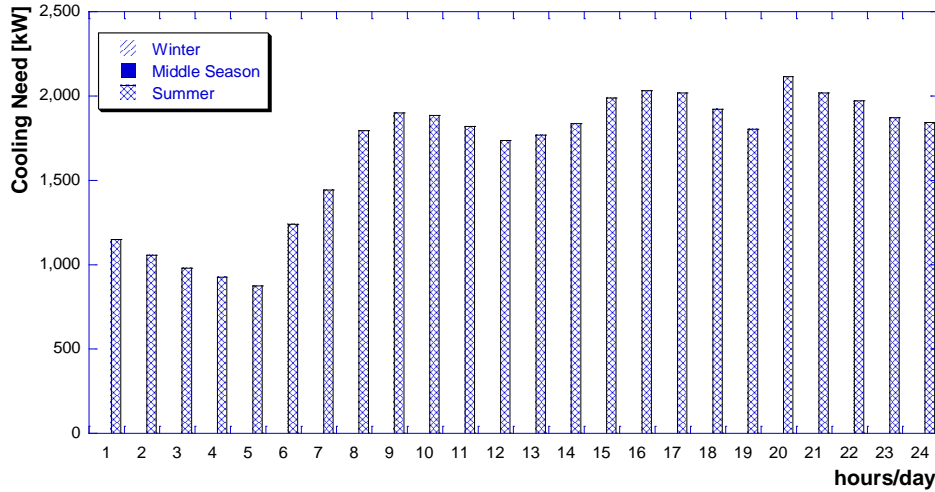
FIGURE 5.5: HOURLY COOLING PROFILES OF THE NETWORK FOR THE THREE TYPICAL DAYS.

Another important aspect concerns the energy production systems included within the considered complex energy network for the fulfillment of users needs. To this respect, the energy network is equipped with two identical internal combustion engines operating as CHP units each one of which characterized by a design electrical power equal to 730 kW. As for the thermal needs, also natural gas auxiliary boilers are included along with a heat pump. The cooling energy, instead, is provided by compressor chillers and absorption chillers. The main characteristics of each production system are listed in Table 5.1.

TABLE 5.1: MAIN PARAMETERS OF THE ENERGY SYSTEMS.

Internal Combustion Engine (each)		
Fuel Type		Natural Gas
Design Electric Power	[kW]	730
Design Thermal Power	[kW]	778
Design Electrical Efficiency	[-]	0.4161
Design Thermal Efficiency	[-]	0.4425
Auxiliary Boilers		
Design Thermal Power	[kW]	11˙600
Design Thermal Efficiency	[-]	0.80
Heat Pump		
Design Thermal Power	[kW]	20˙000
COP	[-]	4
Compression Chillers		
Design Cooling Power	[kW]	2˙200
EER	[-]	4
Absorption Chillers		
Design Cooling Power	[kW]	2˙000
EER	[-]	0.67

With respect to the internal combustion engine, in Figure 5.6 are shown the dimensional curves of the electrical and thermal efficiency as function of the ICE load.
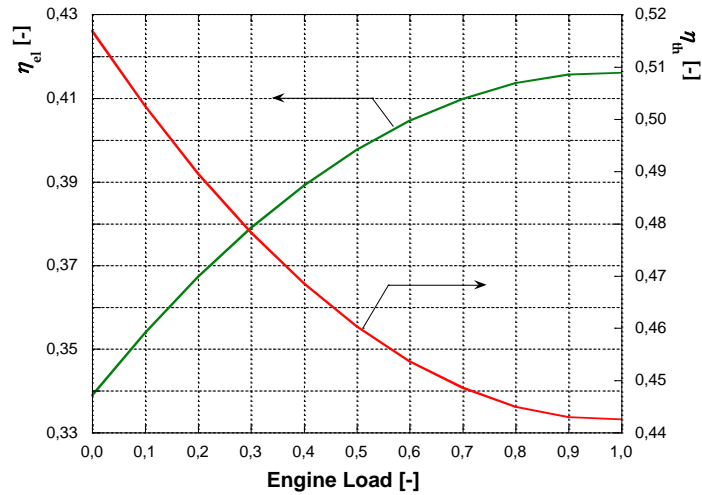
FIGURE 5.6: DIMENSIONAL CURVES FOR ICE OFF DESIGN BEHAVIOR CALCULATION OF ELECTRICAL AND THERMAL EFFICIENCY.

Moreover, with respect to the energy systems operation, it has to be highlighted that with the developed algorithm the heat pump can be powered by both the electricity produced by the ICE and/or by the electricity purchase from the national grid. On the other hand, the absorption chiller can be feed by the thermal power produced by the ICE, the heat pump and/or by the auxiliary boilers.

Finally, for a reason of completeness and to test the proposed algorithm, an economic analysis, based on the yearly time horizon, has been carried-out in order to evaluate the real cost of energy production, namely the one that does not consider the fictitious costs included in the objective function of the software. On this regard, the costs associated to the fuel employment, to the electricity purchase and the maintenance costs have been considered. With respect to the latter, the values assumed for each considered energy system are listed in Table 5.2.

TABLE 5.2: MAINTENANCE COSTS ASSUMED FOR THE ECONOMIC ANALYSIS.

Maintenance Costs		
Internal Combustion Engines	[€/kWh$_e$]	0.020
Auxiliary Boilers	[€/kWh$_t$]	0.005
Heat Pump	[€/kWh$_t$]	0.010
Compressor Chillers	[€/kWh$_c$]	0.006
Absorption Chillers	[€/kWh$_c$]	0.002

In addition, the specific cost of the fuel (*i.e.:* natural gas) has been assumed equal to 0.075 €/kWh while the specific cost of the electricity purchase from the national grid – which is different during the day depending on the time frame – has been assumed equal to 0.250 €/kWh from 9 a.m. to 8 p.m. and equal to 0.125 €/kWh from 9 p.m. to 8 a.m..

5.2.5 Results and discussion

The results of the carried-out analysis are presented in this section with respect to the three considered typical days. Furthermore, all the results are represented by operating a comparison between the COMBO and EGO application to the considered case study.

A first result, shown in Figure 5.7, concerns the computational time employed by the two software for each simulation. To this respect, from the figure it can be noted that in each considered representative day, the computational time of the software COMBO is greater than the one employed by the software EGO. In fact, on one hand, the calculation time required by EGO is in the order of few seconds (ranging from 2 to 5 seconds for a single simulated hour), while for COMBO it varies in the order of few tens of seconds (ranging from 20 to 46 seconds depending on the simulated hour). This result is strongly related to a second results, shown in Figure 5.8 which represents the number of solutions analyzed at each simulation by the two software. In fact, as can be noted from Figure 5.8, the number of solutions evaluated by the software COMBO is much higher than the number of solutions evaluated by the software EGO at each hour (namely simulation) for each representative day. In particular, for the single case the software COMBO analyzes a number of solutions in the order of the million and, more precisely, a value equal to 1˙176˙490 for each hour. The software EGO, instead, evaluates a number of 21˙000 solutions each hour. By combining the results of Figure 5.7 and Figure 5.8, it follows that the software COMBO analyses a range from 25.5 to about 58.8 thousand solutions per second against the software EGO which analyzes between 4.2 and 10.5 thousands of solutions per second. From these results it can be deduced that, on one hand, the software COMBO is probably more suitable to address the design of the network and/or the scheduling forecast. On the other hand, the software EGO is more appropriated in the context of the real-time management of the network.

A further result concerns the so-called cost gap, which consists in the absolute value of the difference between the objective function (including the fictitious costs) and the real cost of the energy production. This parameter, presented in Figure 5.9 with respect to each considered representative day, considers the reliability of the software (COMBO or EGO) since it describes to what extent the results provided by the software differ from the constraints of the desired strategy, which is defined by means of the fictitious costs. On the basis of this considerations, it follows that, in the case of the software respects all the constraints, the resulting cost-gap is equal to zero. The results in terms of cost-gap presented in the figure show that there is a strong agreement between the value of the objective function and the effective cost for the energy production both as it regards the software COMBO and the software EGO.

The last result, which is presented in Figure 5.10 with respect to each considered typical day, concerns the hourly real cost of energy production. To this respect, as can be observed from the figures, the results show that by considering the wintertime and middle season representative days, the total cost of energy production obtained with the implementation of the case study within the software EGO are higher than the one obtained by the implementation of the software COMBO. On the other hand, with respect to the summertime, it results a different behavior since the total real cost of energy production evaluated on the optimal solution obtained with the software EGO almost coincides with the ones obtained with the software COMBO. The main reason of this evidence stands in the different construction of the objective functions of the two algorithms behind the software. In particular, the difference consists in the different definition of the fictitious costs as described in the previous sections. To this respect, in fact, on one hand in the software EGO the fictitious costs have been defined by considering the energy surplus. On the other hand, the software

COMBO considers the energy non-production within the fictitious costs by accounting the eventual energy surplus within the other terms of the fitness function (costs for the electricity purchase and/or cost of the fuel and the maintenance costs). It follows that the results obtained for the solution of EGO and COMBO in terms of real cost of energy production of Figure 5.10 are due to the virtuous behavior from the environmental and/or electricity grid stability viewpoints which is a direct consequence of the different way in which the thermal energy dissipation and the electricity fed into the grid are accounted.

At least, from the figure, it can be pointed out that, according to the tariff scenario chosen from the carried-out analysis, the software COMBO results to have a more convenient approach with respect to the software EGO from the economic point of view. Moreover, on the basis of both the boundary conditions and the tariff scenario, it can be deduced that the different approach at the basis of the two software can involves a lower total cost of energy production in relation to the ratio between the cost of the electricity purchased from the grid and the cost of the fuel introduced into the energy systems.
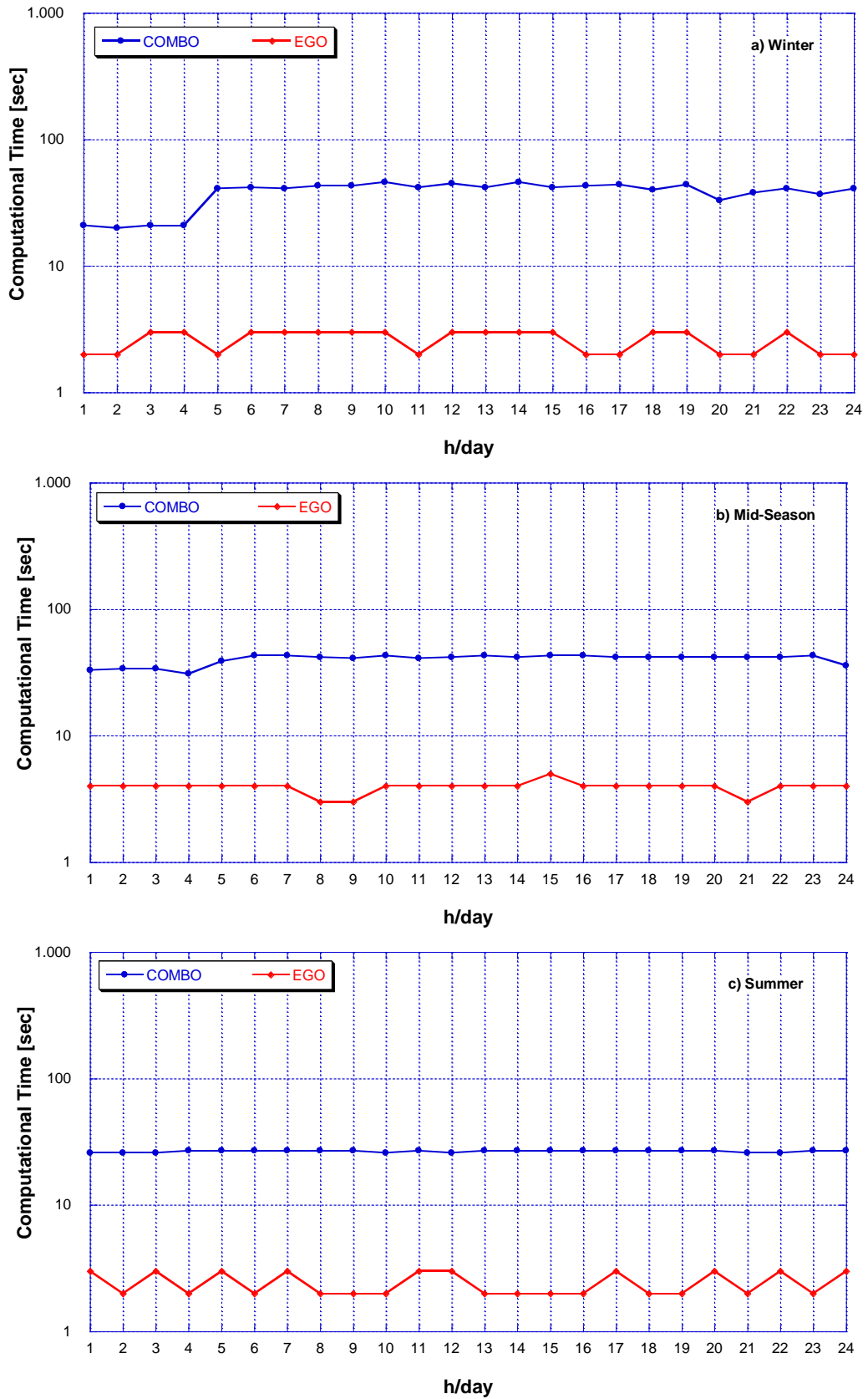
FIGURE 5.7: COMPUTATIONAL TIME RESULTING FROM THE SOFTWARE COMBO AND EGO AS FUNCTION OF THE TYPICAL DAY.
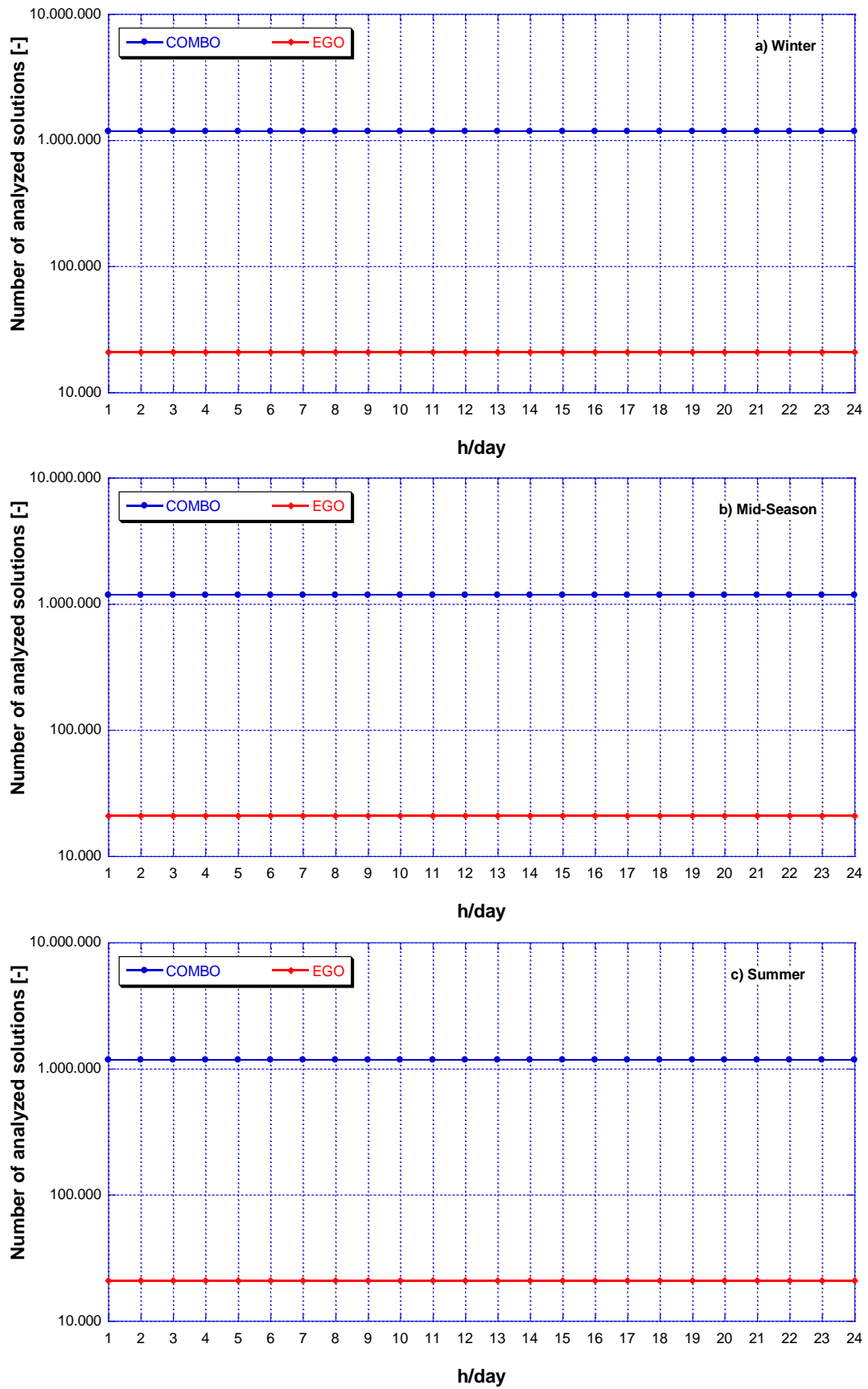
FIGURE 5.8: NUMBER OF SOLUTIONS ANALYZED BY THE SOFTWARE COMBO AND EGO AS FUNCTION OF THE TYPICAL DAY.
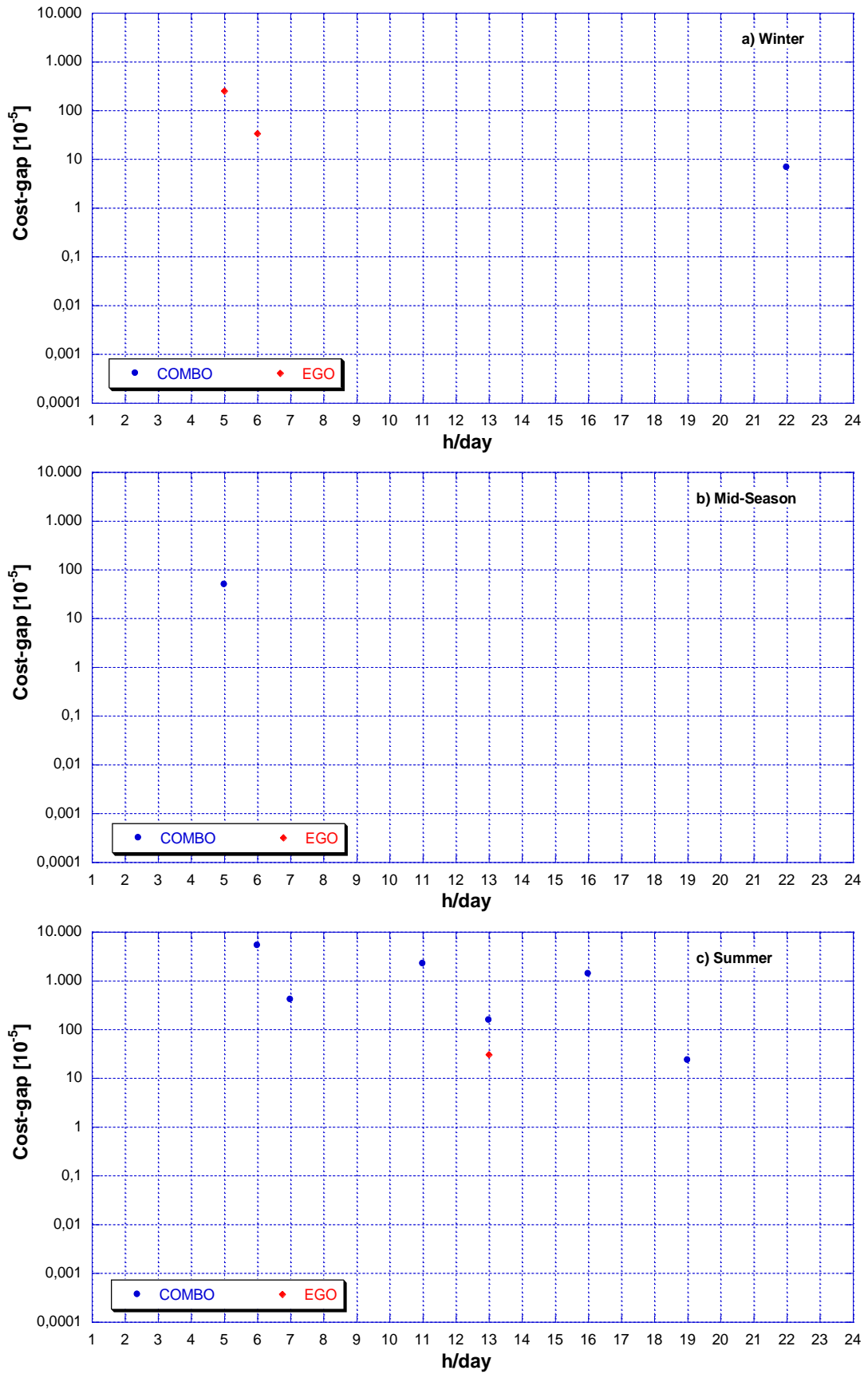
FIGURE 5.9: COSTS GAP FOR THE SOFTWARE COMBO AND EGO, AS A FUNCTION OF THE TYPICAL DAY.
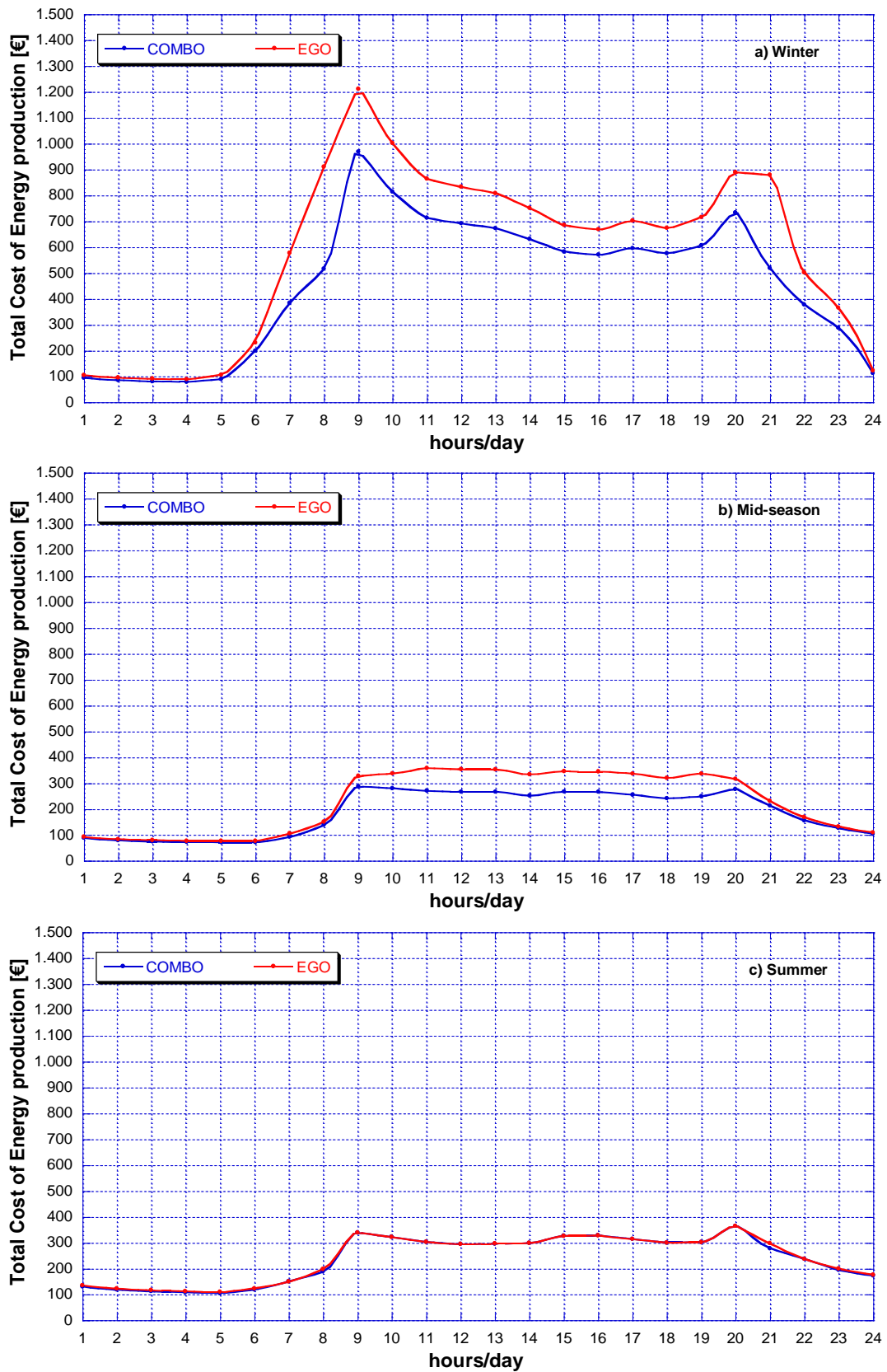
FIGURE 5.10: HOURLY PROFILE OF THE ENERGY PRODUCTION COSTS FOR BOTH SOFTWARE AS A FUNCTION OF THE TYPICAL DAY.

In conclusion, the new software COMBO, realized with the main purpose of evaluating the optimal load allocation between the energy systems connected to a complex electrical, thermal, cooling energies and fuel distribution network allows to potentially analyze all the possible loads combinations among the considered energy systems, to guarantee the fulfillment of the users needs. In the light of the obtained results, it can be outlined that the developed software COMBO allows to find a more accurate solution compared to the genetic algorithm (namely software EGO) since it investigates all the possible load combinations and, therefore, a higher number of solutions. At the same time, this involves longer computational time for the research of the optimal solution.

This comparison highlights that software COMBO is probably more suitable for all those applications such as the network design and/or forecasted scheduling. On the other hand, to address the energy networks real-time management problem, the use of the genetic algorithm is more appropriate. In addition, considering the results in term of total cost of energy production, it can be pointed out that the different approach of the software COMBO (with respect to the software EGO) affects these results. This is mainly due to the different definition of the fictitious costs within the objective function of the two software.

References

[1] Festa, P. (2014, July). A brief introduction to exact, approximation, and heuristic algorithms for solving hard combinatorial optimization problems. In 2014 16th International Conference on Transparent Optical Networks (ICTON) (pp. 1-20). IEEE.

[2] Mellouk, L., Aaroud, A., Benhaddou, D., Zine-Dine, K., Boulmalf, M. Overview of mathematical methods for energy management optimization in smart grids. In 2015 3rd International Renewable and Sustainable Energy Conference (IRSEC), 2015, December, pp. 1-5.

[3] Melhem, F.Y. (2018). Optimization methods and energy management in" smart grids" (Doctoral dissertation).

[4] M. A. Ancona, M. Bianchi, L. Branchini, A. De Pascale, F. Melino, A. Peretto, J. Rosati. Complex Energy Networks Optimization: Part I – Development and Validation of a Software for Optimal Load Allocation. Proceedings of the ASME Turbo Expo 2020, Virtual Conference

[5] M. A. Ancona, M. Bianchi, L. Branchini, A. De Pascale, F. Melino, A. Peretto, J. Rosati. Complex Energy Networks Optimization: Part I – Development and Validation of a Software for Optimal Load Allocation. ASME Journal of Engineering for Gas Turbines and Power, in press.

[6] Ancona, M.A., Branchini, L., De Pascale, A., Di Pietra, B., Melino, F., Puglisi, G., Zanghirella, F. Complex Energy Networks Optimization for Renewables Exploitation and Efficiency Increase. AIP Conference Proceedings 2191, 020007 (2019).

6. Optimization Analysis with Software COMBO

In this chapter will be presented the implementation, for the scheduling optimization of a case study, of the software COMBO, whose mathematical model has been described in the previous chapter along with its validation. In particular, a residential network has been considered as case study and has been evaluated from both an energy and an economic point of view [1,2]. In the following section the main assumptions at the basis of the carried-out analysis will be described and the results will be presented in detail.

6.1 Case study: residential network

The residential neighborhood considered for the investigation is the same of the one presented in the previous Chapter. Briefly, it consists in a small-medium network located in the city of Bologna (North of Italy) and composed by a total of 17 users (13 residential and 4 tertiary). A schematic representation of the considered energy network, in which the 17 users have been highlighted along with the central power station, is represented in Figure 6.1 [3].
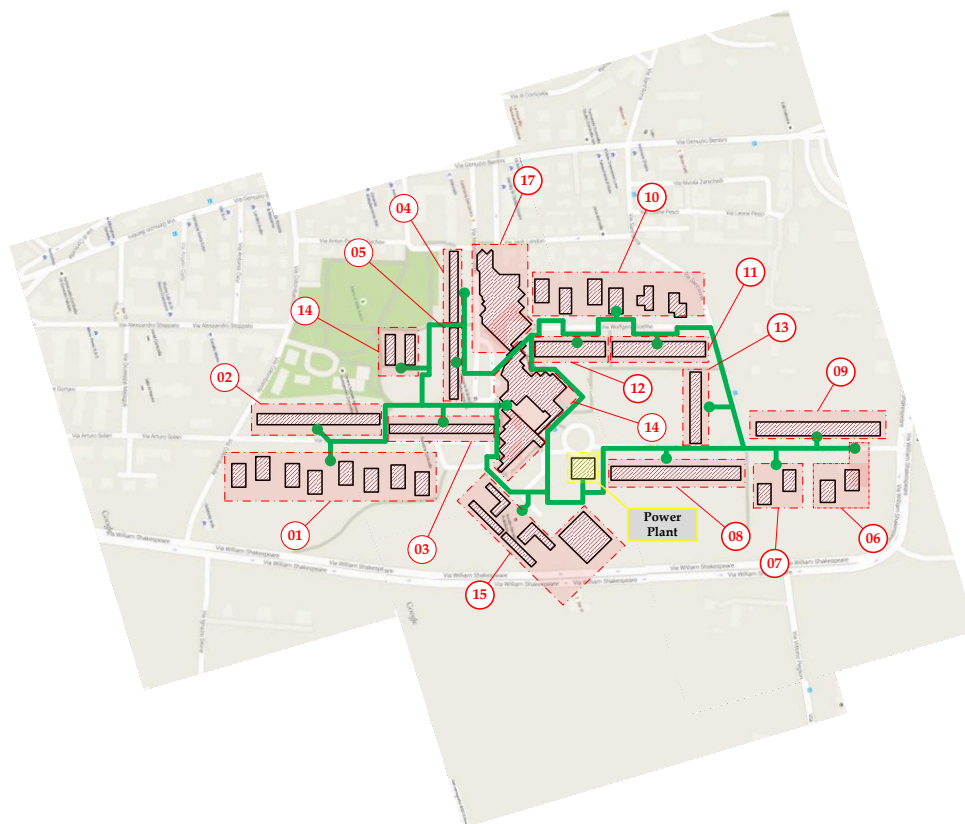
FIGURE 6.1: COMPLEX ENERGY NETWORK SCHEME.

As can be noted from the figure, the energy grid has a double ring structure in which the thermal power plant is located almost in the middle of the network.

6.1.1 Hypotheses and assumptions

A first assumption concerns the hourly electrical, thermal and cooling energies profiles of each considered representative day defined in order to perform an annual evaluation of the network operation. To this respect, it has to be underlined that the users' needs are the same of the ones presented in Figure 5.3, Figure 5.4 and Figure 5.5 in the previous chapter. These hourly profiles, as mentioned before, derives from the analysis of the typology of user and of the seasonal energy needs, the latter summarized in Table 6.1. In particular, from the table it can be observed that both the spring and fall seasons are characterized by the same typology of energy needs, that is the electricity for the electric appliances and the thermal energy for the domestic hot water (DHW) needs. While the electricity needs are registered during the whole year (with a slight variation depending on the season), the thermal needs for the space heating occurs only in the wintertime as well as the cooling needs occurs only in the summertime. It follows that, the spring and the fall season energy needs coincides and, therefore, they can be assumed in the same way and represented by the middle season profile. From these considerations it follows that for the analysis is sufficient considered three representative days: wintertime, middle season and summertime.

TABLE 6.1: TYPOLOGY OF USERS ENERGY NEED AS A FUNCTION OF THE SEASON.

Type of energy need	Spring	Summer	Autumn	Winter
Electricity	✓	✓	✓	✓
Thermal energy (SH)	×	×	×	✓
Thermal energy (DHW)	✓	✓	✓	✓
Cooling energy	×	✓	×	×

As it concerns the repartition of the season during the whole year, the following assumption has been made by considering the typical weather conditions characterizing the location of the network in the North of Italy:

- winter: 183 days:
- middle season: 90 days;
- summer: 92 days.

With respect to the energy production systems assumption, instead, it has been hypothesized that the energy needs of the users connected to the considered energy network are fulfilled by two Internal Combustion Engine (ICE) of different size, operating as combined heat and power units, four natural gas auxiliary boilers and a heat pump for the thermal request, as well as compression and absorption chillers are considered for the fulfillment of the cooling needs. The choice of a different setup, with respect to the one presented in the previous chapter for the software validation, lies into the main purpose of investigating the optimization of the energy systems scheduling by

considering an innovative configuration (namely different from the traditional one) also characterized by two different size of CHP units. Furthermore, it has to be highlighted that the micro-cogenerative approach on the basis of this analysis is based on the minimization (or avoidance) of the electricity sale for the stability and frequency of the national electric grid.

With respect to the considered energy systems, the main design parameters of the selected energy systems are listed in Table 6.2.

TABLE 6.2: DESIGN PARAMETERS OF THE ENERGY PRODUCTION SYSTEMS INCLUDED IN THE CASE STUDY.

Internal Combustion Engine (ICE) #1		
Manufacturer		Jenbacher
Model		JMS 420
Fuel Type		Natural Gas
Design Electric Power	[kW]	1˙415
Design Thermal Power	[kW]	1˙493
Design Electrical Efficiency	[-]	0.419
Design Thermal Efficiency	[-]	0.442
Internal Combustion Engine (ICE) #2		
Manufacturer		EMD
Model		EMD45
Fuel Type		Natural Gas
Design Electric Power	[kW]	45
Design Thermal Power	[kW]	63
Design Electrical Efficiency	[-]	0.325
Design Thermal Efficiency	[-]	0.455
Auxiliary Boilers (AB)		
Design Thermal Power	[kW]	11˙600
Design Thermal Efficiency	[-]	0.80
Heat Pump (HP)		
Design Thermal Power	[kW]	20˙000
COP	[-]	4
Compressor Chillers (CC)		
Design Cooling Power	[kW]	2˙200
EER	[-]	4
Absorption Chillers (AC)		
Design Cooling Power	[kW]	2˙000
EER	[-]	0.67

Furthermore, a Reference Case has been set with the main purpose of highlighting the benefits obtainable with the defined energy production mix (which is almost uncommon for the existing networks) from both the economic and environmental viewpoints. To this respect, the Reference Case consists in an energy generation mix composed by one internal combustion engine (ICE#1 in Table 6.2), the same four auxiliary boilers of the case study and the compressor chillers having the same characteristics listed in the previous Table 6.2. With respect to the internal combustion engine, in line with the current practice in this kind of applications, it has been assumed that it is completely shut down during the middle season and summertime (since in these seasons the thermal needs are

very low and concern, according to the Table 6.1, with the only domestic hot water request). During the wintertime, instead, it has been assumed that the ICE operation occurs at the design load from 9 a.m. to 8 p.m., while it is shut down in the remaining hours. It follows that the remaining request of thermal energy is fulfilled by the auxiliary boilers operation. As it regards the electrical needs, instead, it has been assumed that during the wintertime they are covered by the electricity production from the ICE and the eventual remaining part by the purchase from the national grid. During the middle season and summertime, the electricity needs are entirely covered by the electricity purchase since the internal combustion engine has been supposed to be shut down during these seasons. At least, as it regards the fulfillment of the cooling demand of the users, in the Reference Case it has been assumed to be provided by the only operation of the compressor chillers moved thanks to the electricity purchase from the national grid.

For reasons of completeness, an economic analysis has been performed by evaluating the real cost of energy production, which is calculated without taking into account for the fictitious costs characterizing the objective function of the applied software. To this purpose, a yearly based analysis has been carried-out by considering the cost of the fuel, the costs for the electricity purchase and the maintenance costs. With respect to the latter, the values of the maintenance costs of each production systems are the same listed in Table 5.2. Likewise, the fuel cost (*i.e.:* natural gas) has been hypothesized equal to 0.0075 €/kWh and the cost associated to the electricity purchase from the national grid has been assumed, depending on the time horizon, equal to 0.250 €/kWh (timeframe from 9 a.m. to 8 p.m.) or equal to 0.125 €/kWh (timeframe from 9 p.m. to 8 a.m.).

6.2.2 Results and discussion

The hourly-based energy and economic results arising from the investigation of the aforementioned case study will be presented in this section with respect to the three defined typical days. Furthermore, the energy and economic results concerning the yearly time horizon will be shown and compared with the previously defined Reference Case.

Energy analysis results

A first results of the carried-out analysis, shown in Figure 6.2, concerns the comparison between the total electrical energy required and the production mix within the energy network for each considered representative day.

In more detail, on one hand the figure shows the total energy needs, divided between the user demand and the energy required for the heat pump and/or compressors chillers operation. On the other hand, instead, it shows how this electricity need is fulfilled, namely the production mix (the internal combustion engine production and/or the energy purchased from the national grid). During the winter and middle season, the electricity needs is due, in addition to the users demand, to the energy request for the heat pump operation.

During the summertime, the electrical energy demand involves also the need for the supply of the compressor chillers. As it regards the energy production mix, from Figure 6.2a it can be observed that during the wintertime around 40 % of the electricity daily demand is fulfilled by the internal combustion engine production. In particular, with respect to the hourly need, the percentage covered

by the ICE production ranges between a minimum value equal to 0 % (occurring at 4 a.m.) to a maximum value equal to about 94.7 % (occurring at 6 a.m.) with a daily average equal to about 35.3 %. Obviously, the remaining percentage of needs is fulfilled by the purchase from the electrical national grid.

As it regards the fulfillment mix of the middle seasons, instead, from Figure 6.2b it can be noted that the electricity needs, which is almost due to the users needs and only in a very small percentage to the heat pump operation, is fulfilled in the major part of the day by the purchase from the national grid. To this respect, in fact, only the smaller ICE (namely the ICE#2 listed in Table 6.2) is in operation due to the low thermal need.

During the summertime (see Figure 6.2c), the electricity production mix shows that, from 9 p.m. to 8 a.m. – in which the electricity demand involves only the user and the compressor chiller needs – the entire demand is fulfilled by the only electricity purchase from the national grid. During the central hours of the day, instead, being present also a certain amount of electrical need for the heat pump operation, the production mix involves also the ICE production whose hourly fulfilment percentage ranges between a minimum value equal to about 33.7 % (occurring at 8 p.m.) and a maximum value equal to about 93.5 % (occurring at 5 p.m.).
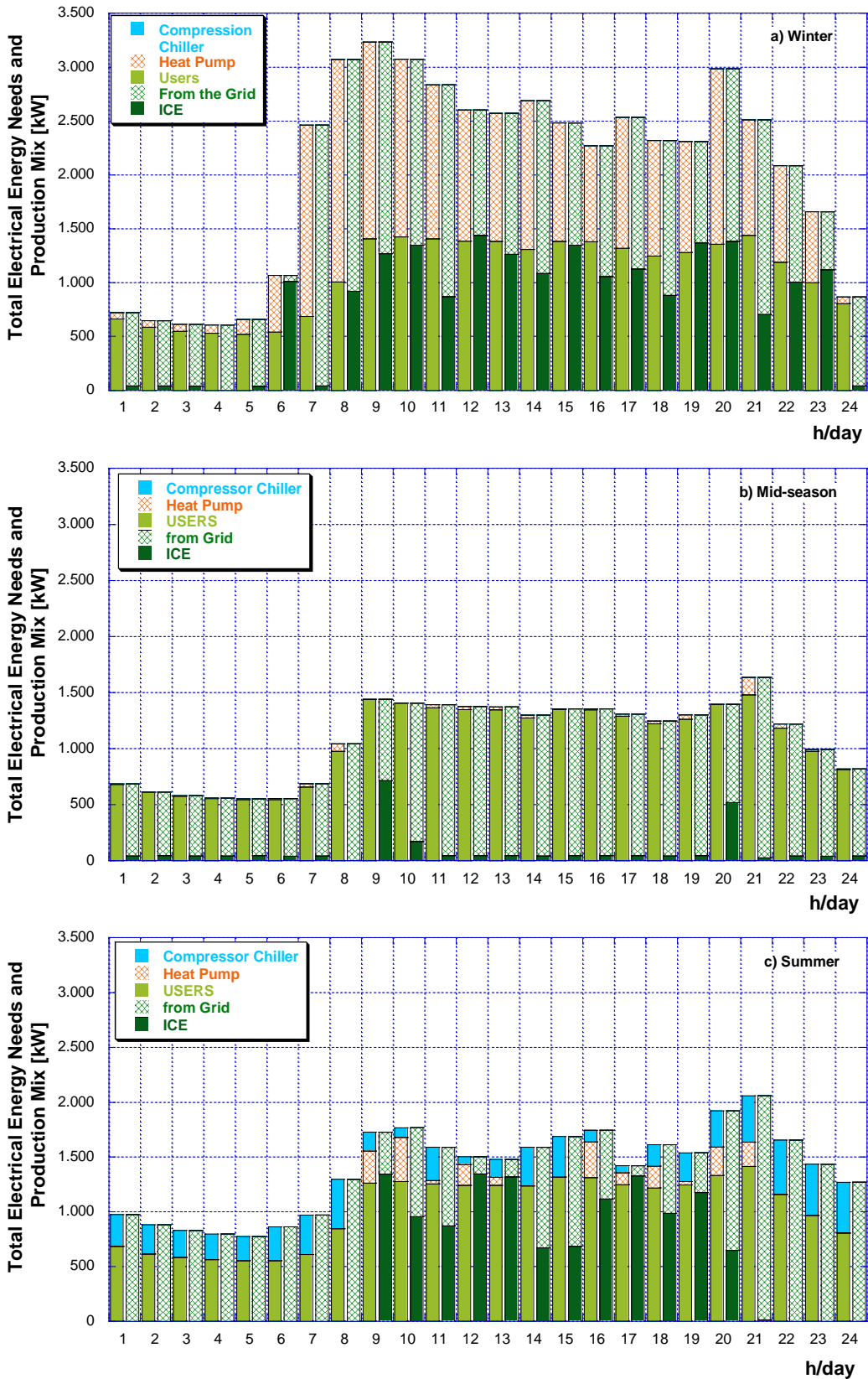
FIGURE 6.2: HOURLY TOTAL ELECTRICAL ENERGY NEEDS ALONG WITH THE ENERGY
PRODUCTION MIX FOR (A) WINTER, (B) MIDDLE SEASON AND (C) SUMMER.

Another result concerns the hourly thermal energy needs which is shown in Figure 6.3 along with the energy production mix for each representative day.

As it regards wintertime and middle season, it must be highlighted that the total thermal needs coincide with the users needs, since the only other possible thermal request within the analyzed network is the one of the absorption chillers, which however are in operation only during summertime. Therefore, in Figure 6.3a and Figure 6.3b only the energy production mix is presented. Conversely, since during the summertime the thermal needs for the absorption chillers operation are present in addition to the users demand, in Figure 6.3c the hourly thermal needs are shown.

More in detail, as it regards the wintertime, the figure shows that great amount of the energy request is satisfied by the heat pump which covers about 73.8 % of the daily need, varying – depending on the hour of the day – from a minimum value equal to about 56.6 % to a maximum value equal to 100 %, occurring at 9 p.m. and 4 a.m. respectively. The internal combustion engine, instead, contributes to fulfill about 16.5 % of the daily needs varying between a minimum value equal to about 0 % at 4 a.m. and a maximum value equal to about 33.3 % at 6 a.m.. At least, the auxiliary boilers contribute only for the 9.7 % on average of the daily demand reaching a maximum value at 9 p.m. equal to about 32.8 % of the hourly need.

During the middle season, the behavior is quite different since the major contribution for the thermal energy fulfillment is due to the ICE production, covering about 52.9 % of the daily need, reaching the maximum value at 8 p.m. when the entire need is completely fulfilled by the internal combustion engine. Also the heat pump contributes with a high percentage to the need fulfillment, covering about 40.4 % of the daily demand. The maximum contribution of the heat pump occurs at 9 p.m. when it covers a percentage of the hourly thermal needs equal to about 94.1 %. As it regards the auxiliary boilers, they contribute only for the 6.7 % of the daily demand reaching the maximum operation at 8 a.m. with a covered percentage equal to about 35.9 %.

As it regards the summertime, it can be noted from Figure 6.3c that from 10 p.m. to 8 a.m. the entire hourly thermal needs are fulfilled by the auxiliary boilers, while in the remaining hours of the day, in which the thermal needs also includes the absorption chillers request, they are fulfilled by the ICE (which covers a percentage between 2.3 % and 100 % of the hourly need), by the HP (which covers a percentage between 0 % and 78.9 % of the hourly need) and by the auxiliary boilers (which cover at least 34.2 % of the hourly need). Overall, the daily need is fulfilled by the ICE, heat pumps and auxiliary boilers by covering respectively the 53.4 %, 34.4 % and 12.2 %. Finally, it has to be underlined that during few hours of summertime occurs a small amount of heat losses through the chimney. However, due to the lower values, the thermal dissipations can be neglected.
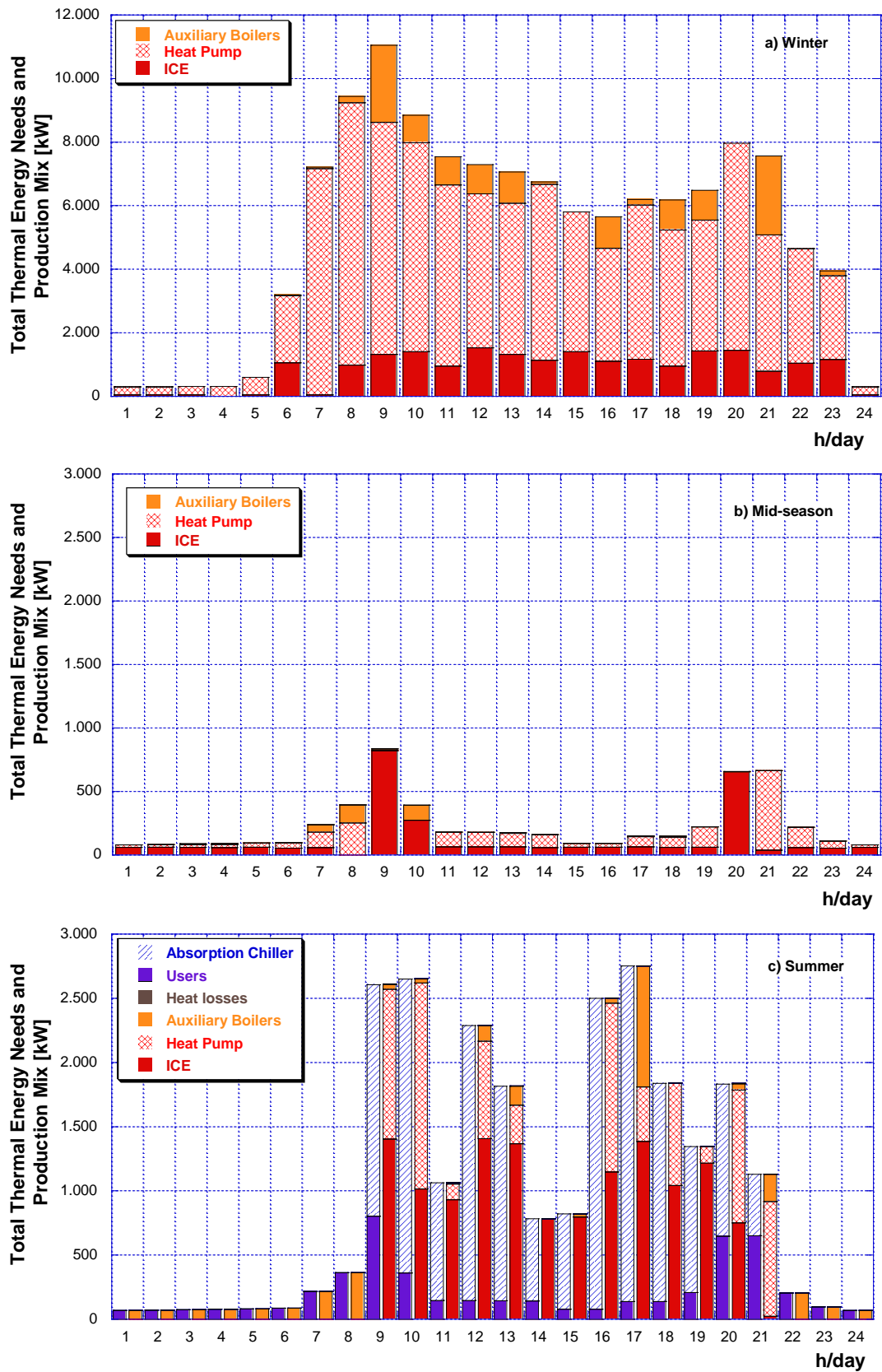
FIGURE 6.3: HOURLY TOTAL THERMAL ENERGY NEEDS ALONG WITH THE ENERGY
PRODUCTION MIX FOR (A) WINTER, (B) MIDDLE SEASON AND (C) SUMMER.

The last result related to the energy analysis concerns the cooling energy demand and production. This result is shown in Figure 6.4 only for the summertime representative day since, according to the hourly load profiles presented in Chapter 5, there is no energy request for cooling applications during the wintertime and middle season.

From the figure it can be noted that the major contribution is due to the compressor chillers which cover about 66.9 % of the daily demand. In particular, from 10 p.m. to 8 a.m., the hourly demand is fulfilled by only the compressor chillers. In the remaining hours of the day, instead, being in operation the ICE since also the thermal and electrical demands are higher than in the nighttime, also the absorption chillers are involved in the energy production mix. Overall, the absorption chillers supply a cooling energy of about 33.1 % of the daily demand.
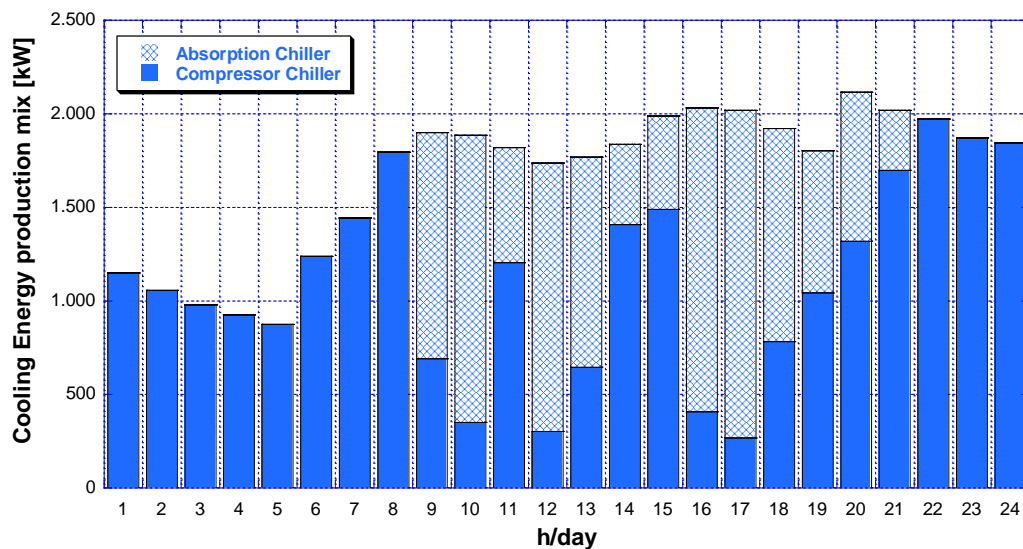
FIGURE 6.4: HOURLY COOLING ENERGY PRODUCTION MIX FOR THE TYPICAL DAY REPRESENTATIVE OF SUMMERTIME.

Economic analysis results

The results of the economic evaluation are shown in Figure 6.5 in terms of the hourly total cost of energy production as function of the considered representative day. To this respect, it has to be underlined that the economic result is shown for the case study and compared with the one of the Reference Case (represented by a red line in the figure). Furthermore, to better understand the obtained total cost of energy production, it has been represented by highlighting the contribution of the maintenance cost, the fuel cost and the electricity purchase cost. From the figure it can be observed that during the wintertime, the greater contribution to the total cost of energy production is due to the cost of the electricity purchase. In fact, it covers about 49 % of the daily cost ranging between a minimum value equal to 3 % and a maximum value equal to around 96 %. The fuel cost, instead, cover a percentage equal to about 39 % of the daily total cost of energy production. Furthermore, to this respect, it has to be pointed out that there is no contribution of the fuel cost at

4 a.m. which correspond, according to Figure 6.2, to the hour in which all the electricity need is covered by the purchase from the national grid. The maximum contribution of the fuel cost, instead, occurs at 6 a.m. being the hourly percentage equal to about 79 %. As it concerns the maintenance costs, their hourly contribution varies between a minimum value equal to about 3 % to a maximum value equal to about 19 % representing about 12 % of the daily total cost of energy production.

With respect to the middle season, shown in Figure 6.5b, it can be noted that the total cost of energy production is almost entirely due to the cost associated to the electricity purchase from the national grid. This contribution, in fact, represents about 89 % of the daily total cost. A lower contribute is due to the fuel cost, since it represents only the 9 % of the daily total cost. The remaining small percentage, instead, is obviously due to the maintenance costs.

Finally, with respect to the summertime (see Figure 6.5c), it can be observed a different behavior of the total cost repartition between the three contributes. In this case, in fact, the major contribution is due to the fuel costs which account for about 53 % of the daily total cost of energy production ranges between an hourly minimum value equal to about 4 % to a maximum value equal to about 84 %. The cost for the electricity purchase, instead, contributes for about 39 % of the daily total cost by varying from a minimum value equal to about 6 % to a maximum value equal to about 90 % which occur respectively at 5 p.m. and at 1 a.m.. The lower contribution, finally, is given by the maintenance costs, as well as for the middle season and wintertime. In fact, in this case, it covers only the 8 % of the total daily cost of energy production.

Furthermore, from the results presented in Figure 6.5 it can be noted that the economic results obtained for the Reference Case – in terms of total cost of energy production – are always higher than (or at least equal to) the ones of the case study. In particular, it results that the total cost of energy production of the Reference Case is almost coincident with the one of the case studies during the night hours, while they diverge during the central hours of the day. To this respect, from the figure it can be observed that the difference between the two cases is more evident during the wintertime and summertime. This is mainly due to a lower consumption of the fuel in the case study with respect to the Reference Case. In fact, as aforementioned in the previous sections, the thermal energy needs fulfillment of the Reference Case is mainly due to the ICE and auxiliary boilers use while in the case study, also a heat pump is considered to cover the thermal demand. The operation of the latter indeed, mainly occurs during the summertime and wintertime involving a decrease in the fuel consumption and, therefore, in the associated cost. Conversely, the heat pump employment during the middle season is lower and this results in a similar trend in the economic results between the case study and the Reference Case.
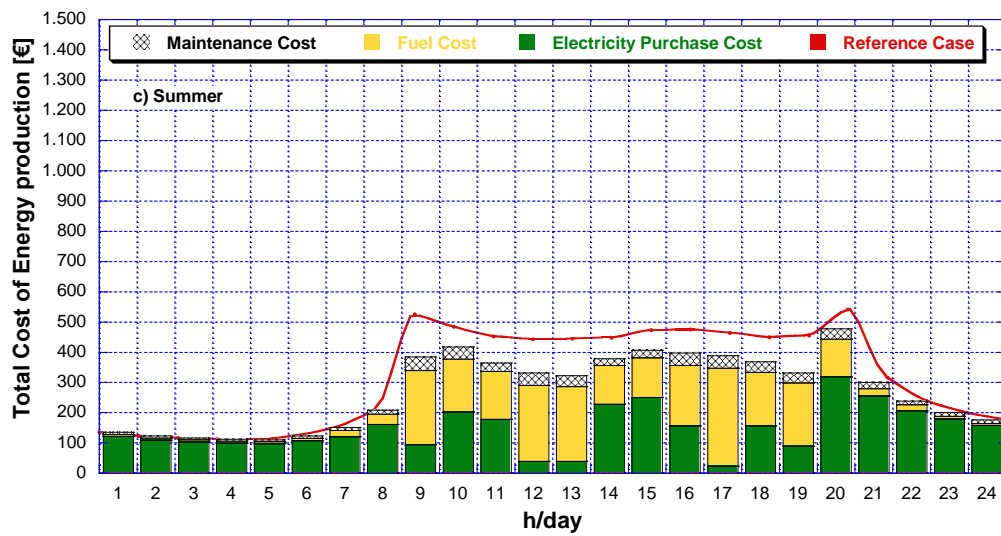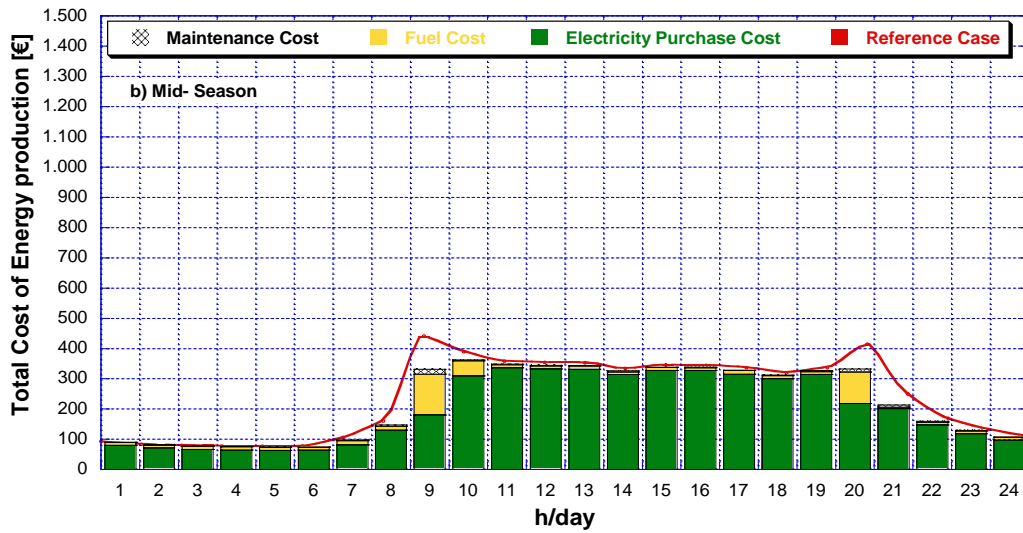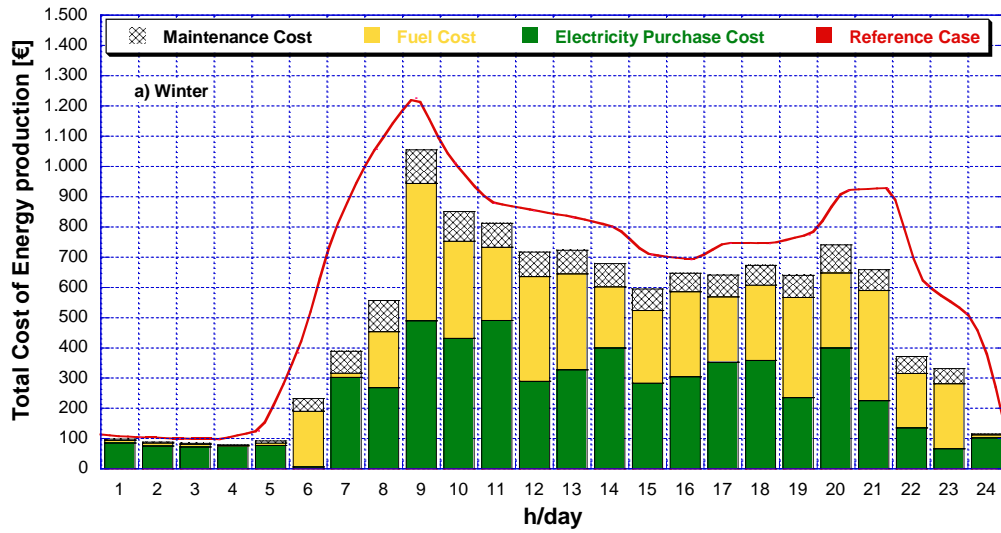
FIGURE 6.5: HOURLY TOTAL COST OF ENERGY PRODUCTION FOR (A) WINTER, (B) MID-SEASON AND (C) SUMMER.

According to the results presented in the previous sections and to the aforementioned seasonal partition, an energy and economic yearly analysis has been conducted for the energy network considered as case study. Furthermore, the same analysis has been also done by considering the Reference Case in order to compare the yearly performance in both cases. To this respect, in Table 6.3 the results of the yearly investigation are presented. The results show that, as it concerns the fuel consumption, there is a reduction of more than 50 % in the case study with respect to the Reference Case. This evidence is mainly due to the heat pump operation (being equal to 17˙371 MWh/y) which involves a significant decrease in the operation of the auxiliary boilers (being equal to 3˙493 MWh/y instead of 20˙568 MWh/y). Moreover, it can be observed that, with respect to the electrical energy, in the considered case study there is an increase in the electricity purchase from the grid with respect to the Reference Case. In both the analyzed scenarios, there is no electricity sold to the national grid.

Finally, due to the results obtained from the energy analysis, it can be noted that the total cost of energy production is lower in the case study than in the Reference Case. To this respect, indeed, there is a decrease equal to about 18 % which demonstrates the economic and energy benefits resulting from the proposed strategy and the application of the software COMBO.

TABLE 6.3: YEARLY EVALUATION RESULTS.

Parameter	Ref. Case	Case Study
Electricity sold to the grid [kWh/y]	128˙704	0
Electricity Purchase [kWh/y]	7˙323˙344	9˙465˙904
Electrical Energy from ICE [kWh/y]	3˙107˙340	4˙909˙482
Fuel Energy [kWh/y]	33˙125˙985	15˙040˙816
Thermal Energy from ICEs* [kWh/y]	3˙277˙910	5˙866˙237
Thermal Energy from AB [kWh/y]	20˙567˙919	3˙493˙436
Thermal Energy from HP [kWh/y]	-	17˙371˙238
Cooling Energy from CC [kWh/y]	3˙680˙686	2˙463˙601
Cooling Energy from AC [kWh/y]	-	1˙217˙084
Total cost of energy production [€/y]	3˙996˙511	3˙261˙979

* ICE #1 and ICE #2 for the Case Study; only ICE #1 for the Reference Case (see Table 1).

References

[1]   M. A. Ancona, M. Bianchi, L. Branchini, A. De Pascale, F. Melino, A. Peretto, J. Rosati. Complex Energy Networks Optimization: Part II – Software Application to a Case Study. Proceedings of the ASME Turbo Expo 2020, Virtual Conference.

[2]   M. A. Ancona, M. Bianchi, L. Branchini, A. De Pascale, F. Melino, A. Peretto, J. Rosati. Complex Energy Networks Optimization: Part II – Software Application to a Case Study. ASME Journal of Engineering for Gas Turbines and Power, in press.

[3]   Ancona, M.A., Branchini, L., De Pascale, A., Di Pietra, B., Melino, F., Puglisi, G., Zanghirella, F. Complex Energy Networks Optimization for Renewables Exploitation and Efficiency Increase. AIP Conference Proceedings 2191, 020007 (2019).

Conclusions

The increasing diffusion of the distributed generation systems as a consequence of the European and international targets in terms of energy efficiency increase, pollutant emissions decrease and fossil fuel consumption reduction, has been resulted in a growing complexity of the existing energy grids. In addition, the electrical grid, as well as the thermal and the cooling ones, shifted towards a smart paradigm in which the end user, called smart user (or prosumer) play an active role since it act both as a producer and as consumer. As a consequence, the concept of complex energy network has been developed, defined as a network for energy supply, consisting in electrical, thermal and cooling networks with centralized and distributed generation – eventually in presence of storage systems. The complexity of the energy networks involves new issue from both the energy systems management and operation viewpoints to prevent the instability and malfunction problems of the network. To this respect, an important aspect lies in the optimization of the production mix and operation of all the energy systems composing the network by maximizing the exploitation of the renewable energy sources, minimizing the fuel consumption and the environmental impact. Furthermore, another important aspect concerns the definition of the optimal design of the networks, in terms of ideal set-up of the energy systems for the electrical, thermal and cooling energy need fulfilment.

To this respect different optimization techniques are adopted in the complex energy networks field such as genetic algorithms, firefly algorithms and particle swarm optimization – as it regards the approximate methods – or linear programming, Mixed Integer Linear Programming and Mixed Integer Non Linear Programming as it concerns the exact methods.

A first part of the research activities focused on the investigation of the thermal grids, namely the district heating networks with a particular attention to the possibility to convert it into a smart district heating network. To this regard, the software IHENA (Intelligent Heat Energy Network Analysis), previously developed by the Energy Systems research group, has been modified in order to evaluate the possibility to convert the user into smart users. In particular, the purpose of the analysis has been focused on the investigation of which user of a given district heating network is more suitable to be chosen for the conversion into a smart user and how the choice of its position will affect the performances of the whole network. To this purpose, a branched and a ring district heating network, representative of the main typology, have been considered and analyzed. The evaluation has been conducted by investigating the design, the smart user evaluation and the management in both considered cases. The results of the carried-out analysis have been shown that the critical user, namely the user resulting from the design evaluation – which is the one characterized by the minimum pressure drop at the uses heat exchanger – is the more suitable to be converted into smart user. To validate this result, the same analysis has been conducted by analyzing an existing medium-size network. Also in this case, results have been shown that the more suitable user to be upgraded in smart user is the critical one resulting from the design evaluation.

A second part of the research activities has been focused on the analysis of the optimal design of the complex energy networks. In particular, a residential neighborhood has been investigated with the main purpose of defining a general methodology to identify the optimal size of the energy systems composing the network. More in detail, starting from a small residential neighborhood

composed by a total of 100 households, a parametric analysis has been carried-out by varying the total number of the considered households up to 1000 units, in order to define the optimal design of each energy system suitable for the energy needs fulfillment as function of the number of the users connected to the network itself. To this respect, the software EGO (Energy Grid Optimizer), previously developed by the Energy Systems research group, has been implemented. The resolution method of this software is based on a genetic algorithm which is a heuristic technique. The results defined the optimal size of each energy systems composing the network for all the considered cases of residential units. Furthermore, an economic evaluation has been carried-out by evaluating both the net present value and the return on investment of each case.

A third part of the research activities has been focused on the investigation of the optimal management of the energy network. To this purpose, an isolated energy grid consisting in a cruise ship has been analyzed by applying the aforementioned software EGO, namely a genetic algorithm-based method. To this respect, starting from the current set-up of the vessel, six different configurations have been developed and analyzed in order to determine the optimal configuration and operational strategy of the energy systems. In detail, three strategies characterized by a standard configuration, namely the current engines regulation, which is typical for this typology of ships, have been considered. Furthermore, the other three developed strategies have been defining by considering a hybrid configuration of the ship, which is mainly used on the military ships field. For each of the developed strategies, the energy, economic and environmental analyses have been conducted. To this respect, a parametric analysis has been carried-out by varying the volume of the thermal storage device in order to point out the optimal and the maximum volume. The results have been shown that all the developed strategies allow to reach both a yearly fuel consumption and dispersed thermal energy decrease compared to current engines operation. Furthermore, the results have been shown that, compared to the current regulation of the vessel, the developed strategies allow to reduce the main pollutant emission (such as CO, CO_2, NO_x etc.) involving also a benefit from an environmental point of view.

The last part of the research activities, indeed, has been focused on the non-heuristic algorithms for the complex energy networks management. To this respect, a novel software, named COMBO, based on a non-heuristic resolution algorithm and able to deal with the nonlinearity of the scheduling optimization problem, has been developed. In detail, the software allows to create all the possible combinations of the energy systems loads and to evaluate each one of them with the main purpose of finding the optimal solution, namely the configuration that minimizes the fitness function consisting in the total cost of the energy production. Therefore, to validate the realized software, a residential neighborhood has been considered and implemented within the software COMBO. The same case study has been also implemented with the software EGO in order to evaluate the results obtained with the heuristic and non-heuristic algorithm-based software. The results of the carried-out analysis have been shown that the software COMBO allows to investigate a greater number of solutions with respect to EGO, but with longer computational time. However, considering the number of solutions evaluated for the unit of time step, it must be highlighted that COMBO evaluates from 25.5 to 58.8 thousand solutions per second, while EGO investigates a number of solutions per second ranging between 4.2 and 10 thousand. As a consequence, COMBO is probably more suitable for the network design and/or forecasted scheduling, while the software EGO is more appropriate for the real-time management. Furthermore, by considering the results in term of total cost of energy production, it follows that the different approach of the software COMBO (with respect to the software EGO) affects these results. The difference between the

obtained results is mainly due to the definition of the fictitious costs of the objective function of the two software.

Finally, the software COMBO has been implemented to a case study consisting in an existing residential neighborhood network. To this purpose, a Reference Case, characterized by an energy systems setup including one internal combustion engine, a natural gas auxiliary boiler and a compression chiller has been defined being representative of the most common configuration for energy distribution networks. This Reference Case have been determined with the main purpose of evaluating the energy and economic advantages achievable with the proposed energy generation mix, which is quite unusual for this typology of networks. The energy results of the carried-out analysis have been pointed out the optimal production mix of the energy systems. Furthermore, from the economic point of view, the results have been shown that the proposed energy system mix allows to reduce the annual total costs of energy production. In conclusion, the comparison allowed to demonstrate the benefits – from energy and economic viewpoints – achievable with the proposed strategy and with the application of the developed software.

List of tables

List of figures

APPENDIX A

In this Appendix A, the prototype designed and developed during the PhD is presented. Due to the recent development of this technology, which has been gained ground in particular in the last decades because of the specific environmental legislations in terms of refrigerants use, a briefly description of the magnetocaloric effect principle is firstly provided. Therefore, the 3D model of the designed devices is presented together with a detail description of each component of which it is composed by outlined the main characteristics. Finally, the realized magnetocaloric prototype is shown.

Magnetocaloric Effect

The magnetocaloric effect (MCE) mainly consists in the magnetic material thermal response as a consequence of the exposition to a magnetic field variation due to the intrinsic property of the substance. Thus, by considering an adiabatic process, when the so-called magnetocaloric material (MCM) is affected by a magnetic field variation, a reversible change in temperature occurs. Otherwise, if the field variation is realized in an isothermal process, a reversible change on magnetic entropy occurs.

In more detail, the thermodynamic cycle, shown in Figure A.1, is characterized by four main steps: (*i*) adiabatic magnetization; (*ii*) isomagnetic enthalpic transfer; (*iii*) adiabatic demagnetization and (*iv*) isomagnetic entropic transfer. The magnetization process consists in the introduction of a magnetocaloric material into a magnetic field generated by two permanent magnets, with a consequent increase of its temperature. Then, the refrigerant fluid absorbs and discharged the heat from the MCM to the environment while the magnetic field is held constant to prevent the dipoles from reabsorbing the heat. When the MCM is sufficiently cooled, the magnetocaloric substance and the secondary fluid are separated. Successively, during the demagnetization phase, the MCM is removed from the magnetic field while the entropy remains constant. The magnetic dipoles are randomly oriented so the magnetocaloric materials cools down. At least, holding the magnetic field constant to prevent the material reheating, the refrigerant fluid removes the heat energy from the MCM, so the cooling effect occurs.
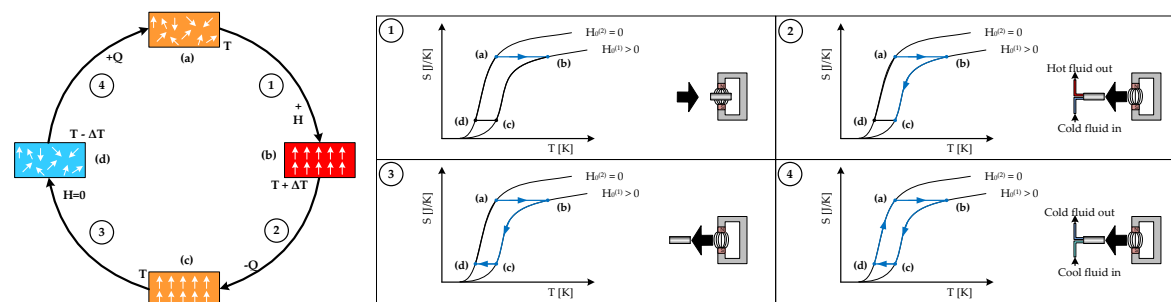
FIGURE A.1: THERMODYNAMIC CYCLE OF THE MAGNETIC REFRIGERATION ALONG WITH THE WORKING PRINCIPLE.

Magnetocaloric refrigerator prototype

The prototype of the developed magnetocaloric refrigerator is a rotary permanents magnet magnetic device composed by four stationary regenerative beds, which contain the magnetocaloric material (and in particular, gadolinium) and a rotating permanent magnet designed with two high field and two low field regions. Overall, the realized device is composed by four main components: (*i*) magnetic system; (*ii*) drive system; (*iii*) regenerative beds; (iv) hydraulic system. A 3D model developed by using the modelling software CREO Parametric is represented in Figure A.2.
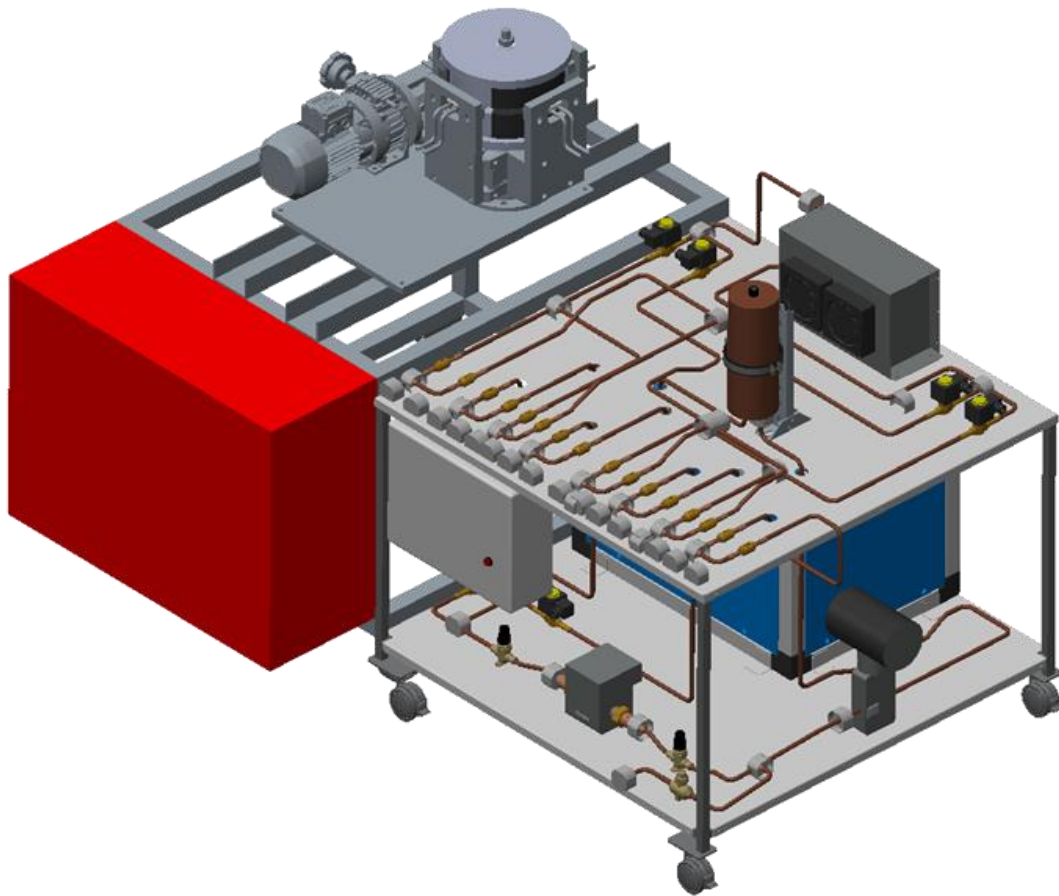
FIGURE A.2: 3D MODEL OF THE DEVELOPED PROTOTYPE.

Magnetic system

The magnetic system represents the rotating part of the prototype. It consists of two couple of composite magnets based on Halbach's configuration each of which is fixed on a cobalt-iron structure, to obtain two permanent magnets, positioned between two rotating parallel discs, since they are attached to the shaft.

The 3D model and the magnetic flux density regions of the magnetic systems are shown respectively in Figure A.3 and Figure A.4.
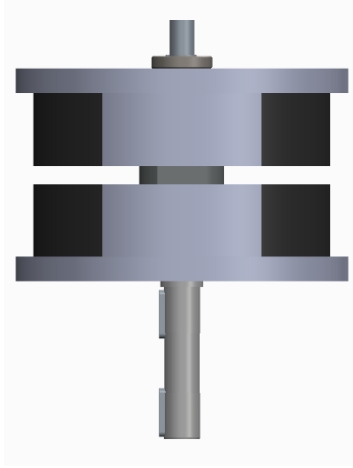
FIGURE A.3: 3D MODEL OF THE MAGNETIC SYSTEM.
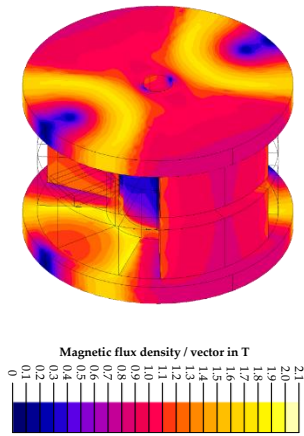
FIGURE A.4: MAGNETIC FLUX DENSITY REGIONS.

As it concerns the magnetic field generated by the magnetic systems, the simulated and the measured magnetic field are presented in Figure A.5. These values have been represented with respect to the degree corresponding to the permanent magnets. In fact, as can be noted from the previous figures, the magnets do not cover 360° but only a degree equal to about 120° each. Furthermore, according to the figure, the maximum magnetic field is equal to about 1.35 T.
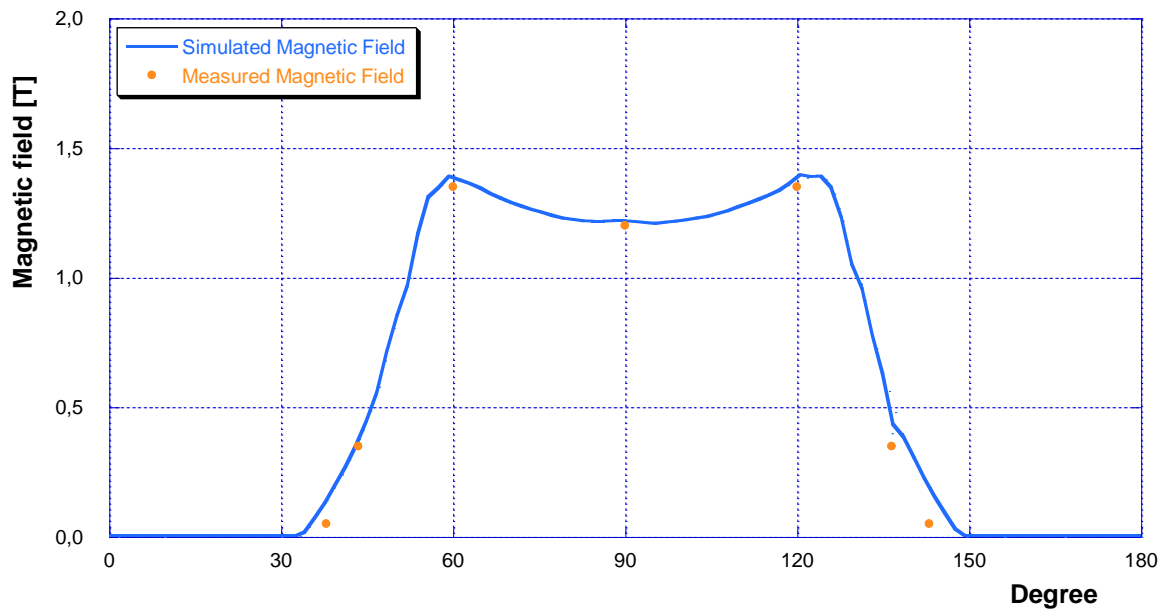
FIGURE A.5: SIMULATED MAGNETIC FIELD COMPARED TO THE EFFECTIVE MEASURED MAGNETIC FIELD.

The drive system consists of a six poles three-phases asynchronous motor driven by inverter characterized by a nominal power equal to 0.25 kW and a nominal torque equal to 2.7 Nm. It is cooled by an external ventilation system and is equipped with a plastic radial fan running. This motor can operate in both direction of rotation, depending on the phases. The bearings are axially pre-loaded radial ball, lubricated for life with the grease. The motor is coupled with a mechanical speed variator. This component is able to be brought up to the acceptable torque limit, without any sliding of the kinematic mechanisms. For reason of output rotational speed values, a combined gearbox, characterized by a reduction factor equal to 250:1 has been added to the kinematic chain. The dynamic efficiency (by means the maximum efficiency reached after a certain number of operating hours, defined as the ratio between the inlet and outlet power) of this component is equal to 52%. In addition, the system is equipped with an optical encoder to detect the angular position of the input shaft and a programmable shift controller which allows to simultaneously operation of the valve and the magnetic system since, the fluid flow direction is provided by the angular position between the stator and rotor, that is between the regenerative beds and the magnets.

This configuration, shown in Figure A.6, have chosen to face the necessity to obtain a low rotational output speed despite of the efficiency. The main characteristics of the drive systems, in terms of efficiency, mechanical power and mechanical torque are shown in Figure A.7 as function of the rotational speed. As can be noted from the figure, the drive system efficiency (red line) linearly ranges between a minimum value about equal to 8% and a maximum value equal to 25% respectively for an output speed from 0.5 rpm to 2.65 rpm. AS it concerns the mechanical power and the mechanical torque of the kinematic chain, indeed, it can be noted that by increasing the rotational speed, the mechanical torque exponentially decreases, while the mechanical power linearly increases.
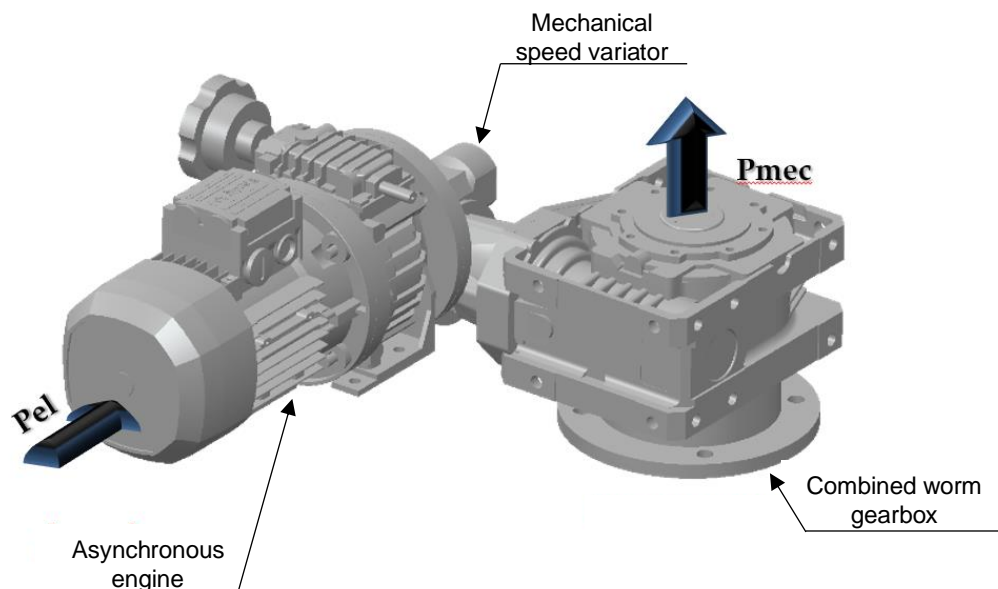
FIGURE A.6: 3D MODEL OF THE DRIVE SYSTEM.
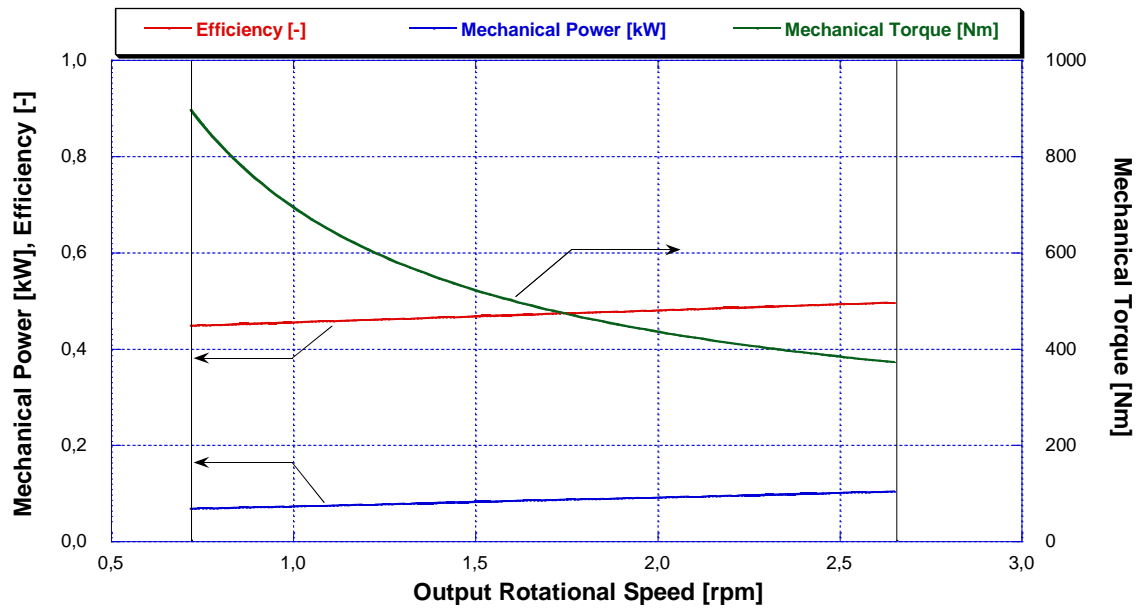
FIGURE A.7: DRIVE SYSTEM EFFICIENCY, MECHANICAL POWER AND MECHANICAL TORQUE AS FUNCTION OF OUTPUT ROTATIONAL SPEED.

Regenerative beds

The stator part of the device is represented by four AMR beds arranged spacing 90° each other, as is shown in Figure A.8. This configuration allows the magnetization (or demagnetization) of the two-opposite regenerators, by the permanent magnets each quarter of revolution.
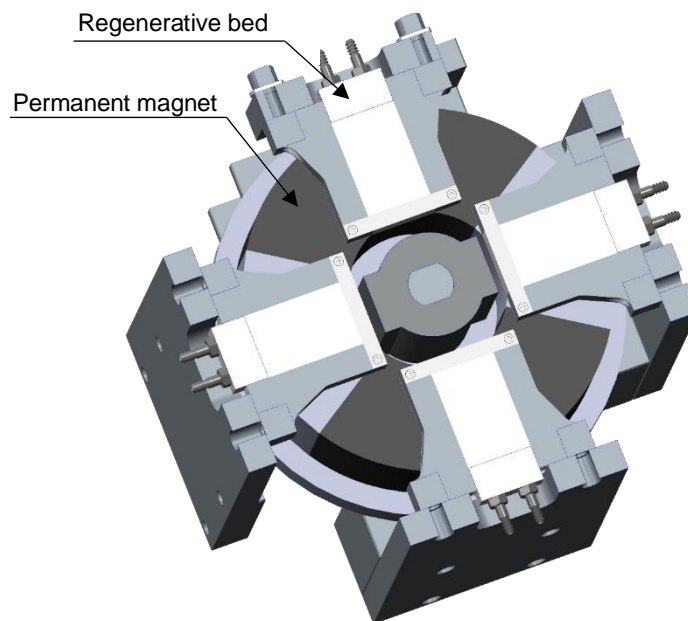
FIGURE A.8: 3D MODEL OF THE REGENERATIVE BEDS ARRANGEMENT.

As is shown in Figure A.9, each regenerator consists of parallel plates of magnetocaloric material in a polycarbonate casing, a low heat conducting polymer (0.20 W/mK) with good mechanical properties in terms of working pressure and temperature resistance. The total mass of gadolinium employed in the four regenerator is about equal to 0.5 kg. Each regenerator is 13 mm high, 100 mm long and 44 mm wide. As it regards the MCM, gadolinium has been selected as refrigerant, arranged in parallel plates with a thickness equal to 0.25 mm. Overall, a total amount of gadolinium equal to 0.5 kg has been employed. Water has been chosen as working fluid.
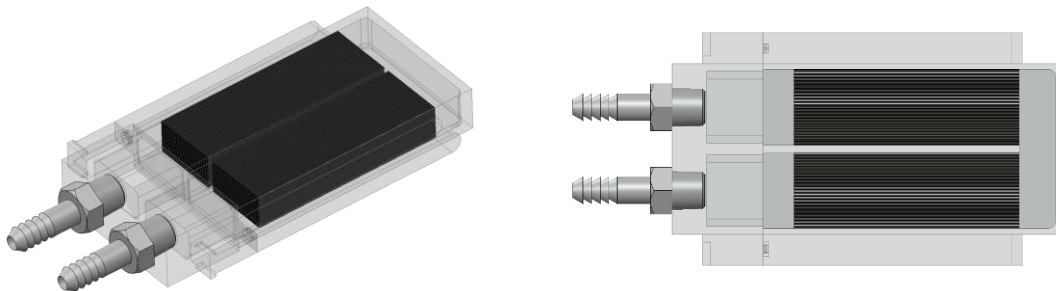
FIGURE A.9: 3D MODEL OF THE REGENERATIVE BED.

In order to maximize the magnetocaloric effect, the regenerators are arranged between the two magnets with a gap of 1 millimeter above and below. In this respect, the magnetocaloric effect, as was said before, depends on the adiabatic temperature of the material.

Finally, in Figure A.10, the gadolinium adiabatic temperature as function of the initial temperature, namely the temperature it is characterized before the magnetization/demagnetization process, has been shown. These values have been experimentally evaluated by applying a magnetic field about equal to the one described in the previous section. Furthermore, as can be observed from the figure, the temperature span ranges from a minimum value about equal to 1 K to a maximum value equal to 4.3 K. The purpose of the design of the regenerators is to obtain a regenerative effect run by run (*i.e.:* the increase of the temperature span due to the inversion of the water path from the magnetization phase to the demagnetization step).
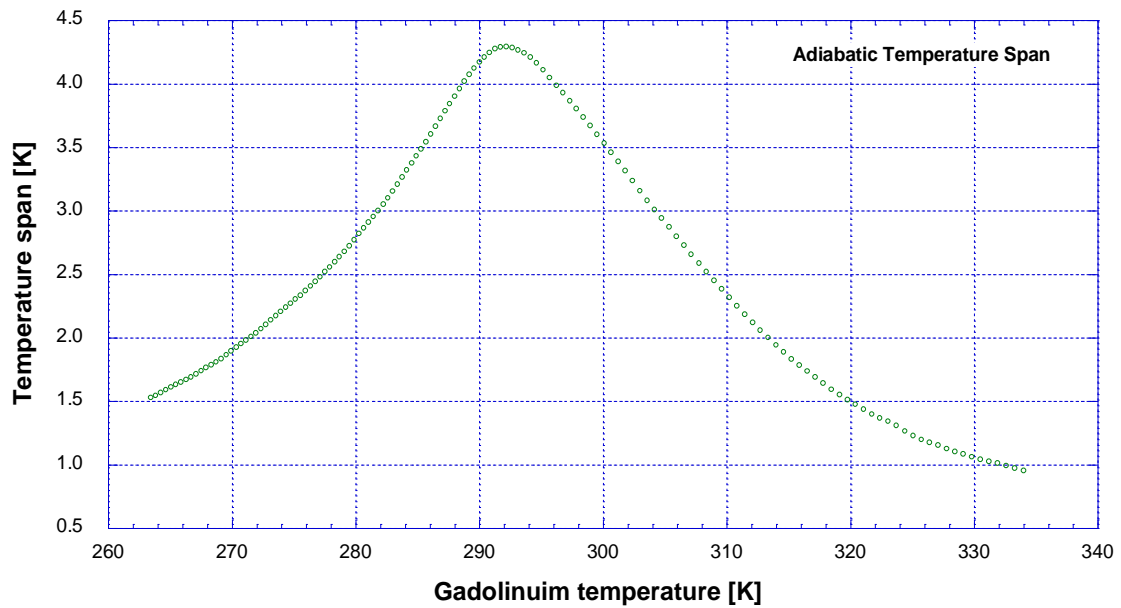
FIGURE A.10: GADOLINIUM ADIABATIC TEMPERATURE UNDER A MAGNETIC FIELD ABOUT EQUAL TO 1.4 TESLA.

Hydraulic system

the schematic layout of the hydraulic system is represented in Figure A.11a. The choice of using only one pump for the water circulation led to a high complexity in the circuit to guarantee the implementation of the active magnetic regenerative cycle. In fact, by the use of a series of on/off valve, is possible to switch the working fluid direction each quarter revolution.

(a)   (b)
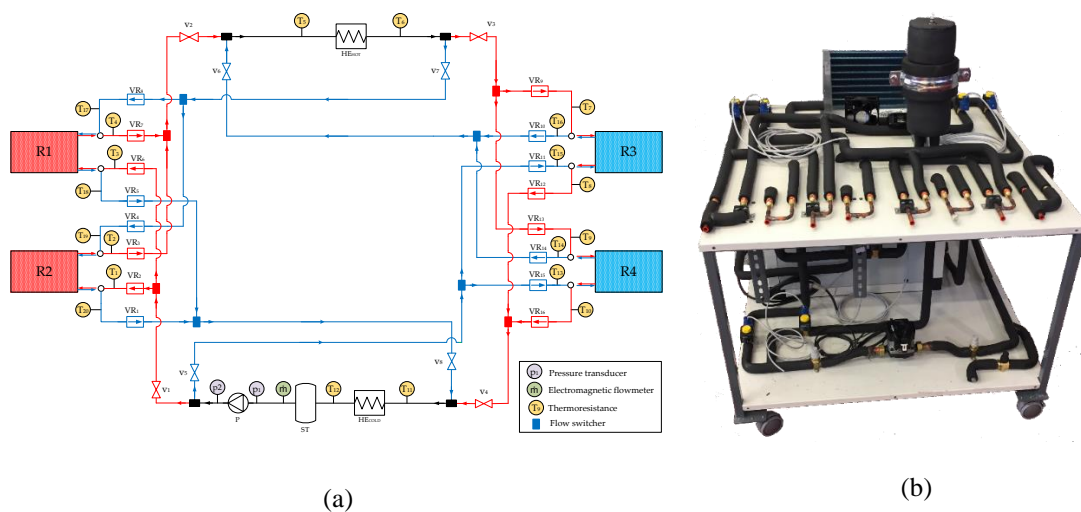
FIGURE A.11: (*a*) HYDRAULIC SYSTEM LAYOUT ALONG WITH THE MEASUREMENT DEVICES AND (*b*) THE REALIZED TEST BENCH.

More in detail, the cold fluid is pushed into the magnetized regenerators (by means the two red rectangles) by the pump in order to remove the heat and dispersed it by the heat exchanger (HE$_{hot}$). At this point, the working fluid is sent to the demagnetized regenerative beds (by means the two blue rectangles) where a new heat exchange occurs before the water is sent to the cold room (represented by the heat exchanger HE$_{cold}$) where the refrigeration effect occurs.

The hydraulic circuit realized on the basis of the layout is shown in Figure A.11b. This circuit represents a first realization of the layout of Figure A.11a and, for this reason, it is characterized by non-optimized dimension, being its size equal to about one cube meter.

Data acquisition and control system

In order to test the developed prototype, a data acquisition and control system, whose schematic representation is shown in Figure A.12, have been also realized with the aim of measuring the main parameter – such as temperature, pressure and mass flow rate in different points of the prototype. In particular, thermoresistance has been chosen for temperature acquisition upstream and downstream of each regenerator and for the cold and hot heat exchanger. These sensors allow to verify and evaluate the effective active magnetic regenerative cycle. As it regards the pressure transducer, two devices have been placed upstream and downstream of the pump to evaluate the pressure drop, and an electromagnetic flowmeter has been placed for the mass flow value acquisition. Moreover, an optical encoder has been installed to detect the angular position of the magnets in order to control the series of valve, by which their switch the water flow direction change occurs. The data acquisition and instrumental control system has been implemented by using Labview.
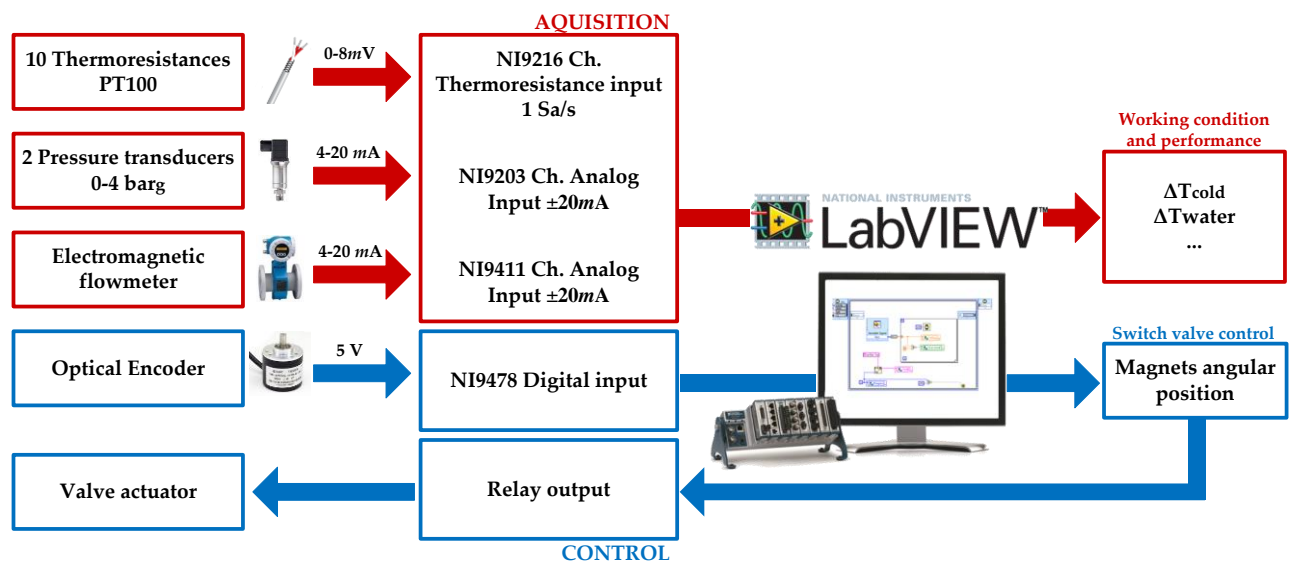
FIGURE A.12: SCHEMATIC REPRESENTATION OF THE DATA ACQUISITION AND CONTROL SYSTEM.

The final realized prototype, which represents the first magnetocaloric refrigeration developed by the University of Bologna, is shown in Figure A.13.

FIGURE A.13: REALIZED MAGNETOCALORIC PROTOTYPE.

A first preliminary test has been conducted on the developed prototype presented in Figure A.13 in order to analyze the thermodynamic performances. To this respect, a single regenerative bed has been considered to evaluate the effect on the gadolinium temperature due to the iteration of the regenerative bed with the magnetic field. Hence, by considering each thermodynamic cycle composed by the following steps:

1. gadolinium magnetization and heat exchange with the fluid (water);
2. fluid heat discharged into the environment;
3. gadolinium demagnetization and heat exchange with the fluid;
4. fluid heat exchange with the cooling cell;

the gadolinium temperature has been investigated by considering a certain number of cycles. The results of the analysis are shown in Figure A.14.

As can be noted from the figure, there is an initial period, corresponding to the starting of the machine in which the gadolinium temperature is quite constant at each step of the cycle (namely at each timestep) and therefore, once the steady state is reached, the temperature behavior begins to decrease. Finally, after a certain number of timestep, the results of the test shown an overall decrease of the gadolinium temperature from quite more of 300 K to about 297.3 K. This first results
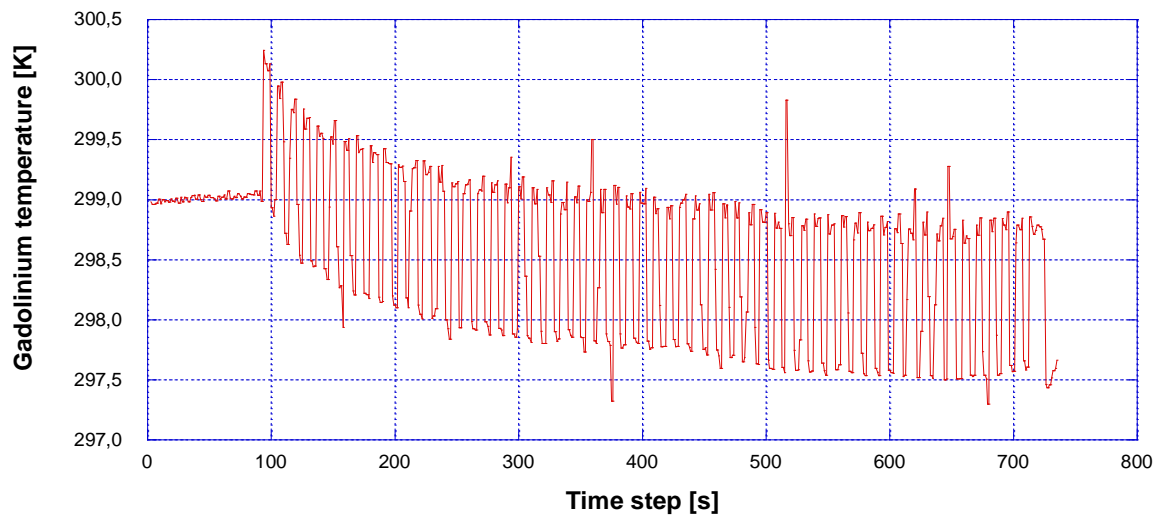
FIGURE A.14: GADOLINIUM TEMPERATURE BEHAVIOR.

APPENDIX B
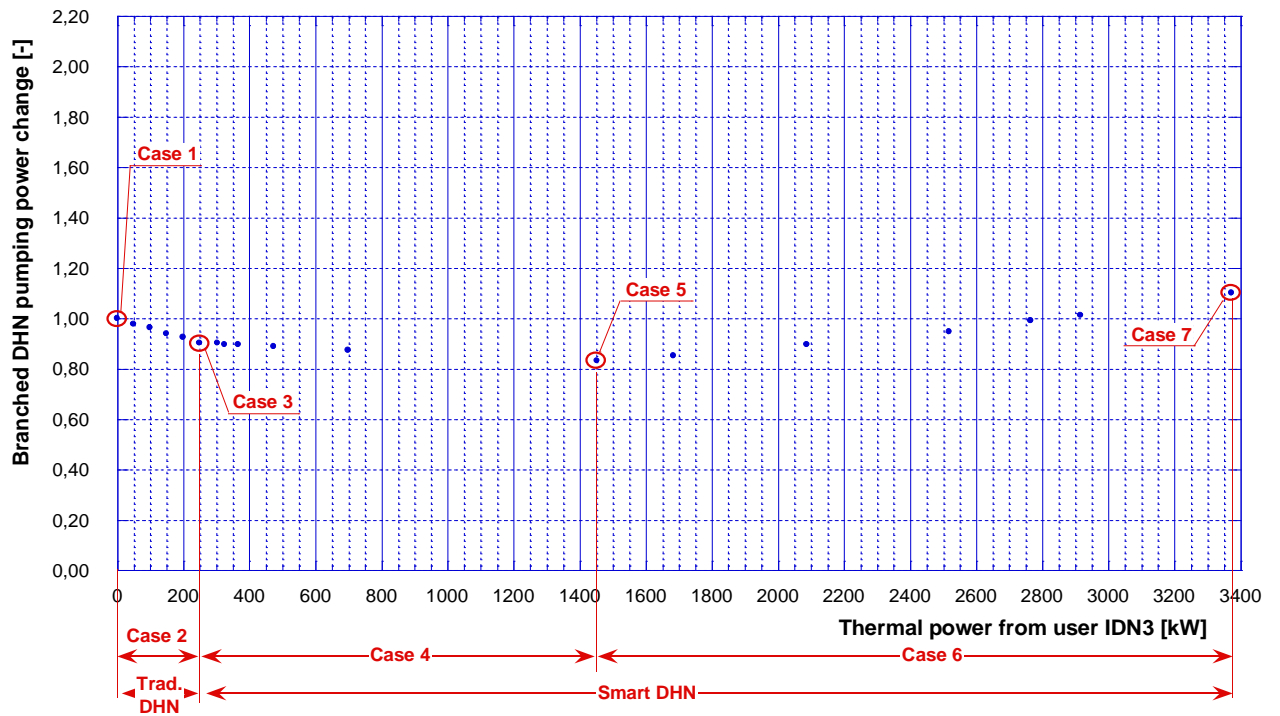
FIGURE B.1: VARIATION OF THE DHN PUMPING POWER IN THE CASE OF SMART USER IDN3 FOR THE BRANCHED DHN.
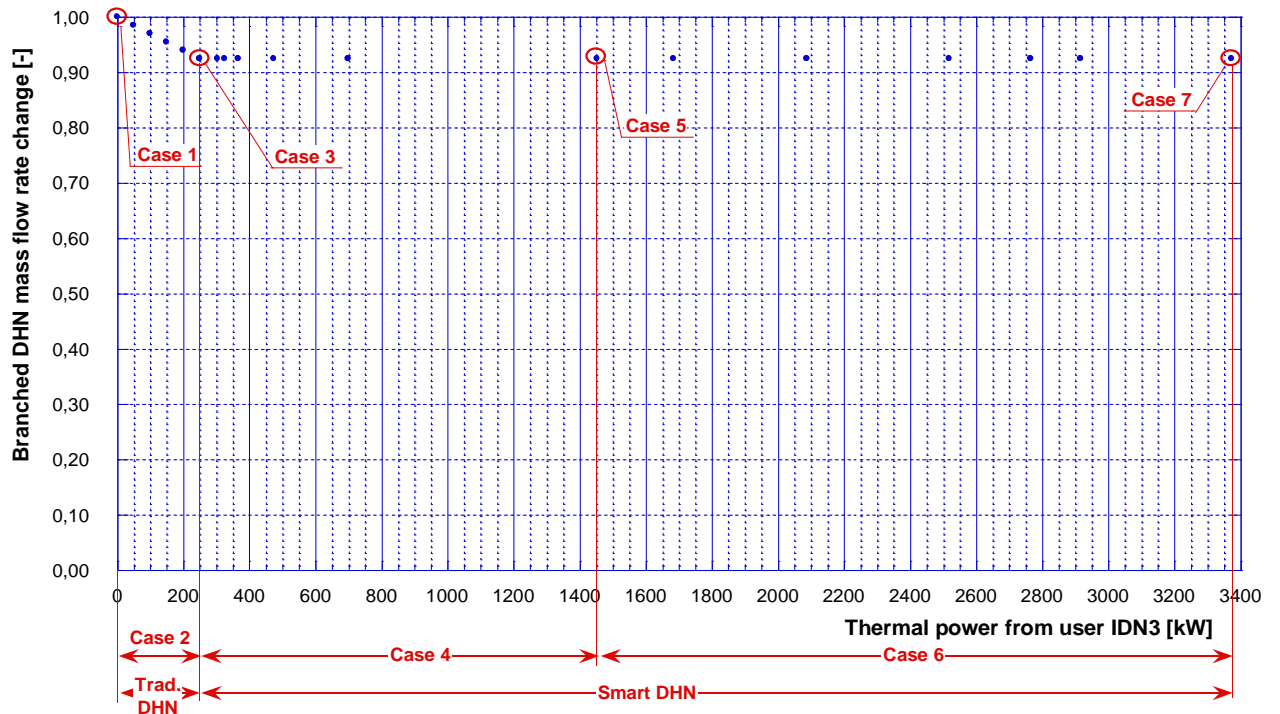
FIGURE B.2: VARIATION OF THE DHN MASS FLOW RATE IN THE CASE OF SMART USER IDN3 FOR THE BRANCHED DHN.
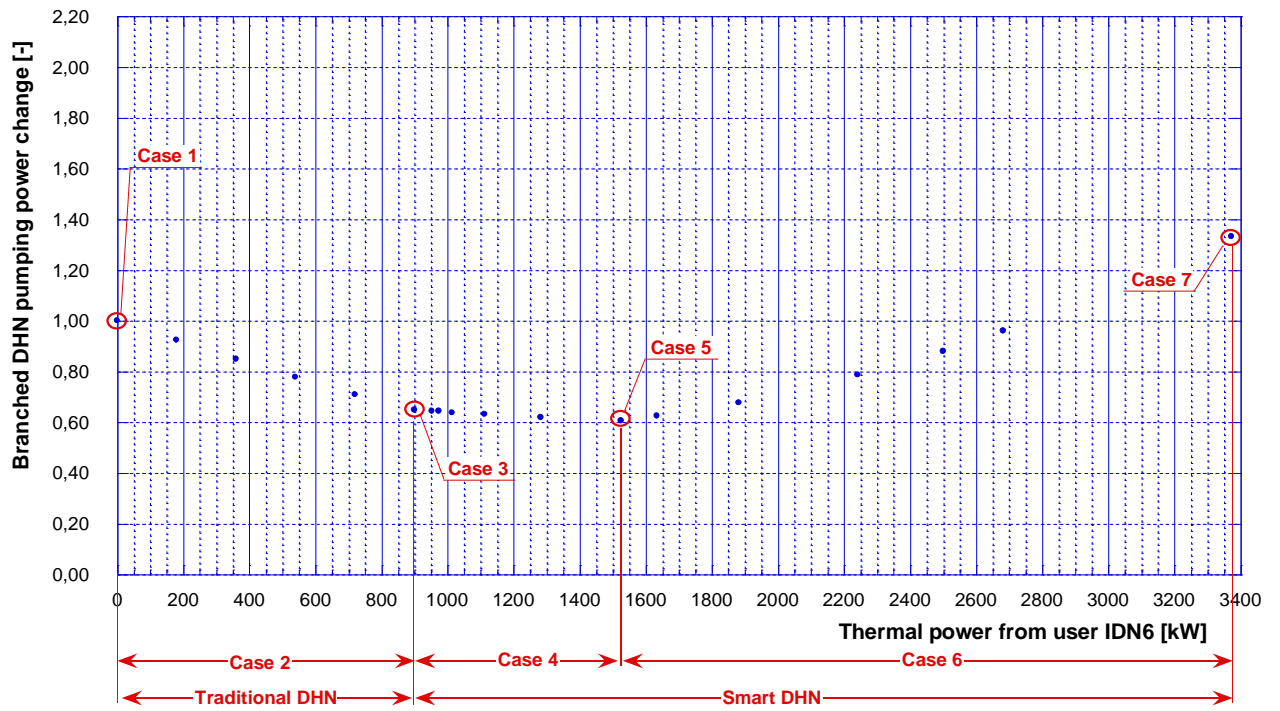
FIGURE B.3: VARIATION OF THE DHN PUMPING POWER IN THE CASE OF SMART USER IDN6
FOR THE BRANCHED DHN.
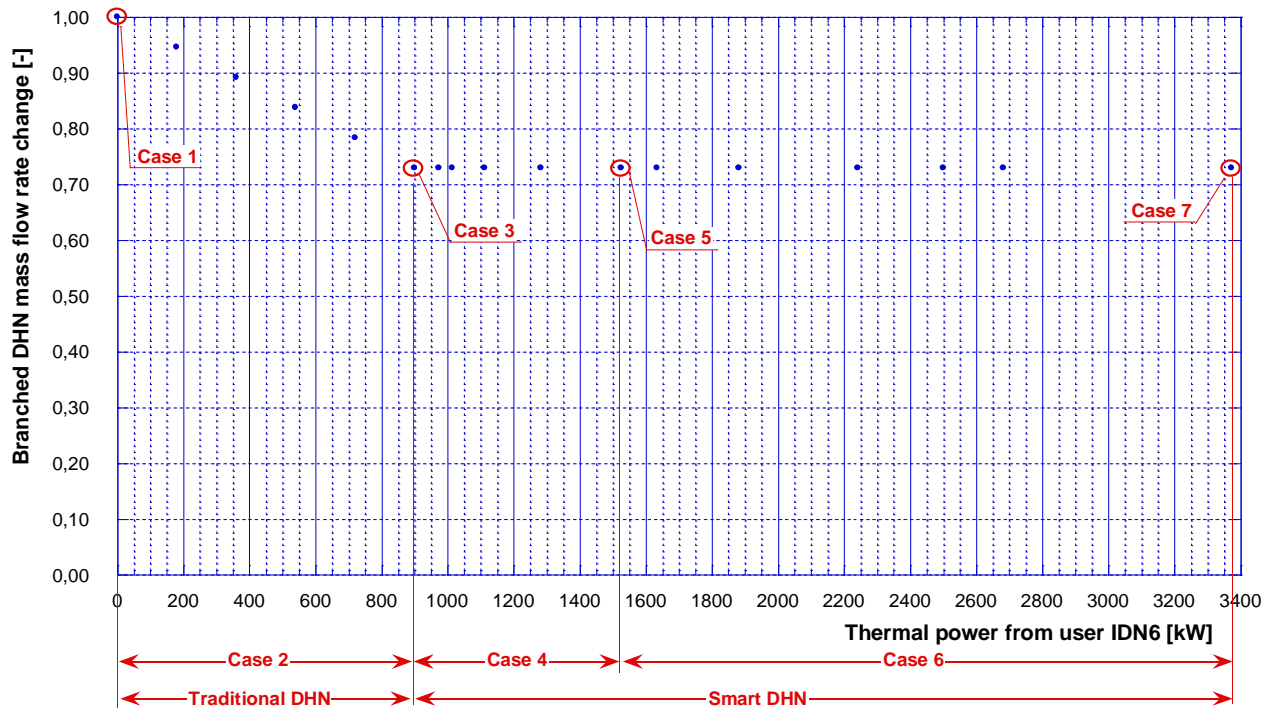
FIGURE B.4: VARIATION OF THE DHN MASS FLOW RATE IN THE CASE OF SMART USER IDN6
FOR THE BRANCHED DHN.
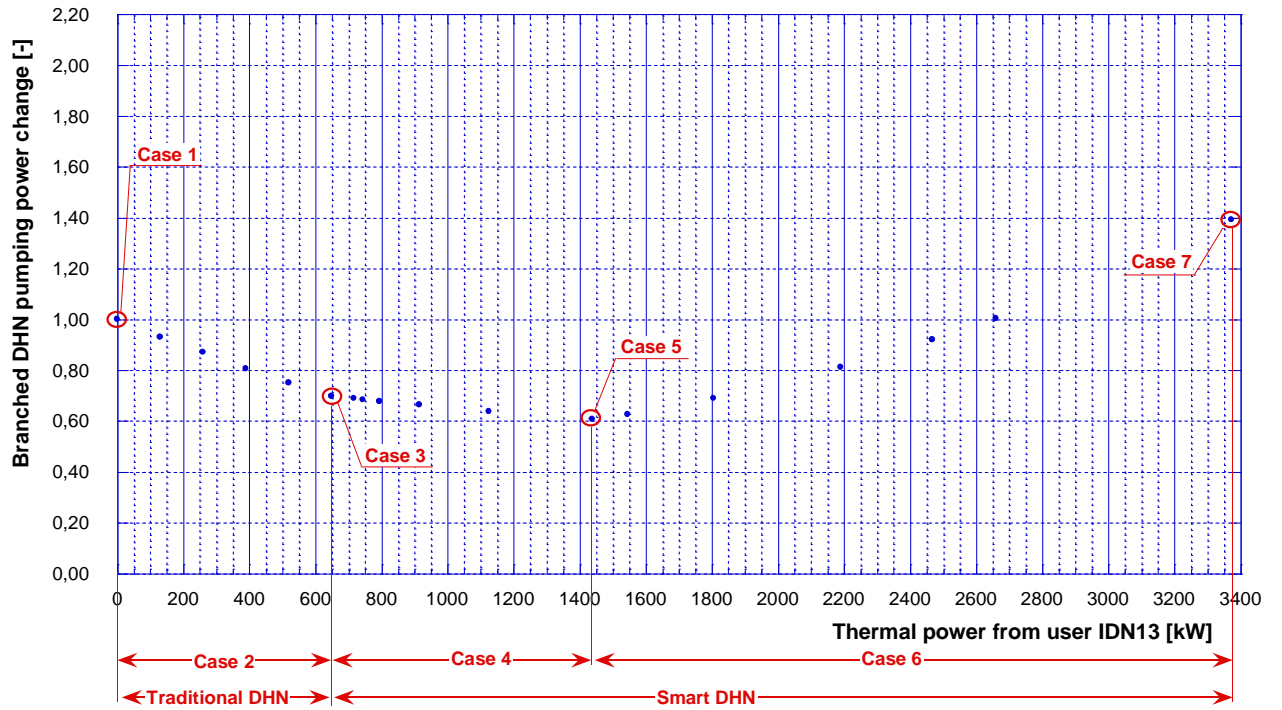
FIGURE B.5: VARIATION OF THE DHN PUMPING POWER IN THE CASE OF SMART USER IDN13 FOR THE BRANCHED DHN.
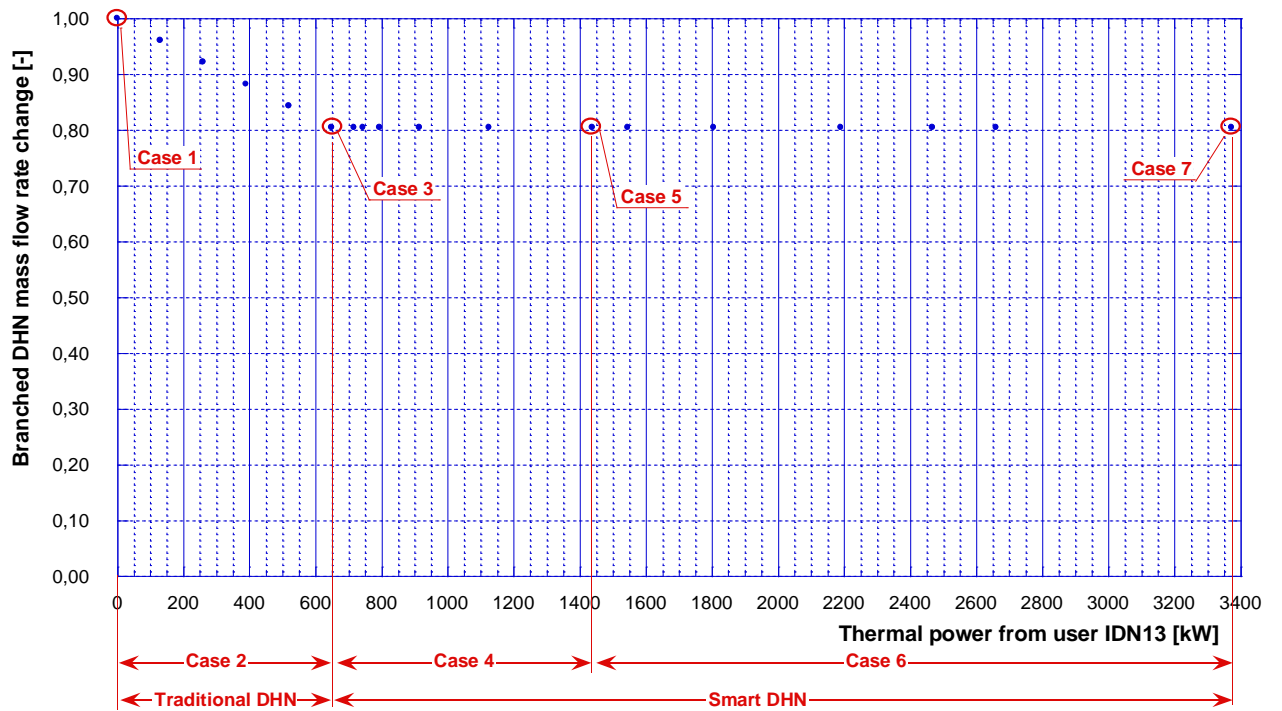
FIGURE B.6: VARIATION OF THE DHN MASS FLOW RATE IN THE CASE OF SMART USER IDN13 FOR THE BRANCHED DHN.
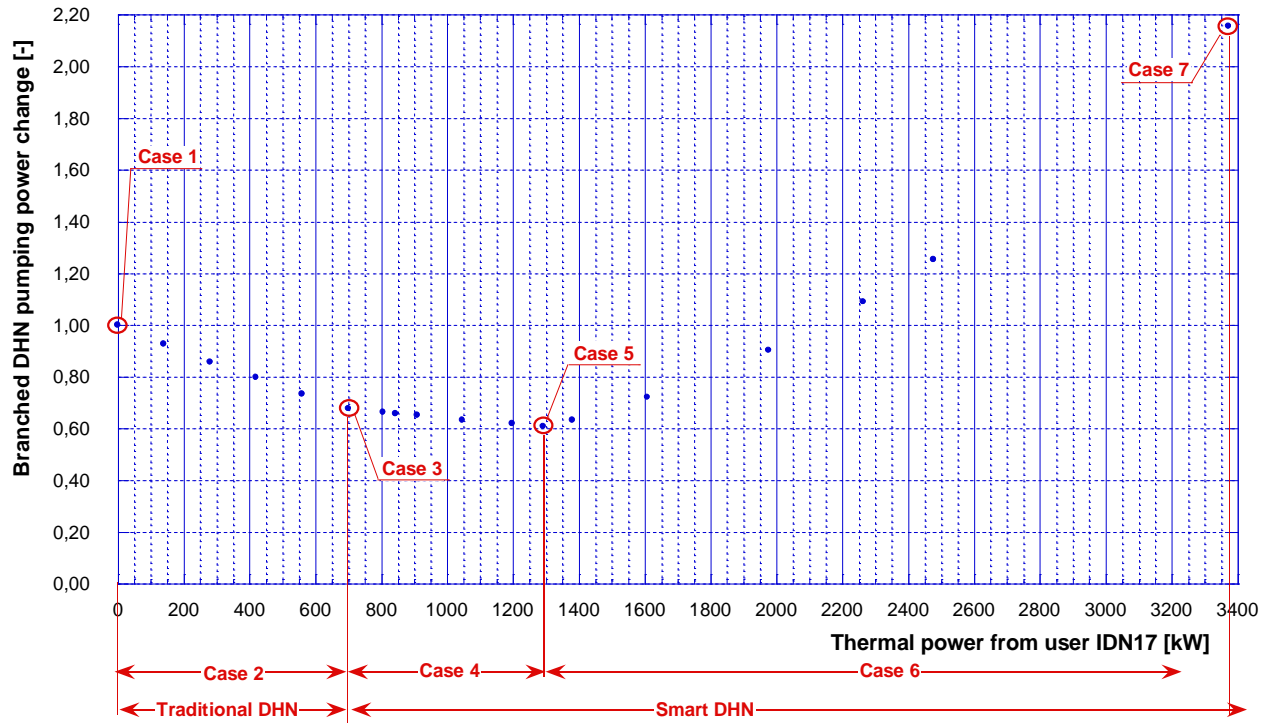
FIGURE B.7: VARIATION OF THE DHN PUMPING POWER IN THE CASE OF SMART USER IDN17 FOR THE BRANCHED DHN.
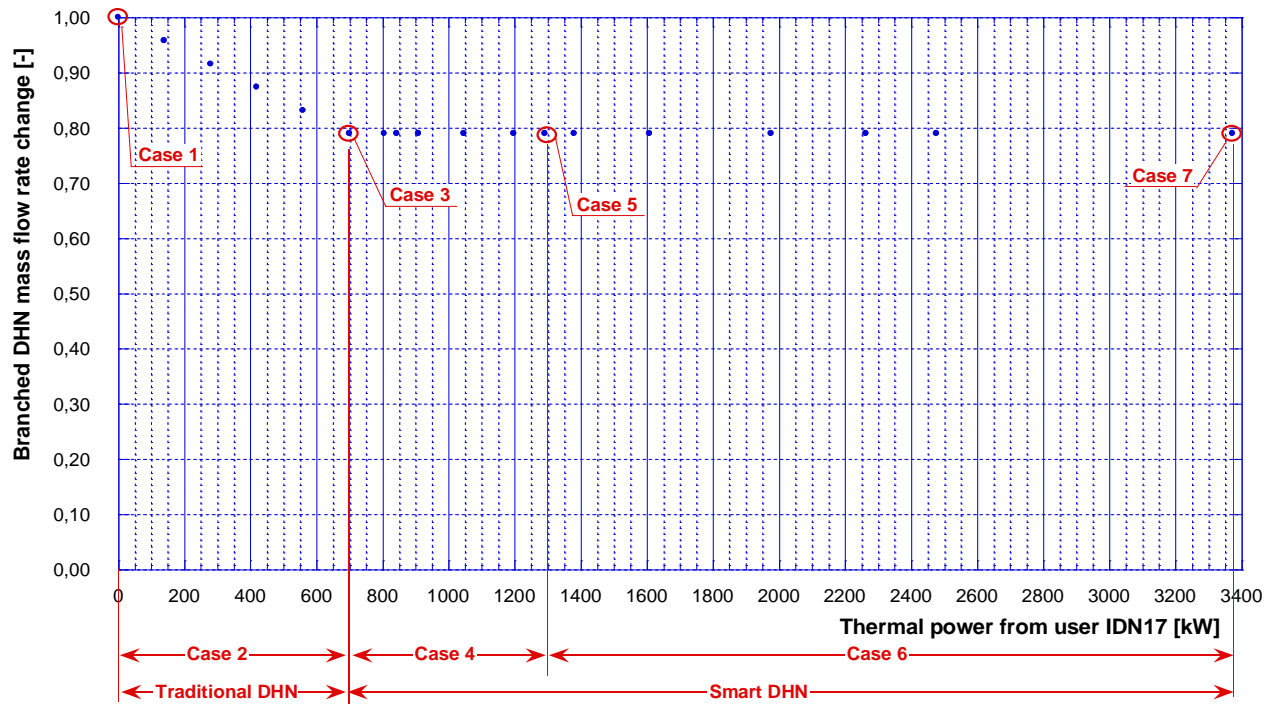
FIGURE B.8: VARIATION OF THE DHN MASS FLOW RATE IN THE CASE OF SMART USER IDN17 FOR THE BRANCHED DHN.
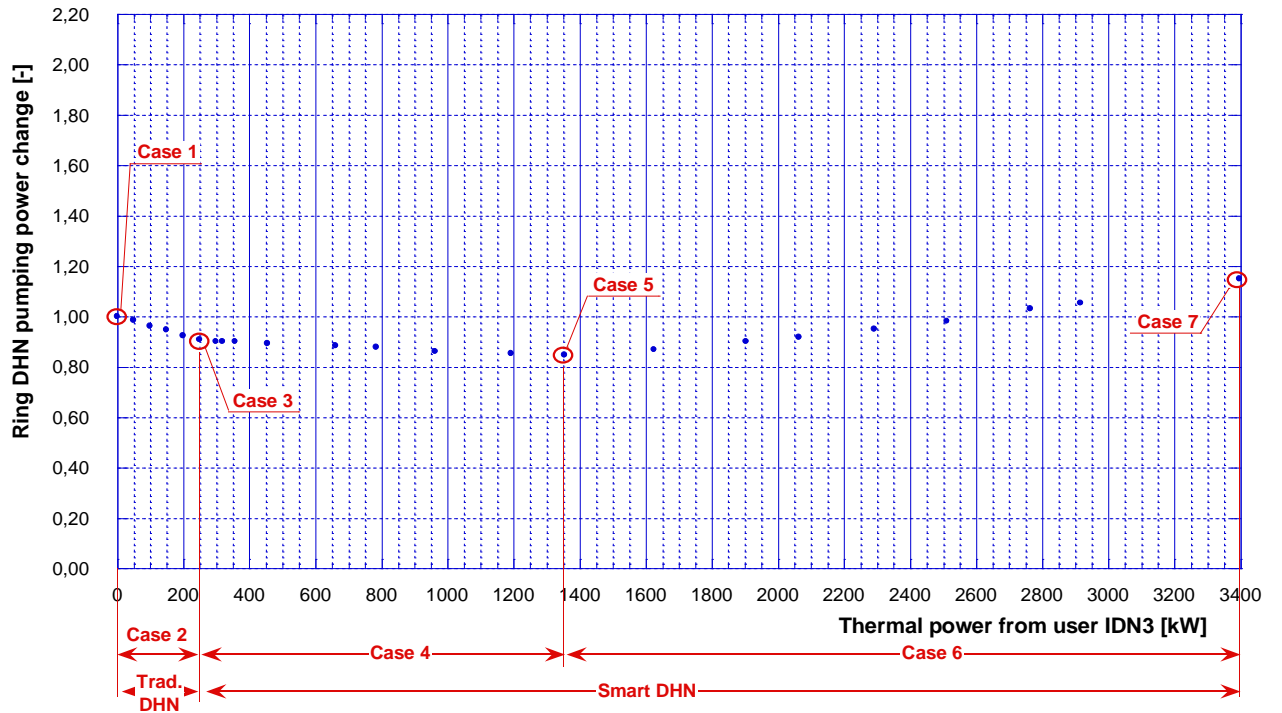
FIGURE B.9: VARIATION OF THE DHN PUMPING POWER IN THE CASE OF SMART USER IDN3
FOR THE RING DHN.
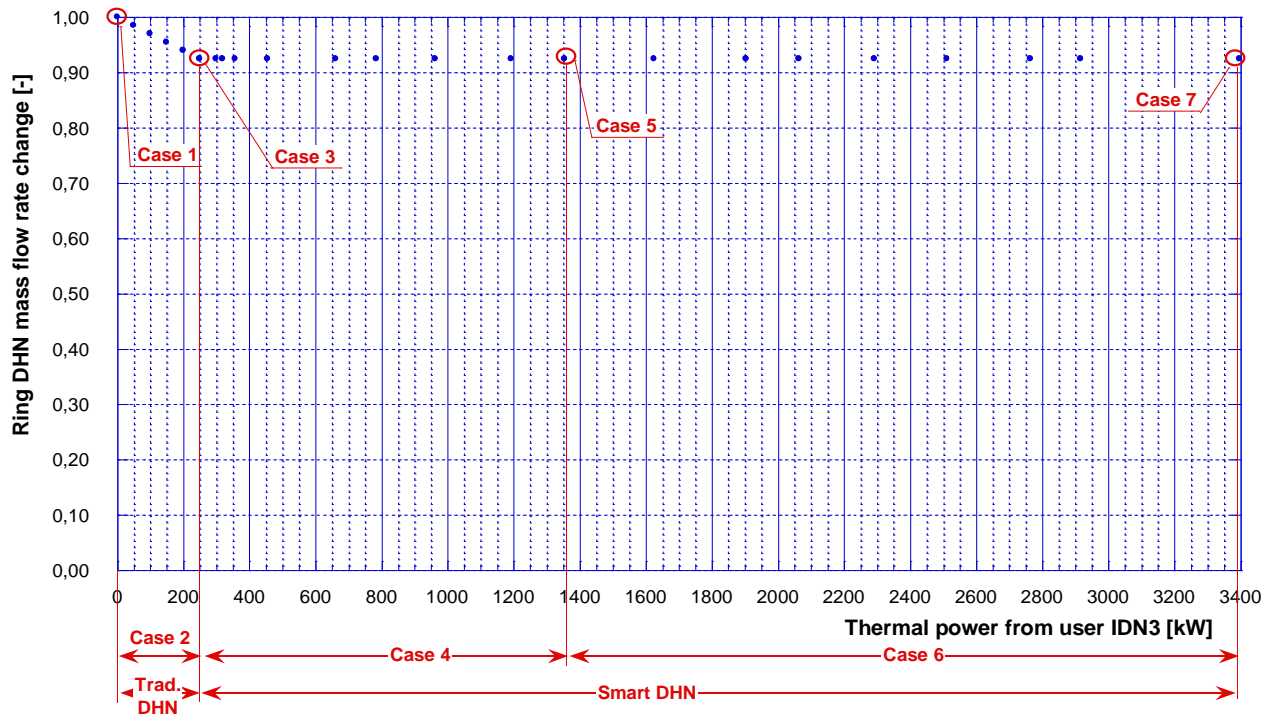
FIGURE B.10: VARIATION OF THE DHN MASS FLOW RATE IN THE CASE OF SMART USER
IDN3 FOR THE RING DHN.
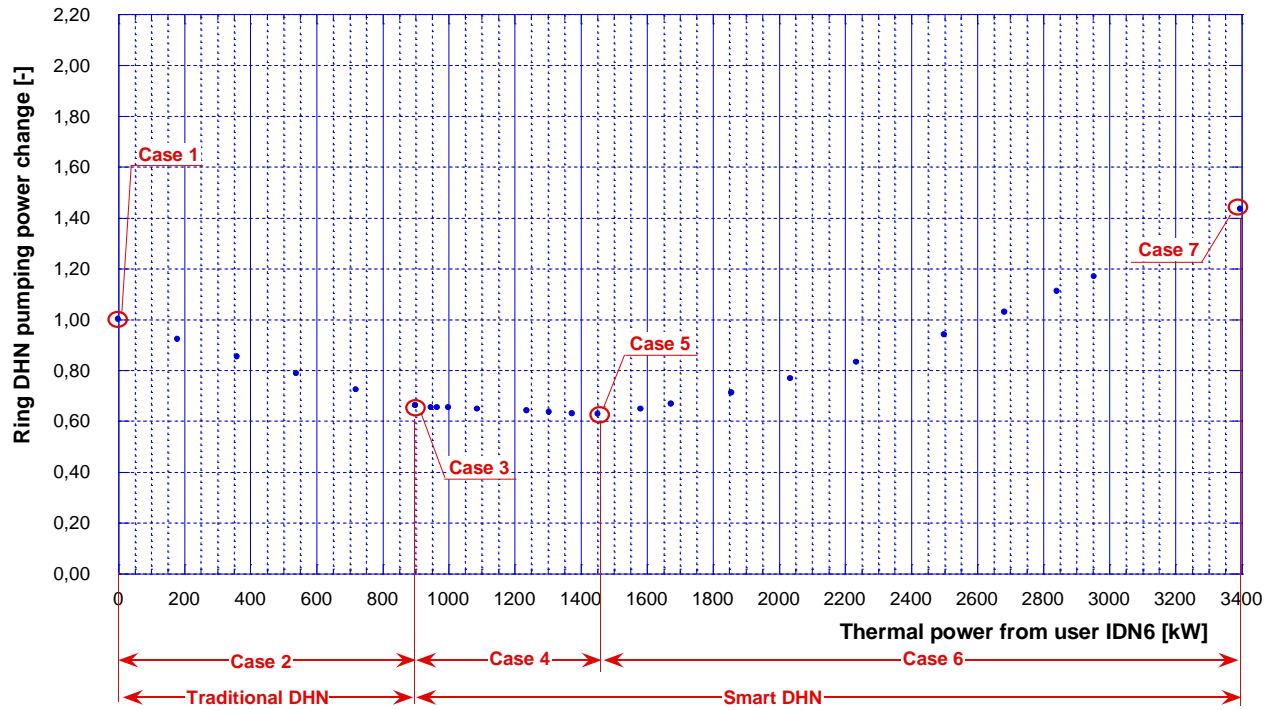
FIGURE B.11: VARIATION OF THE DHN PUMPING POWER IN THE CASE OF SMART USER IDN6 FOR THE RING DHN.
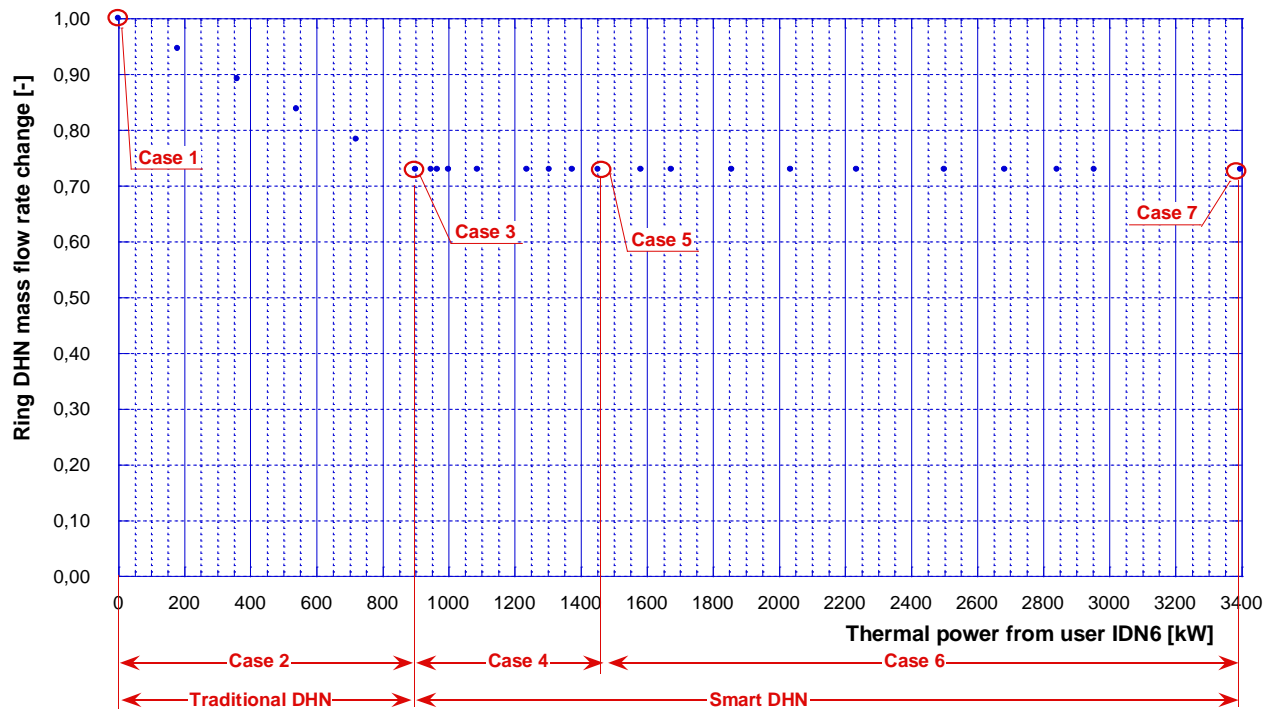
FIGURE B.12: VARIATION OF THE DHN MASS FLOW RATE IN THE CASE OF SMART USER IDN6 FOR THE RING DHN.
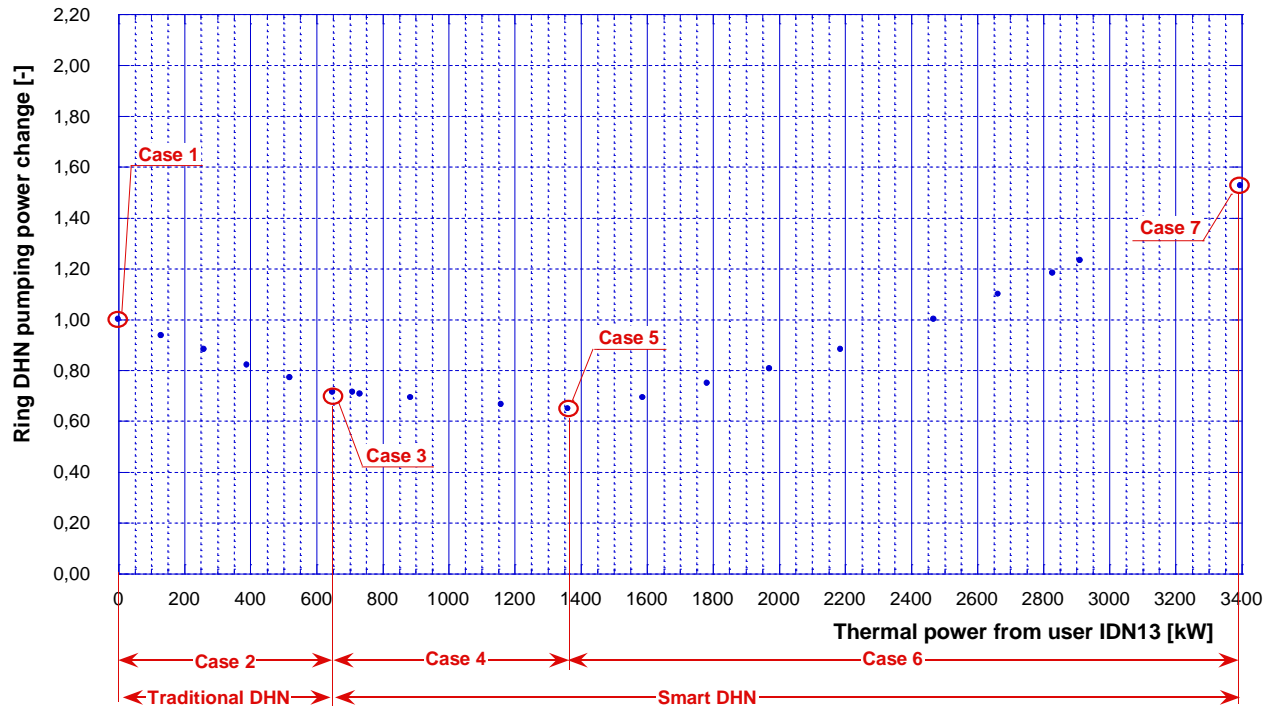
FIGURE B.13: VARIATION OF THE DHN PUMPING POWER IN THE CASE OF SMART USER
IDN13 FOR THE RING DHN.
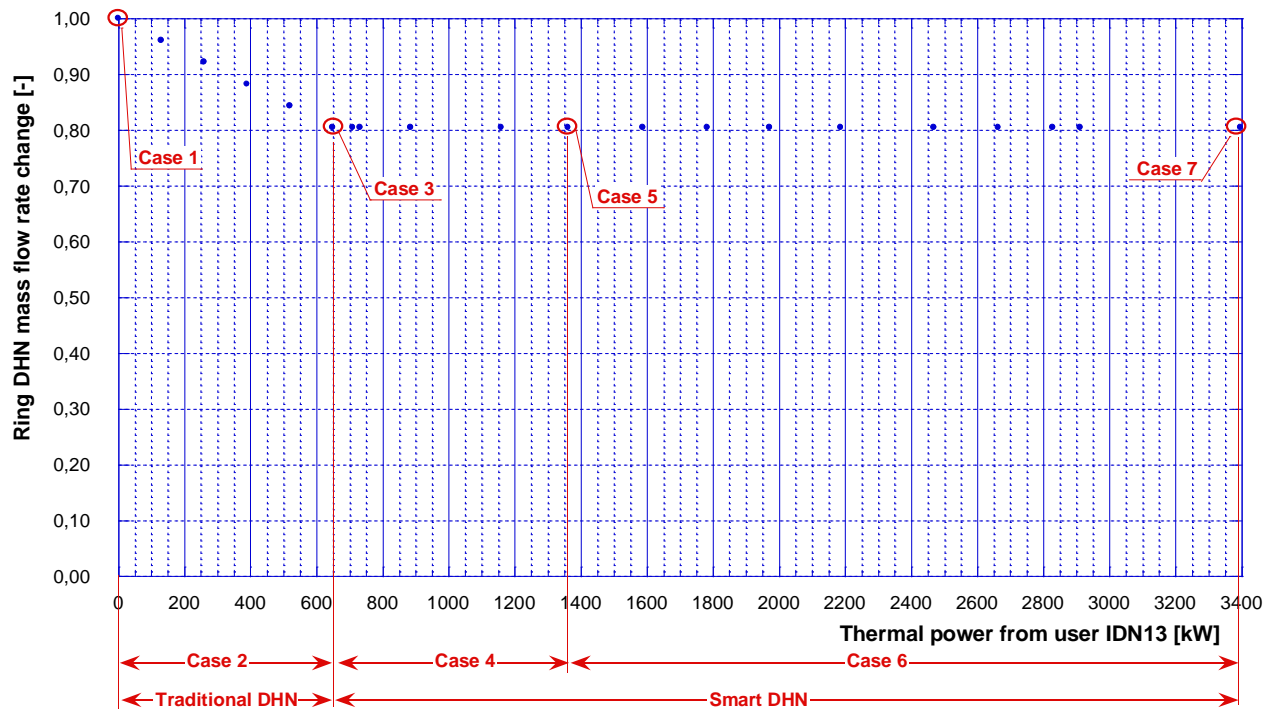
FIGURE B.14: VARIATION OF THE DHN MASS FLOW RATE IN THE CASE OF SMART USER
IDN13 FOR THE RING DHN.
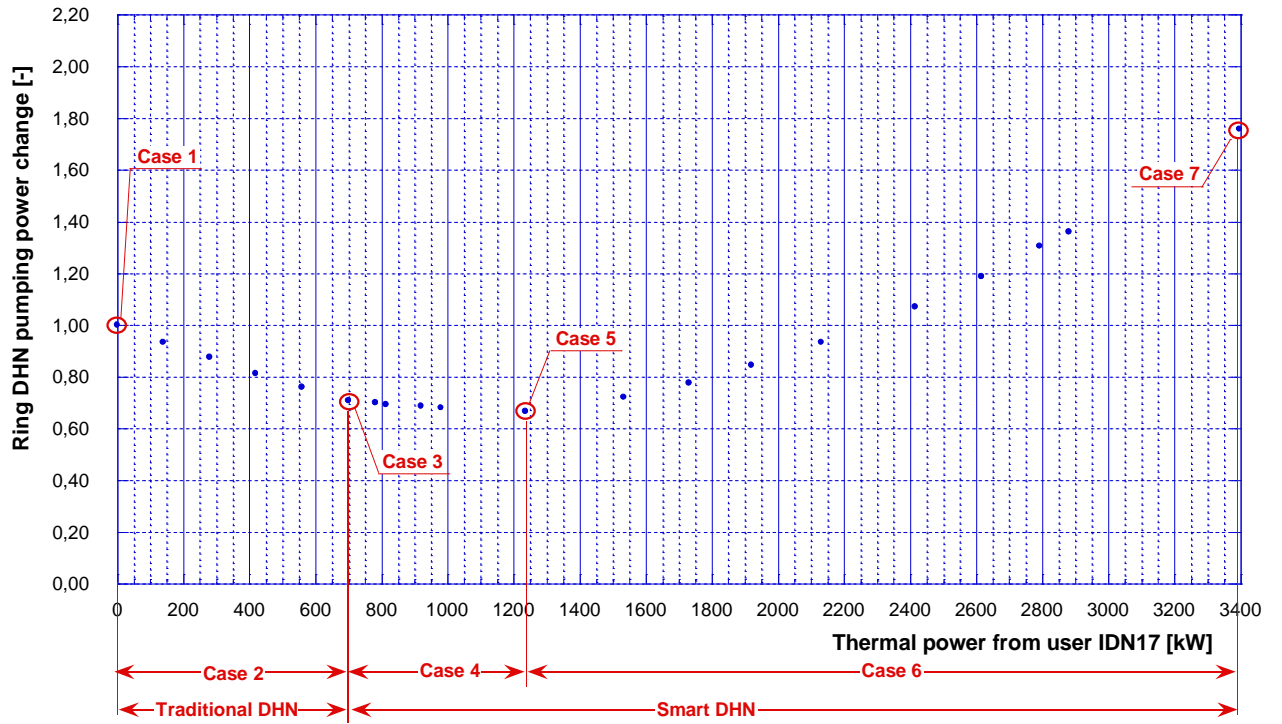
FIGURE B.15: VARIATION OF THE DHN PUMPING POWER IN THE CASE OF SMART USER IDN17 FOR THE RING DHN.
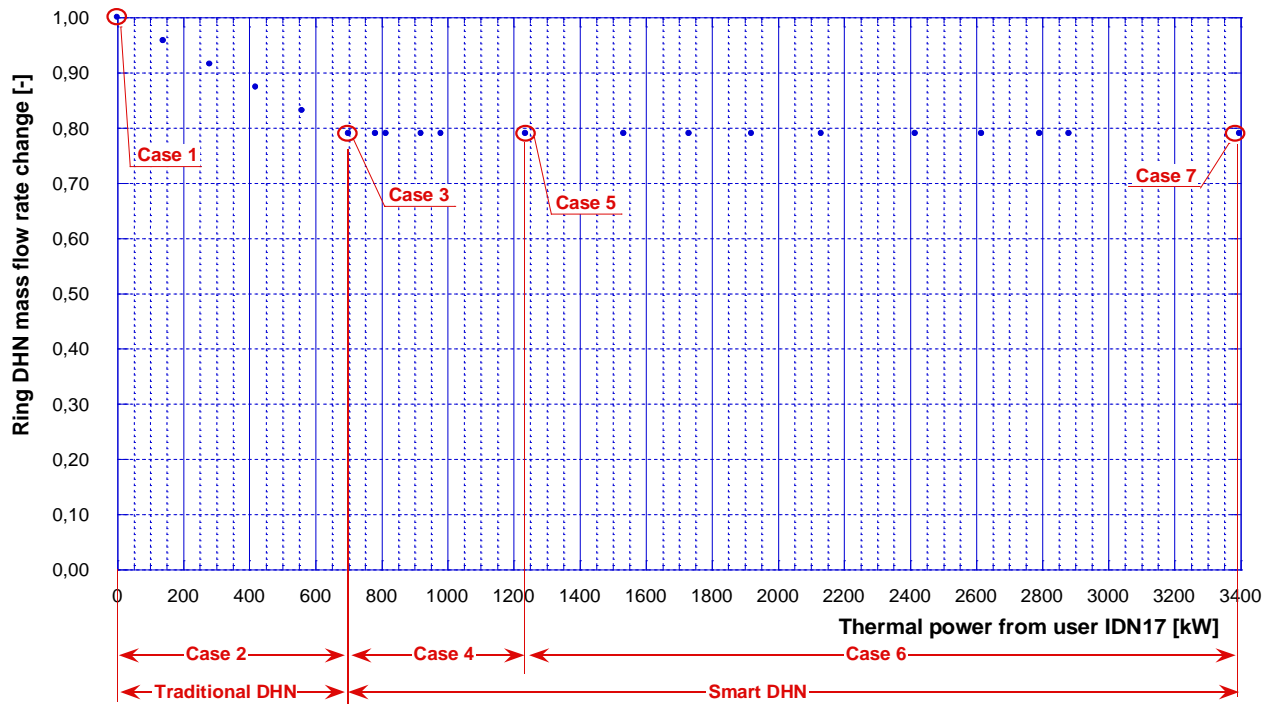
FIGURE B.16: VARIATION OF THE DHN MASS FLOW RATE IN THE CASE OF SMART USER IDN17 FOR THE RING DHN.

FIGURE C.1: NETWORK SETTING IN CASE 1 (IN RED COLOR THE CRITICAL PATH).
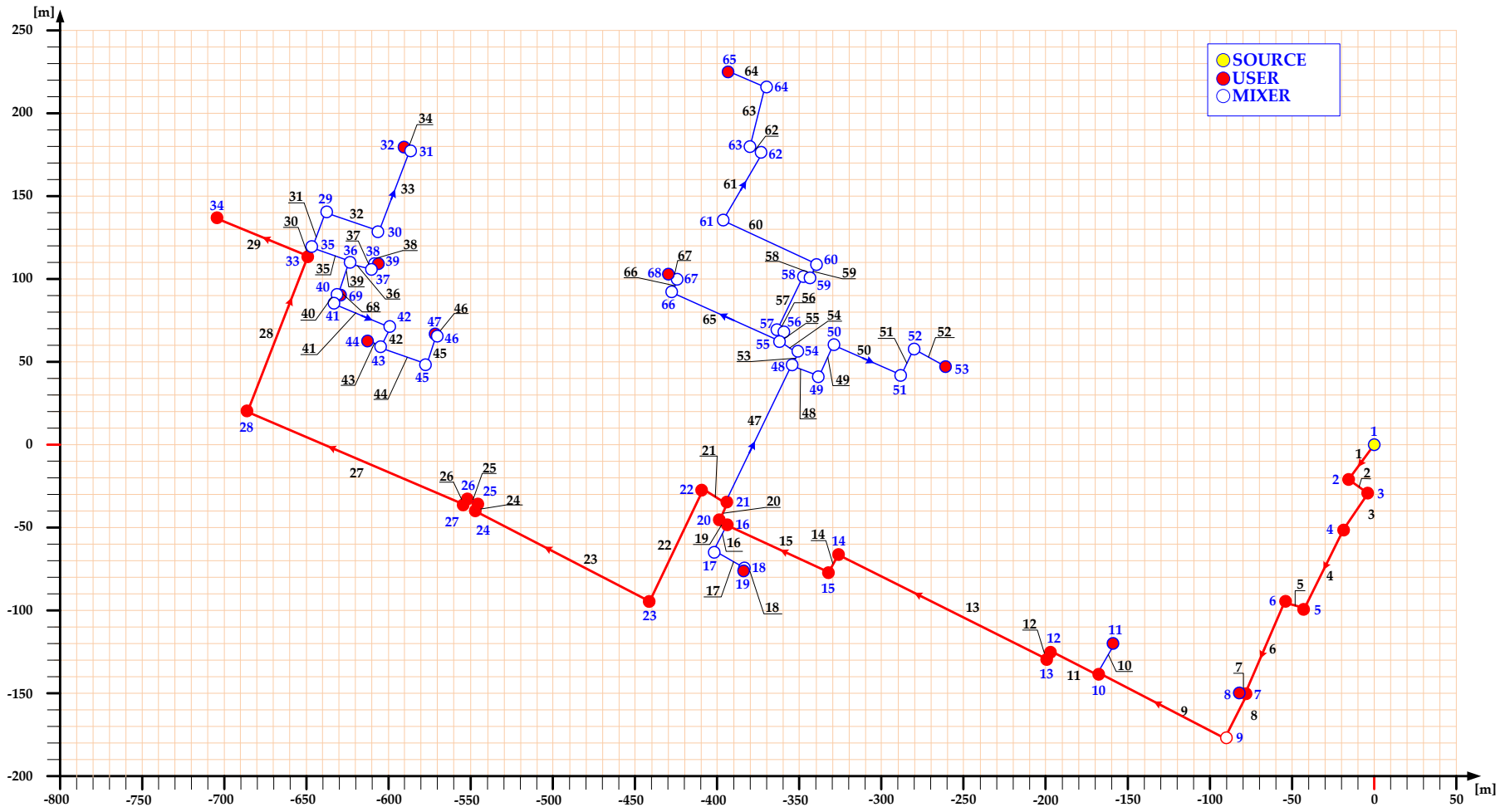
FIGURE C.2: NETWORK SETTING IN CASE 2 (IN RED COLOR THE CRITICAL PATH).
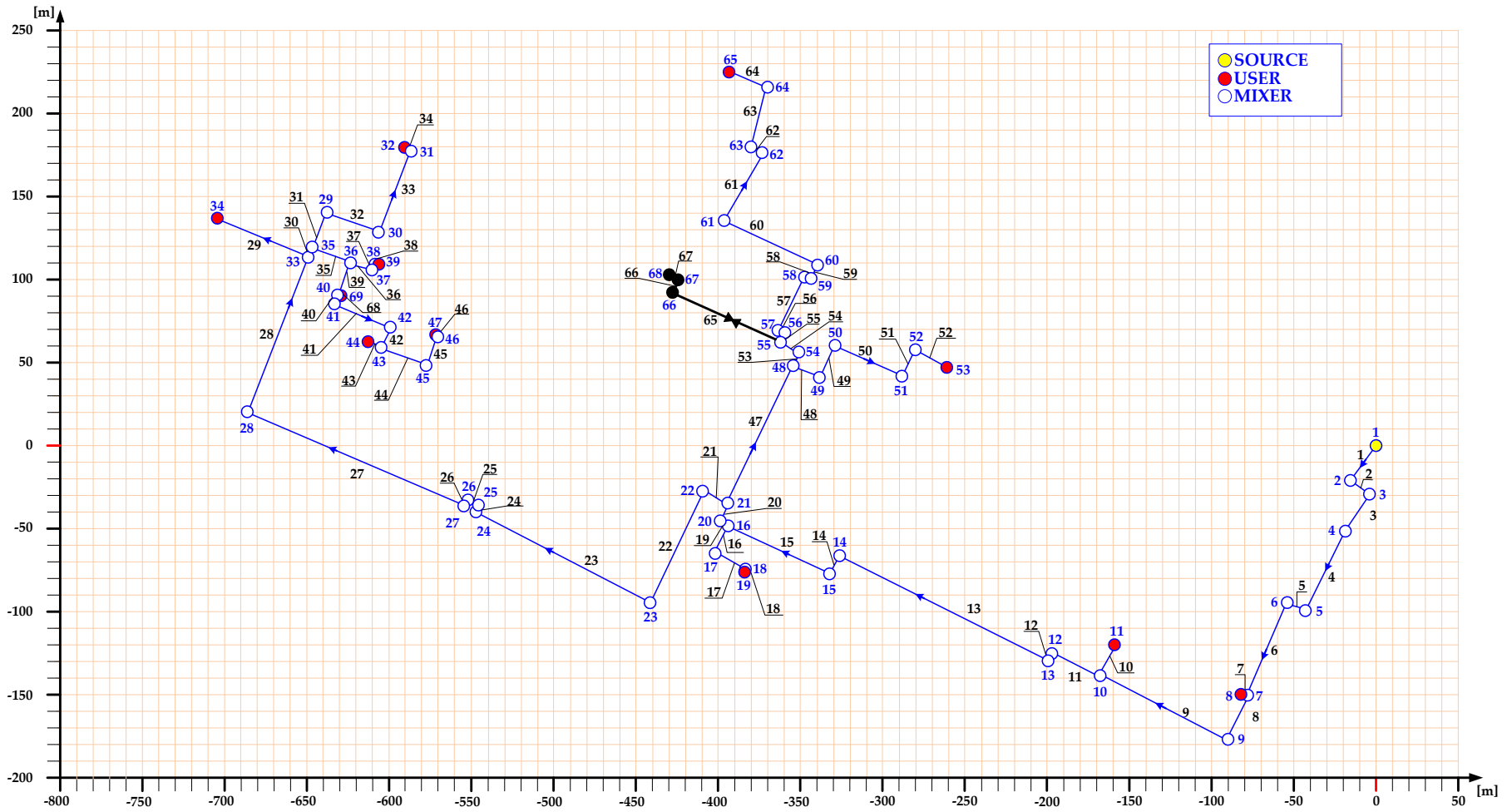
FIGURE C.3: NETWORK SETTING IN CASE 3 (IN BLACK COLOR THE CLOSED PIPES).
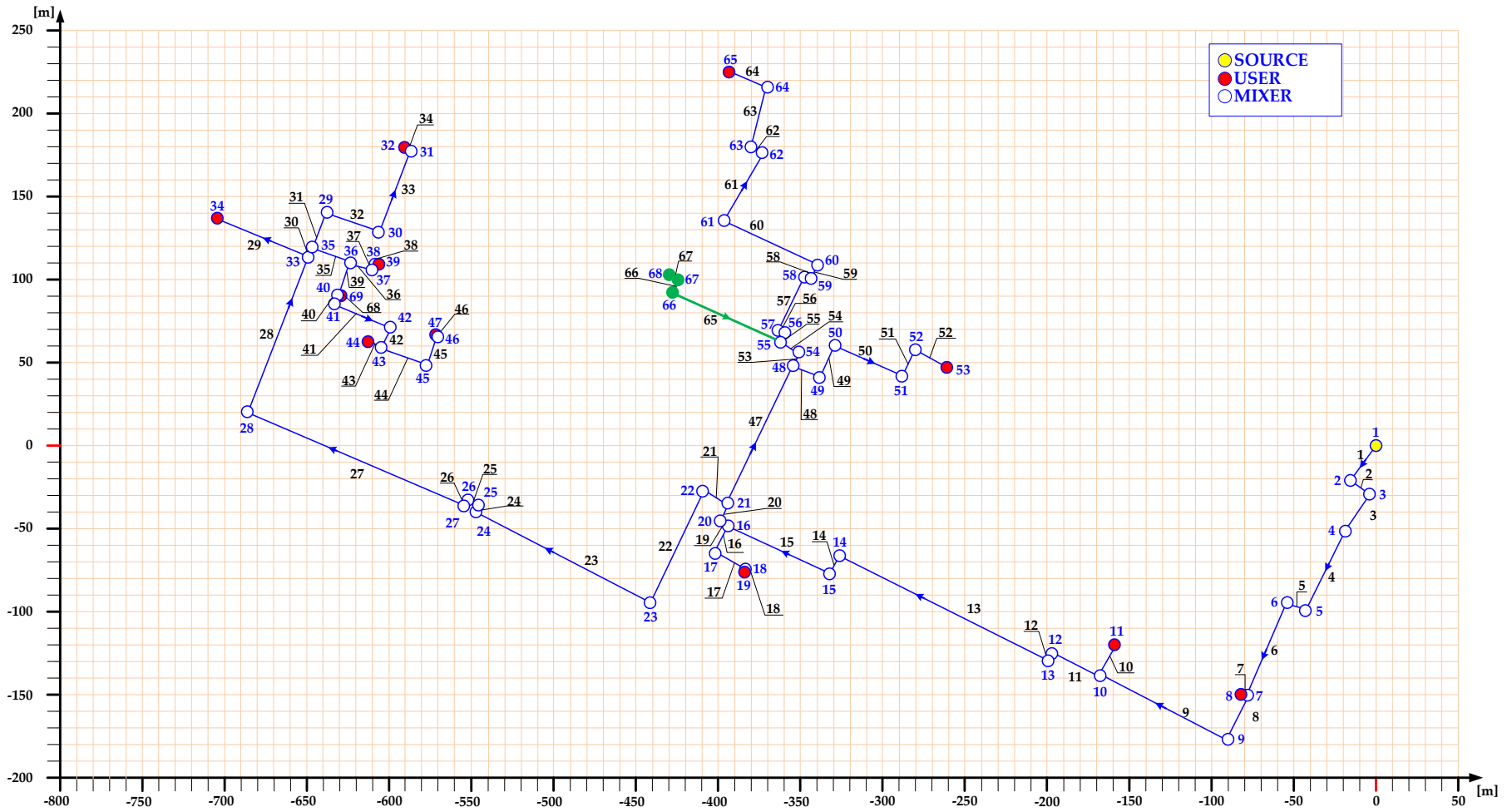
FIGURE C.4: NETWORK SETTING IN CASE 4 (IN GREEN COLOR THE REVERSE FLOW PIPES WITH RESPECT TO THE DESIGN CASE).
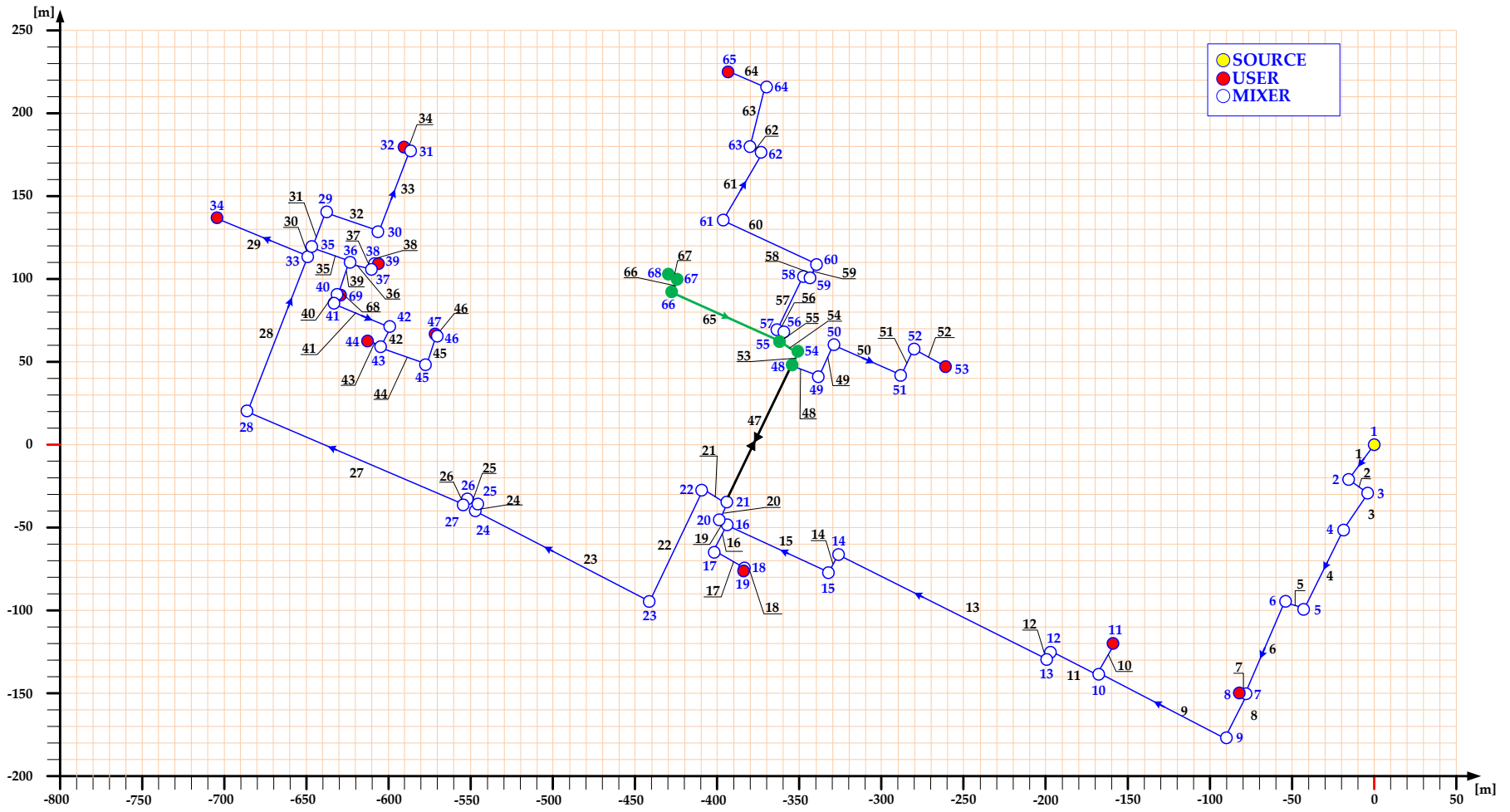
FIGURE C.5: NETWORK SETTING IN CASE 5 (IN GREEN COLOR THE REVERSE FLOW PIPES WITH RESPECT TO THE DESIGN CASE, IN IN BLACK COLOR THE CLOSED PIPES).
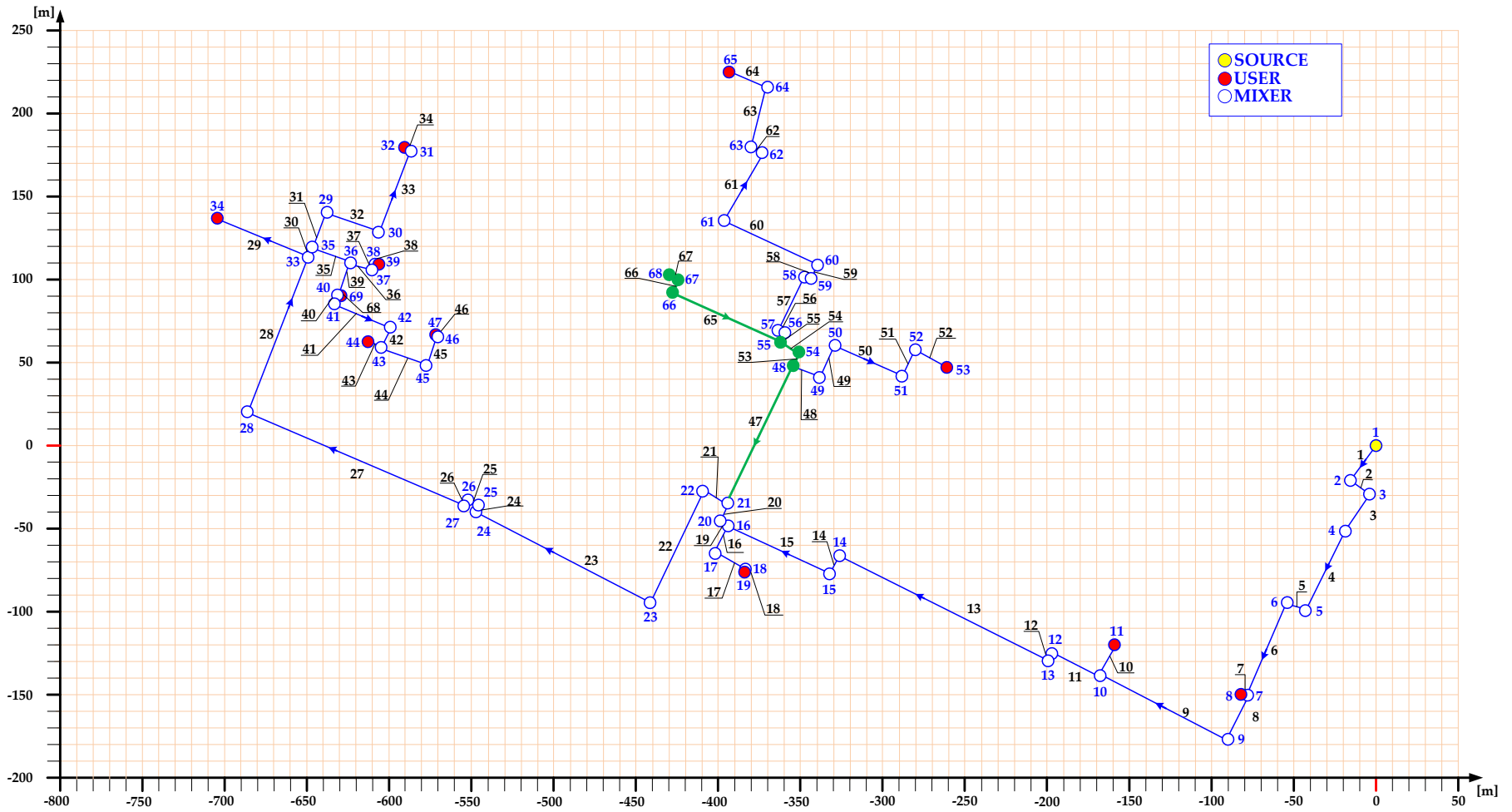
FIGURE C.6: NETWORK SETTING IN CASE 6 AND IN CASE 7 (IN GREEN COLOR THE REVERSE FLOW PIPES WITH RESPECT TO THE DESIGN CASE).
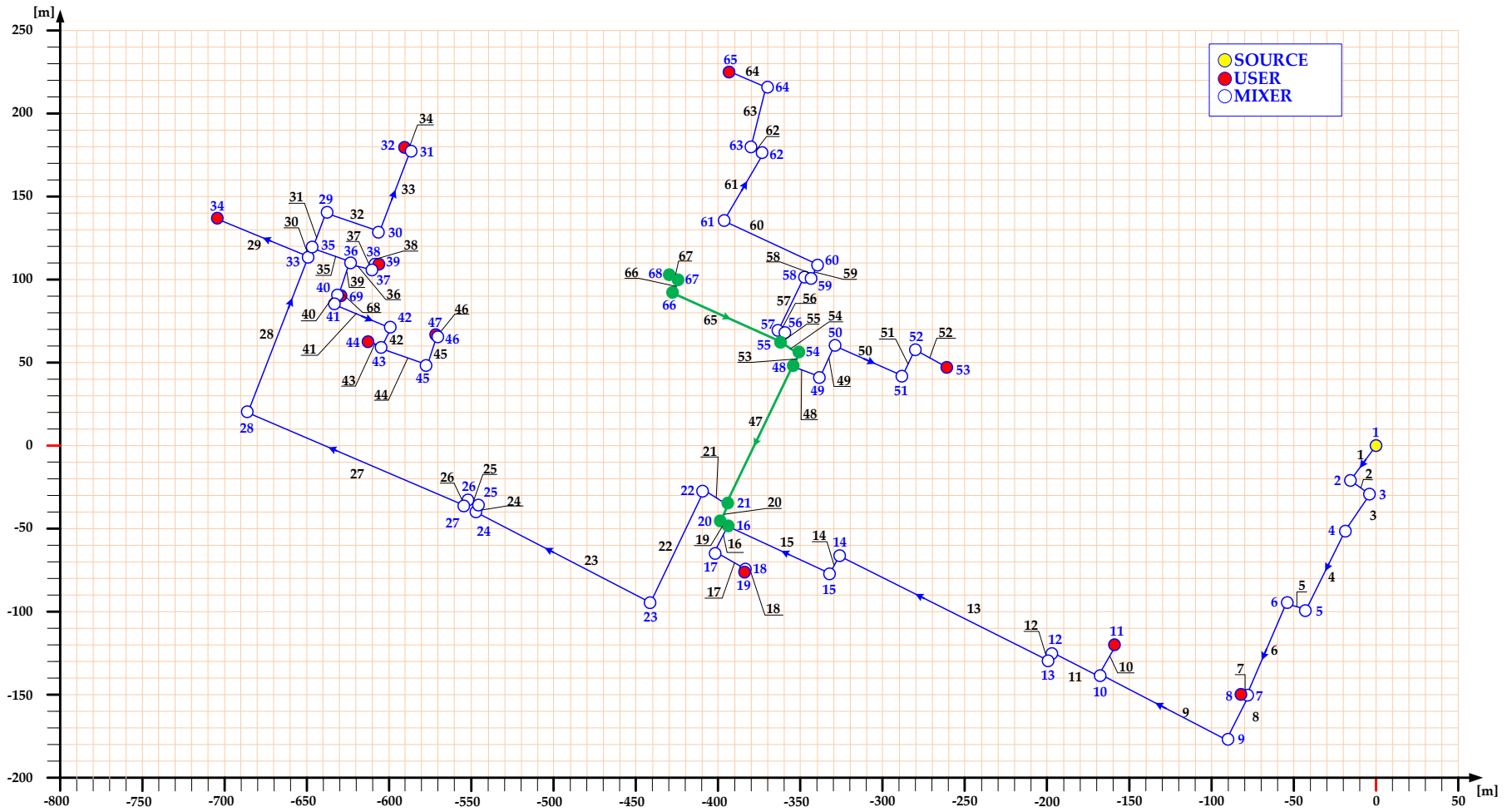
FIGURE C.7: NETWORK SETTING IN CASE 8 WITH P_{TH} 68=10˙273 KW (IN GREEN COLOR THE REVERSE FLOW PIPES WITH RESPECT TO THE DESIGN CASE).
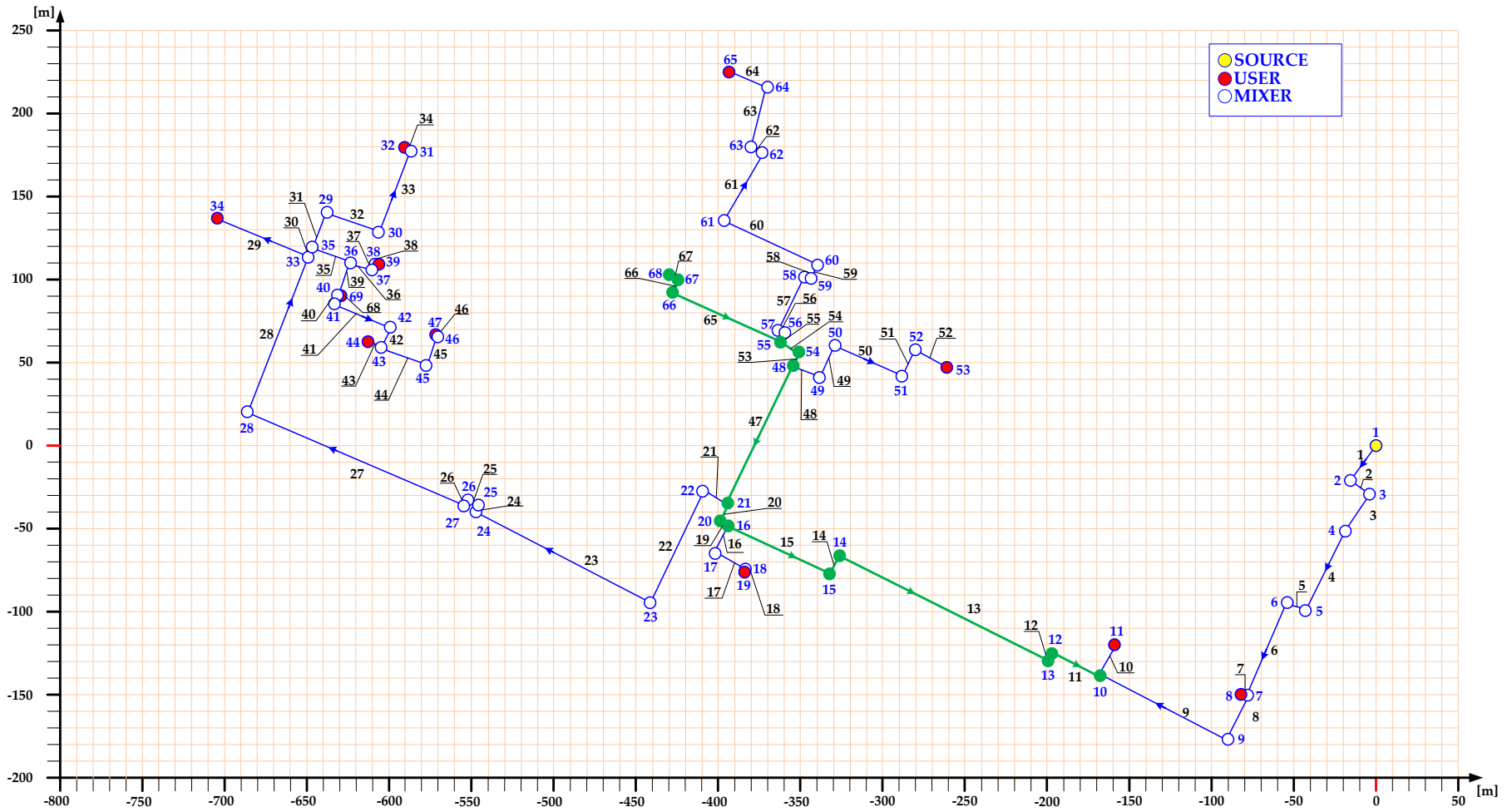
FIGURE C.8: NETWORK SETTING IN CASE 8 WITH P_{TH} 68=11375 KW (IN GREEN COLOR THE REVERSE FLOW PIPES WITH RESPECT TO THE DESIGN CASE).
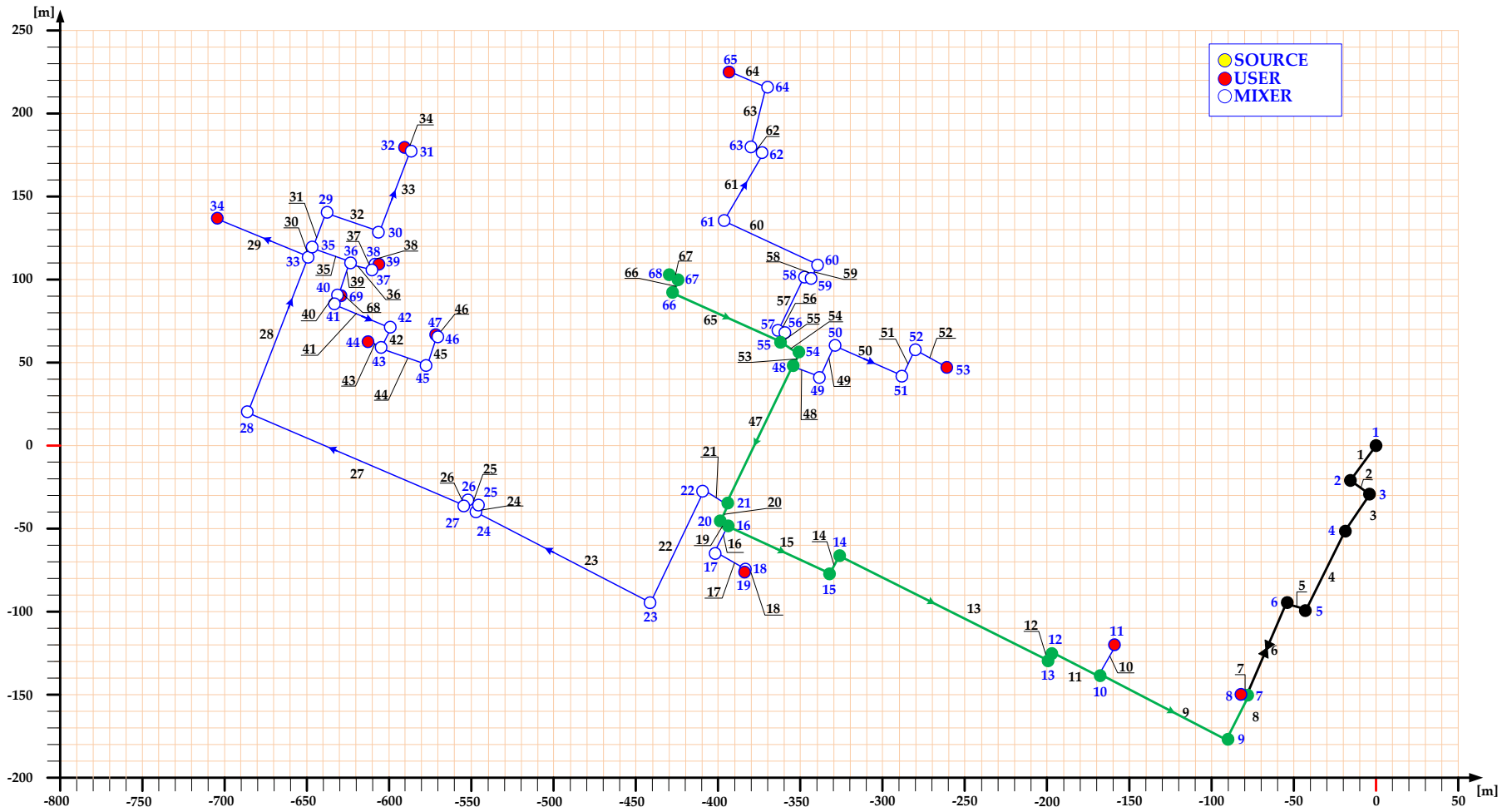
FIGURE C.9: NETWORK SETTING IN CASE 9 (IN GREEN COLOR THE REVERSE FLOW PIPES WITH RESPECT TO THE DESIGN CASE, IN IN BLACK COLOR THE CLOSED PIPES).

APPENDIX D
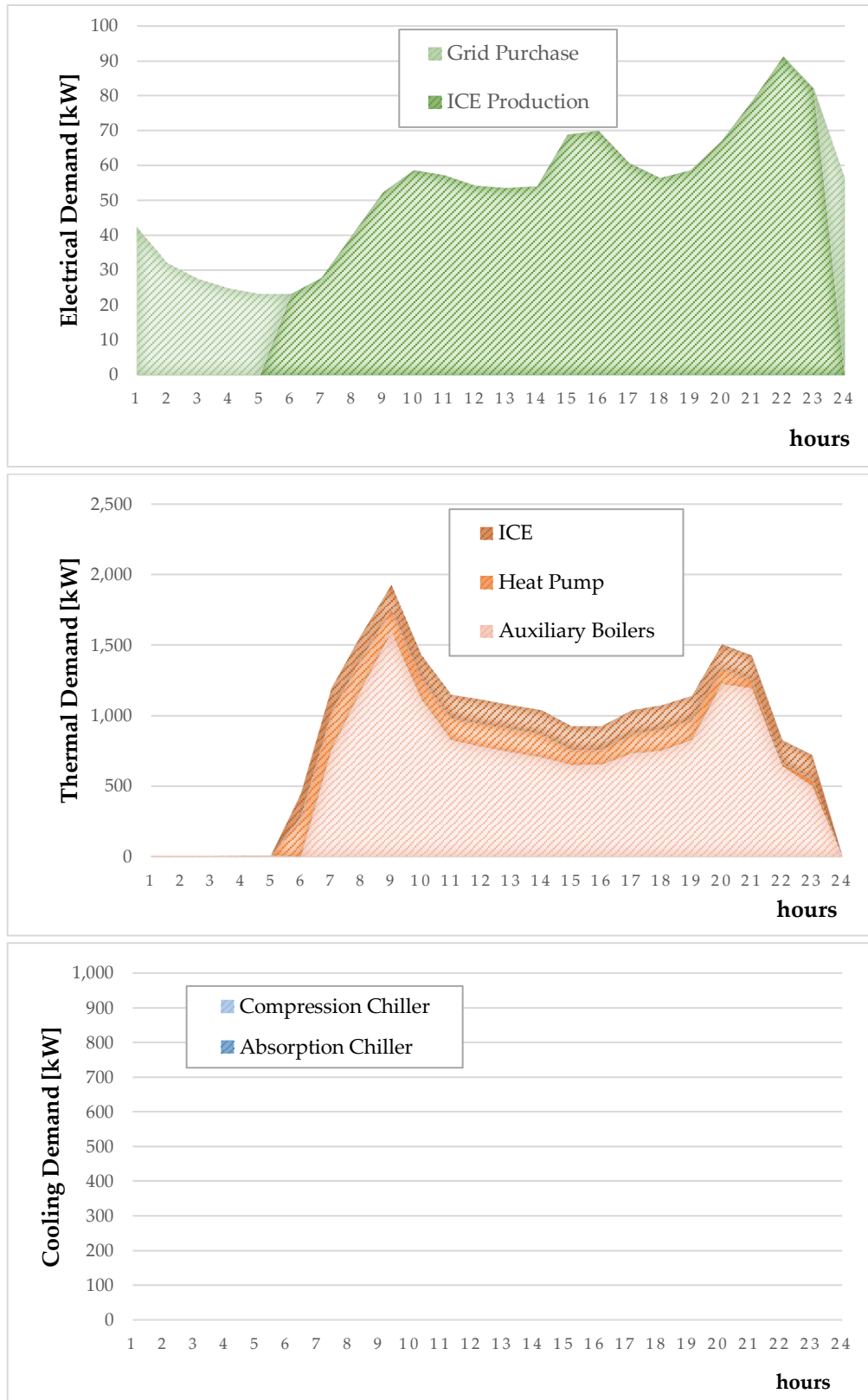
FIGURE D.1: HOURLY ELECTRICAL, THERMAL AND COOLING PROFILE IN THE CASE OF 200 HOUSEHOLDS FOR WINTER SEASON.
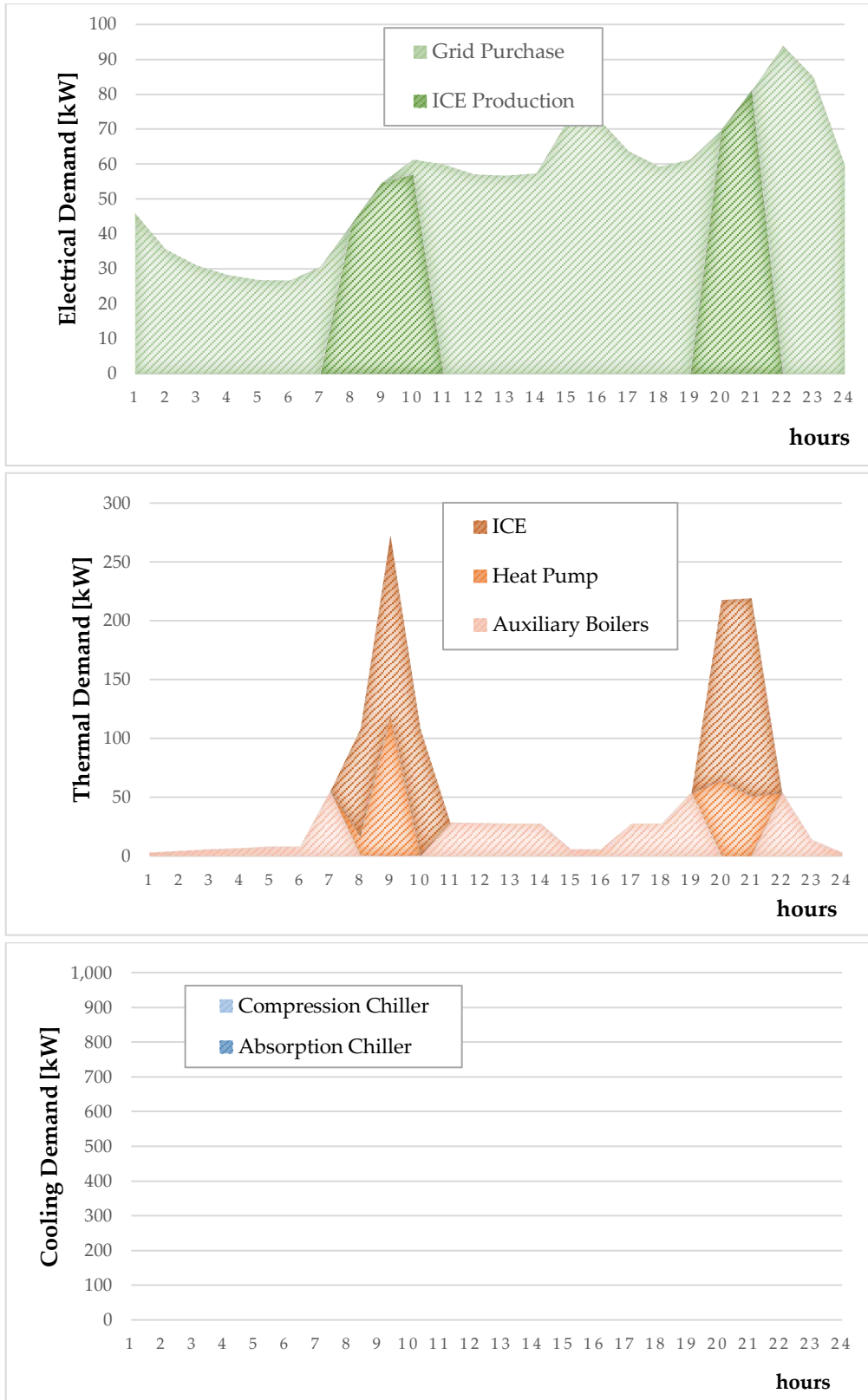
FIGURE D.2: HOURLY ELECTRICAL, THERMAL AND COOLING PROFILE IN THE CASE OF 200 HOUSEHOLDS FOR MIDDLE SEASON.
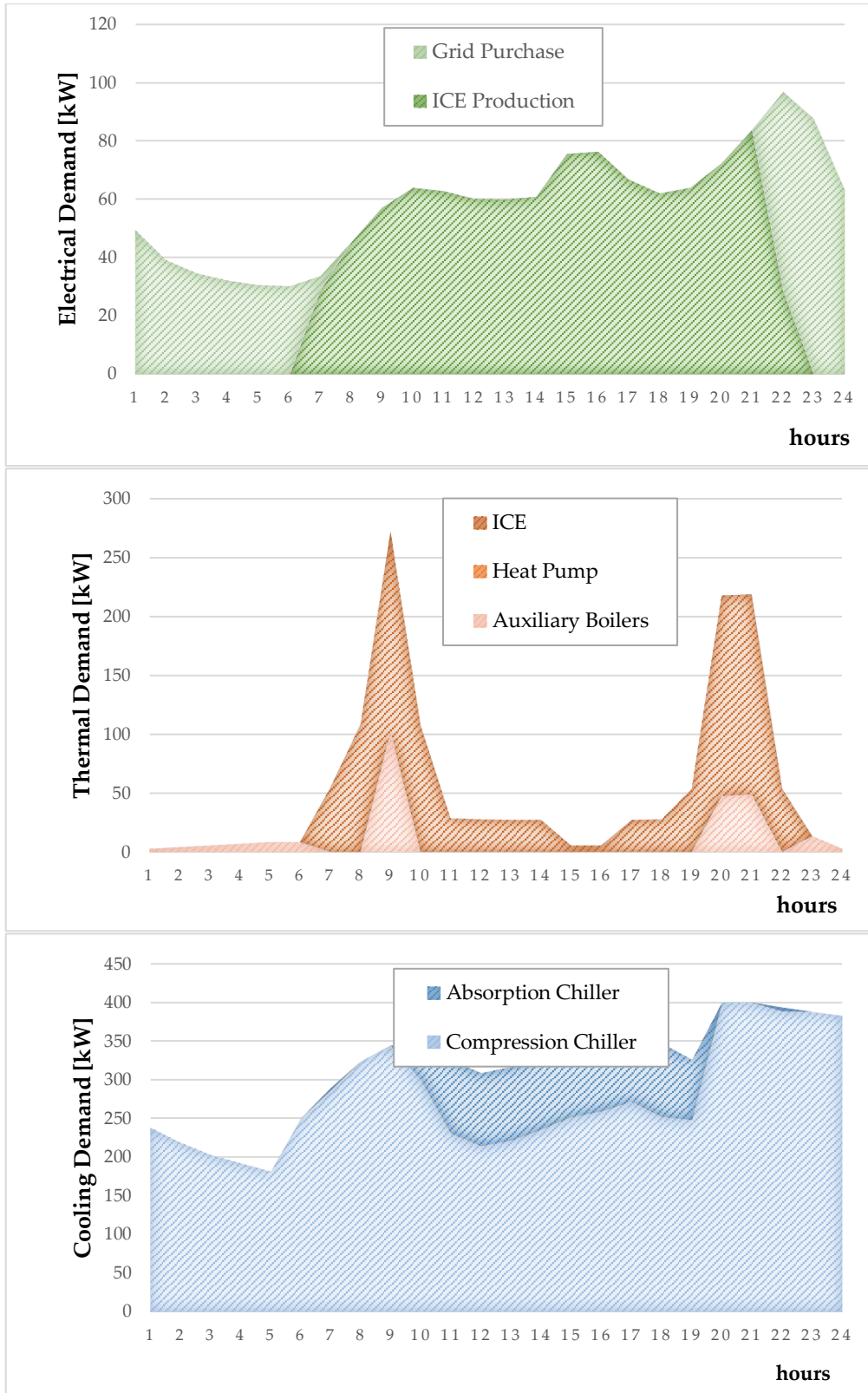
FIGURE D.3: HOURLY ELECTRICAL, THERMAL AND COOLING PROFILE IN THE CASE OF 200 HOUSEHOLDS FOR SUMMER SEASON.
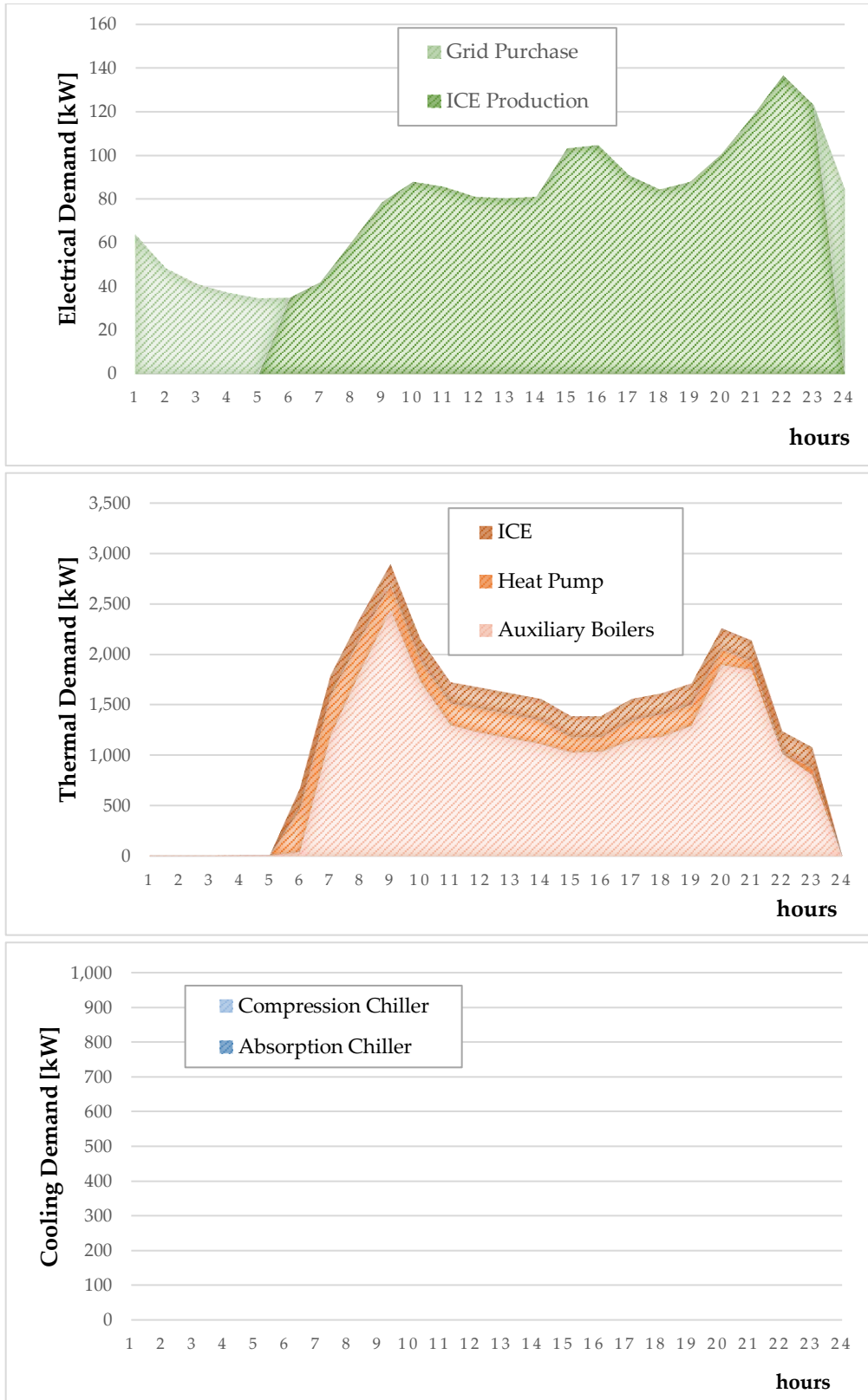
FIGURE D.4: HOURLY ELECTRICAL, THERMAL AND COOLING PROFILE IN THE CASE OF 300 HOUSEHOLDS FOR WINTER SEASON.
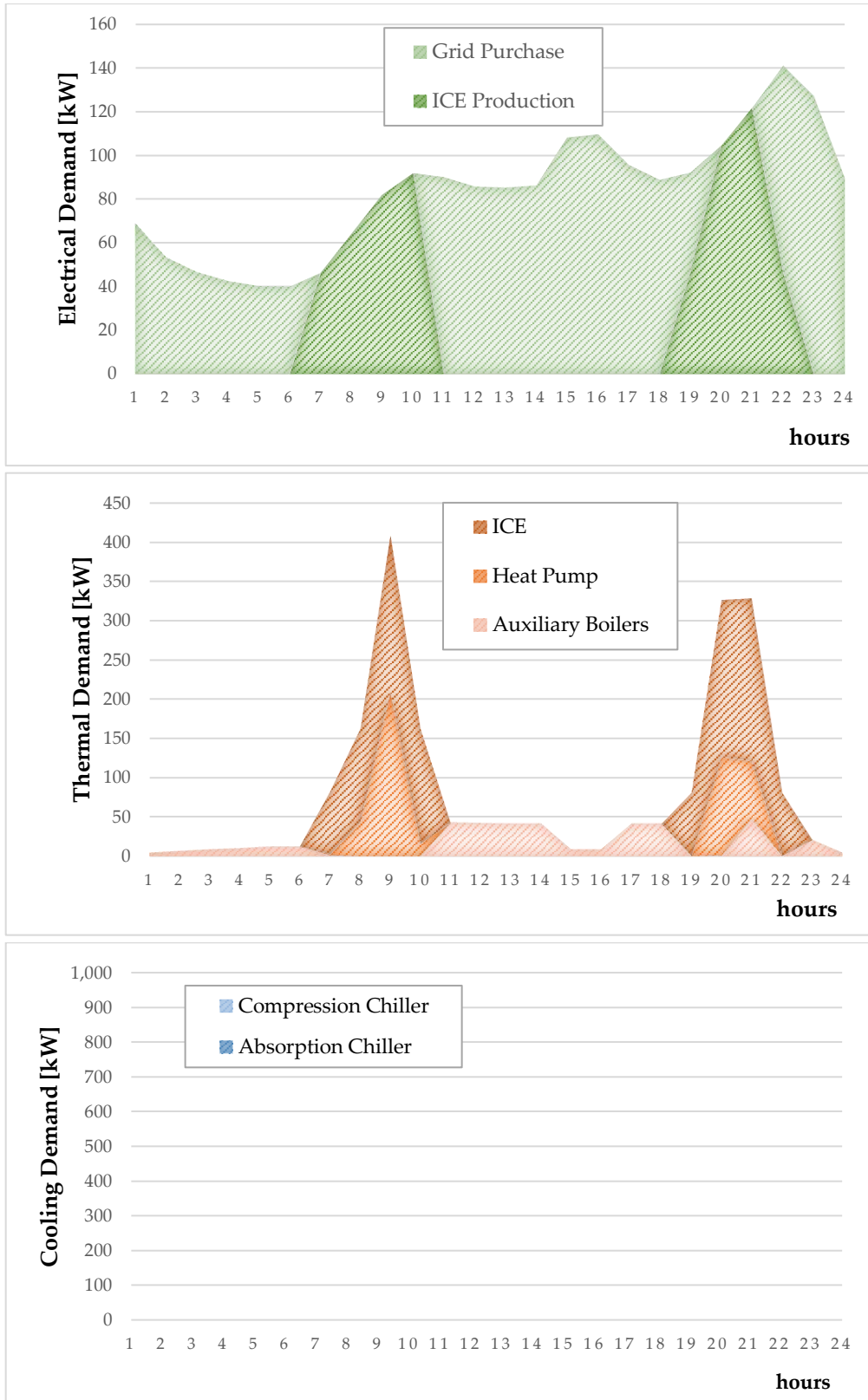
FIGURE D.5: HOURLY ELECTRICAL, THERMAL AND COOLING PROFILE IN THE CASE OF 300 HOUSEHOLDS FOR MIDDLE SEASON.
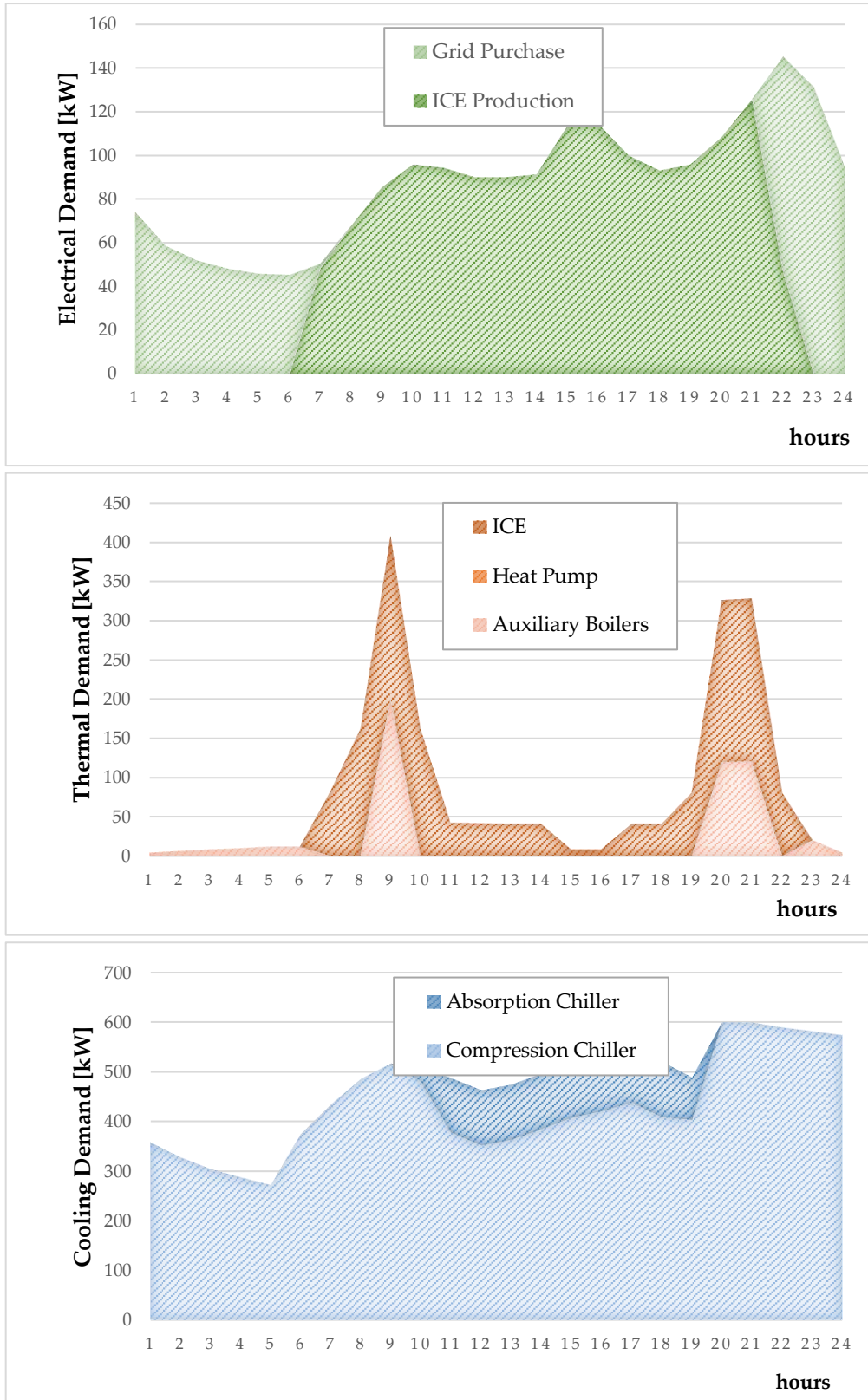
FIGURE D.6: HOURLY ELECTRICAL, THERMAL AND COOLING PROFILE IN THE CASE OF 300 HOUSEHOLDS FOR SUMMER SEASON.
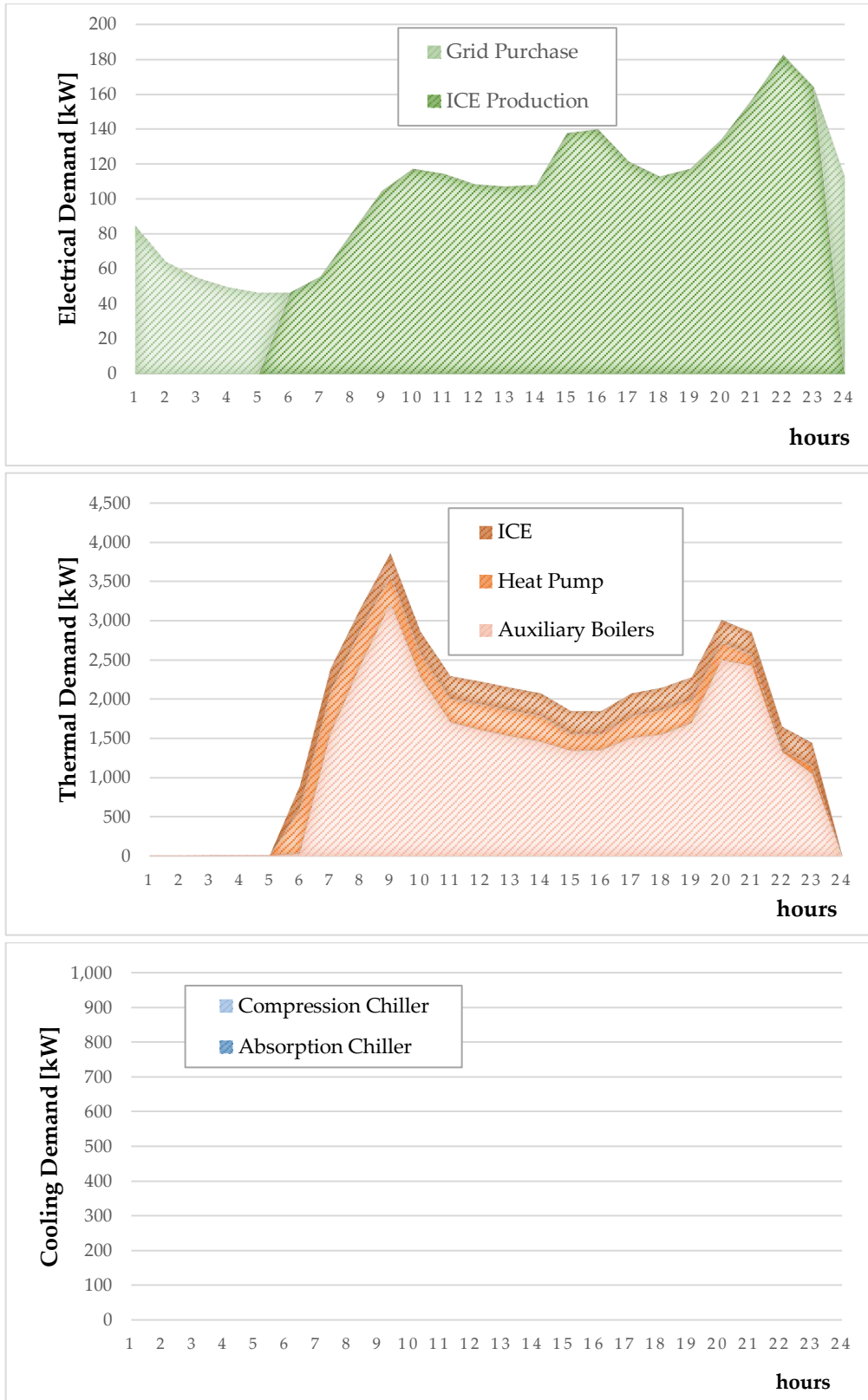
FIGURE D.7: HOURLY ELECTRICAL, THERMAL AND COOLING PROFILE IN THE CASE OF 400 HOUSEHOLDS FOR WINTER SEASON.
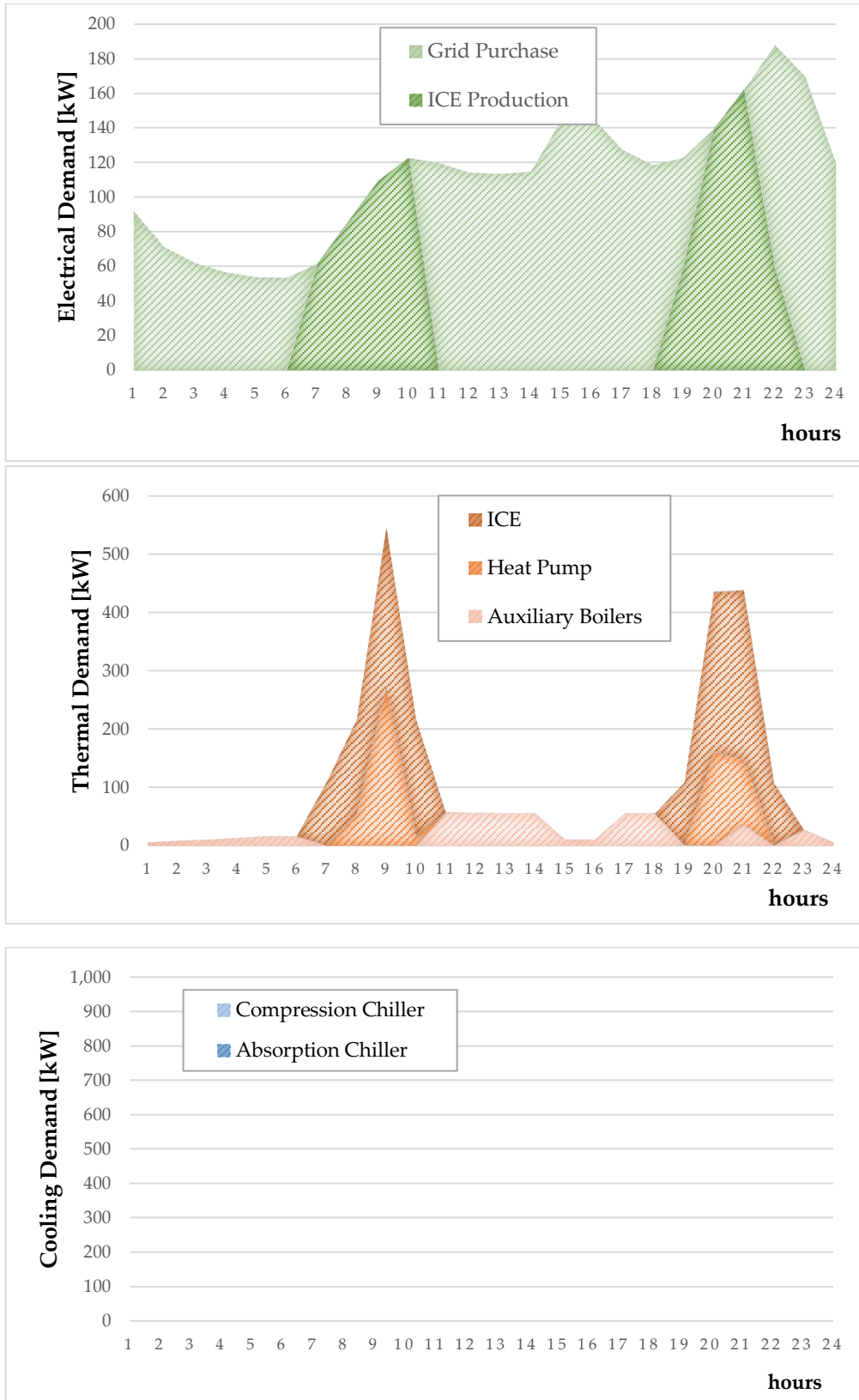
FIGURE D.8: HOURLY ELECTRICAL, THERMAL AND COOLING PROFILE IN THE CASE OF 400 HOUSEHOLDS FOR MIDDLE SEASON.
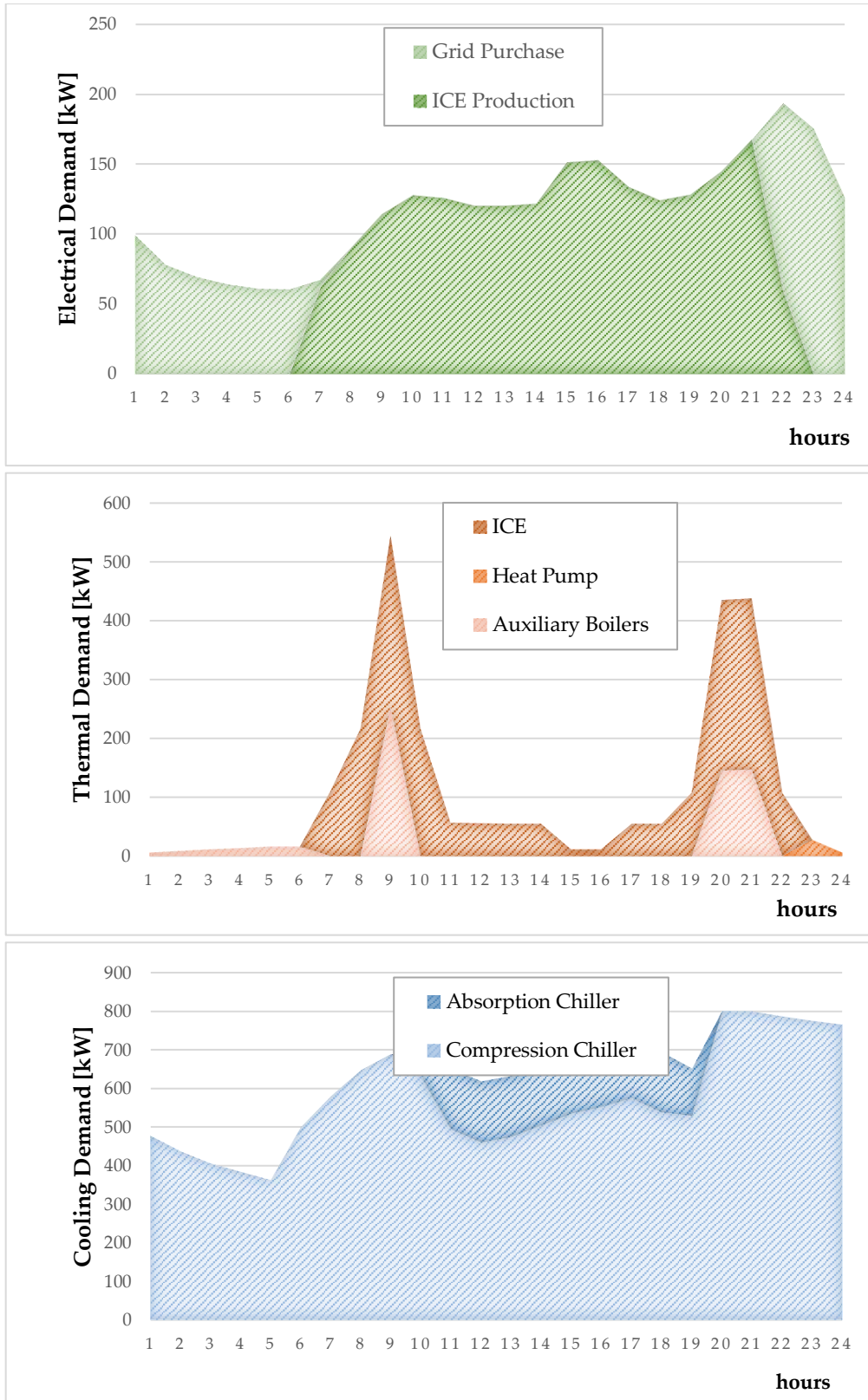
FIGURE D.9: HOURLY ELECTRICAL, THERMAL AND COOLING PROFILE IN THE CASE OF 400 HOUSEHOLDS FOR SUMMER SEASON.
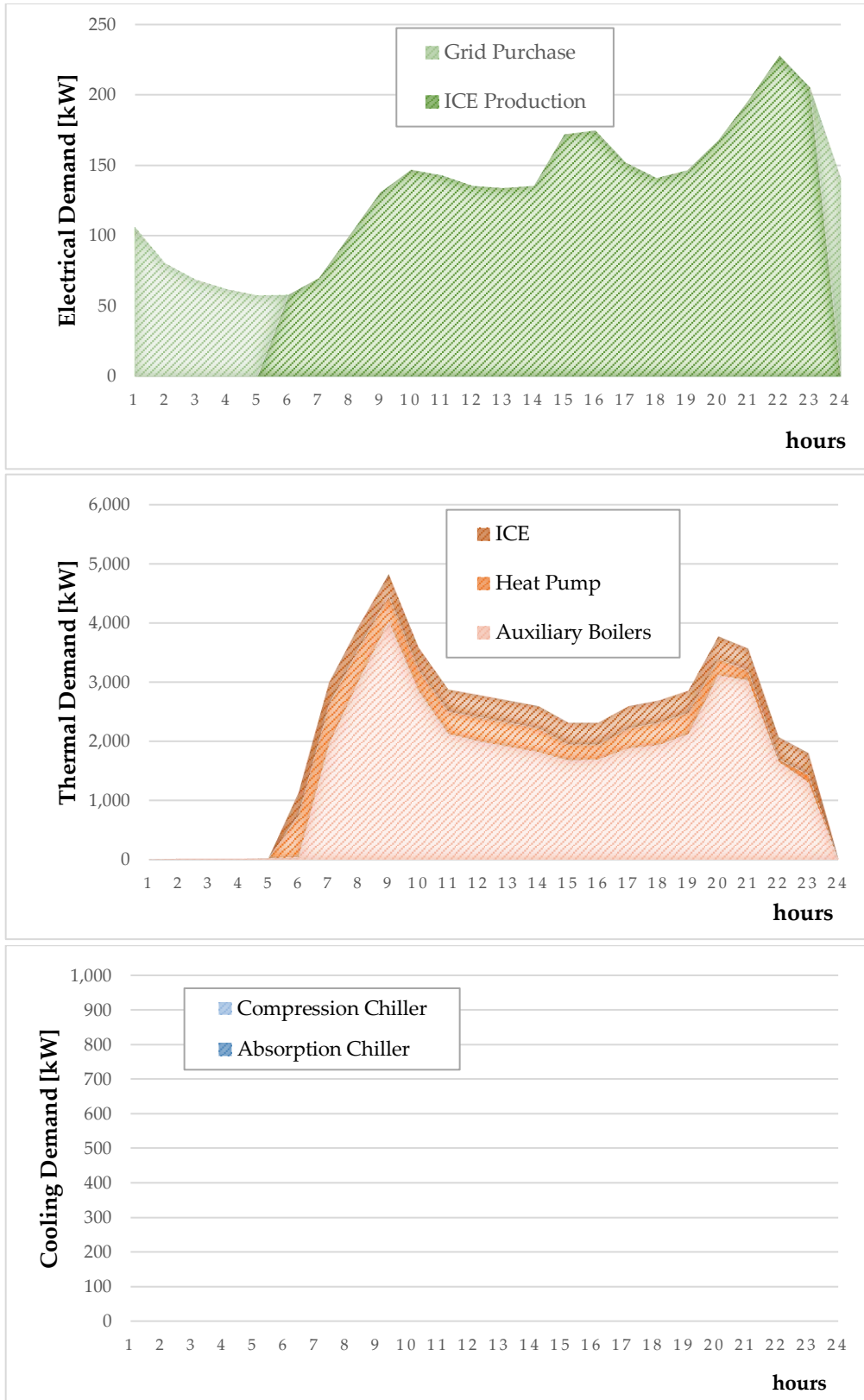
FIGURE D.10: HOURLY ELECTRICAL, THERMAL AND COOLING PROFILE IN THE CASE OF 500 HOUSEHOLDS FOR WINTER SEASON.
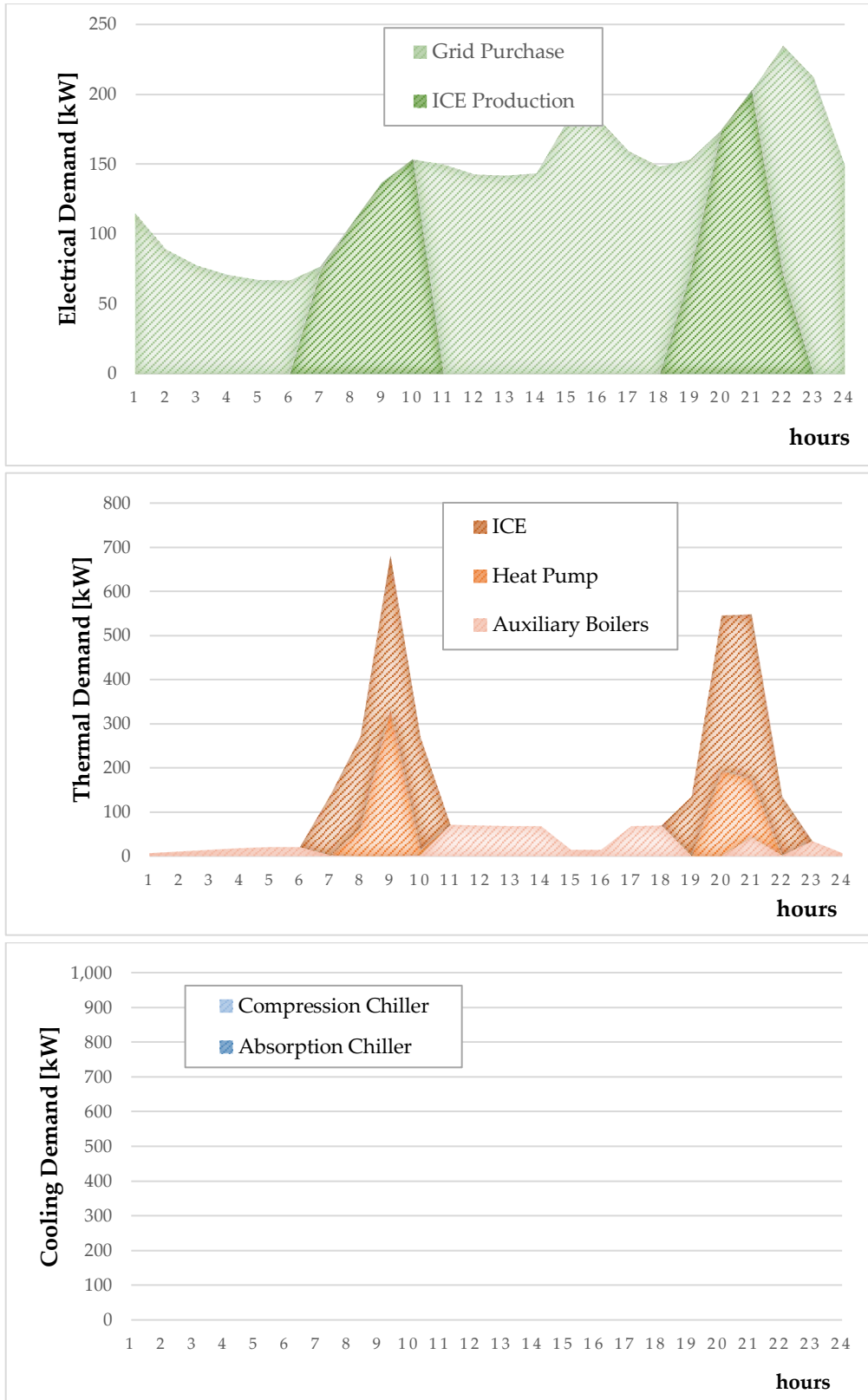
FIGURE D.11: HOURLY ELECTRICAL, THERMAL AND COOLING PROFILE IN THE CASE OF 500 HOUSEHOLDS FOR MIDDLE SEASON.
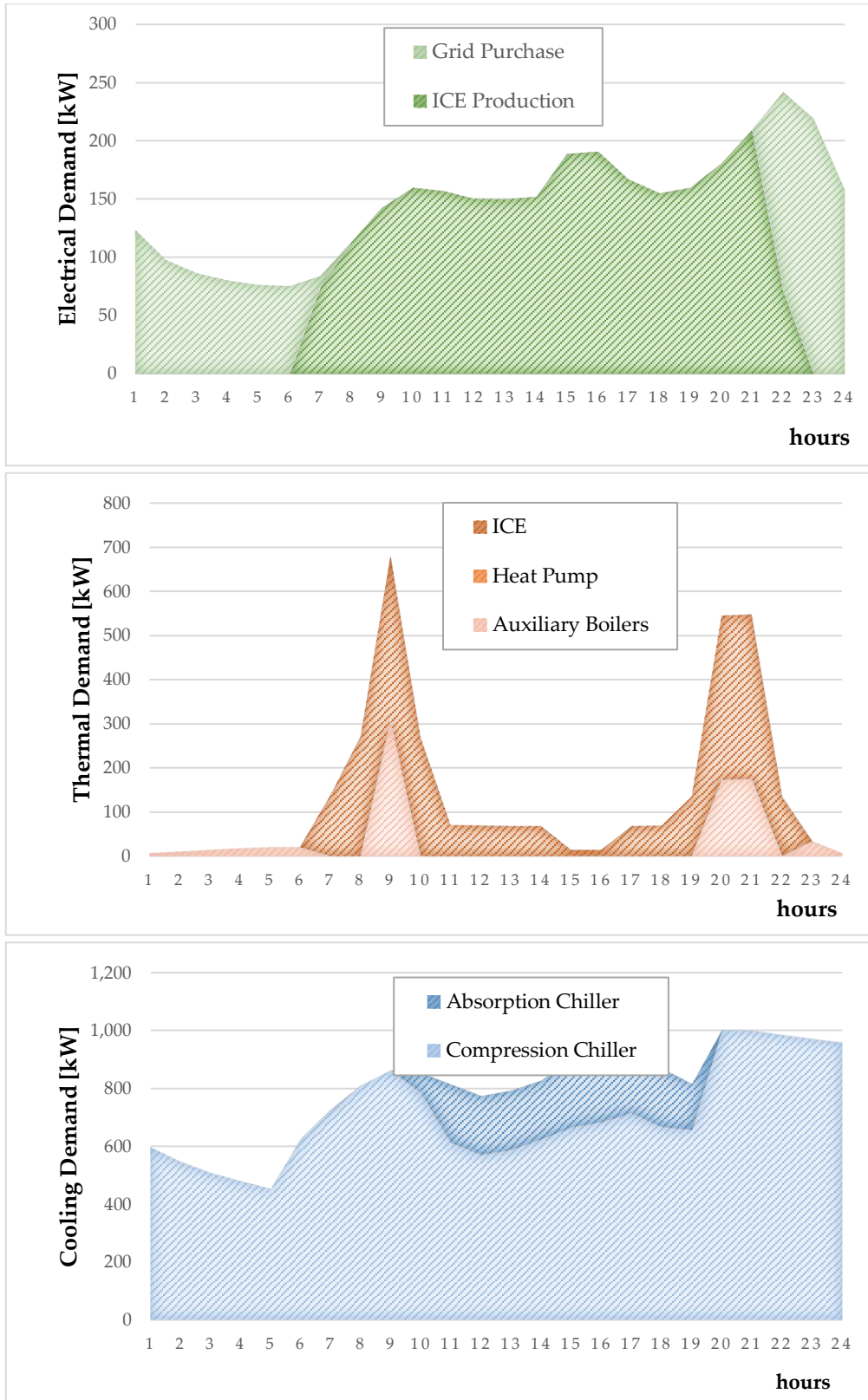
FIGURE D.12: HOURLY ELECTRICAL, THERMAL AND COOLING PROFILE IN THE CASE OF 500 HOUSEHOLDS FOR SUMMER SEASON.
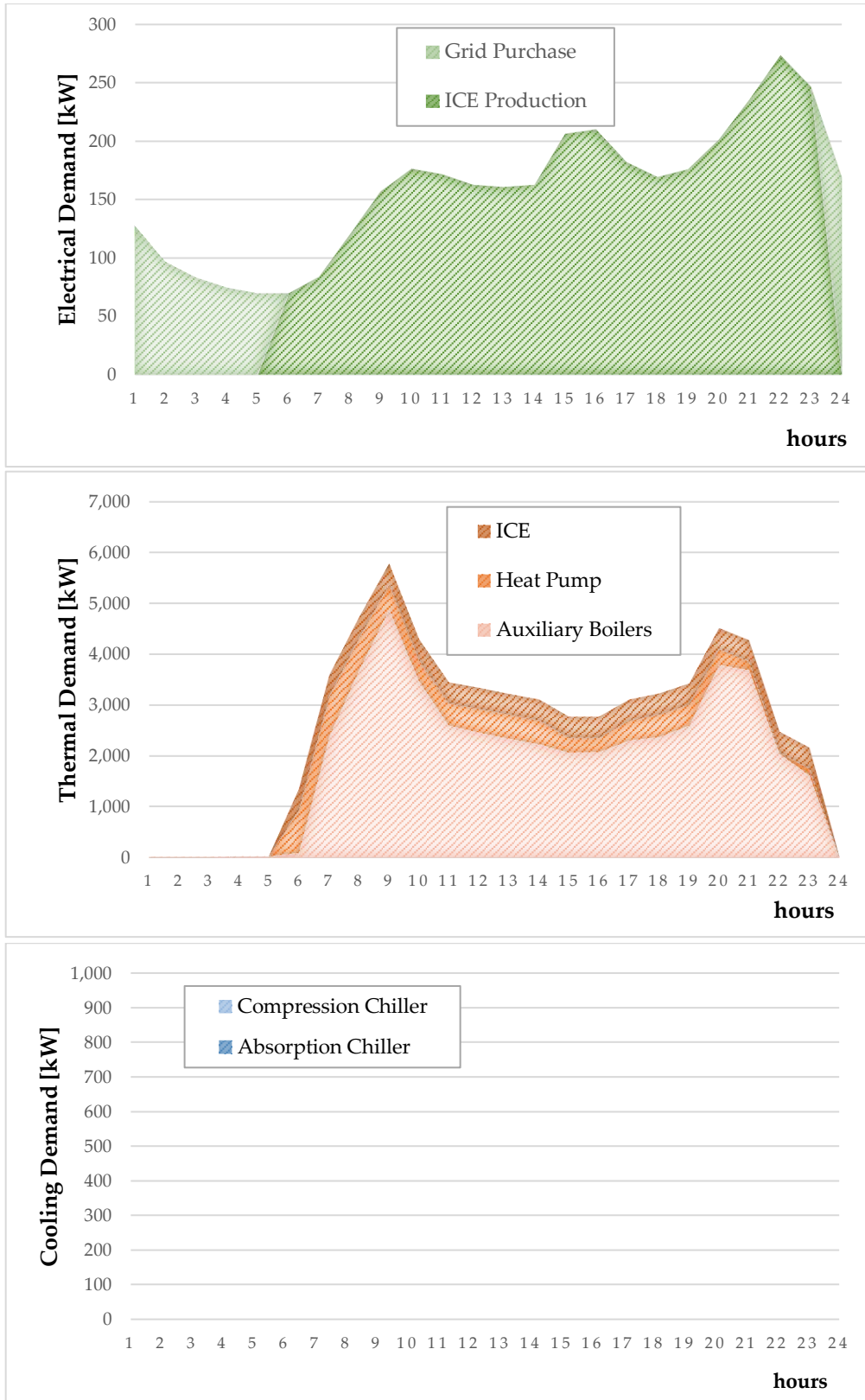
FIGURE D.13: HOURLY ELECTRICAL, THERMAL AND COOLING PROFILE IN THE CASE OF 600 HOUSEHOLDS FOR WINTER SEASON.
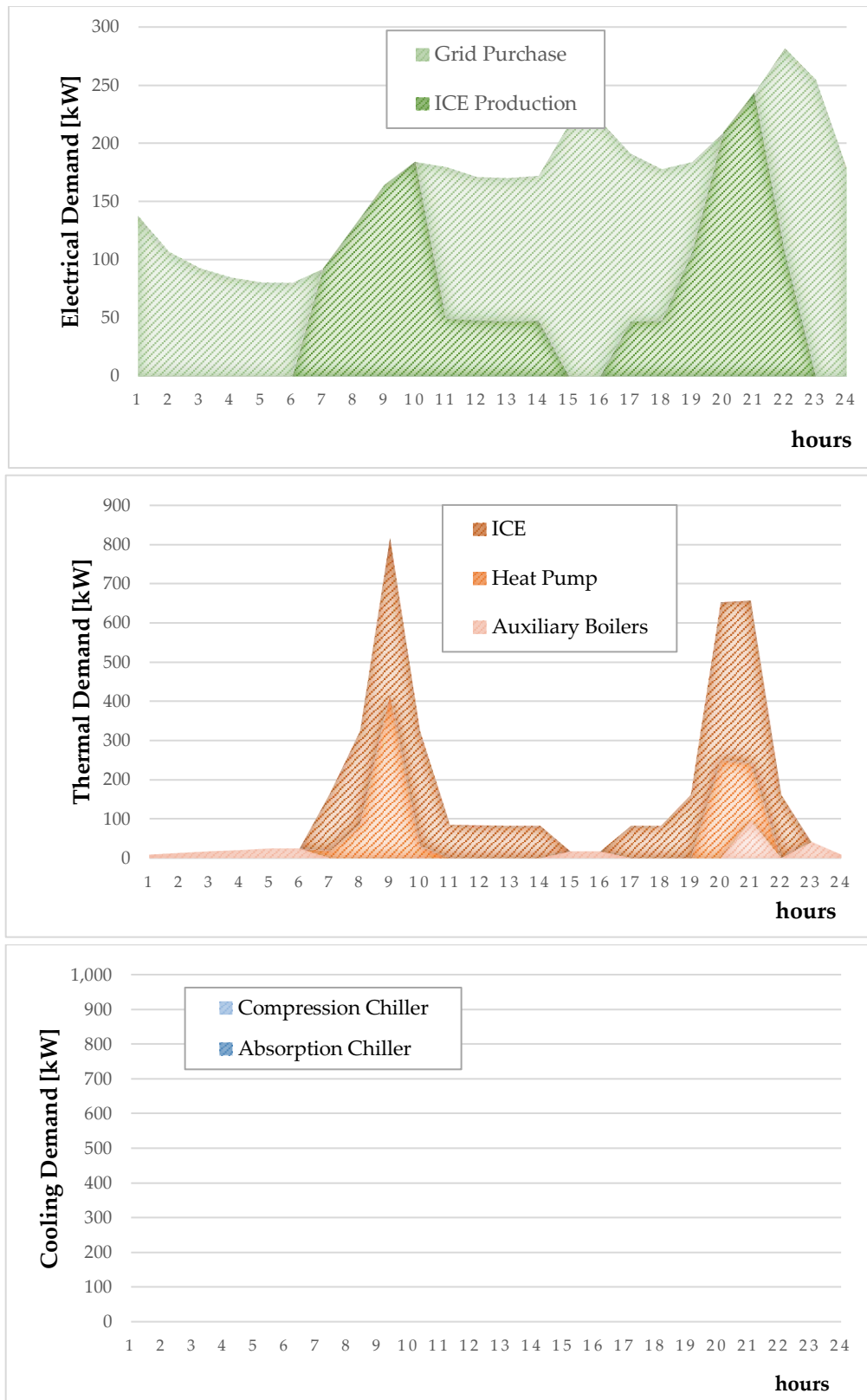
FIGURE D.14: HOURLY ELECTRICAL, THERMAL AND COOLING PROFILE IN THE CASE OF 600
HOUSEHOLDS FOR MIDDLE SEASON.
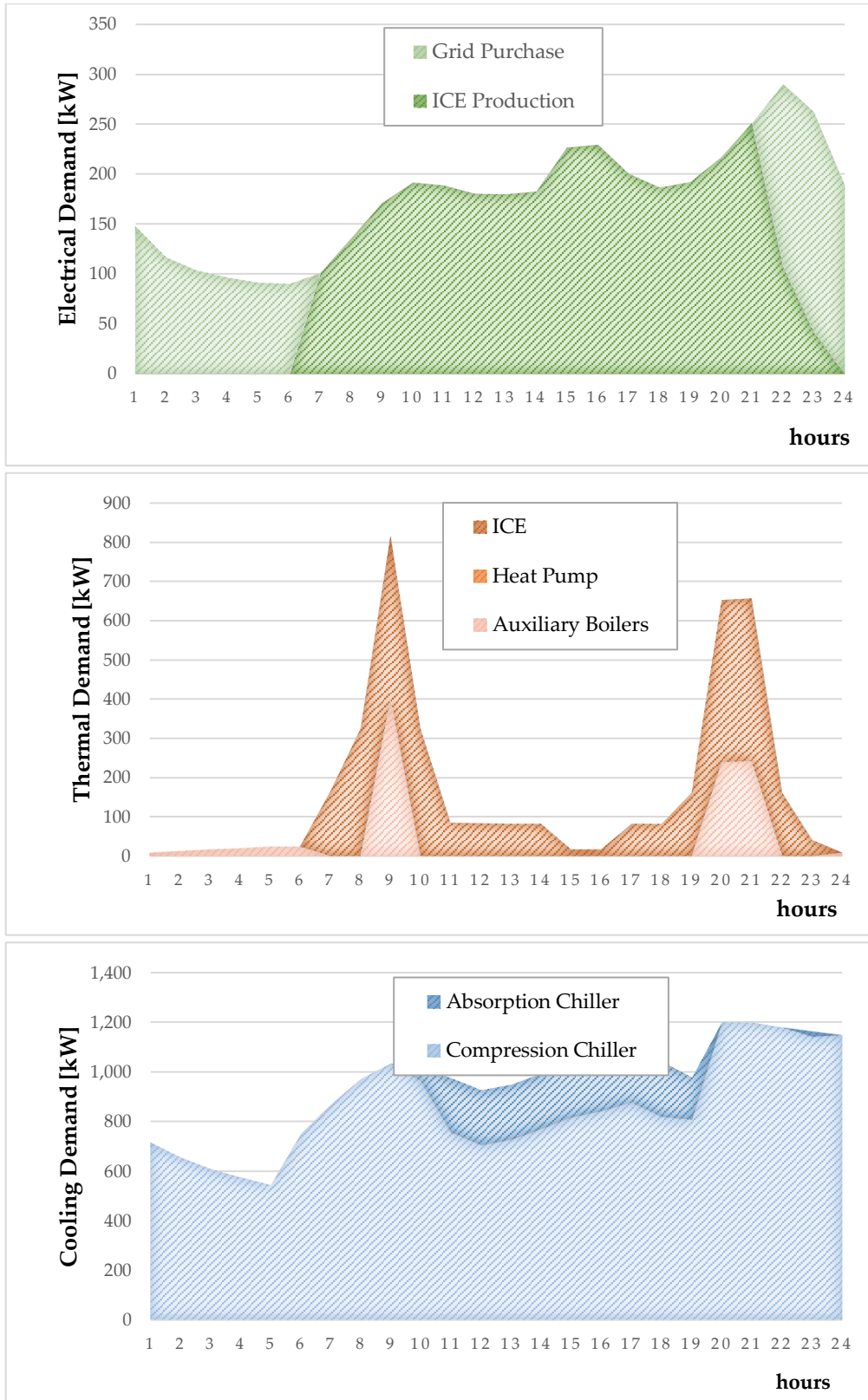
FIGURE D.15: HOURLY ELECTRICAL, THERMAL AND COOLING PROFILE IN THE CASE OF 600 HOUSEHOLDS FOR SUMMER SEASON.
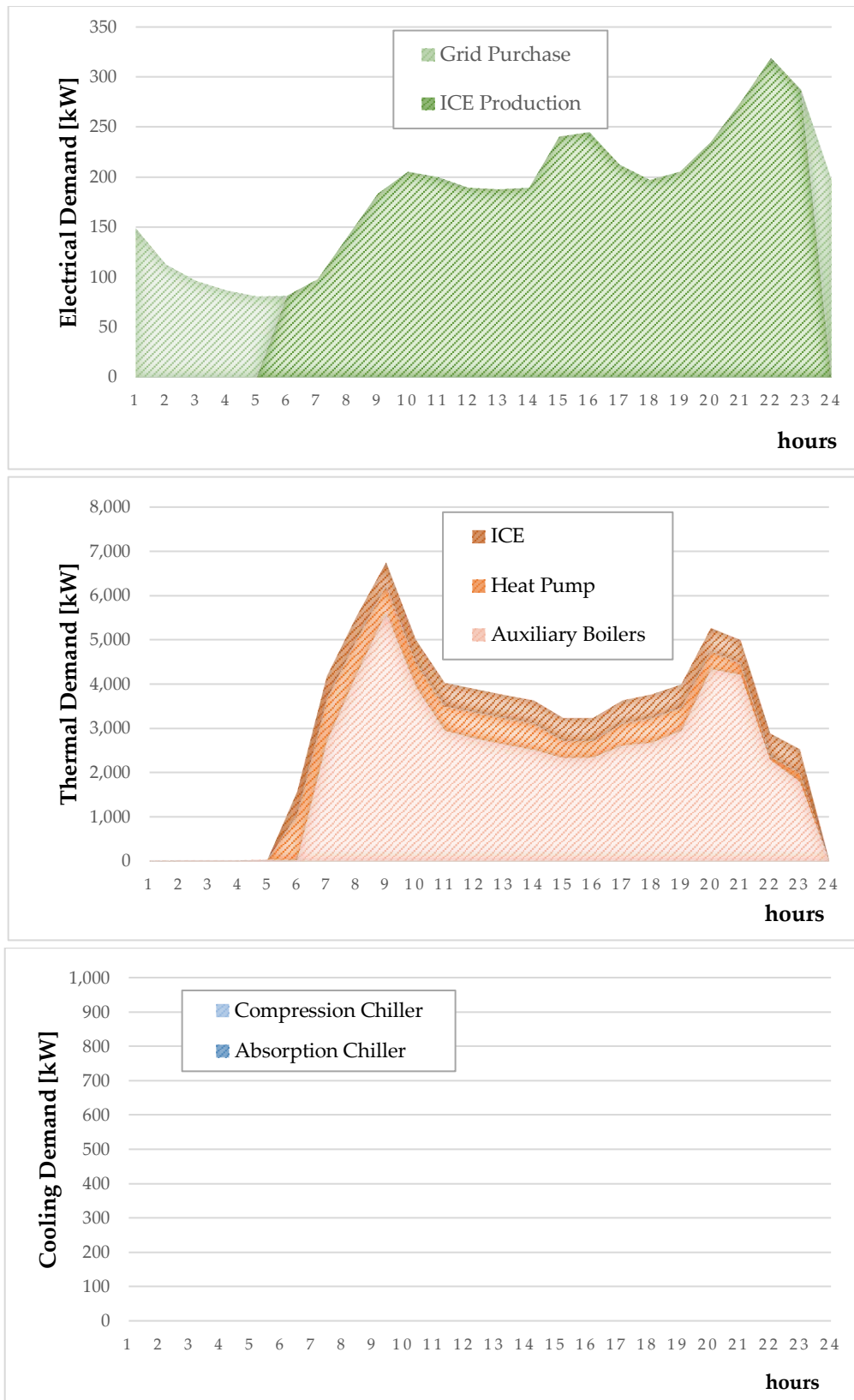
FIGURE D.16: HOURLY ELECTRICAL, THERMAL AND COOLING PROFILE IN THE CASE OF 700 HOUSEHOLDS FOR WINTER SEASON.
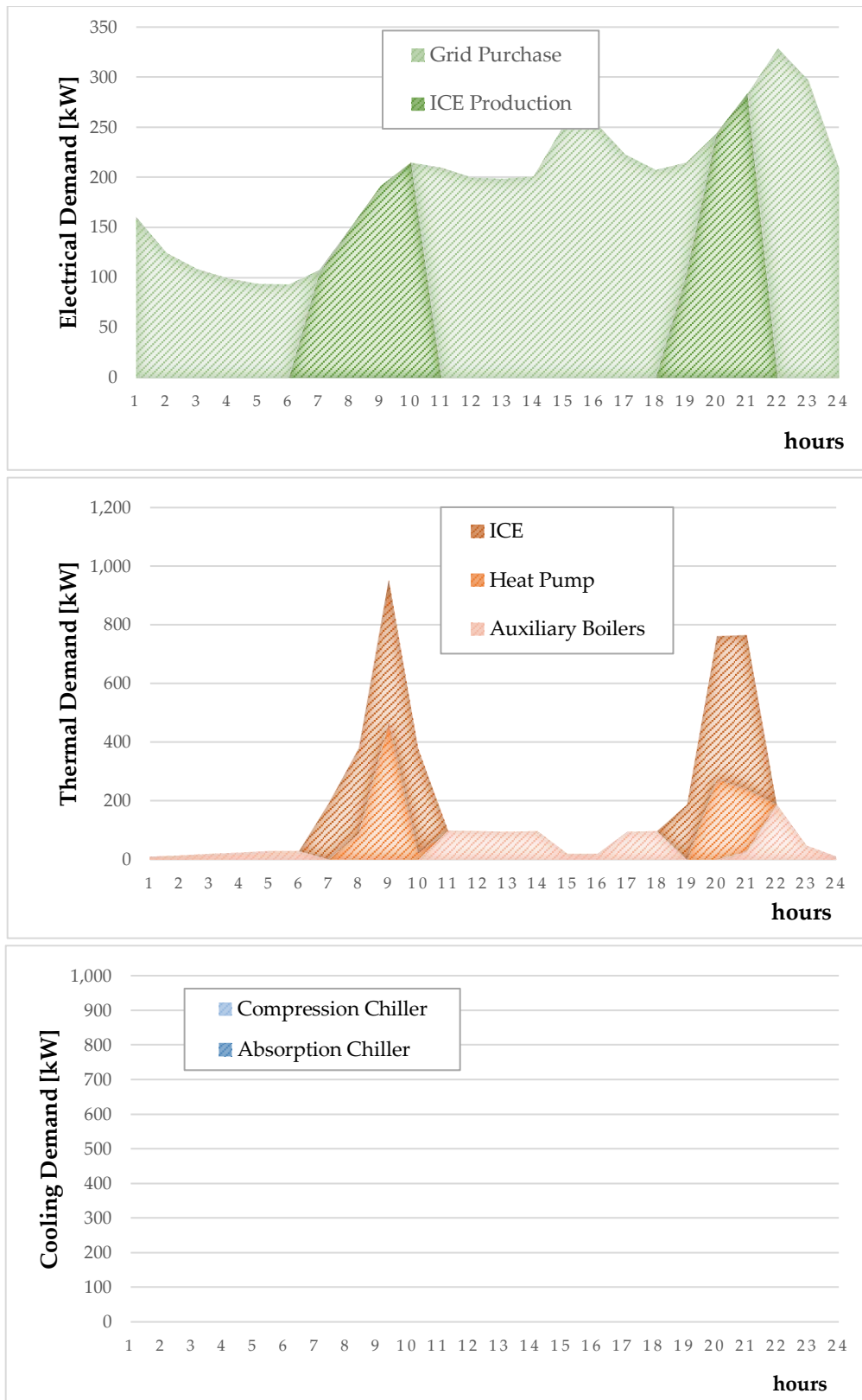
FIGURE D.17: HOURLY ELECTRICAL, THERMAL AND COOLING PROFILE IN THE CASE OF 700 HOUSEHOLDS FOR MIDDLE SEASON.
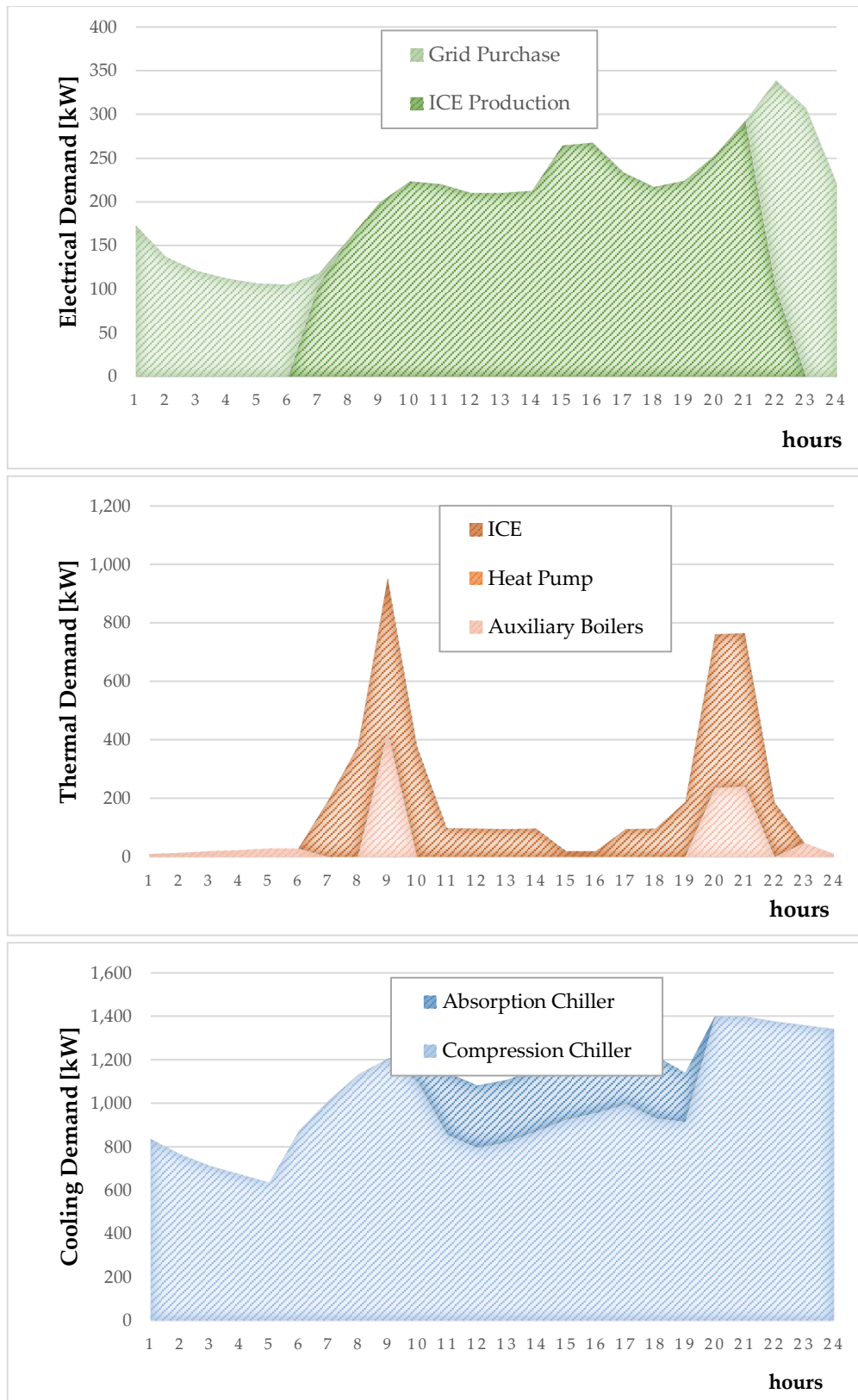
FIGURE D.18: HOURLY ELECTRICAL, THERMAL AND COOLING PROFILE IN THE CASE OF 700
HOUSEHOLDS FOR SUMMER SEASON.
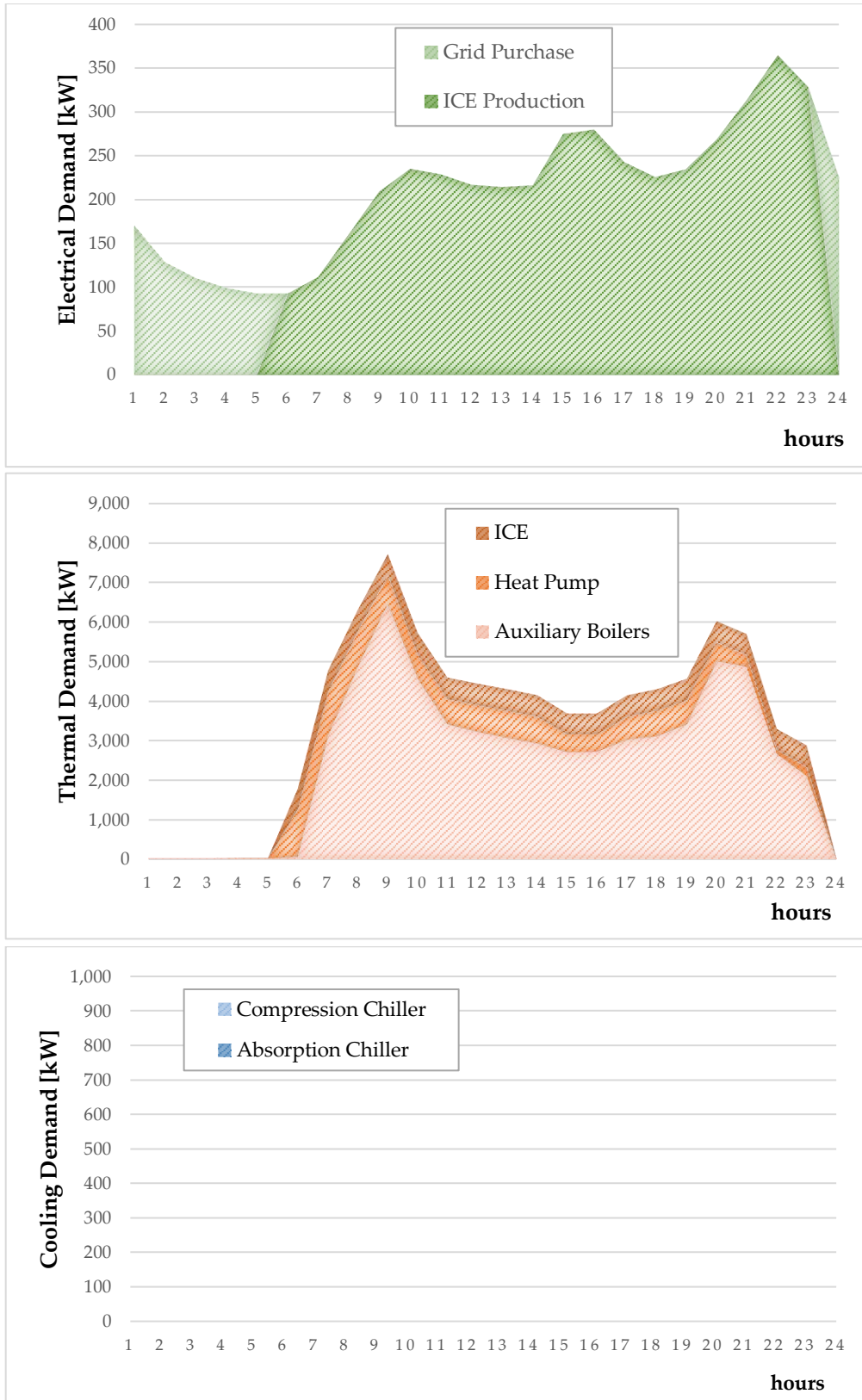
FIGURE D.19: HOURLY ELECTRICAL, THERMAL AND COOLING PROFILE IN THE CASE OF 800
HOUSEHOLDS FOR WINTER SEASON.
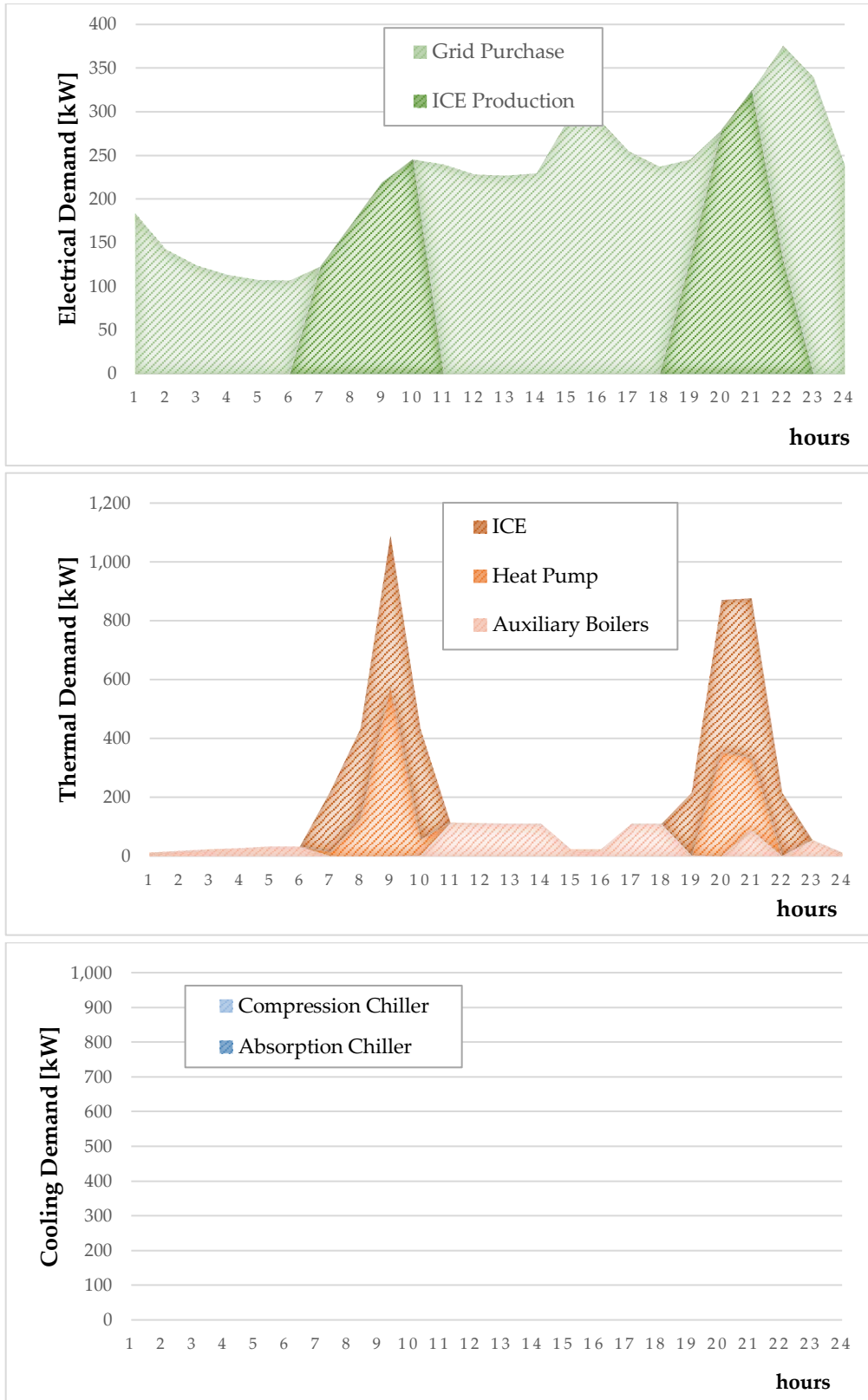
FIGURE D.20: HOURLY ELECTRICAL, THERMAL AND COOLING PROFILE IN THE CASE OF 800 HOUSEHOLDS FOR MIDDLE SEASON.
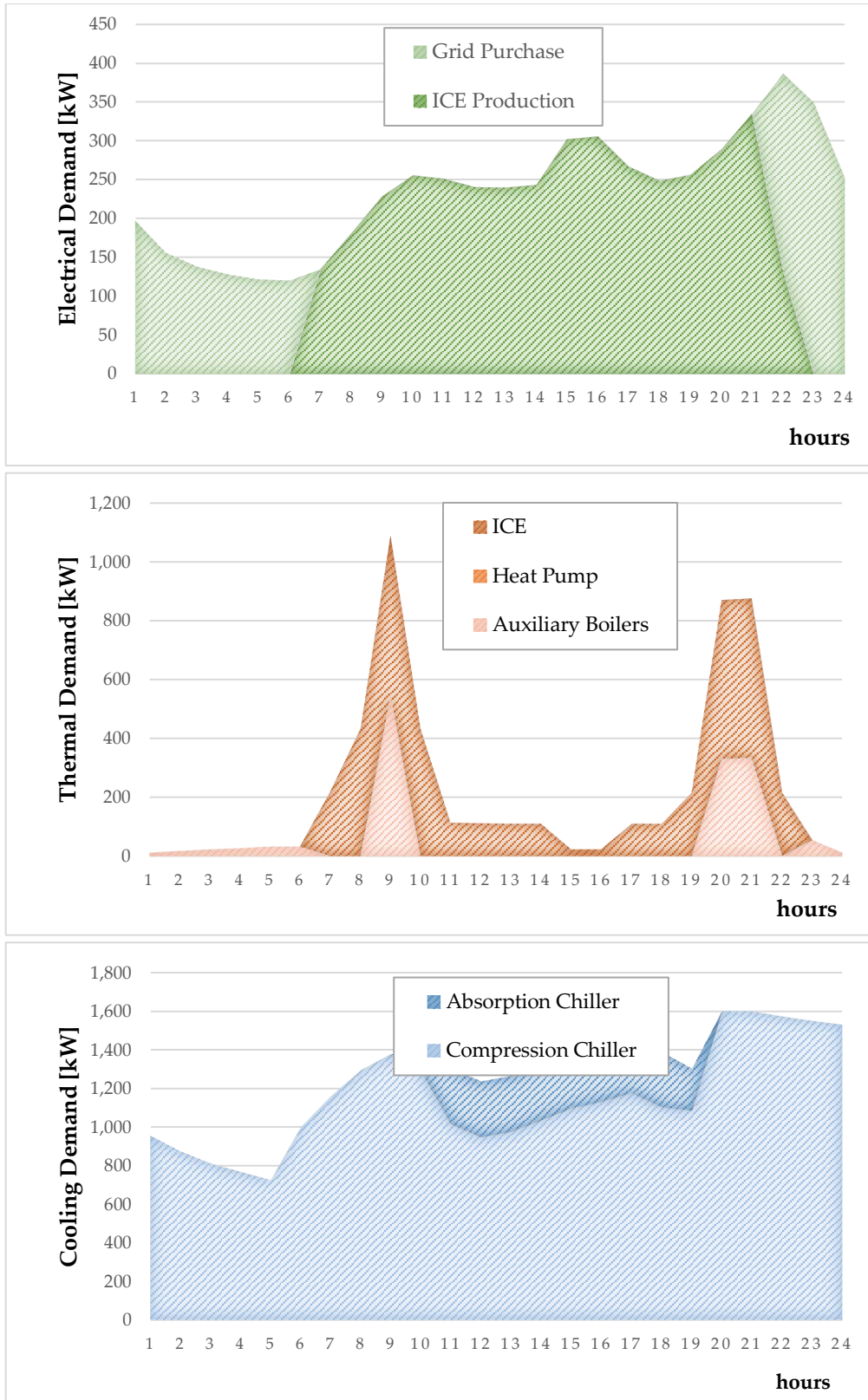
FIGURE D.21: HOURLY ELECTRICAL, THERMAL AND COOLING PROFILE IN THE CASE OF 800 HOUSEHOLDS FOR SUMMER SEASON.
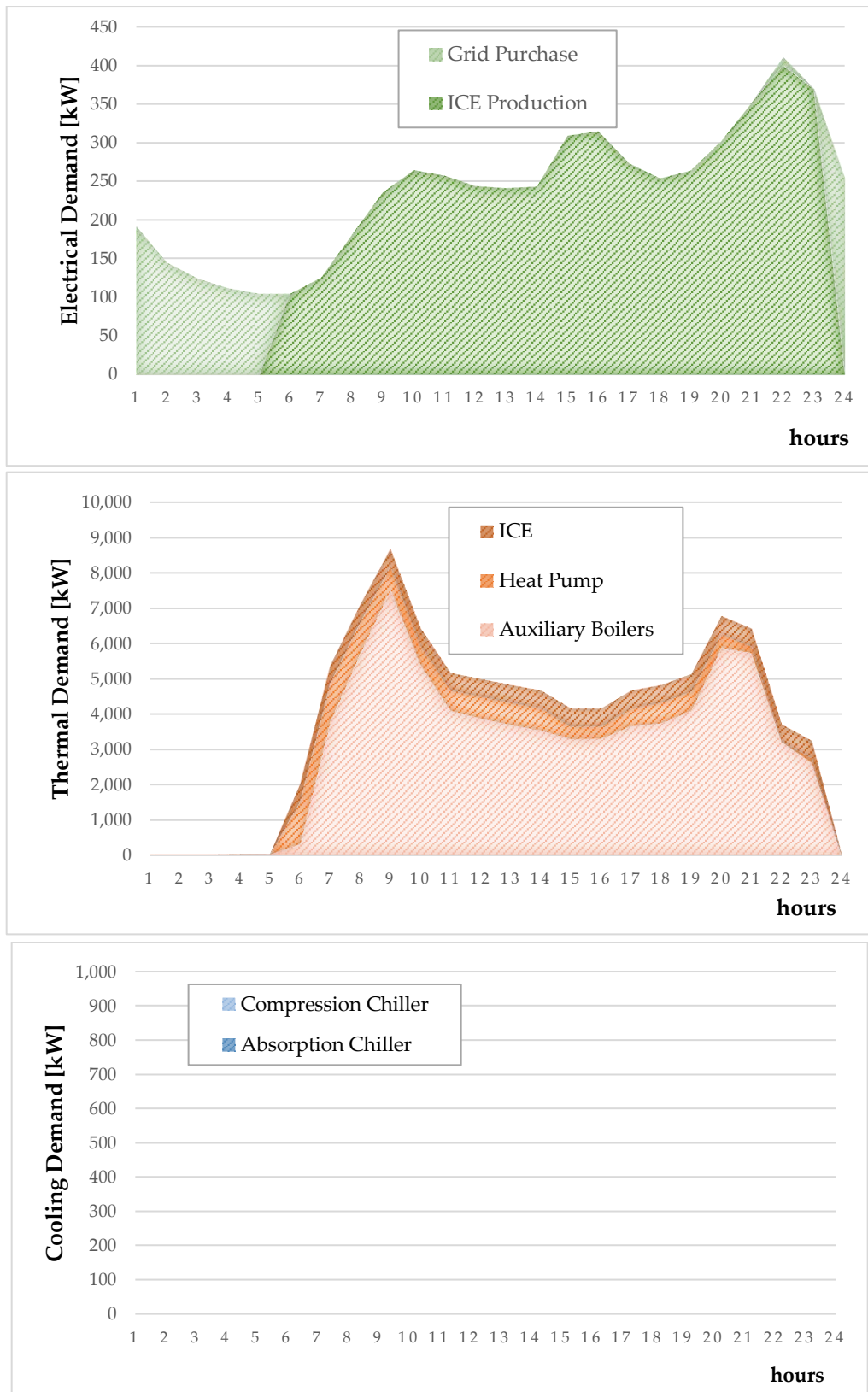
FIGURE D.22: HOURLY ELECTRICAL, THERMAL AND COOLING PROFILE IN THE CASE OF 900 HOUSEHOLDS FOR WINTER SEASON.
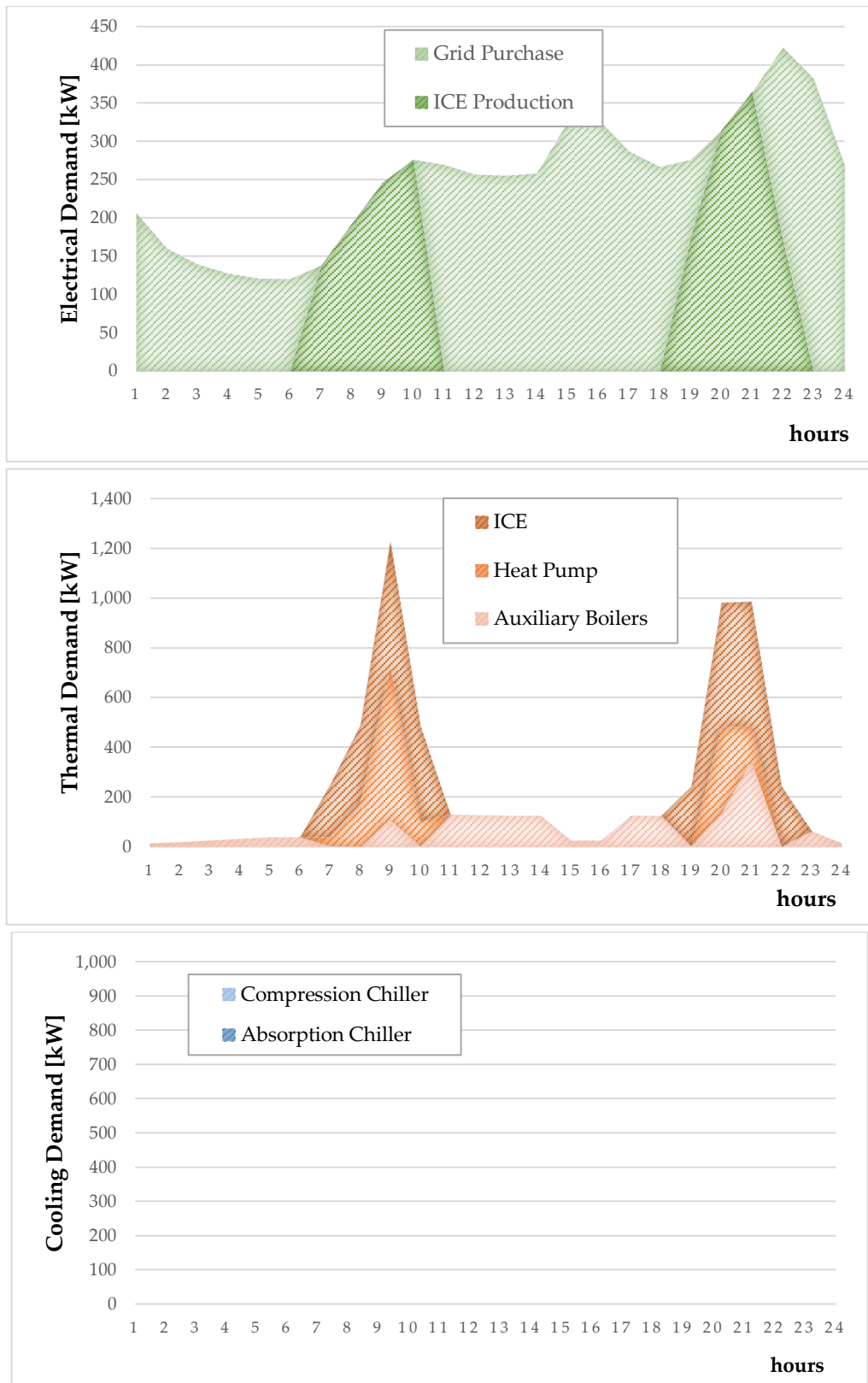
FIGURE D.23: HOURLY ELECTRICAL, THERMAL AND COOLING PROFILE IN THE CASE OF 900 HOUSEHOLDS FOR MIDDLE SEASON.
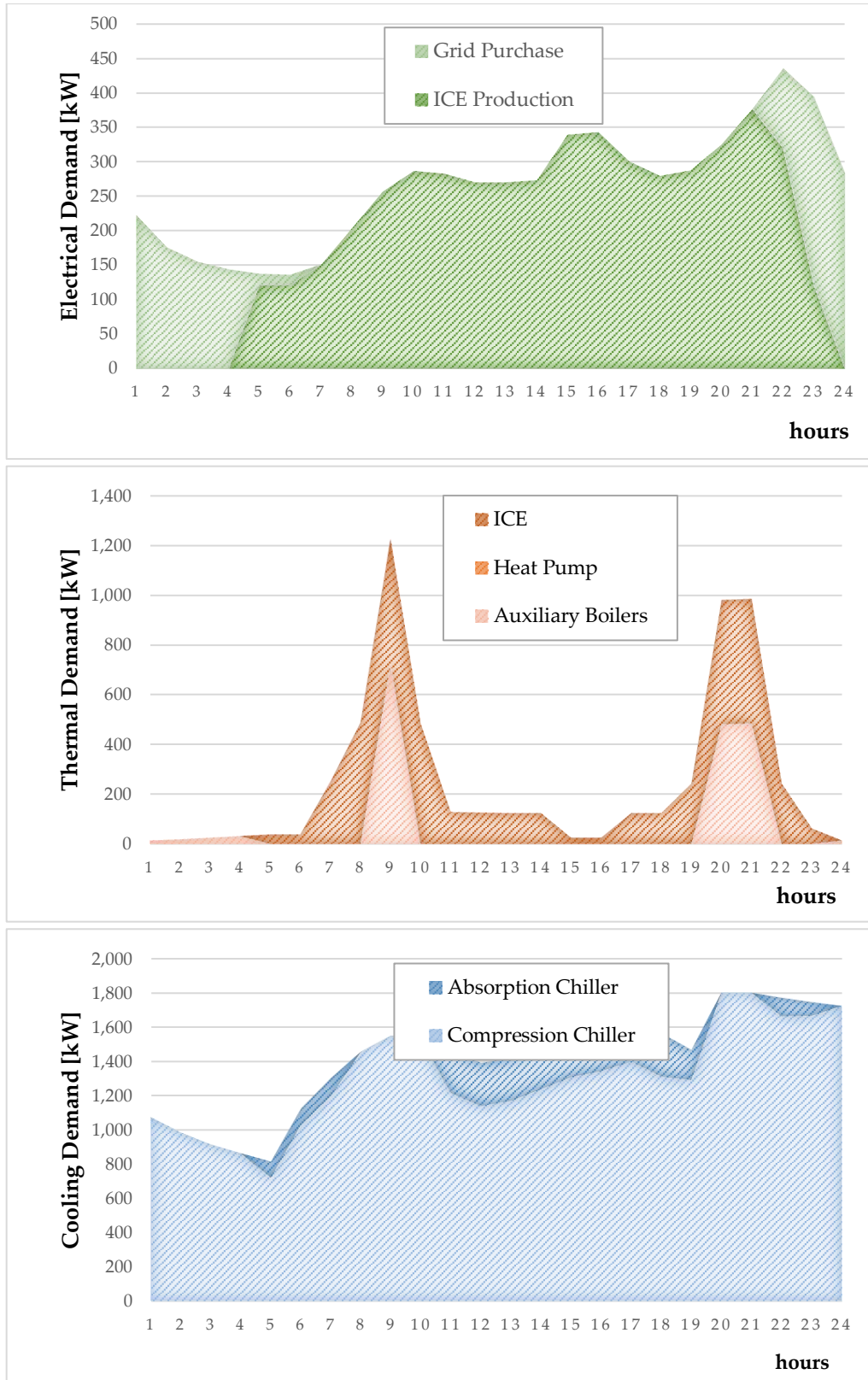
FIGURE D.24: HOURLY ELECTRICAL, THERMAL AND COOLING PROFILE IN THE CASE OF 900 HOUSEHOLDS FOR SUMMER SEASON.
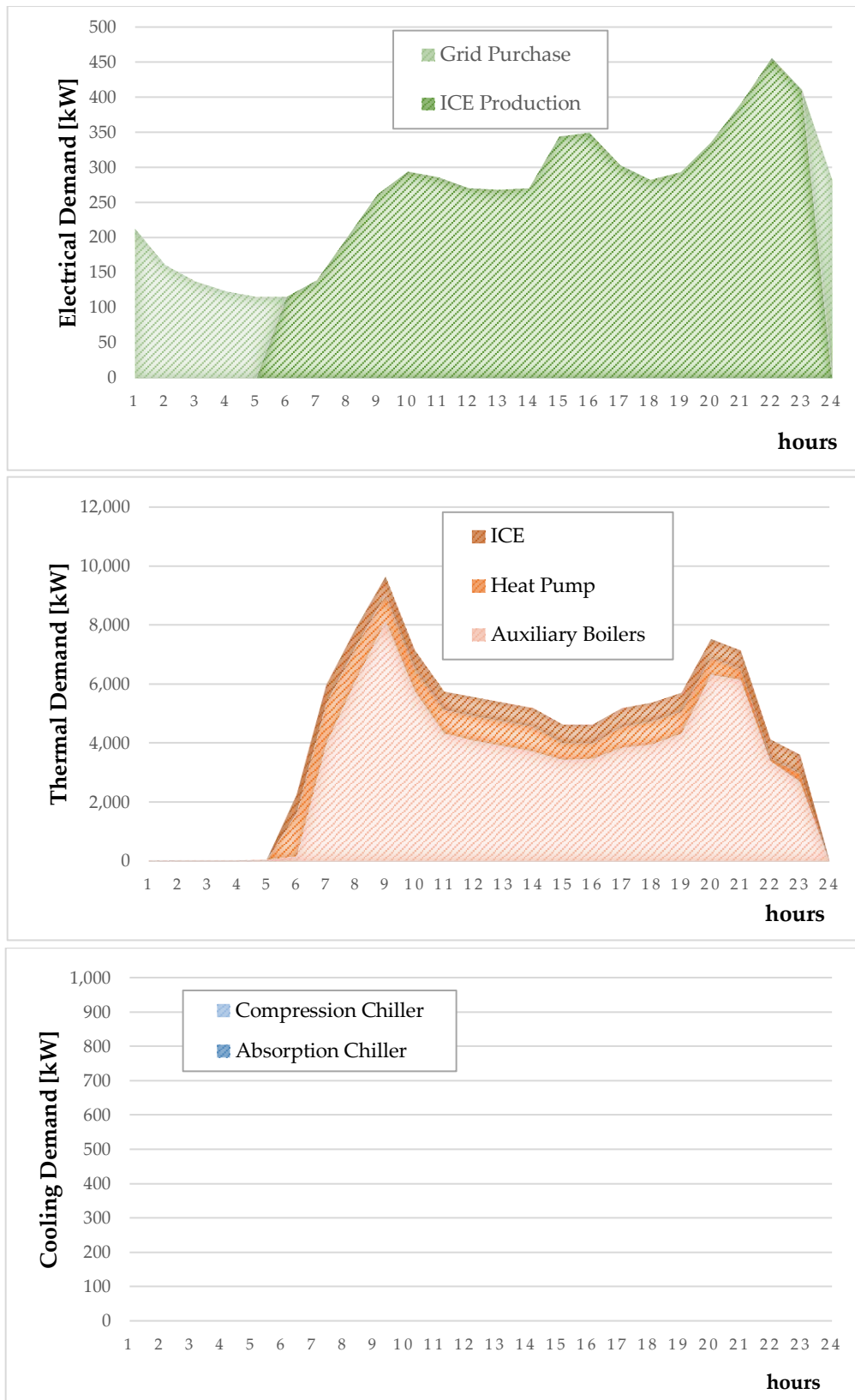
FIGURE D.25: HOURLY ELECTRICAL, THERMAL AND COOLING PROFILE IN THE CASE OF 1000 HOUSEHOLDS FOR WINTER SEASON.
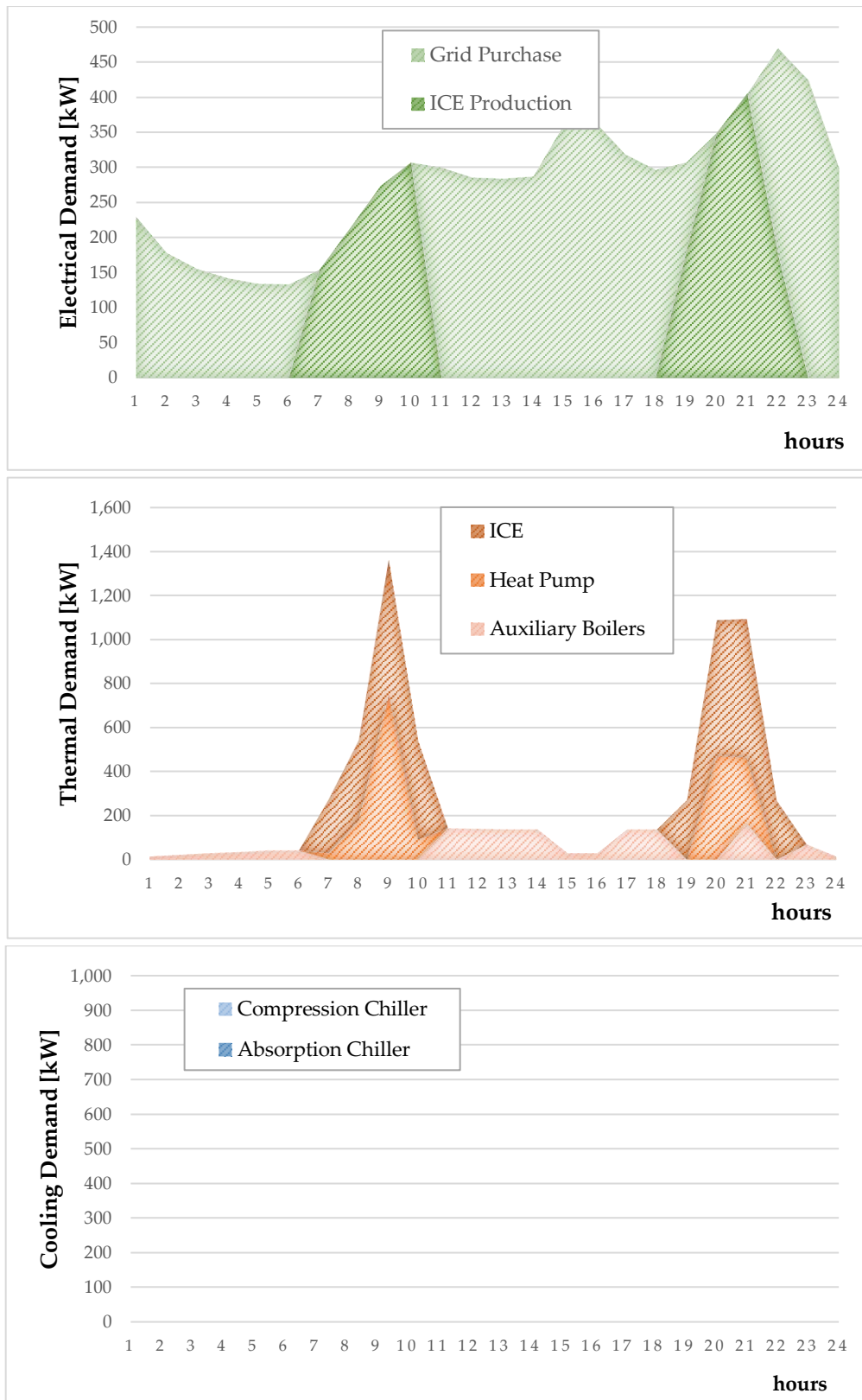
FIGURE D.26: HOURLY ELECTRICAL, THERMAL AND COOLING PROFILE IN THE CASE OF 1000
HOUSEHOLDS FOR MIDDLE SEASON.
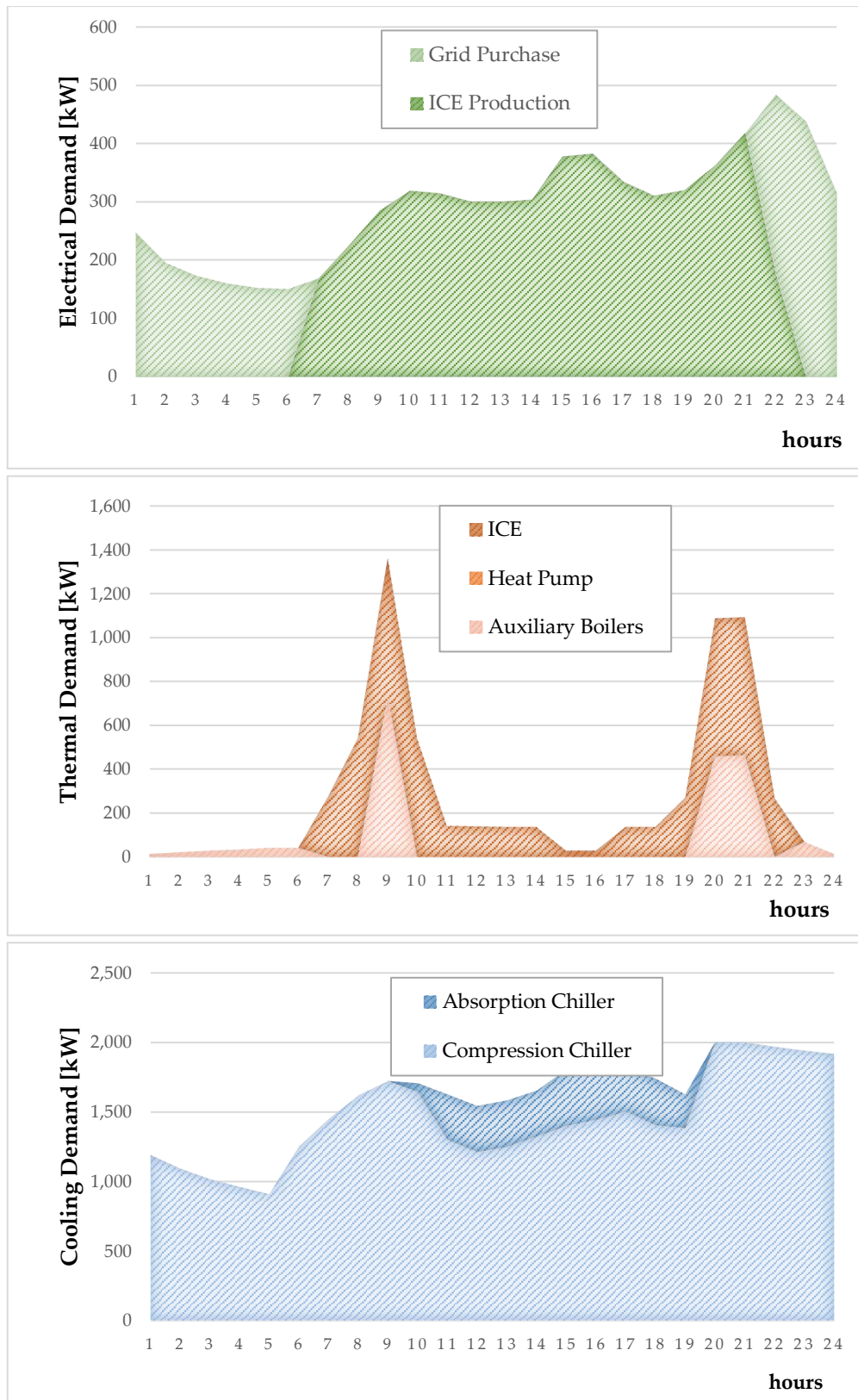
FIGURE D.27: HOURLY ELECTRICAL, THERMAL AND COOLING PROFILE IN THE CASE OF 1000
HOUSEHOLDS FOR SUMMER SEASON.